

Gastroesophageal reflux and *Helicobacter pylori*: a review

F Pace and G Bianchi Porro

Subject headings gastroesophageal reflux/therapy; *Helicobacter pylori*; epidemiology; peptic ulcer/therapy; stomach neoplasms/therapy; *Helicobacter* infections

Pace F, Porro GB. Gastroesophageal reflux and *Helicobacter pylori*: a review. *World J Gastroenterol*, 2000;6(3):311-314

INTRODUCTION

Since the observation by Labenz *et al* that eradication of *Helicobacter pylori* (*Hp*) infection may be followed by development of reflux esophagitis in a relevant proportion of duodenal ulcer patients previously not affected by gastroesophageal reflux disease (GERD)^[1], a growing attention has been given to the potential interactions between *Hp* and GERD. Epidemiological studies have now demonstrated that the prevalence of GERD is steadily increasing in the developed countries^[2], as is the incidence of adenocarcinoma of the esophagus^[3], its most dangerous complication, while the prevalence of peptic ulcer and gastric cancer is falling^[4], in parallel with a falling prevalence of *Hp* infection in the western countries^[5]. It is therefore tempting to causally relate these phenomena. Despite the number of original papers and of reviews dealing with this topic, at least 3 issues are still debated: ① Does *Hp* infection interfere with the pathogenesis of GERD? ② Is the anti-secretory effect of *Hp* infection of any clinical relevance in the management of GERD patients? ③ Does long-term proton pump inhibitors (PPI) therapy accelerate development of atrophic changes in *Hp* +ve GERD patients? Finally, the relationship(s) between *Hp* and Barrett's esophagus may deserve some importance.

Department of Gastroenterology, L. Sacco University Hospital, Milan, Italy

Dr. Fabio Pace graduated from the Palermo Medical University in 1979. He is at present senior consultant at the Department and Chair of Gastroenterology of Milan, "L. Sacco" Hospital, Milan, Italy. His main interests are in the field of GI Motility, GERD disease and functional gastrointestinal disorders. He is author of more than 150 original papers.

Correspondence to: G. Bianchi Porro, Divisione di Gastroenterologia, Ospedale Polo Universitario "L. Sacco", Via G. B. Grassi, 74, I-20157 Milano

Tel. +39-02-35799438, Fax. +39-02-35799232

Email. pace@spm.it

Received 2000-03-20 Accepted 2000-04-28

The present review will focus on these 4 issues. The interested reader may also refer to some recent papers, dealing with the same subject^[6-9].

Hp AND PATHOGENESIS OF GERD

Several studies have now convincingly shown that the prevalence of *Hp* infection in patients with reflux esophagitis is somewhat lower than in normal subjects; in a careful review of 26 papers on this topic, O'Connor summarizes the data existing as follows: the overall prevalence of *Hp* infection in 2182 adult GERD patients is 40.3%, as compared with 50.2% in the 2010 controls^[9]. He concludes that this "difference in prevalence (is) intimating that the pathogenesis of GERD might be related in some way to the absence of *Hp*". In our view, more simplistically, the only link between *Hp* infection and GERD lies on the degree of gastric acid secretion, and through this, on esophageal acid exposure. In patients with a predisposition to GERD but without a clinical manifestation of GERD (symptoms and/or esophageal lesions), eradication of *Hp* may trigger it, disclosing the clinical picture. On the contrary, patients harboring the infection, may be protected if the infection involves the corpus (i.e. the acid-producing part of the gastric mucosa), because the amount of acid secretion and hence the esophageal acid exposure is reduced. In fact, no single paper has ever been published so far focusing on *Hp* infection as a pathogenetic (aggressive or defensive) factor of GERD-perse. On the contrary, El-Serag *et al* have now clearly demonstrated that, for the above reasons, corpus gastritis is protective against reflux esophagitis^[10]. They have investigated 302 subjects, 154 of whom with endoscopic signs of esophagitis; there was no difference between patients with and controls without esophagitis in the overall infection rates with *Hp* infection. Compared with controls, corpus gastritis was less frequent and less severe in patients with esophagitis. Finally, in a multivariate logistic analysis, age, sex, smoking status, and the presence of chronic corpus gastritis exerted a significant influence on the presence of reflux esophagitis. This latter variable, however, showed an odds ratio of 0.46% only (95% confidence interval of 0.27-0.79), a value which is, albeit statistically significant, of doubtful clinical relevance.

In summary, the pathogenetic relationship

between *Hp* infection and GERD are probably weak and of indirect nature, being related to the amount of gastric acid secretion, a factor which is necessary but not indispensable for inducing GERD. The most relevant GERD pathogenetic factor is, as universally known, the occurrence of transient relaxation of the lower esophageal sphincter^[11], a factor which has not, to the best of our knowledge, been observed to be influenced by *Hp* gastric infection.

Is the antisecretory effect of *Hp* infection of any clinical relevance in the management of GERD patients?

A profound inhibition of acid secretion is the mainstay of treatment for reflux esophagitis, in particular in cases of moderate to severe RE^[12]. Therefore, the influence of *Hp* on the efficacy of acid-lowering treatment may be important for patients with RE. Verdu *et al*^[13] showed that omeprazole produces a greater decrease in gastric acidity in subjects with *Hp* infection than in those who are *Hp* negative, and that omeprazole produces a smaller decrease in gastric acidity after *Hp* infection has been cured^[14]. Similar findings have been obtained by Labenz *et al*^[15], who showed that in 17 FU patients, *Hp* eradication resulted in a marked decrease of the pH-increasing effect of omeprazole (24h median gastric pH: 5.5 vs 3.0, $P < 0.002$) that was most pronounced during night time. Base line intragastric pH remained unchanged after eradication (median gastric pH: 1.0 vs 1.1, $P = 0.05$). The same authors have also shown that this effect persisted for at least 1 year after *Hp* eradication^[16], whereas others have been shown that it is shared by other PPIs, such as lansoprazole^[17].

Despite this *Hp* mediated exaggeration of the effect of acid-suppressive drugs on intragastric pH is clearly proven, there is little evidence that this effect has any clinical relevance for the treatment of GERD patients with PPI. One reason is that the effect, due to the logarithmic scale of pH, a variation of one pH unit from 5 to 6 is 10 000 times less important than a variation from 1 to 2. The small variation in acid secretory capacity due to *Hp* colonisation is only "visible" when the acid secretion is already potentially reduced by PPI, but is otherwise unimportant.

Direct evidence shows in fact that, during acid suppressive therapy with ranitidine or omeprazole, *Hp* +ve or -ve GERD patients show a similar reduction of esophageal acid exposure, the entity of which is only influenced by the type of drug received^[18]. Furthermore, both groups of GERD patients require the same dose of omeprazole during long-term maintenance treatment to prevent symptomatic and endoscopic relapse^[19], and *Hp* status seems not to be an important prognostic

factor during long-term maintenance therapy with PPI; in a study conducted on 103 patients with RE grade 1 or 2, randomized to maintenance therapy with lansoprazole 15 or 30 mg daily for 12 months, it was observed that *Hp* infected patients relapsed as early as patients who were not infected^[20].

The only discordant piece of evidence comes from the very large study of Holtman *et al*^[21], who claims of a significantly better acute response of *Hp* +ve GERD patients treated with the PPI pantoprazole in comparison to *Hp* -ve; however, the difference of healing rates between the two groups after 8wk of 40mg daily was quite small (96.4% vs 91.8%, $P < 0.05$) and no difference at all was observed in GERD symptoms between infected and noninfected patients. There is therefore enough evidence to say, at least, that PPI maintenance therapy does not need to be titrated upon *Hp* status^[19]. It is therefore to be fully agreed upon the recommendation that "testing for *Hp* infection is not indicated in patients on long term treatment or in those considered for treatment with a proton pump inhibitor for GERD", as stated by the recent guidelines of the American College of Gastroenterology^[22].

Does long-term proton pump inhibitors (PPI) therapy accelerate development of atrophic in *Hp* +ve GERD patients?

Several studies have shown that treatment with PPI is associated with the worsening of gastritis (increase in severity score, spreading from the antrum to corpus and fundus)^[23-25]. Because superficial corpus gastritis may lead to atrophic gastritis, the increased body inflammation in *Hp* positive patients observed during short term PPI therapy may lead to atrophic gastritis during long term PPI treatment. This has been observed so far after omeprazole administration^[26], but the study was criticized in particular for the incorporation of an inappropriate control group^[27]. Moreover, the findings have not been confirmed by a randomized Swedish study comparing the efficacy of omeprazole maintenance treatment and antireflux surgery over a 3-years follow-up^[28]. Thus, on the basis of available evidence, long-term treatment with PPI up to 10 years appears to be a perfectly safe therapy^[29].

***Hp* INFECTION AND BARRETT'S ESOPHAGUS**

The interest in BE is still growing since the early description of this entity in 1950^[30] for two main reasons: ① BE is associated with GERD, and also with an increased risk of adenocarcinoma^[31], thus representing a link between a common benign condition and a rare very malignant disease; ② The incidence of adenocarcinoma of the esophagus and cardia is increasing at the fastest rate among gastrointestinal (and also non GI) human

cancers^[3]. Since *Hp* exhibits a special affinity for gastric-type epithelium, and since *Barrett's* metaplasia contains columnar-lined epithelium, it is to be expected that *Hp* will also be able to attach the *Barrett's* epithelium, at least of the gastric type, independently from any involvement of *Hp* infection in the pathogenesis of esophageal mucosal inflammation.

It seems that the prevalence of *Hp* infection of the stomach in BE patients is not different from that exhibited by controls, roughly one third of the subjects^[9]. The colonization of metaplastic epithelium by the bacterium has been tested only in a minority of studies, but appears to be marginally lower^[9]. It seems therefore that the stomach represents the primary site of infection, with secondary colonization of columnar mucosa in the esophagus. Furthermore, most *Hp* positive patients show a very low bacterial load in their metaplastic epithelium, and no significant difference has been found in the severity of inflammatory changes between *Hp* +ve and *Hp* -ve *Barrett's* esophagus patients^[32]. Finally, recent work has confirmed that within the esophagus, *Hp* adheres only to gastric type metaplasia, which is not considered premalignant for adenocarcinoma^[33]. In conclusion, it is most probable that *Hp* has no etiologic role on the development of *Barrett's* esophagus, nor in the esophagitis associated with this metaplastic change; the colonization of *Barrett's* epithelium probably reflects only a shift from gastric antrum.

Another intriguing point is the prevalence of *Hp* infection and the intestinal metaplasia of the gastric cardia. It is in fact at present not known whether inflammation of the cardia indicates GERD and/or is a manifestation of gastritis caused by *Hp*. Recently two studies have shed some light on this issue^[34,35]: in the first, biopsies were obtained from the antrum, corpus and cardia from 135 *Hp*-infected patients with gastritis, ulcer disease, or RE. One hundred and thirty-two (97.7%) of them showed active carditis, resembling antral gastritis in most patients, but with less marked bacterial density and inflammatory process^[34]. The authors conclude that *Hp* gastritis commonly involves the cardia, that intestinal metaplasia in the cardia is a common finding in *Hp* gastritis, but that the cardia lower histologic density of the bacteria and inflammatory responses in comparison to the antrum are not clear. In the second work^[35], 22 GERD patients and 11 controls were compared in relationship to endoscopic and biptic evaluation of inflammation, *Hp* infection and intestinal metaplasia in distal esophagus, cardia, fundus and antrum. It turned out that neither the prevalence of *Hp* infection (controls 48%; GERD 41%) nor cardia inflammation (controls 41%; GERD 40%) differed between the two groups. All 11 controls and 22 of

23 (96%) patients with GERD and cardia inflammation had *HP* infection. Cardia intestinal metaplasia was more common among controls (22%) than among GERD patients (3%, $P = 0.01$); all patients with cardia intestinal metaplasia had cardia inflammation, 7 had *Hp* infection, and 6 had metaplasia elsewhere in the stomach. The authors conclude that the prevalence of cardia inflammation is similar in patients with and without GERD, and is associated with *Hp* infection. Also, in this study, cardia intestinal metaplasia is associated with *Hp* related cardia inflammation ($P = 0.01$) and intestinal metaplasia elsewhere in the stomach, indicating that it is distinct from *Barrett's* esophagus.

The final point is the association, if any, between *Hp* infection and *Barrett's* associated adenocarcinoma. Again, two recent works have contributed to the improvement of our knowledge on this previously uninvestigated issue^[36,37]. Qaddus *et al* report on 19 cases of adenocarcinoma arising in BE, who were examined for the presence of *Hp* after staining with three different techniques: all sections of BE, with or without dysplasia, adenocarcinoma and stomach (when available) were uniformly negative for the presence of *Hp*. The authors conclude that neither gastric nor esophageal infection with *Hp* is a requisite for the development of adenocarcinoma in BE^[36].

The second study aimed at comparing the prevalence of *Hp* and increasing grades of dysplasia. Biopsies from 19 malignant and 94 benign cases of BE were analyzed histologically for *Hp*; 34% of non-dysplastic *Barrett's* epithelium was colonized with *Hp* compared with only 17% of dysplastic/malignant-cases ($P = 0.04$). No relationship was found between *Hp* status and ① length of BE; ② the presence of strictures or ulcers; ③ previous anti-reflux surgery. The authors therefore confirmed that *Hp* colonization of BE is not particularly common, and that a negative correlation exists with increasing severity of dysplasia^[37].

To summarize, from both studies it appears that it is unlikely that a causal relationship exists between *Hp* infection and *Barrett's* associated adenocarcinoma.

REFERENCES

- 1 Labenz J, Blum AL, Bayerdorffer E, Meining A, Stolte M, Borsh G. Curing *Helicobacter pylori* infection in patients with duodenal ulcer may provoke reflux esophagitis. *Gastroenterology*, 1997; 112:1442-1447
- 2 Howard PJ, Heading RC. Epidemiology of gastro-oesophageal reflux disease. *World J Surg*, 1992;16:288-293
- 3 Pera M, Cameron AJ, Trastek VF, Carpenter HA, Zinsmeister AR. Increasing incidence of adenocarcinoma of the esophagus and esophagogastric junction. *Gastroenterology*, 1993;104:910-913
- 4 El-Serag HB, Sonnenberg A. Opposite time trends of peptic ulcer and reflux disease. *Gut*, 1998;43:327-333
- 5 Marshall BJ. Epidemiology of *H. pylori* in western countries. in: Hunt RH, Tytgat GN. *Helicobacter pylori*. Basic mechanism to clinical cure. Dordrecht: Kluwer Acad Pub, 1994:75-84
- 6 Xia HH, Talley NJ. *Helicobacter pylori* infection, reflux esophagitis and atrophic gastritis: an unexplored triangle. *Am J Gastroenterol*,

- 1998;93:394-400
- 7 Richter JE, Falk GW, Vaezi MF. Helicobacter pylori and gastroesophageal reflux disease: the bug may not be all bad. *Am J Gastroenterol*, 1998;93:1800-1802
- 8 Pace F, Bianchi Porro G. Gastro-oesophageal reflux and Helicobacter pylori. *Ital J Gastroenterol Hepatol*, 1998;30(Suppl 3):289-293
- 9 O'Connor HJ. Helicobacter pylori and gastro-oesophageal reflux disease clinical implications and management. *Aliment Pharmacol Ther*, 1999;13:117-127
- 10 El-Serag BH, Sonnenberg A, Jamal MM, Inadomi JM, Crooks LA, Feddersen RM. Corpus gastritis is protective against reflux oesophagitis. *Gut*, 1999;45:181-185
- 11 Dodds WJ, Dent J, Hogan WJ, Helm JF, Hauser R, Patel GK, Egide MS. Mechanism of gastroesophageal reflux in patients with reflux esophagitis. *N Engl J Med*, 1982;307:1547-1552
- 12 Chiba N, De Gara CJ, Wilkinson JM, Hunt RH. Speed of healing and symptom relief in grade II to IV gastroesophageal reflux disease: a meta-analysis. *Gastroenterology*, 1997;112:1798-1810
- 13 Verdu EF, Armstrong D, Fraser R, Viani F, Idstrom J, Cederberg C, Blum AL. Effect of Helicobacter pylori status on intragastric pH during treatment with omeprazole. *Gut*, 1995;36:539-543
- 14 Verdu EF, Armstrong D, Idstrom JP, Labenz J, Stolte M, Dorta G, Borsch G, Blum AL. Effect of curing Helicobacter pylori infection on intragastric pH during treatment with omeprazole. *Gut*, 1995;37:743-748
- 15 Labenz J, Tillenburg B, Peitz U, Idstrom JP, Verdù E, Stolte M, Blum AL. Helicobacter pylori augments the pH-increasing effect of omeprazole in patients with duodenal ulcer. *Gastroenterology*, 1996;110:725-732
- 16 Labenz J, Tillenburg B, Peitz U, Idstrom JP, Verdù E, Stolte M, Bosch G, Blum AL. Efficacy of omeprazole one year after cure of Helicobacter pylori infection in duodenal ulcer patients. *Am J Gastroenterol*, 1997;92:576-578
- 17 Van Herwaarden MA, Samson M, Van Nispen CHM, Mulder PGH, Smout AJP. The effect of Helicobacter pylori eradication on intragastric pH during dosing with lansoprazole or ranitidine. *Aliment Pharmacol Ther*, 1999;13:731-740
- 18 Peters FT, Kuipers EJ, Ganesh S, Sluiter WJ, Klinkenberg-Knol EC, Lamers CB, Kleibeuker JH. The influence of Helicobacter pylori on esophageal acid exposure in GERD during acid suppressive therapy. *Aliment Pharmacol Ther*, 1999;13:921-926
- 19 Schenk BE, Kuipers EJ, Klinkenberg-Knol EC, Eskes SA, Meuwissen SGM. Helicobacter pylori and the efficacy of omeprazole therapy for gastroesophageal reflux disease. *Am J Gastroenterol*, 1999;94:884-887
- 20 Hatlebakk JG, Berstad A. Prognostic factors for relapse of reflux oesophagitis and symptoms during 12 months of therapy with omeprazole. *Aliment Pharmacol Ther*, 1997;11:1093-1099
- 21 Holtmann G, Cain C, Malfertheiner P. Gastric Helicobacter pylori infection accelerates healing of reflux esophagitis during treatment with the proton pump inhibitor pantoprazole. *Gastroenterology*, 1999;117:11-16
- 22 Howden CW, Hunt RH. Guidelines for the management of Helicobacter pylori infection. *Am J Gastroenterol*, 1998;93:2330-2338
- 23 Kuipers EJ, Uytterlinde AM, Pena AS, Hazenberg HJA, Bloemena E, Lindeman J, Klinkenberg Knol E, Meuwissen SGNM. Increase of Helicobacter pylori associated corpus gastritis during acid-suppressive therapy: implications for longterm safety. *Am J Gastroenterol*, 1995;90:1401-1406
- 24 Logan RPH, Walker MM, Misiewicz JJ, Gummett PA, Karim QN, Baron JH. Changes in intragastric distribution of Helicobacter pylori during treatment with omeprazole. *Gut*, 1995;36:12-16
- 25 Eissele R, Brunner G, Simon B, Solcia E, Arnold R. Gastric mucosa during treatment with lansoprazole: Helicobacter pylori is a risk factor for argyrophil cell hyperplasia. *Gastroenterology*, 1997;112:707-715
- 26 Kuipers EJ, Lundell L, Klinkenberg-Knol EC, Havu N, Festen HPM, Liedman B, Lamers CBHW, Jansen JBMJ, Dalenback J, Snel P, Nelis GF, Meuwissen SGNM. Atrophic gastritis and Helicobacter pylori infection in patients with reflux esophagitis treated with omeprazole or fundoplication. *N Engl J Med*, 1996;334:1018-1022
- 27 Genta RM. Acid suppression and gastric atrophy: sifting fact from fiction. *Gut*, 1998;43(Suppl 1):35-38
- 28 Lundell L, Miettinen P, Myrvold HE, Pedersen SA, Thor K, Andersson A, Hattlebakk J, Janatuinen E, Lecander C, Liedman B, Nystrom P, and the NORDIC GERD STUDY GROUP. Lack of effect of acid suppression therapy on gastric atrophy. *Gastroenterology*, 1999;117:319-326
- 29 Labenz J. Does Helicobacter pylori affect the management of gastroesophageal reflux disease? (Editorial). *Am J Gastroenterol*, 1999;94:867-869
- 30 Barrett NR. Chronic peptic ulcer of the oesophagus and "oesophagitis". *Br J Surg*, 1950;38:175-182
- 31 Hameeteman W. Barrett's esophagus and adenocarcinoma. In: Bianchi Porro G, Pace F, eds. *Argomenti di patologia esofagea*, Vol. 3. Milano: Springer Verlag Italia, 1998:5-27
- 32 Loffeld RJLF, Ten Tije BJ, Arends JW. Prevalence and significance of Helicobacter pylori in patients with Barrett's esophagus. *Am J Gastroenterol*, 1992;87:1598-1600
- 33 Sharma VK, Demian SE, Taillon D, Vasuveda R, Howden CW. Examination of tissue distribution of Helicobacter pylori within columnar-lined esophagus. *Dig Dis Sci*, 1999;44:1165-1168
- 33 Hackelsberger A, Guenther T, Schultze V, Labenz J, Roessner A, Malfertheiner P. Prevalence and pattern of Helicobacter pylori gastritis in the gastric cardia. *Am J Gastroenterol*, 1997;92:2220-2224
- 35 Goldblum JR, Vicari JJ, Falk GW, Rice TW, Peek RM, Easley K, Richter JE. Inflammation and intestinal metaplasia of the gastric cardia: the role of gastr oesophageal reflux and H. pylori infection. *Gastroenterology*, 1998;114:633-639
- 36 Quidus MR, Henley JD, Sulaiman RA, Palumbo TC, Gnepp DR. Helicobacter infection and adenocarcinoma arising in Barrett's esophagus. *Hum Pathol*, 1997;28:1007-1009
- 37 Wright TA, Myskow M, Kingsnorth AN. Helicobacter pylori colonization of Barrett's esophagus and its progression to cancer. *Dis Esophagus*, 1997;10:196-200

Management of difficult inflammatory bowel disease: where are we now?

D.S. Rampton

Subject headings inflammatory bowel diseases/therapy; colitis/therapy; Crohn disease/therapy; endoscopy, gastrointestinal; social support; azathioprine

Rampton DS. Management of difficult inflammatory bowel disease: where are we now? *World J Gastroentero*, 2000;6(3):315-323

INTRODUCTION

Medical care of patients with inflammatory bowel disease (IBD) comprises general measures and specific pharmacological, nutritional, endoscopic and surgical therapies (Table 1)^[1-3]. In this paper, current management options for patients with two commonly difficult presentations of IBD, acute severe ulcerative colitis (UC) and steroid-refractory or dependent ileocaecal Crohn's disease (CD), are discussed. Practical considerations and newer developments are emphasized.

MANAGEMENT OF ACUTE SEVERE ULCERATIVE COLITIS

These patients should be admitted immediately to a gastroenterology ward for close joint medical, surgical and nursing care. The nutrition team and a stoma therapist in patients likely to need surgery should be involved promptly. Patients undergoing an acute attack of UC need to be made aware from the outset that they have a one in four chance of failing to respond to the primary treatment (intravenous steroids), and thus need either cyclosporin or colectomy during their admission (Table 1).

Establishing the diagnosis, extent and severity of disease

A carefully targeted history and appropriate investigations can help establish the diagnosis (Table 2) in patients presenting for the first time and, in those with established UC, to exclude infection and to assess disease extent (if not already known) and severity.

Blood and stool tests Stool should be sent to look for

Reader & Consultant Gastroenterologist, Gastrointestinal Science Research Unit and Digestive Diseases Research Centre, St Bartholomew's & Royal London School of Medicine and Dentistry, London E1 2AD, UK

Correspondence to: Dr. DS Rampton, Royal London Hospital, London? E1 1BB, UK

Tel +44-171-7442, Fax. +44-171-7441

Email. drampton@mds.qmw.ac.uk

Received 2000-02-22 Accepted 2000-04-22

pathogens, and serology checked for amoebiasis, strongyloidiasis and schistosomiasis. Blood tests are better for establishing the activity of UC than making the diagnosis or identifying its extent. However, a raised platelet count is more common in UC than in infective colitis. The best measures of disease activity are haemoglobin, platelet count, ESR, C-reactive protein^[4] and serum albumin.

Sigmoidoscopy and rectal biopsy Cautious rigid or flexible sigmoidoscopy in the unprepared patient, and without excessive air insufflation, provides immediate confirmation of active colitis. Sigmoidoscopy also allows biopsy for histology: to minimise the risks of bleeding and perforation a small superficial biopsy should be taken from the posterior rectal wall less than 10 cm from the anal margin using small-cupped forceps. Anecdotally, colonoscopy may cause colonic perforation and dilatation in acute severe UC, and although some authorities have reported that it is both safe and useful for decision-making^[5], most patients can be managed satisfactorily without it. In patients with established UC, rectal biopsy is not routinely necessary. However, in those presenting for the first time, infective colitis may be suggested by an acute, focal and superficial inflammatory infiltrate with minimal goblet cell depletion and preservation of crypt architecture^[6]. Although colitis due to *Clostridium difficile*, cytomegalovirus, amoebiasis and *Crohn's* disease often has characteristic macroscopic appearances, histology may confirm these diagnoses.

Plain abdominal X-ray A plain film at presentation can be used to assess disease extent, since faecal residual visible on X-ray usually indicates sites of uninfamed colonic mucosa. Plain abdominal X-ray is also used to assess disease severity and in particular to exclude colonic dilatation (diameter > 5.5 cm) in sick patients, however, the gas pattern on a plain film may be misleading if there has been excessive air insufflation during a sigmoidoscopy or colonoscopy done shortly beforehand. In patients with suspected colonic perforation, the diagnosis can be confirmed by erect chest X-ray or a lateral decubitus abdominal film.

Radiolabelled leucocyte scans The intensity and extent of colonic uptake one hour after injection of autologous ⁹⁹Tc-HMPAO or ¹¹¹Indium-labelled leukocytes provides information about disease

activity and particularly extent, respectively, where doubt exists in patients with UC. Colonic uptake of leucocytes is not of course specific for UC and positive results are obtained in other inflammatory colonic diseases.

Table 1 Principles of management of acute severe ulcerative colitis

GENERAL MEASURES	
Explanation, psychosocial support	- patient support groups
Specialist multidisciplinary care	- physicians, surgeons, nutrition team, nurses, stoma therapist, counsellor
ESTABLISHING THE DIAGNOSIS, EXTENT/SITE AND SEVERITY	
	- clinical evaluation
	- FBC, ESR, C-reactive protein, albumin, LFTs, amoebic serology
	- stool microscopy, culture, C. difficile toxin
	- limited sigmoidoscopy and biopsy
	- plain abdominal X-ray
	- consider radiolabelled leucocyte scan
MONITORING PROGRESS	
	- daily clinical assessment
	- stool chart
	- 4-hrly temperature, pulse
	- daily FBC, ESR, C-reactive protein, urea and electrolytes, albumin
	- daily plain abdominal X-ray
SUPPORTIVE TREATMENT	
	- i.v. fluids, electrolytes (Na, K), blood transfusion
	- nutritional supplementation
	- heparin s.c.
	- haematinics (folate)
	- avoid antidiarrhoeals (codeine, loperamide, diphenoxylate), opiates, NSAIDs
	- rolling manoeuvre (if colon dilating)
SPECIFIC TREATMENT	
Medical	- corticosteroids i.v. (hydrocortisone or methylprednisolone) then p.o. (prednisolone)
	- continue 5-ASA p.o. in patients already taking it; otherwise start when improvement begins
	- antibiotics for very sick febrile patients, or when infection suspected
	- consider cyclosporin i.v. then p.o.) for steroid non-responders at 4-7 days
Surgical (for non-responders at 5-7 days, toxic megacolon, perforation, massive haemorrhage)	- panproctocolectomy with ileoanal pouch or permanent ileostomy
	- subtotal colectomy with ileorectal anastomosis (rarely)

Table 2 Management of active ileocaecal Crohn's disease. General measures, monitoring progress and supportive treatment are essentially as for ulcerative colitis

ESTABLISHING THE DIAGNOSIS, EXTENT/SITE AND SEVERITY	
	- clinical evaluation
	- FBC, ESR, C-reactive protein, ferritin, folate, B12, albumin, LFTs, Ca, Mg, Zn
	- stool microscopy, culture, C difficile toxin
	- plain abdominal X-ray
	- consider colonoscopy and biopsy, small bowel barium radiology, ultrasound, CT, MRI, leucocyte scan
SPECIFIC TREATMENT (separately or in combination)	
Medical	- corticosteroids i.v. (hydrocortisone or methylprednisolone) then p.o. (prednisolone or budesonide CR)
	- continue high dose mesalazine (Pentasa or Asacol) in patients already taking it; otherwise start when improvement begins
	- consider metronidazole, ciprofloxacin; also broad spectrum antibiotics for very sick febrile patients, or when infection/collection suspected
	- consider azathioprine/6-mercaptopurine (slow response) or anti TNF antibodies (infliximab) for steroid non-responders
Nutritional	- liquid formula diet
Endoscopic	- balloon dilatation
Surgical	- resection or stricturoplasty

Monitoring progress

Progress is monitored by twice daily clinical assessment, stool chart and 4-hourly measurement of temperature and pulse. Blood count, ESR, C-reactive protein, routine biochemistry and plain abdominal X-ray should be done daily in sick patients. The two most useful variables in predicting the outcome of the acute attack are stool frequency and C-reactive protein at three days: patients with values above 8 stools/day or 45 mg/L, respectively, have an 85% chance of failing to respond to intravenous steroids and needing cyclosporin or surgery during their admission^[4] (Table 1).

Supportive treatment

Intravenous fluids and blood Most patients require intravenous fluids and electrolytes, particularly potassium, to replace diarrhoeal losses. Serum potassium concentration should be maintained at or above 4 mmol/L, since hypokalaemia may predispose to colonic dilatation. Blood transfusion is recommended if the haemoglobin falls below 100g/L.

Nutritional support Patients can usually eat normally, with liquid protein and calorie supplements if necessary. Very sick patients may need total parenteral nutrition.

Anticoagulation Because active UC is associated with a high risk of venous and arterial thrombo-embolism^[7], patients should be given prophylactic subcutaneous heparin (e.g. low molecular mass heparin 3000-5000 U daily). Heparin does not appear to increase rectal blood loss even when given intravenously^[8].

Drugs to avoid Antidiarrhoeal drugs (loperamide, codeine phosphate, diphenoxylate), opioid analgesics, antispasmodics and anticholinergic drugs should not be prescribed in active UC since they may provoke acute colonic dilatation^[9]. Patients should also avoid NSAIDs in view of their adverse effects on the clinical course of IBD^[10]. If relief of mild pain is needed, oral paracetamol appears to be safe, while severe pain suggests colonic dilatation or perforation needing urgent intervention.

Rolling manoeuvre In very sick patients, particularly those with clinical and/or radiological evidence of incipient colonic dilatation, rolling into the prone or knee-elbow position for 15 minutes every two hours may aid in the evacuation of gas per rectum, particularly from the transverse colon^[11].

Specific medical treatment

The cornerstone of specific medical treatment of acute severe UC remains corticosteroids^[1,12]. Aminosalicylates and antibiotics have minor roles. Cyclosporin has become a useful option, but oral

azathioprine and 6-mercaptopurine are too slow to work in patients with acute steroid-refractory attacks (Table 1).

Corticosteroids Hydrocortisone (300 mg/d-400 mg/d) or methyl prednisolone (40 mg/d-60 mg/d) are given intravenously. There is no advantage in giving higher doses, although continuous infusion may be more effective than once or twice daily boluses^[12]. On this treatment, about 70% patients improve substantially in 5 d-7 d. They are then switched to oral prednisolone (40 mg/d-60 mg/d), the dose being tapered to zero over 2-3 months. Conventionally, failure to respond to intravenous steroids after 7 d indicates urgent colectomy, but introduction of intravenous cyclosporin can now be considered as an alternative.

Aminosalicylates Aminosalicylates in full dose are continued in patients already taking them at the time of admission, and well enough to take oral medication, but do not have a primary therapeutic in acute severe UC. In case patients given aminosalicylates for the first time prove to be allergic to, or intolerant of them, initiation of these drugs is best delayed until the patient shows sufficient improvement on intravenous steroids to switch to oral treatment.

Antibiotics Although one study has suggested a role for adjunctive oral tobramycin^[13], the use of antibiotics is usually restricted now to very sick febrile patients, or to those in whom an infective component to their colitis is strongly suspected. Under such circumstances, a combination of antibiotics, for example ciprofloxacin or a cephalosporin with metronidazole, is often given.

Cyclosporin The only current evidence-based indication for cyclosporin in IBD is steroid-refractory acute severe UC. In a single small controlled trial^[14], the results of which have been largely confirmed by subsequent experience^[15,16], intravenous (4 mg·kg⁻¹·d⁻¹) for about 5 d) followed by oral (5 mg·kg⁻¹·d⁻¹-8 mg·kg⁻¹·d⁻¹) cyclosporin, given with continued corticosteroids, averted colectomy in the acute phase in 80% of patients failing to respond to 5 d-7 d of intravenous steroids alone. Enthusiasm for this approach has to be tempered by the frequency of relapse necessitating colectomy (up to 50%) that follows withdrawal of cyclosporin, and by its serious adverse effects which in turn demand frequent monitoring of cyclosporin blood levels and serum biochemistry in treated patients. The therapeutic range for monoclonal radioimmunoassay is 250 µg/L⁻¹-400 µg/L⁻¹ during intravenous treatment, and 150 µg/L⁻¹-300 µg/L⁻¹ as the trough level on oral treatment. Biochemical disturbances induced by cyclosporin include

hyperkalaemia, hypomagnesaemia and hyperuricaemia, as well as renal dysfunction. The most serious side effects of cyclosporin are opportunistic infections (20% patients) including pneumocystis carinii pneumonia, on account of which co-administration of prophylactic trimethoprim/sulphamethoxazole may be advisable; renal impairment, including a small reduction in glomerular filtration rate in most patients and, sometimes, an interstitial nephritis which is not always reversible on stopping cyclosporin; hypertension (30% patients); hepatotoxicity (up to 20%); and epileptic fits (3%), due to penetration of the blood-brain barrier by a vehicle, cremophor, in cyclosporin and essentially confined to patients with low serum cholesterol and/or magnesium concentration. Less serious side-effects include nausea, headache, paraesthesiae and hypertrichosis.

Further studies are needed to determine optimal usage of cyclosporin in UC. For example, precisely when should patients be given the drug, will a lower dose (2 mg·kg⁻¹·d⁻¹ iv) be as effective but safer, should trimethoprim/sulphamethoxazole be coprescribed as prophylaxis against pneumocystis carinii infection, and should oral cyclosporin or azathioprine be prescribed after the intravenous treatment? It is clear, however, that intravenous cyclosporin can be invaluable in patients with steroid-refractory acute severe UC, not least for buying time for improving their nutrition prior to, and/or preparing them psychologically for surgery.

Azathioprine and 6-mercaptopurine Oral azathioprine and 6-mercaptopurine are very effective in inducing and maintaining remission in patients with steroid-refractory or dependent IBD. Unfortunately, however, they take up to 4 months to exert their effect and are thus inappropriate for acute severe UC.

Possible new treatments The possible roles of anti-TNF-α antibody^[17], antibodies and antisense oligonucleotides to leucocyte/endothelial cellular adhesion molecules^[18], and intravenous heparin^[8] require further evaluation in controlled clinical trials.

Surgery

A colorectal surgeon should be involved in the care of patients with acute severe UC throughout their admission. Indications for urgent colectomy, which is required in about 25% of patients with acute severe colitis, include toxic colonic dilatation which does not respond within 24 h to intensification of medical treatment with rolling^[11,12], antibiotics and nasogastric suction, and deterioration or failure to improve on medical therapy in 5 d-7 d. Emergency surgery, after immediate resuscitation, is required in the rare patients, who develop colonic perforation or massive colonic haemorrhage.

Details of the surgical options available (pan-proctocolectomy with ileoanal pouch or permanent ileostomy, or, rarely, sub-total colectomy with ileorectal anastomosis) and their elective indications, are beyond the scope of this review.

MANAGEMENT OF ACTIVE CROHN'S DISEASE

Treatment of CD depends not only on disease activity and site, as in UC, but also needs to be tailored according to the patient's clinical presentation^[2,3]. Inflammation (Table 2), obstruction, abscess and fistula require different therapeutic approaches, and need to be distinguished by appropriate investigation before specific treatment is begun.

Assessment of disease activity

Its heterogeneous presentation makes assessment of disease activity in CD more complicated than in UC. For clinical trials, a large number of multifactorial clinical and/or laboratory-based scoring systems, such as the Crohn's Disease Activity Index (CDAI), has been devised, but none is suitable for ordinary clinical use^[2]. The working definitions of the American College of Gastroenterology^[2] are more practicable. Many patients with active CD can be looked after as outpatients, but those with moderate-severe and severe-fulminant disease need prompt, and in the latter instance immediate, hospital admission.

General measures

As for UC, patients with active CD should be looked after by a multi-disciplinary team with special expertise in IBD in a gastroenterology clinic or ward. Options for treatment (medical, nutritional, surgical) are wider than in UC, and it is essential that the patient is kept fully informed about his/her illness, and takes a place at the centre of the therapeutic decision-making process^[2,3].

Establishing the diagnosis and clinicopathological problem

In many patients, the diagnosis of CD and identification of its principal site will have been made before the current relapse. Investigations, therefore, are directed primarily to clarifying the dominant clinicopathological process so as to optimise subsequent treatment. In those individuals presenting acutely for the first time, the diagnosis needs to be established (Table 2).

Clinical evaluation Terminal ileal and ileocaecal CD usually present with pain, diarrhoea and/or a tender mass in the right iliac fossa. Inflammation and abscess tend to cause constant pain, often with fever; in patients with small bowel obstruction, the pain is more generalised, intermittent, colicky and associated with borborygmi, abdominal distension and vomiting. Where the diagnosis of CD has not yet been made, an appendix mass, caecal

carcinoma, lymphoma and, in some ethnic groups, ileocaecal tuberculosis require careful consideration.

Blood tests As in UC, the main value of blood tests is in assessing and monitoring disease activity, which is related directly to the platelet count, ESR and C-reactive protein and inversely to serum haemoglobin and albumin. However, in very sick patients, particularly with extensive small bowel disease and steatorrhoea, there may be laboratory evidence of malnutrition and malabsorption (anaemia, low serum iron, folate, Vit.B12, albumin, calcium, magnesium, zinc, essential fatty acids).

Endoscopy and biopsy In patients with right iliac fossa pain where the diagnosis of CD is in doubt, colonoscopy to the terminal ileum, with biopsies, is helpful. It can also be used to balloon-dilate short strictures. In established Crohn's colitis, colonoscopy during acute relapse is not routinely necessary and may be unsafe. In previously undiagnosed patients, digital rectal examination and sigmoidoscopy may show rectal induration or ulceration, or the presence of perianal disease. Furthermore, biopsy of macroscopically normal rectal mucosa may reveal epithelioid granulomata in a minority of patients with overt CD more proximally.

Plain abdominal X-ray A plain film is essential if intestinal obstruction is suspected. It may also hint at a mass in the right iliac fossa, and is often helpful, as in UC, in estimating extent or severity of Crohn's colitis.

Barium radiology Because it may exacerbate obstructive symptoms and pre-existing perforation, conventional barium follow through and small bowel enema should be avoided in severely ill patients with small bowel disease. In many centres, colonoscopy, because it allows biopsy and when necessary balloon dilatation of strictures, is used in preference to barium enema in patients with suspected large bowel and terminal ileal disease. Contrast fistulography is useful for the clarification of anatomical connections in patients with abdominal sinuses or fistulae.

Radiolabelled leucocyte scans ⁹⁹Tc-HMPAO or ¹¹¹Indium-leucocyte scanning can be helpful to identify, non-invasively, not only sites of large bowel inflammation, as in UC, but also in the small intestine. Delayed scanning can also be helpful in identifying intra-abdominal abscesses.

Ultrasound, CT scan and magnetic resonance imaging (MRI) Abdominal ultrasound and CT scan can be very useful in active CD, allowing not only the evaluation but also the percutaneous drainage of localised collections. CT also plays a central role in

defining abdominal fistulous tracks and sinuses, while endoluminal ultra sound and MRI are particularly useful for the anatomical delineation of perianal abscesses and fistulae.

Supportive treatment

Patients with active CD, like those with acute severe UC, need meticulous supportive treatment, including, as necessary, intravenous fluids and electrolytes, blood transfusion and prophylactic subcutaneous heparin^[7](Table 2).

Dietary advice and nutritional support All patients should be carefully assessed in relation to their nutritional intake and status, the latter clinically by measurement of body mass index [mass (kg)/height (m)²; (normal >20)]. Patients with stricturing small bowel CD should avoid high residue foods (e.g. citrus fruit segments, nuts, sweetcorn, uncooked vegetables) which might cause bolus obstruction. Special dietary and nutritional modifications are needed for patients with extensive small bowel CD or short bowel syndrome. Sick inpatients may need enteral or parenteral nutrition to restore nutritional deficits, while liquid formula diets offer effective primary therapy for some patients with active small bowel CD.

Smoking Patients with CD who smoke should be strongly advised to stop, since this habit has a major adverse effect on the long-term natural history of the disease, particularly in women^[19].

Drugs Codeine phosphate and loperamide are useful for the control of diarrhoea in patients with small bowel CD or resection; they should, as in UC, be avoided in active Crohn's colitis in case they provoke colonic dilatation. Cholestyramine sachets (4 g one to three times daily) reduce watery diarrhoea due to bile salt malabsorption induced by extensive terminal ileal disease or resection. Haematinics (Fe, folate, Vit.B12), calcium, magnesium, zinc and fat soluble Vit. (A,D,E,K) may be needed for the replacement of particular deficiencies, as may appropriate drugs for incipient or established osteoporosis.

Drugs to avoid NSAIDs may precipitate relapse of CD, as of UC^[10], and should be avoided. Likewise, in patients with small bowel stricturing due to CD, delayed release drugs should not be prescribed in case they cause bolus obstruction.

SPECIFIC TREATMENT OF ACTIVE ILEOCAECAL CROHN'S DISEASE

Therapeutic options include drugs, liquid formula diet and surgery, as separate alternatives or in combination, depending on the individual patient's age, presentation and personal preference (Table 2)^[2,3].

Drug therapy

Corticosteroids In active disease, oral steroids provide the quickest and most reliable response, 60%-80% patients improving in 3 wk-4 wk. Conventionally, prednisolone (40 mg·d⁻¹-60 mg·d⁻¹) is used, the dose being tapered by 5 mg every 7 d-10 d once improvement has begun. Very sick patients, or those needing to be fasted because of intestinal obstruction, need intravenous corticosteroids at least initially (e.g. hydrocortisone 300 mg·d⁻¹-400 mg·d⁻¹, methyl prednisolone 40 mg·d⁻¹-60 mg·d⁻¹). In patients able to take oral treatment in whom systemic steroid side effects are a major problem, a useful recent advance is the introduction of an oral controlled ileal release formulation of budesonide (Entocort CR, Budenofalk) (9 mg·d⁻¹). This steroid approaches prednisolone in efficacy, but because of first-pass metabolism, has fewer systemic side-effects and causes much less adrenocortical suppression, albeit at greater financial cost^[20]. Up to 20% of patients with CD may be difficult to wean off steroids after relapse. Of these, many will be able partially or totally to discontinue steroid therapy on introduction of an aminosalicilate or immunomodulatory agent.

Aminosalicilates Patients with only moderately active ileocaecal disease, most of whom can be treated as outpatients, can be tried on high dose oral mesalazine (e.g. Pentasa 2 g b.d., Asacol 1.2 g t.d.s.)^[21,22]; about 40% will go into remission in 2-3 months on such treatment, which may be preferred by individuals reluctant to use prednisolone.

Metronidazole and other antibiotics Metronidazole alone^[23] or in combination with ciprofloxacin^[24] is moderately effective in mild moderately active CD, but is insufficiently potent for use as sole therapy in patients ill enough to need hospital admission. Treatment needs to be given for up to 3 months, but may be confounded by nausea, vomiting, an unpleasant taste and/or patients' unwillingness to abstain from alcohol during this time. More seriously, metronidazole taken long-term may cause a peripheral neuropathy not always reversible on its discontinuation. The place of other antibiotics such as clarithromycin, clofazimine and rifabutin has not yet been adequately established in controlled trials. Conventional antituberculous therapy was not beneficial in a controlled trial in CD^[25]. Antibiotics such as amoxycillin, trimethoprim, ciprofloxacin and metronidazole are sometimes useful for the treatment of diarrhoea or steatorrhoea due to bacterial overgrowth in patients with small bowel CD.

Azathioprine and 6-mercaptopurine Patients not

responding to or dependent on corticosteroids who, because of extensive disease or previous resection, need to avoid operative treatment, can be treated with adjunctive oral azathioprine ($2\text{--}2.5\text{ mg}\cdot\text{kg}^{-1}\cdot\text{d}^{-1}$) or 6-mercaptopurine ($1\text{--}1.5\text{ mg}\cdot\text{kg}^{-1}\cdot\text{d}^{-1}$); the dose of steroids is reduced as improvement occurs^[26-28]. Such patients must be well enough to wait for up to four months for this to become apparent. Hopes that intravenous azathioprine could be used to accelerate response in active Crohn's have not been confirmed in a controlled trial^[29]. Up to 20% of patients cannot tolerate azathioprine because of nausea, rash, fever, arthralgia, upper abdominal pain and headache; in a minority of these patients, a switch to 6MP may avert these problems. More seriously, both drugs may cause acute pancreatitis in about 3% of patients, particularly in the first few weeks of treatment. Their other potentially serious side effects, bone marrow depression (which occurs in 2% patients) and cholestatic hepatitis, necessitate blood tests every two weeks for the first two months of therapy: thereafter, white cell count, platelet count and liver function tests should be monitored every 2 months^[30]. Opportunistic infections and a serious form of glandular fever have been reported in patients on azathioprine or 6MP. Although existing data in IBD is reassuring^[31], very long-term use, as in transplant patients, may yet prove to increase the risk of malignancy. Indeed, the risk of skin cancer makes it advisable to recommend to white patients on azathioprine or 6MP that they avoid excessive exposure to sunlight. Homozygous deficiency of 6-thiopurine methyl transferase (6TPMT), the enzyme responsible for the safe metabolic breakdown of azathioprine and 6-MP, occurs in about 0.2% of the population and may contribute to the occasionally serious side-effects of both drugs and its routine assay is not yet available. Allopurinol, by inhibiting xanthine oxidase, reduces metabolism of azathioprine. Patients on this drug should not be given either thiopurine. Usage of azathioprine and 6-mercaptopurine in CD is long term. However, in patients maintained in remission on azathioprine or 6MP, the risk of relapse after four years of treatment appears to be similar whether the drug is continued or stopped^[32]. In view of the potential toxicity of the long-term use of these drugs, their withdrawal should be considered in patients still in remission after four years treatment.

Methotrexate Methotrexate, given weekly as a 25 mg intramuscular injection, improves symptoms and reduces steroid requirements in chronically active steroid-dependent CD^[33], but its potential side effects (bone marrow depression, hepatic fibrosis, pneumonitis, opportunistic infections) restrict its use to the very small number of patients

with difficult CD refractory to safer treatments. Although a lower dose (12.5 mg weekly), given orally, may also prove beneficial in CD^[34], all patients given methotrexate need careful blood monitoring.

Mycophenolate mofetil In an unblinded trial in complicated CD, this newer immunomodulatory drug appeared to act quicker and produce fewer side-effects than azathioprine^[35] and double-blind controlled trials are needed to confirm these results.

Cyclosporin Has not been confirmed as useful in active ileocaecal CD^[38-40].

Anti-TNF-alpha antibody The first specific cytokine-related therapy to reach the bedside in CD is infliximab, a mouse-human chimeric (cA2) antibody to-TNF-alpha^[36-38]; this drug was launched in the USA in 1998 and in Europe in 1999. In patients with CD refractory to steroids and/or conventional immunosuppressive drugs, a single infusion of infliximab produced, at 4 weeks, some improvement in 64% patients, compared with 17% after placebo; remission occurred in 33% patients treated with infliximab but only 4% of those given placebo^[39]. Relapse tends to recur in the ensuing months: repeated infusions every 4 wk-8 wk may produce more lasting remissions^[40]. Infliximab is administered as a single^[40] or, to obtain a more prolonged response, multiple intravenous infusions^[40,41] at 4 wk-8 wk intervals, each given over 2 hours. The dose is $5\text{ mg}\cdot\text{kg}^{-1}$ per infusion, and the cost about £1000 (US \$1600) per infusion. Common minor side-effects include headache, nausea and upper respiratory tract infections. Serious, but not opportunistic, infections including salmonella enterocolitis, pneumonia and cellulitis have been reported. Infusion reactions occur in up to 20% patients, are usually mild and respond to antihistamines: however, adrenaline and corticosteroids should also be available when infusions are given. The development of human antichimeric antibodies (HACA) in up to 15% patients may cause a serum sickness reaction and diminished clinical response to repeated infusions. A lupus syndrome has been associated with anti-double-stranded DNA antibodies and cardiolipin antibodies in rheumatoid patients given infliximab. Rapid healing and fibrosis may precipitate bowel obstruction in patients with small intestinal strictures. Lastly, there are several reports of lymphoma in rheumatoid and Crohn's patients given infliximab, although whether these are due to the drug or the underlying disease is not yet clear. The benefits, or otherwise, of coprescription of azathioprine or 6-mercaptopurine in patients given anti-TNF antibody are not yet established. By analogy with the effects

of methotrexate in infliximab-treated patients with rheumatoid arthritis, conventional immunosuppressive drugs may have a synergistic effect and reduce the incidence of the development of autoantibodies and other adverse effects. It is conceivable, however, that immunosuppressive agents could increase the risk of lymphoma in patients on infliximab^[42]. In the future, selection of patients to be treated with anti-TNF antibody may depend not only on the disease phenotype (eg fistulating disease), but also their genotype. Preliminary evidence suggests that CD patients who are pANCA positive, and have particular TNF microsatellite haplotypes, for instance, show a poor response to infliximab.

Dietary therapy

In patients with a poor response to, or preference for avoiding corticosteroids, in those with extensive small bowel disease, and in children, an alternative primary therapy is a liquid formula diet. This can be either elemental (amino acid-based), protein hydrolysate (peptide-containing) or polymeric (containing whole protein and not therefore hypoallergenic), and is given for 4–6 weeks as the sole nutritional source^[43]. This approach is probably as effective as corticosteroid therapy in the short term, about 60% patients achieving remission. Unfortunately, after the resumption of a normal diet, many patients relapse (50% at six months). Whether this can be prevented by selective and gradual reintroduction of particular foods to which individual patients are not intolerant^[44], or by the intermittent use of further enteral feeding for short periods, remains to be proven. The success of enteral nutrition as a primary therapy for CD is also limited by its cost, the unpleasant taste of some of the available preparations and the need often to give the feed by nasogastric tube or percutaneous gastrostomy. Such therapy does, nevertheless, offer a valuable alternative in the compliant minority of adults for whom it is appropriate.

Surgery

In patients whose ileocaecal disease fails to respond to drug or dietary therapy, particularly if they have short segment (less than 20 cm) rather than extensive disease, surgery is indicated. Indeed, some patients prefer surgery at presentation to the prospect of pharmacological or nutritional treatment of uncertain duration; there is no controlled data to confirm which approach is best. After surgery, there is a 50% chance of recurrent symptoms at 5 years and of further surgery at 10 years.

SPECIFIC TREATMENT OF OTHER PRESENTATIONS OF ACTIVE CROHN'S DISEASE

Obstructive small bowel Crohn's disease In patients presenting with obstructive symptoms and signs,

with appropriate abnormalities on plain abdominal X-ray, the principal difficulty lies in deciding whether stricturing is due to active inflammation, fibrosis with scarring or even adhesions. Sometimes laboratory markers (e.g. raised platelet count, ESR, C-reactive protein) and/or radiolabelled leucocyte scan can help to identify individuals with active inflammatory Crohn's, but in most instances a short trial of intravenous corticosteroids is given in addition to intravenous fluids and, if necessary, nasogastric suction. Parenteral nutrition is required if resumption of an oral diet is not likely in 5–7 d. If the stricture is in the upper jejunum, terminal ileum or colon, enteroscopic or colonoscopic balloon dilatation can be undertaken^[45]; the value of concomitant local injection of triamcinolone around the stricture is as yet unclear. In patients not settling after 48 h–72 h of conservative treatment, surgery is needed, options being local resection or, for short and/or multiple strictures, stricturoplasty. Patients responding to conservative therapy should be advised to take a low residue diet to reduce the chance of recurrent symptoms.

Intra-abdominal abscess Ultra sound, CT scan and/or radiolabelled leucocyte scan are usually used to confirm suspected intra-abdominal abscess in patients with Crohn's. Broad spectrum antibiotics are given and the abscess drained percutaneously under radiological control, and/or surgically. Subsequent treatment is usually of the underlying pathological process, for example, ileocaecal inflammation.

Intestinal fistula The relevant anatomical connections are clarified using contrast radiology, CT, endoluminal ultra sound and/or MRI. Restitution of nutritional well being is required using enteral or parenteral nutrition. Where there is no obstruction distal to the site of intestinal fistulae, medical therapy with oral, rectal or intravenous metronidazole and/or oral azathioprine or 6-mercaptopurine^[26] cause some fistulae to heal. Uncontrolled reports suggest that intravenous cyclosporin may heal fistulous Crohn's, while a controlled trial shows anti-TNF- α antibody (infliximab) infusions to be a promising option^[41]. Most patients with enterocutaneous, vesical or vaginal fistulae, however, require surgical resection of the fistula and local resection of involved intestine and/or other viscera.

Perianal disease Non-suppurative perianal CD may respond to oral metronidazole^[46] and/or ciprofloxacin given for up to three months, and to azathioprine or 6-mercaptopurine in the long term^[26]. Successful healing of >50% perianal (and other) fistulae was reported in 62% patients treated with three intravenous infusions of anti-TNF- α

antibody (infliximab) compared with 26% of those given placebo^[41]. Although in this study it is not clear whether the fistulous tracks, rather than simply their openings on to the skin, healed, and reopening of fistulae was common in the 6 months after treatment was stopped, infliximab may prove a useful advance in therapy. Patients with suppurating perianal CD need surgery, minimised as far as possible and abscesses should be drained and loose (seton) sutures inserted to facilitate the continued drainage of chronic fistulae. Defunctioning ileostomy or colostomy is of uncertain benefit.

Crohn's colitis The treatment of active Crohn's colitis closely resembles that of active UC (Table 1). In contrast to UC, oral metronidazole (400 mg b.d. for up to three months), if tolerated, can be used in patients with only moderately active disease who wish to avoid corticosteroids or aminosalicylates: the response rate is up to 50%^[23]. There is no data to support the use of cyclosporin. Meta-analysis data suggest that Crohn's colitis, like ileocaecal disease, responds to a liquid formula diet^[43]. In patients who require total colectomy, permanent ileostomy is usually preferred to an ileoanal pouch because of the high incidence of pouch breakdown and sepsis in CD. Ileorectal anastomosis is an option in patients with rectal sparing, though recurrence requiring further surgery is far more common than after ileostomy. In rare individuals with refractory segmental colitis, local resections of short diseased segments can be performed. Toxic megacolon is even more rare in acute severe Crohn's than it has become in UC.

Oral and upper gastrointestinal Crohn's disease

Treatment of oral and upper gastrointestinal CD follows the usual principles outlined above. Patients with oral Crohn's are best managed in close conjunction with specialists in oral medicine: controlled trial data are lacking, but options include topical, intral esional and oral steroids as well as oral thiopurines and liquid formula diet. Duodenal Crohn's may respond to omeprazole^[47]; endoscopic balloon dilatation of strictures can be helpful, but surgery other than stricturoplasty may be technically demanding and complicated by fistulation.

MEDICAL TREATMENT OF IBD—THE FUTURE

Improvements in future medical treatments are likely to take several directions. First, conventional therapies, such as steroids and aminosalicylates, are likely to be made available in formulations which focus delivery more accurately on the site of disease and thereby further reduce systemic side effects. More excitingly, the increase in our knowledge of the aetiology and pathogenesis of IBD will inevitably lead to the development of more selectively targeted pharmacological agents, of

which the first to reach clinical application has been anti-TNF-alpha antibody. Gene therapy, for example applied topically to involved gut mucosa, may prove an important step forward in UC and Crohn's as in other chronic inflammatory diseases outside the gut. The choice of treatment in individual patients with IBD will depend not only on the phenotypic expression of their disease, but also on their genotype.

Whatever therapeutic advances are made in the coming years, the management of patients with IBD, whether apparently straightforward or difficult, will continue to depend on close collaboration between physicians, surgeons, specialist nurses, dieticians, radiologists, pathologists and counsellor, and a clinical geneticist may need to join this team. Most importantly, the patient with IBD must be looked upon as a person rather than a case. As treatment becomes more complex, and the options more varied, it is essential that the patient remains at the centre of the decision-making process, and the individual with IBD must be the final arbiter of the type of treatment he or she is to be given.

REFERENCES

- Kornbluth A, Sachar DB. Ulcerative colitis practice guidelines in adults. *Am J Gastroenterol*, 1997;92:204-211
- Hanauer SB, Meyers S. Management of Crohn's disease in adults. *Am J Gastroenterol*, 1997;92:559-566
- Rampton DS. Management of Crohn's disease. *Br Med J*, 1999; 319:1480-1485
- Travis SPL, Farrant JM, Ricketts C. Predicting outcome in severe ulcerative colitis. *Gut*, 1996;38:905-910
- Alemayehu G, Järnerot G. Colonoscopy during an attack of severe ulcerative colitis is a safe procedure and of great value in clinical decision making. *Am J Gastroenterol*, 1991;86:187-190
- Surawicz CM, Haggit RC, Husseman M, McFarland LV. Mucosal biopsy diagnosis of colitis: acute self-limited colitis and idiopathic inflammatory bowel disease. *Gastroenterology*, 1994; 107:755-763
- Thromboembolism Risk Factors (THRIFT) Consensus Group. Risk of and prophylaxis for venous thromboembolism in hospital patients. *Br Med J*, 1992;305:567-57
- Evans RC, Shim Wong V, Morris AI, Rhodes JM. Treatment of corticosteroid-resistant ulcerative colitis with heparin: a report of 16 cases. *Aliment Pharmacol Ther*, 1997;11:1037-1040
- McInerney GT, Sauer WG, Baggenstoss H, Hodgson JR. Fulminating ulcerative colitis with marked colonic dilatation: a clinicopathologic study. *Gastroenterology*, 1962;42:244-257
- Bjarnason I, Hayllar J, MacPherson AJ, Russell AS. Side effects of non steroidal antiinflammatory drugs in small and large intestine in humans. *Gastroenterology*, 1993;104:1832-1847
- Present DH, Wolfson D, Gelernt IM, Rubin PH, Bauer J, Chapman ML. Medical decompression of toxic megacolon by "rolling". *J Clin Gastroenterol*, 1988;10:485-490
- Marion JF, Present DH. The modern medical management of acute severe ulcerative colitis. *Eur J Gastroenterol Hepatol*, 1997; 9:831-835
- Burke DA, Axon ATR, Clayden SA. The efficacy of tobramycin in the treatment of ulcerative colitis. *Aliment Pharmacol Ther*, 1990; 4:123-129
- Lichtiger S, Present DG, Kornbluth A, Gelernt I, Bauer J, Galler G, Michelassi F, Hanauer SB. Cyclosporin in severe ulcerative colitis refractory to steroid therapy. *New Eng J Med*, 1994;330: 1841-1845
- Sandborn WJ. A critical review of cyclosporin therapy in inflammatory bowel disease. *Inflamm Bowel Dis*, 1995;1:48-63
- Kornbluth A, Present DG, Lichtiger S, Hanauer SB. Cyclosporin for severe ulcerative colitis: a user's guide. *Am J Gastroenterol*, 1997;92:1424-1428
- Evans RC, Clarke L, Heath P, Stephens S, Morris AI, Rhodes JM. Treatment of ulcerative colitis with an engineered human anti-TNF-

- alpha antibody CDP571. *Aliment Pharmacol Ther*, 1997;11:1031-1035
- 18 Yacyshyn BR, Bowen-Yacyshyn MB, Jewell L. A placebo-controlled trial of ICAM-1 antisense oligonucleotide in the treatment of Crohn's disease. *Gastroenterology*, 1998;114:1133-1142
 - 19 Sutherland LR, Ramcharan S, Bryant H, Fick G. Effect of cigarette smoking on recurrence of Crohn's disease. *Gastroenterology*, 1990;98:1123-1128
 - 20 Rutgeerts P, Lofberg R, Malchow H, Lamers C, Olaison G, Jewell D, Danielsson A, Goebell H, Thomsen OO, Lorenz-Meyer H, Hodgson H, Persson T, Seidegaard C. A comparison of budesonide with prednisolone for active Crohn's disease. *New Eng J Med*, 1994;331:842-845
 - 21 Singleton JW, Hanauer SB, Gitnick GL, Peppercorn MA, Robinson MG, Wruble LD, Krawitt EL. Mesalamine capsules for the treatment of active Crohn's disease: results of a 16 week trial. *Gastroenterology*, 1993;104:1293-1301
 - 22 Tremaine WJ, Schroeder KW, Harrison JM, Zinsmeister AR. A randomised, double blind, placebo controlled trial of the oral mesalamine (5-ASA) preparation, Asacol, in the treatment of symptomatic Crohn's colitis and ileocolitis. *J Clin Gastroenterol*, 1994;19:278-282
 - 23 Ursing B, Alm T, Barany F. A comparative study of metronidazole and sulphasalazine for active Crohn's disease: the cooperative Crohn's disease study in Sweden. II Result. *Gastroenterology*, 1982;83:550-562
 - 24 Prantera C, Zannoni F, Scribano ML, Berto E, Andreoli A, Kohn A, Luzzi C. An antibiotic regimen for the treatment of active Crohn's disease: a randomized controlled clinical trial of metronidazole plus ciprofloxacin. *Am J Gastroenterol*, 1996;91:328-332
 - 25 Swift GL, Srivastava ED, Stone R, Pullan RD, Newcombe RG, Rhodes J, Wilkinson S, Rhodes P, Roberts G, Lawrie BW, Evans KT, Jenkins PA, Williams GT, Strohmeyer G, Kreuzpaintner G, Thomas GAO, Calcraft B, Davies PS, Morris TJ, Morris J. Controlled trial of anti tuberculous chemotherapy for two years in Crohn's disease. *Gut*, 1994;35:363-368
 - 26 Pearson DC, May GR, Fick GH, Sutherland LR. Azathioprine and 6mercaptopurine in Crohn's disease: a metaanalysis. *Ann Intern Med*, 1995;122:132-142
 - 27 Ewe K, Press AG, Sing CC. Azathioprine combined with prednisone or monotherapy with prednisone in active Crohn's disease. *Gastroenterology*, 1993;105:367-372
 - 28 D'Haens G, Geboes K, Ponette E, Penninckx F, Rutgeerts P. Healing of severe recurrent ileitis with azathioprine therapy in patients with Crohn's disease. *Gastroenterology*, 1997;112:1475-1481
 - 29 Sandborn WJ, Tremaine WJ, Wolf DC. Lack of effect of intravenous administration on time to respond to azathioprine for steroid-treated Crohn's disease. *Gastroenterology*, 1999;117:527-535
 - 30 Connell WR, Kamm MA, Ritchie JK, Lennard-Jones JE. Bone marrow toxicity caused by azathioprine in inflammatory bowel disease: 27 years of experience. *Gut*, 1993;34:1081-1085
 - 31 Connell WR, Kamm MA, Dickson M, Balkwill AM, Ritchie JK, Lennard-Jones JE. Long term neoplasia risk after azathioprine treatment in inflammatory bowel disease. *Lancet*, 1994;343:1249-1252
 - 32 Bouhnik Y, Lémann NM, Mary JY, Scemama G, Tai R, Matuchansky C, Modigliani R, Rambaud JC. Long term follow up of patients with Crohn's disease treated with azathioprine or 6-mercaptopurine. *Lancet*, 1996;347:215-219
 - 33 Feagan BG, Rochon JR, Fedorak RN, Irvine EJ, Wild G, Sutherland L, Steinhart AH, Greenberg GR, Gillies R, Hopkins M, Hanauer SB, McDonald JWD. Methotrexate for the treatment of Crohn's disease. *New Eng J Med*, 1995;332:292-297
 - 34 Oren R, Moshkowitz M, Odes S, Becker S, Keter D, Pomeranz I, Shirin C, Reisfeld I, Broider E, Lavy A, Fich A, Eliakim R, Patz J, Villa Y, Arber N, Gilat T. Methotrexate in chronic active Crohn's disease. *Am J Gastroenterol*, 1997;92:2203-2209
 - 35 Neurath MF, Wanitschke R, Peters M, Krummenauer F, Meyer zum Buschenfelde K-H, Schlaak JF. Randomised trial for mycophenolate mofetil versus azathioprine for treatment of chronic active Crohn's disease. *Gut*, 1999;44:625-628
 - 36 Brynskov J, Freund L, Rasmussen SN, Lauritsen K, Schaffalitzky de Muckadell O, Williams N, MacDonald AS, Tanton R, Molina F, Campanini MC, Bianchi P, Ranzi T, di Palo FQ, Malchow Moller A, Thomsen OO, Tage-Jensen U, Binder V, Riis P. A placebo controlled, double-blind randomised trial of cyclosporin therapy in active Crohn's disease. *New Eng J Med*, 1989;321:845-850
 - 37 Feagan BJ, MacDonald JWD, Rochon JR. Low dose cyclosporin for the treatment of Crohn's disease. *New Eng J Med*, 1994;330:1846-1851
 - 38 Stange EF, Modigliani R, Pena AS, Wood AJ, Feutren G, Smith PR. European trial of cyclosporin in chronic active Crohn's disease. *Gastroenterology*, 1995;109:774-782
 - 39 Targan SR, Hanauer SB, van Deventer SJH, Mayer L, Present DH, Braakman T, DeWoody KL, Schaible TF, Rutgeerts PJ. A short term study of chimeric monoclonal antibody cA2 to tumour necrosis factor alpha for Crohn's disease. *New Eng J Med*, 1997;337:1029-1035
 - 40 Rutgeerts P, D'Haens G, Targan S, Vasilasak E, Hanauer SB, Present DH, Mayer L, van Hogeand RA, Braakman T, DeWoody KL, Schaible TF, van Deventer SJH. Efficacy and safety of retreatment with anti tumour necrosis factor antibody (infliximab) to maintain remission in Crohn's disease. *Gastroenterology*, 1999;117:761-769
 - 41 Present DH, Rutgeerts P, Targan S, Hanauer SB, Mayer L, van Hogeand RA, Podolsky DK, Sands BE, Braakman T, DeWoody KL, Schaible TF, van Deventer SJH. Infliximab for the treatment of fistulas in Crohn's disease. *New Eng J Med*, 1999;340:1398-1405
 - 42 Bickston SJ, Lichstenstein GR, Arseneau KO, Cohen RB, Cominelli F. The relationship between infliximab treatment and lymphoma in Crohn's disease. *Gastroenterology*, 1999;117:1433-1437
 - 43 Griffiths AM, Ohlsson A, Sherman PM, Sutherland LR. Meta-analysis of enteral nutrition as a primary therapy of active Crohn's disease. *Gastroenterology*, 1995;108:1056-1067
 - 44 Riordan AM, Hunter JO, Cowan RE. Treatment of active Crohn's disease by exclusion diet: East Anglian Multicentre Controlled Trial. *Lancet*, 1993;342:1131-1134
 - 45 Couckuyt H, Gevers AM, Coremans G, Hiele M, Rutgeerts P. Efficacy and safety of hydrostatic balloon dilatation of ileocolonic Crohn's strictures: a prospective longterm analysis. *Gut*, 1995;36:577-580
 - 46 Bernstein LH, Frank MS, Brandt LJ, Boley SJ. Healing of perineal Crohn's disease with metronidazole. *Gastroenterology*, 1980;79:357-365
 - 47 Dickinson JB. Is omeprazole helpful in inflammatory bowel disease. *J Clin Gastroenterol*, 1994;8:317-319

Treatment of *Helicobacter pylori* infection: analysis of Chinese clinical trials

Yu Yuan Li and Wei Hong Sha

Subject headings *Helicobacter* infection/therapy; clinical trials; evaluating studies, *Helicobacter pylori*

Li YY, Sha WH. Treatment of *Helicobacter pylori* infection: analysis of Chinese clinical trials. *World J Gastroentero*, 2000;6(3):324-325

INTRODUCTION

Eradication of *Helicobacter pylori* (*Hp*) infection is generally not easy. Various clinical regimens have been recommended in the literature. With the experience from the other countries and the practice in China, Chinese doctors have tried many regimens. In this study, we collected and pooled the data from Chinese literature to evaluate the effect of different regimens in Chinese patients infected with *Hp*.

MATERIALS AND METHODS

Papers published from 1990 to 1997 were reviewed. The papers were cited from the index "Chinese Literature of Science and Technology, (Medicine)", Published by the Medical Information Institute of China, Beijing, and from the Chinese bio medical disks (CBMDISC). Papers were selected according to the following criteria: ① the papers must be published in full text; ② data must be from original studies from author's own unit; ③ *Hp* status must be determined using histology, microbiology and urea breath test; and ④ the studies should be appropriately designed and reported. If several papers were published from the same data source, the one with the best data was included.

RESULTS

Monotherapy Monotherapy has been fully proved to be not effective in *Hp* eradication, with a eradication rate between 10%-45%.

Dual therapy Proton pump inhibitor (PPI) dual therapy was introduced from western countries to China, whereas furazolidone was developed in China. The data are shown in Tables 1,2.

Triple therapy PPI and bismuth triplies were main regimens recommended. Furazolidone was fully practiced in China. Their results are shown in Tables 3-5.

Department of Gastroenterology, First Municipal People's Hospital of Guangzhou 510180, Guangdong Province, China

Correspondence to: Prof. Yu Yuan Li, Head of Department of Gastroenterology, First Municipal People's Hospital of Guangzhou, 602 Ren Min Bei Road, Guangzhou 510180, Guangdong Province, China

Received 2000-01-23 **Accepted** 2000-03-19

Quadruple therapy Only two studies were available using 1 week course of bismuth, PPI and two antibiotics. The eradication rates were 91% and 93%, and the occurrence rate of side effect being 33%^[19,20].

Table 1 PPI dual therapy

Authors	Ome	Amo	Eradication(%)	Healing(%)	Side effect
Zhou YH ^[11]	20 bid×14	500 qid×14	30/33 (91)	31/33 (94)	12%
Zhou YH ^[11]	20 qd×14	500 qid×14	31/35 (89)	32/35 (91)	
Nie YQ ^[2]	20 bid×14	500 qid×14	10/13 (77)	12/13 (92)	15%
Li YY ^[3]	20 bid×14	500 qid×14	8/11 (73)	9/11 (82)	
Hu FL ^[4]	20 bid×14	750 bid×14	13/22 (59)	18/22 (82)	
Zhou Y ^[5]	20 bid×14	750 qid×14	30/36 (83)	36/36 (100)	2.7%

Ome: omeprazole Amo: amoxycillin

Table 2 Furazolidone dual therapy

Authors	Furazolidone	Antibiotics	Eradication(%)	Side effect
Xiao SD ^[6]	100 qid×14	CBS 120 qid×14	66/90 (73)	
Mao PJ ^[7]	100 tid×28	Ran 150 bid×28	10/17 (59)	8.9%
Mao PJ ^[7]	100 tid×28	Ome 20 qd×28	15/18 (83)	
Li YN ^[8]	200 tid×7	CBS 110 qid×28	34/34 (100)	
Li YN ^[8]	100 qid×7			
Li YN ^[8]	100 tid×14	CBS 110 qid×28	21/23 (91)	
Li YN ^[8]	50 tid×14	CBS 110 qid×28	13/21 (62)	
Xi BG ^[9]	200 tid×14	CBS 110 qid×28	24/24 (100)	

CBS: bismuth Ran: ranitidine Ome: omeprazole

Table 3 Triple therapy with Furazolidone

Authors	Fu	Antibiotics	Antibiotics	Eradication(%)	Side effect
Liu WZ ^[10]	200 bid×7	CBS 240 bid×7	Cla 500 bid×7	12/12(100)	57%
Liu WZ ^[10]	100 bid×7	CBS 240 bid×7	Cla 250 bid×7	25/27(93)	7.4%
Huang YS ^[11]	100 tid×5	Met 400 tid×5	Genta 40 tid×5	25/26(96)	
Xiao SD ^[6]	100 qid×10	CBS 120 qid×10	Met 200 qid×10	74/75(78)	
Chen JP ^[12]	100 qid×28	CBS 120 qid×28	Tetra 250 qid×28	35/54(65)	

Cla: clarithromycin Genta: gentamycin Tetra: tetracyclin

Table 4 Hp eradication with CBS triple therapy

Authors	CBS	Amo	Met	Eradication(%)	Side effect
Jia BQ ^[13]	120 qid×14	250 qid×14	200 qid×14	328/440(87)	7.8%
Jia BQ ^[13]	240 bid×14	500 bid×14	400 bid×14	139/156(89)	7.8%
Chen SP ^[14]	240 bid×14	1000 bid×14	400 bid×14	33/46(71)	
Li QN ^[15]	240 bid×14	500 bid×14	400 bid×14	13/16(81)	37.5%
Geng Z ^[16]	110 qid×14	500 qid×14	200 qid×14	64/76(84)	
Zhou LY ^[17]	120 qid×14	250 qid×14	200 qid×14	56/73(77)	
Li YY ^[18]	120 qid×14	250 qid×14	200 qid×14	20/25(80)	28%

Table 5 PPI triple therapy

Authors	PPI	Antibiotics	Cla	Eradication(%)	Side effect
Chen SP ^[14]	Ome 20 bid×7	Amo 1000 bid×7	500 bid×7	43/48(90)	21.1%
Chen SP ^[14]	Ome 20 bid×14	Amo 1000 bid×14	500 bid×14	45/47(96)	
Liu WZ ^[10]	Lan 30 bid×7	Fu 200 bid×7	500 bid×7	11/12(92)	10%
Liu WZ ^[10]	Lan 30 qd×7	Fu 100 bid×7	250 bid×7	27/30(90)	
Li QN ^[15]	Lan 30 bid×7	Met 400 bid×7	250 bid×7	14/16(86)	18.8%
Li QN ^[15]	Lan 30 bid×7	Met 400 bid×7	500 bid×7	15/16(94)	25%

DISCUSSION

Eradication of *Hp* is considered to be confirmed when the tests of *Hp* continue to be negative for at least 4 weeks after the discontinuation of treatment^[21]. Great efforts have been made to establish regimens with good efficacy and safety. It is recognized in western countries that a good regimen should reach the eradication rate of intention to treat (ITT) > 80% and per protocol (PP) > 90%^[22]. In most Chinese papers only the rate of PP was available, therefore used in this review. In consideration of high resistant rates to antibiotic and the high prevalence of *Hp* in the country, a regimen with a PP eradication rate > 85% should be accepted in our practice. With this standard we found that both PPI triple therapy and bismuth triple therapy with a two-week course were good for Chinese patients. The former had high adverse events and the latter was more expensive. In most treatment, the dosage of antibiotics was cut down in order to reduce the side effects. It was shown that the low-dose triple therapies could yield high eradication rates in Chinese patients because they had lower body weight. The limited data with one-week quadruple therapy showed that it could be a good alternative especially for the patients who failed to other regimens. Monotherapy and dual therapy were not suitable in practice because of their poor efficacy. These findings agree with the data from western literatures^[23].

The presence of resistant *Hp* strains is a severe problem in China and influences the efficacy of treatments. The resistant rates to metronidazole were reported to be between 28%-80%, and clarithromycin, <5%. However, there has been no reported resistance to bismuth, amoxycillin, furazolidone and tetracycline. These antibiotics should be used to replace metronidazole if the resistance exists. Some studies recommended furazolidone, which was less expensive, with low resistance but more adverse events.

Recently the consensus reports from European, American and Asia Pacific areas recommended the following regimens^[22,24,25]: ① PPI (ome 20 mg or lan 30 mg) + Cla 500 mg + Amo 1000mg; ② PPI + Cla 250/500 mg + Met 400 mg; ③ RBC/Bis + Cla 500 mg + Met 400 mg/Amo; and ④ PPI + Bis + Met + Tetra.

All were used twice daily for the one-week course. These regimens had a good efficacy in western countries, but have not been extensively examined in China. RBC is still unavailable in China. The preliminary results from our group showed that Lan30 + Cla500 + Met400 regimen reached a 93% eradication rate, but Lan30 + Cla250 + Met400 only 77%^[26]. More studies are needed before their establishment in this country.

REFERENCES

- 1 Zhou YH, Wu XL. Control study of different doses of omeprazole and a moxycillin on eradication of *Helicobacter pylori*. *Xiandai Xiaohuabing Zhengdu an Yu Zhiliao*, 1995; 6:202-204
- 2 Nie YQ, Li YY, Wu HS. Eradication of *Helicobacter pylori* and duodenal ulcer recurrence. *Zhonghua Xiaohua Neijing Zazhi*, 1997; 14:351-353
- 3 Li YY, Wu HS, Nie YQ, Zhou SF. Effect of losec and amoxycillin on treatment of duodenal ulcer and eradication of *Helicobacter pylori*. *Guangzhou Yiyao*, 1995; 26:24-26
- 4 Hu FL, Huang ZL, Wang JM, Jia BQ, Liu XG, Xie PY. Eradication of *Hp* and its effect on the cure and recurrence of duodenal ulcer. *Zhonghua Xiaohua Zazhi*, 1996; 16:106-108
- 5 Zhou Y, Yu JP. Study of relationship between *Helicobacter pylori* and bleeding in peptic ulcer diseases. *Weichangbingxue He Ganbingxue Zazhi*, 1997; 6: 162-165
- 6 Xiao SD, Liu WZ, Lin GJ. Multi-center study of *Hp* eradication using colloidal bismuth subcitrate combinative therapy. *Zhonghua Xiaohua Zazhi*, 1995; 15(Suppl):16-18
- 7 Mao PJ, Guo YM. Effect of omeprazole on peptic ulcer bleeding and *Helicobacter pylori* eradication. *Shanghai Yixue*, 1996; 19: 359-360
- 8 Li YN, Xia ZW, Xi BG, Ye SM, Yang XS. Effect of colloidal bismuth subcitrate combined with furazolidone on *Helicobacter pylori* associated gastritis. *Zhonghua Xiaohua Zazhi*, 1995; 15: 203-205
- 9 Xi BG, Li YN, Ye SM. Effect of furazolidone and colloid bismuth on *Hp* infection. *Zhonghua Neike Zazhi*, 1995; 34: 118-119
- 10 Liu WZ, Lu BL, Xiao SD, Xu WW, Shi Y, Zhang DZ. Clarithromycin in combined short-term triple therapy for eradication of *Helicobacter pylori* infection. *Zhonghua Neike Zazhi*, 1996; 35: 803-805
- 11 Huang CS, Yang YS. Clinical observation of five-day antibiotic therapy to reduce the recurrence of duodenal ulcer. *Zhonghua Xiaohua Zazhi*, 1995; 15: 117-119
- 12 Chen JP, Xu CP. Effect of *Helicobacter pylori* infection and post-eradication of the organism on serum gastrin. *Linchuang Xiaohuabing Zazhi*, 1996; 8: 153-155
- 13 Liu XG, Jia BQ. *Helicobacter pylori* eradication with low dose amoxycillin-metronidazole-colloidal bismuth subcitrate triple therapy: a nation-wide cooperative clinical study in China. *Zhonghua Xiaohua Zazhi*, 1996; 16: 192-194
- 14 Chen SP, Chen ZQ, Bei L, Wen SH. Omeprazole, clarithromycin and amoxycillin therapy for *Helicobacter pylori* infection. *Zhonghua Neike Zazhi*, 1996; 35: 799-800
- 15 Li QL, Li YY, Wu HS, Sha WH. Lansoprazole in the treatment of *Hp* positive duodenal ulcer. *Xin Xiaohuabingxue Zazhi*, 1997; 5: 808-809
- 16 Gen Z, Zhang ZA, Zhen XZ. Significance of *Helicobacter pylori* eradication to the cure of functional dyspepsia. *Zhongyuan Yikan*, 1997; 24: 17-18
- 17 Zhou LY, Lin SR, Yu ZL. Multi-center clinical study of peptic colloid bismuth triple therapy on *Helicobacter pylori* eradication. *Linchuang Xiaohuabing Zazhi*, 1997; 3: 6-7
- 18 Li YY, Wu HS, Nie YQ, Li QL. Effect of low dose triple therapy on peptic ulcer and *Helicobacter pylori* eradication. *Xin Yixue*, 1996; 27: 245-246
- 19 Fan BH. Effect of *Helicobacter pylori* eradication on peptic ulcer recurrence. *Nantong Yixueyuan Xuebao*, 1996; 16: 568-569
- 20 Li YY. Control of *Helicobacter pylori* positive duodenal peptic colloid bismuth triple and quadruple therapy. *Xinyixue*, 1998; 29: 293-295
- 21 Price A. The Sydney system: histologic division. *Am J Gastroenterol*, 1991; 86: 209-222
- 22 Chiba N. Analysis of antibiotic therapy on *Hp* eradication. *Am J Gastroenterol*, 1992; 87: 1716-1719
- 23 The European *Helicobacter pylori* study group: current European concepts in the management of *Helicobacter pylori* infection. The Maastricht Consensus Report. *Gut*, 1997; 41: 8-13
- 24 Howden CW. For what condition is there evidence-based justification for treatment of *H. pylori* infection. *Gastroenterology*, 1997; 113(Suppl): 5107-5112
- 25 Lam SK, Talley NJ. *Helicobacter pylori* consensus: report of the 1997 Asia Pacific Consensus Conference on the management of *Helicobacter pylori* infection. *J Gastroenterol Hepatol*, 1998; 13: 1-12
- 26 Hu PJ, Li YY, Chen WH, Cui Y, Nie YQ. Effect of clarithromycin, metronidazole and lansoprazole on the treatment of *Hp* infection. *Zhonghua Xiaohua Zazhi*, 1997; 17: 204-206

Protective effects of prostaglandin E1 on hepatocytes

Xian Ling Liu and Dai Ming Fan

Subject headings prostaglandin E1; hepatitis; liver injury; hepatic; cytoprotective effects; lipid microspheres

Liu XL, Fan DM. Protective effects of prostaglandin E1 on hepatocytes. *World J Gastroenterol*, 2000;6(3):326-329

INTRODUCTION

Numerous studies have demonstrated the protective action of prostaglandin E1 (PGE1) on experimental animal models of liver injury and on patients with fulminant viral hepatitis. It could act on PGE1 receptor of the diseased vessels to dilate them and increase portal venous flow, improve the microcirculation of the liver, clear the metabolites of the liver cells, and increase oxygen supply to the liver tissues. PGE1 could also accumulate at the inflammatory portion, inhibit the release of lethal factors, stabilize the membrane of liver cells and lysosome, inhibit the active oxygen, and promote the proliferation of the liver cells. It is now used to treat fulminant hepatic failure.

PROTECTIVE ACTION OF PGE1 ON EXPERIMENTAL ANIMAL MODELS OF LIVER INJURY

The protective action of PGE1 has been shown on both experimental animal models of liver injury and patients with fulminant viral hepatitis. Beck *et al*^[1] examined the effects of long-term PGE treatment on liver and stomach in cirrhotic rats. Cirrhosis was induced by bile duct ligation. Sham-operation was performed as controls. Half of the rats received a PGE1 analogue, misoprostol (PGE1) (10 µg orally, daily) on d 1-d 29 postoperation, and the others received placebo only. Liver chemistry, portal pressures, and levels of prostaglandin E2, leukotriene B4, myeloperoxidase, and collagen in hepatic and gastric tissue of all rats on d 31 were determined. PGE1-treated cirrhotic rats had less hepatosplenomegaly, lower serum alanine aminotransferase levels, and portal pressures and higher arterial pressure than placebo-treated

cirrhotic rats. Hepatic and gastric leukotriene B4, myeloperoxidase and collagen levels were significantly lower in the PGE1-treated compared with placebo-treated cirrhotic rats. Placebo-treated cirrhotic rats had greater spontaneous and ethanol-induced gastric damage and failed to show gastric hyperemic response to ethanol, whereas PGE1-pretreated rats did. PGE1 did not significantly affect sham-operated rats. Beck suggested that long-term PGE1 administration was cytoprotective for both the liver and gastric mucosa in cirrhotic rats.

An animal model of hepatocytic necrosis was established by Gu^[2] with injection of D-galactosamine into peritoneal cavity. Examination at regular intervals after injection of PGE showed that the level of increased serum TB, ALT and GST and the degree of histological changes in the liver were less marked in PGE-treated animals ($n = 34$) than those in PGE-untreated animals ($n = 29$), suggesting that PGE has definite protective effect on experimental hepatocytic necrosis.

The effects of PGE1.CD on dimethylnitrosamine (DMN)-induced acute liver damage with intravascular coagulation in rats were biochemically and histopathologically investigated by Suzuki^[3]. PGE1.CD was administered i.v. 30 min before and 24 h after DMN-intoxication (pretreatment) and 30 min or 4 h to 24 h after DMN-intoxication (post-treatment). Pretreatment with PGE1.CD ($0.2-2 \mu\text{g}\cdot\text{kg}^{-1}\cdot\text{min}^{-1}$) dose-dependently suppressed the decrease of platelet counts and the elevation of blood biochemical parameters (PT, HPT, GOT, GPT, LDH, LAP, T-Bil) caused by DMN-intoxication. PGE1.CD ($0.5 \mu\text{g}\cdot\text{kg}^{-1}\cdot\text{min}^{-1}$ or over) significantly suppressed the DMN-induced histopathological changes (occurrence of hemorrhage and necrosis). Post-treatment with PGE1.CD ($2 \mu\text{g}\cdot\text{kg}^{-1}\cdot\text{min}^{-1}$) also suppressed the liver damage. Furthermore, pretreatment with PGE1.CD ($2 \mu\text{g}\cdot\text{kg}^{-1}\cdot\text{min}^{-1}$) not only suppressed the disruption of hepatocytes, but also prevented the damages of sinusoidal endothelial cells and lysosomal membrane, and it reduced the increase of lipid peroxidation. PGE1.CD ($1 \mu\text{g}\cdot\text{kg}^{-1}\cdot\text{min}^{-1}$ or over) significantly suppressed the decrease of hepatic tissue blood flow caused by DMN-intoxication. These results demonstrate that PGE1.CD has therapeutic efficacy against DMN-induced acute liver damage in rats, therefore, it will be clinically useful for the treatment of severe hepatitis such as fulminant hepatitis with intravascular coagulation in the sinusoid.

Institute of Digestive Disease, Xijing Hospital, Fourth Military Medical University, Xi'an 710032, Shaanxi Province, China

Dr. Xian Ling Liu, received Ph.D degree in 1998 from the Fourth Military Medical University. Attending physician in the department of gastroenterology, major in liver cirrhosis and gastric cancer, having 17 papers published.

Correspondence to: Dai Ming Fan, MD. Institute of Digestive Disease, Xijing Hospital, Fourth Military Medical University, 15 Western Changle Road, Xi'an 710032, Shaanxi Province, China
Tel. 0086-29-3375226, Fax. 0086-29-2539041
Email. isabelliu412@yahoo.com

Received 2000-02-07 **Accepted** 2000-03-29

PGE1 AND SEVERE HEPATITIS

The effect of PG on patients with fulminant and subfulminant viral hepatitis (FHF) was studied by Sinclair^[4]. Seventeen patients presented with FHF secondary to hepatitis A ($n = 3$), hepatitis B ($n = 6$), and non-A, non-B (NANB) hepatitis ($n = 8$). Fourteen of the 17 patients had stage III or IV hepatic encephalopathy (HE). The mean aspartate transaminase (AST) was $1844 \text{ U/L} \pm 1246 \text{ U/L}$, bilirubin $232 \text{ } \mu\text{mol/L} \pm 135 \text{ } \mu\text{mol/L}$, prothrombin time (PT) $34 \text{ s} \pm 18 \text{ s}$, partial thromboplastin time (PTT) $73 \text{ s} \pm 26 \text{ s}$, and coagulation Factors V and VII $8\% \pm 4\%$ and $9\% \pm 5\%$, respectively. Intravenous PGE1 was initiated 24 h-48 h later after a rise in AST ($2195 \text{ U/L} \pm 1810 \text{ U/L}$), bilirubin ($341 \text{ } \mu\text{mol/L} \pm 148 \text{ } \mu\text{mol/L}$), PT ($36 \text{ s} \pm 15 \text{ s}$), and PTT ($75 \text{ s} \pm 18 \text{ s}$). Twelve of 17 responded rapidly with a decrease in AST from $1540 \text{ U/L} \pm 833 \text{ U/L}$ to $188 \text{ U/L} \pm 324 \text{ U/L}$. Improvement in hepatic synthetic function was indicated by a decrease in PT from $27 \text{ s} \pm 7 \text{ s}$ to $12 \text{ s} \pm 1 \text{ s}$ and PTT from $61 \text{ s} \pm 10 \text{ s}$ to $31 \text{ s} \pm 2 \text{ s}$, and an increase in Factor V from $9\% \pm 4\%$ to $69\% \pm 18\%$ and Factor VII from $11\% \pm 5\%$ to $71\% \pm 20\%$. Five responders with NANB hepatitis relapsed upon discontinuation of therapy, with recurrence of HE and increases in AST and PT, and improvement was observed upon retreatment. After 4 wk of intravenous therapy oral PGE2 was substituted. Two patients with NANB hepatitis recovered completely and remained in remission 6 mos and 12 mos after cessation of therapy. Two additional patients maintained in remission after 2 mos and 6 mos of PGE2. No relapses were seen in the patients with hepatitis A virus and hepatitis B virus infection. Liver biopsies in all 12 surviving patients restored to normal. In the five non-responders an improvement in hepatic function was indicated by a fall in AST ($3767 \text{ U/L} \pm 2611 \text{ U/L}$ to $2142 \text{ U/L} \pm 2040 \text{ U/L}$), PT ($52 \text{ s} \pm 25 \text{ s}$ to $33 \text{ s} \pm 18 \text{ s}$), and PTT ($103 \text{ s} \pm 29 \text{ s}$ to $77 \text{ s} \pm 44 \text{ s}$), but all deteriorated and died of cerebral edema ($n = 3$) or liver transplantation ($n = 2$). These results suggest that PGE has beneficial effect on FHF.

According to the severity, hepatic failure was divided into early stage, typical symptom stage and late stage. A treatment group of 55 cases received PGE1 therapy and a control group received basic support therapy only. The results showed that difference of the total effective rate was not significant between these two groups, but in the early stage of hepatic failure, the effective rate in the treatment group was markedly higher than that in the control group. In addition, incidence of hepato-renal syndrome was lower in the treatment group^[2]. This study indicates that division of severe viral hepatitis into three stages for evaluation of therapeutic effect is rational and useful and early use of PGE1 may certainly show some efficacy.

While orthotopic liver transplantation (OLT) has become the treatment of choice for most

irreversible end-stage liver diseases, its role in patients with hepatitis B (HBV) infection is controversial. A high risk of reinfection of the transplanted graft, associated with significant morbidity and mortality, has been reported. Although passive and active immunization can delay the reappearance of virus in the allograft, there is not yet an effective therapy for recurrent HBV infection in liver transplant recipients. Twenty-eight OLT in 25 patients with acute and chronic HBV infections were performed^[5]. Twelve of the patients were HBV DNA-negative, six were HBV DNA-positive, and seven were not tested prior to transplantation. Only 19 patients surviving more than 100 days after transplantation were considered to have sufficient duration of follow-up (mean 734 days) to include in the analysis of recurrence. Five (26%) were free of recurrent disease at the time of last follow-up (mean 1031 days). Recurrent HBV in the allograft, as defined by positive immunoperoxidase stains of biopsy sections for viral antigens, was detected in 74% at a mean of 134 d posttransplantation. Histological changes of viral hepatitis were evident in 13 of 14 with positive immunostaining. Twelve of the 14 patients were treated, on an open trial basis, with intravenous and oral prostaglandin E (PGE) because of deteriorating clinical condition. Eleven of the twelve responded to PGE with an initial drop in serum transaminases, improvement in coagulopathy and resolution of encephalopathy. One patient failed to respond and died of myocardial infarction within 9 d of institution of therapy. Three of the eleven patients with an initial response relapsed and died of liver failure as a direct result of recurrent HBV after 13 d, 16 d and 37 d of treatment in association with generalized sepsis. Eight of the 12 patients (67%) had a sustained favorable response to PGE therapy (mean follow-up 737 days). All patients with a sustained response had accompanying improvement in histology and reduction in viral antigen staining in hepatocytes. Treatment with PGE appeared to be of benefit in recurrent HBV infection of the transplanted liver with an initial response rate of 92% and a sustained response rate of 67%.

The efficacy of PGE1 was demonstrated in the treatment of another 4 patients with subfulminant hepatitis of viral hepatitis B^[6]. Three patients suffered from hepatic encephalopathy of the first degree, and the remaining one of the second degree. In three patients the clinical and biochemical improvement came relatively quickly, followed by recovery. In one patient, due to drug intolerance, the treatment was discontinued on the third day. The recurrence of illness was noted with the moderate increase of serum aminotransferase activities without clinical deterioration, necessitating no further use of prostaglandin E1.

Bojic suggested that prostaglandin E1, applied in the treatment of patients with subfulminant form of hepatitis, has favorable effect on the course of illness.

In a rare case of severe acute hepatitis A complicated by pure red cell aplasia (PRCA), plasma exchange transfusion and glucagon-insulin (GI) therapy improved the consciousness, but bilirubin, transaminase levels, and IgM anti-HAV titer remained high. Intravenous administration of lipophilized PGE1 (lipo-PGE1) was added to the GI therapy. Bilirubin and transaminase levels were normalized in the wk 8 after the initiation of this combination therapy (17 wk after admission). The combined use of lipo-PGE1 with plasma exchange and GI therapy appeared to be useful for the severe hepatitis in this patient^[7].

Two patients with HIV infection developed acute hepatitis B with liver insufficiency and hepatic encephalopathy. After alprostadil infusion was begun, they improved quickly and got a full recovery^[8].

MECHANISMS OF HEPATIC CYTOPROTECTION OF PGE1

Indocyanine green disappearance enhanced by PGE1

Indocyanine green (ICG) is a reliable indicator reflecting hepatocyte function and hepatic blood flow. PGE1 has been indicated to increase hepatic blood flow and protect the hepatocyte. Tsukada^[9] found that PGE1 administration increased ICG-K in the liver cirrhosis (LC) and chronic hepatitis (CH) groups with normal liver function, and the ICG-K response was dose dependent when the dosage of PGE1 ranged from $0.01 \mu\text{g}\cdot\text{kg}^{-1}\cdot\text{min}^{-1}$ to $0.05 \mu\text{g}\cdot\text{kg}^{-1}\cdot\text{min}^{-1}$.

Inhibitory effects of PGE1 on T-cell mediated cytotoxicity

The effects of PGE1 on cell-mediated cytotoxicity against hepatocytes were investigated using *in vitro* cytotoxic assay system by Ogawa^[10]. Isolated liver cells from normal C57BL/6 mice were used as the target cells, and effector cells were obtained from spleens of C57BL/6 mice in which experimental hepatitis had been induced by immunization with syngeneic liver antigens. In this assay system, spleen T cells adhering to nylon wool demonstrated a high cytotoxic activity against target liver cells. The cytotoxicity was markedly reduced by PGE1 at concentrations greater than 10^{-7}mol/L . Maximum suppressive activity was obtained when PGE1 was continuously present during the assay period. By contrast, indomethacin, a specific inhibitor of prostaglandin synthesis, enhanced the cytotoxic activity of effector cells. These data seem to indicate that exogenously added PGE1 has an inhibitory effect on cell-mediated cytotoxicity of effector spleen cells against target hepatocytes.

PGE1 enhance DNA synthesis of injured liver after partial hepatectomy by stimulating cyclic AMP production and increasing ATP level in hepatic tissue

D-galactosamine (D-gal) damaged rats were infused with PGE1 through peripheral vein for 40 min. before and after partial hepatectomy. DNA synthesis following 68% partial hepatectomy was severely inhibited by the pretreatment of D-galactosamine. PGE1 infusion ($0.5 \mu\text{g}\cdot\text{kg}^{-1}\cdot\text{min}^{-1}$, $1.0 \mu\text{g}\cdot\text{kg}^{-1}\cdot\text{min}^{-1}$) enhanced the DNA synthesis inhibited by D-gal 600 mg/kg significantly ($P < 0.01$). After 20 min of PGE1 infusion cyclic AMP levels of liver tissue was increased as compared with saline infusion in D-gal (600 mg/kg) damaged rat ($P < 0.05$). Twenty min and 3 h after partial hepatectomy, ATP levels of liver tissue was enhanced in PGE1 treated group ($P < 0.05$). These results suggest that PGE1 enhances DNA synthesis of injured liver after partial hepatectomy by the mechanism of stimulating cyclic AMP production and increasing ATP level in hepatic tissue^[11].

PGE1 could accelerate the recovery of mitochondrial respiratory function after reperfusion, stabilization of membrane microviscosity

PGE1 has been indicated to increase hepatic blood flow and protect the hepatocyte. Kurokawa *et al*^[12] found that PGE1 could accelerate the recovery of mitochondrial respiratory function after reperfusion. When PGE1 was continuously administered to rats from 24 h before giving a dose of carbon tetrachloride, deranged serum glutamic pyruvic transaminase levels and prothrombin time were significantly reduced 12 h after intoxication compared with controls. A similar effect of PGE1 was seen at 24 h in D-galactosamine-intoxicated rats. Liver histology showed a comparable attenuation of injury in these rats. These results were consistent with reported effects of PGE2, suggesting that both prostaglandins may share a common pathway in protection against liver injury. When PGE1 or 16,16'-dimethyl PGE2 was added to the medium of primary cultured rat hepatocytes, lipid peroxidation-dependent killing of the cells by tert-butyl hydroperoxide was significantly attenuated without affecting the extent of malondialdehyde accumulation compared with controls. Both prostaglandins significantly reduced the extent of increased plasma membrane microviscosity of these cells. Masaki *et al*^[13] concluded that PGE1 and PGE2 may possess cytoprotective effects on liver parenchymal cells through stabilization of membrane microviscosity, which may contribute to protection against liver injury.

While the mechanisms of prostaglandin on protecting liver injury are not well understood, it has been demonstrated that dimethyl PGE2

abrogates the induction of tumour necrosis factor, leukotriene B4 (LTB4) and procoagulant activity by macrophages as well as attenuating the expression of major histocompatibility class antigens on the surface of hepatocytes, and may inhibit viral replication. From the present research, we came to a conclusion that increasing hepatic blood flow, accelerating the recovery of mitochondrial respiratory function after reperfusion, stabilizing the membrane microviscosity, decreasing the cell-mediated cytotoxicity against hepatocytes, enhancing DNA synthesis by stimulating cyclic AMP production and increasing ATP level in hepatic tissue made PGE1 as a hepatic cytoprotective agent.

TOXIC EFFECTS OF INTRAVENOUS AND ORAL PGE THERAPY ON PATIENTS WITH LIVER DISEASE

Prostaglandins are cytoprotective agents that have been shown to benefit patients with a variety of acute and chronic liver diseases. Few data exist on the frequency of adverse effects of prostaglandins in these patients. Catral *et al.*^[14] retrospectively studied 105 patients with liver disease who were treated with either i.v. or oral PGE. Forty-four patients with primary nonfunction after liver transplantation and 36 patients with fulminant hepatic failure received i.v. PGE1 for 4.5 d \pm 2.6 d and 12.6 d \pm 10.9 d, respectively. Twenty-five patients with recurrent hepatitis B viral infection after liver transplantation received oral PGE1 for 105 d \pm 94 d or PGE2 for 464 d \pm 399 d. Twenty-six of 80 patients (33%) receiving i.v. PGE1 developed gastrointestinal and/or cardiovascular side effects and 8% developed arthritis. Twenty-three (92%) of 25 patients who received high-dose oral PGE1 or PGE2 incurred arthritis and/or gastrointestinal adverse effects. Twenty-five patients received prolonged PGE therapy (oral >60d; i.v. >28d). Of this group, 23 (92%) developed clubbing and cortical hyperostosis resembling hypertrophic osteoarthropathy. All adverse effects were dose related and resolved with reduction or cessation of therapy. PGE therapy resulted in a wide spectrum of multisystem adverse effects which were reversible with reduction or cessation of therapy. Although the administration of PGE was safe and generally well tolerated, close medical supervision is necessary to avoid serious side effects.

RECENT ADVANCES IN LIPID MICROSPHERE TECHNOLOGY FOR TARGETING PROSTAGLANDIN DELIVERY

Although PGE1 exhibits pharmacological activities in free form, it has been hypothesized and experimentally verified that carrier can target them more effectively at lower doses, thus causing fewer

side effects. Lipid microspheres (LM) with a diameter of 0.2 μ m are drug carriers prepared from soybean oil and lecithin, and the drug is incorporated within the LM. Lipo-PGE1 is LM preparations of PGE1 that are designed to accumulate at the vascular lesions. The newly developed lipo-PGE1 (lipo-AS013) could overcome the disadvantages of the preparation currently available^[15]. Lipo-AS013, a precursor of PGE1, is considered superior to free PGE1 in terms of its chemical stability and the retention ratio in LM in the body.

REFERENCE

- 1 Beck PL, McKnight GW, Kelly JK, Wallace JL, Lee SS. Hepatic and gastric cytoprotective effects of long term prostaglandin E1 administration in cirrhotic rats. *Gastroenterology*, 1993;105:1483-1489
- 2 Gu CH, Cao R, Wang GX, Li MT, Liu SY. Protective effect of prostaglandin E on hepatocytes and its value of early treatment of severe viral hepatitis. *Zhonghua Neike Zazhi*, 1991;30:17-20
- 3 Suzuki A, Hagino M, Yasuda N, Sagawa K, Terawaki T, Ogawa M, Kondo K, Hamanaka N, Tanaka M, Aze Y. Inhibitory effects of prostaglandin E1.alpha.-cyclodextrin (PGE1.CD) on dimethylnitrosamine-induced acute liver damage in rats. *Nippon Yakurigaku Zasshi*, 1995;105:221-229
- 4 Sinclair SB, Greig PD, Blendis LM, Abecassis M, Roberts EA, Phillips MJ, Cameron R, Levy GA. Biochemical and clinical response of fulminant viral hepatitis to administration of prostaglandin E. A preliminary report. *J Clin Invest*, 1989;84:1063-1069
- 5 Flowers M, Sherker A, Sinclair SB, Greig PD, Cameron R, Phillips MJ, Blendis L, Chung SW, Levy GA. Prostaglandin E in the treatment of recurrent hepatitis B infection after orthotopic liver transplantation. *Transplantation*, 1994;58:183-192
- 6 Bojic I, Begovic V, Mijuskovic P. Treatment of patients with subfulminant forms of viral hepatitis B using prostaglandin E1. *Vojnosanit Pregl*, 1995;52:471-475
- 7 Tomida S, Matsuzaki Y, Nishi M, Ikegami T, Chiba T, Abei M, Tanaka N, Osuga T, Sato Y, Abe T. Severe acute hepatitis A associated with acute pure red cell aplasia. *J Gastroenterol*, 1996;31:612-617
- 8 Reus S, Priego M, Boix V, Torrens D, Portilla J. Can alprostadil improve liver failure in HIV infected patients with severe acute viral hepatitis. *J Infect*, 1998;37:84-86
- 9 Tsukada K, Sakaguchi T, Aono T, Ishizuka D, Fujita N, Hatakeyama K. Indocyanine green disappearance enhanced by prostaglandin E1 in patients with hepatic resection. *J Surg Res*, 1996;66:64-68
- 10 Ogawa M, Mori T, Mori Y, Ueda S, Yoshida H, Kato I, Iesato K, Wakashin Y, Wakashin M, Okuda K. Inhibitory effects of prostaglandin E1 on T-cell mediated cytotoxicity against isolated mouse liver cells. *Gastroenterology*, 1988;94:1024-1030
- 11 Shimura T, Miyazaki M, Koshikawa H, Takahashi O, Sugawara H, Fujimoto S, Okui K. Cyclic AMP and ATP-mediated stimulation of DNA synthesis following partial hepatectomy by prostaglandin-E1 in D-galactosamine injured liver. *Nippon Geka Gakkai Zasshi*, 1985;86:1618-1624
- 12 Kurokawa T, Nonami T, Harada A, Nakao A, Sugiyama S, Ozawa T, Takagi H. Effects of prostaglandin E1 on the recovery of ischemia-induced liver mitochondrial dysfunction in rats with cirrhosis. *Scand J Gastroenterol*, 1991;26:269-274
- 13 Masaki N, Ohta Y, Shirataki H, Ogata I, Hayashi S, Yamada S, Hirata K, Nagoshi S, Mochida S, Tomiya T, Ohno A, Ohta Y, Fujiwara K. Hepatocyte membrane stabilization by prostaglandins E1 and E2: favorable effects on rat liver injury. *Gastroenterology*, 1992;102:572-576
- 14 Catral MS, Altraif I, Greig PD, Blendis L, Levy GA. Toxic effects of intravenous and oral prostaglandin E therapy in patients with liver disease. *Am J Med*, 1994;97:369-373
- 15 Mizushima Y, Hoshi K. Review: recent advances in lipid microsphere technology for targeting prostaglandin delivery. *J Drug Target*, 1993;1:93-100

Original Articles

Zonula occludin toxin, a microtubule binding protein

Wen Le Wang, Rui Liang Lu, MariaRosaria DiPierro and Alessio Fasano

Subject headings microtubules; microtubule proteins; microtubule-associated proteins; intercellular junctions; vibrio cholerae; cholera toxin; zonula occluding toxin

Wang WL, Lu RL, DiPierro M, Fasano A. Zonula occludin toxin, a microtubule binding protein. *World J Gastroentero*, 2000;6(3):330-334

Abstract

AIM To investigate the interaction of Zot with microtubule.

METHODS Zot affinity column was applied to purify Zot-binding protein(s) from crude intestinal cell lysates. After incubation at room temperature, the column was washed and the proteins bound to the Zot affinity column were eluted by step gradient with NaCl ($0.3 \text{ mol} \cdot \text{L}^{-1}$ – $0.5 \text{ mol} \cdot \text{L}^{-1}$). The fractions were subjected to 6.0%–15.0% (w/v) gradient SDS-PAGE and then transferred to PVDF membrane for N-terminal sequencing. Purified Zot and tau protein were blotted by using anti-Zot or anti-tau antibodies. Finally, purified Zot was tested in an *in vitro* tubulin binding assay.

RESULTS Fractions from Zot affinity column yielded two protein bands with a M_r of 60kU and 45kU respectively. The N-terminal sequence of the 60kU band resulted identical to β -tubulin. Zot also cross-reacts with anti-tau antibodies. In the *in vitro* tubulin binding assay, Zot co-precipitate with Mt, further suggesting that Zot possesses tubulin-binding properties.

CONCLUSION Taken together, these results suggest that Zot regulates the permeability of intestinal tight junctions by binding to intracellular Mt, with the subsequent activation of the intracellular signaling leading to the permeabilization of intercellular tight junctions.

Center for Vaccine Development Division of Gastroenterology, University of Baltimore at Maryland, Baltimore, MD 21201, USA

Wen Le Wang obtained his medical degree from Norman Bethune University of Medical Sciences in 1987 and M.S. in Biochemistry at West China University of Medical Sciences in 1993. He had worked in medical university and institute for three years in China. He is currently a Ph.D. candidate in the Program of Biochemistry and Molecular Biology at University of Maryland, Baltimore. He has 8 papers published.

Correspondence to: Alessio Fasano, Division of Pediatric GI & Nutrition, Center for Vaccine Development University of Maryland School of Medicine, 685 W. Baltimore Street, Rm 480, Baltimore, MD 21201, USA

Tel. 001-410-706-7376, Fax. 001-410-706-6205

Email. afasano@umaryland.edu

Received 2000-03-04 Accepted 2000-04-25

INTRODUCTION

Vibrio cholerae, the human intestinal pathogen responsible for the diarrhoeal disease cholera, elaborates a large number of extracellular proteins, including several virulence factors. The severe dehydrating diarrhoea characteristic of cholera is induced by cholera toxin (CT). A number of epidemiological studies^[1-4] have shown a concurrent occurrence of the CT genes (ctx-A and ctx-B) and the genes for two other virulence factors elaborated by *V. cholerae*, zonula occludens toxin (Zot)^[5] and accessory cholera toxin (Ace)^[6]. Zot increases the intestinal permeability by rearranging the intestinal cell cytoskeleton strategically located to modulate intercellular tight junctions^[7]. However, the first step of Zot signaling after the protein internalization remains to be established.

Microtubules (MT) are intracellular structures functionally and anatomically related to the cell cytoskeleton. MTs are composed of α -tubulin and β -tubulin. Factors known to regulate microtubule dynamic include microtubule-associated proteins (MAPs). Neuronal MAPs, the most abundant of which are MAP2 and tau, stimulate MT assembly^[8,9]. The best characterized function of MT network polymers is the bi-directional movement of membrane vesicles driven by the MT-based motor proteins, kinesin and cytoplasmic dynein. Different cargoes can be transported via MT-dependent vesicles, including various types of endocytic and exocytic vesicles^[10,11]. Connection of actin filament network has been found^[12]. In eukaryotic organisms, various cell functions, including cell shape and mobility require coordinational interaction between actin and MT cytoskeleton^[13].

In our study, we found that when cell lysates from mammalian tissues passed through a Zot affinity column, two proteins bound to Zot, the N-terminal sequence of one of these two proteins revealed that it corresponded to tubulin; Zot cross-reacted with antibody against Tau, another well described MAP isolated from mammalian brain; by using a microtubule binding assay, Zot was found co-precipitated with MT. Taken together, these results suggest that Zot is a new member of MAPs family. This Zot property may be involved in the Zot signaling leading to the regulation of intercellular TJ.

MATERIAL AND METHODS

Purification of 6-his Zot

Plasmid pSU111, containing the clone Zot gene in a pQE-30 vector with a 6-histidine tag at its N-terminal, was grown in LB medium with 20 g/L glucose, 25 $\mu\text{g/L}$ kanamycin and 200 $\mu\text{g/L}$ ampicillin at 37°C with vigorous mixing until the A_{600} reached 0.7–0.9. Cultures were then induced with 2 $\text{mmol}\cdot\text{L}^{-1}$ isopropylthio- β -D-galactoside (IPTG, Fisher), followed by an additional 2 h culture period at 37°C with vigorous shaking. The cells were harvested by centrifugation at 4 000 $\times g$ for 20 min and resuspended in buffer A (6 $\text{mol}\cdot\text{L}^{-1}$ Guanidine-HCl, 0.1 $\text{mol}\cdot\text{L}^{-1}$ Na-phosphate, 0.01 $\text{mol}\cdot\text{L}^{-1}$ Tris-HCl, pH 8.0; 5 mL/g wet cell weight). After stirring for 1 h at room temperature, the mixture was centrifuged at 10 000 $\times g$ for 30 min at 4°C. A 50% slurry of Superflow (QIAGEN, 1 mL/g wet cell) was added to the supernatant and stirred for 1 h at room temperature. The mixture was loaded onto a 5 cm \times 1.5 cm column and washed sequentially with buffer A, buffer B (8 $\text{mol}\cdot\text{L}^{-1}$ urea, 0.1 $\text{mol}\cdot\text{L}^{-1}$ Na-phosphate, 0.01 $\text{mol}\cdot\text{L}^{-1}$ Tris-HCl, pH 8.0) and buffer C (8 $\text{mol}\cdot\text{L}^{-1}$ urea, 0.1 $\text{mol}\cdot\text{L}^{-1}$ Na-phosphate, 0.01 $\text{mol}\cdot\text{L}^{-1}$ Tris-HCl, pH 6.3). Each wash step was continued until the A_{280} of the flow-through was less than 0.01. His-Zot was eluted by addition of 250 $\text{mmol}\cdot\text{L}^{-1}$ imidazole (1,3-diaza-2,4-cyclopentadiene) to buffer C. After dialysis against urea, the eluate was diluted 200–500 times in PBS, stirred with 50% slurry Superflow (1 mL/g wet cell weight) for 2 h at room temperature, loaded onto another 5 cm \times 1.5 cm column, washed with phosphate-buffered saline (PBS) and eluted with 250 $\text{mmol}\cdot\text{L}^{-1}$ imidazole in PBS. Purity of the His-Zot protein was established by sodium dodecyl sulfate-polyacrylamide gel electrophoresis (SDS-PAGE) analysis and Western blot using polyclonal anti-Zot antibodies.

Analytical procedures

SDS-PAGE It was carried out on a 50 $\text{g}\cdot\text{L}^{-1}$ –150 $\text{g}\cdot\text{L}^{-1}$ gradient gel, stained with Coomassie brilliant blue dye, destained by 75 $\text{mL}\cdot\text{L}^{-1}$ acetic acid with 100 $\text{mL}\cdot\text{L}^{-1}$ methanol and dried with Gel Drying Film (Promega).

Western blot analysis Following SDS-PAGE, proteins were transferred onto polyvinylidene difluoride (PVDF) membrane (MILLIPORE). Non-specific binding sites were blocked by PBS with 50 $\text{mL}\cdot\text{L}^{-1}$ milk plus 1 $\text{g}\cdot\text{L}^{-1}$ Tween-20. Primary and secondary antibodies were rabbit polyclonal anti-Zot antibody and anti-rabbit IgG (peroxidase conjugate, Sigma), respectively. Films were exposed with ECL detection reagent (Amersham) for 1 min, and developed by Konica SRX-101 developer.

Immobilization of his-Zot to AminoLink plus column

One mg of his-Zot in 4 mL coupling buffer (0.1 $\text{mol}\cdot\text{L}^{-1}$ sodium phosphate, 0.15 $\text{mol}\cdot\text{L}^{-1}$ NaCl, pH 7.2) and 40 μL of 5 $\text{mol}\cdot\text{L}^{-1}$ sodium cyanoborohydride, were added to an equilibrated AminoLink plus column (Pierce) and gently mixed overnight at 4°C. After washing with coupling buffer, 4 mL of 1 $\text{mol}\cdot\text{L}^{-1}$ Tris-HCl (pH 7.4) and 40 μL of 5 $\text{mol}\cdot\text{L}^{-1}$ sodium cyanoborohydride were added to the column followed by gently mixing for 30 minutes at room temperature to block the remaining active sites. The column was washed with 1 $\text{mol}\cdot\text{L}^{-1}$ NaCl and stored in PBS containing 0.5 $\text{g}\cdot\text{L}^{-1}$ sodium azide.

Preparation of human tissue plasma membranes

Adult human brain tissues were obtained from the Brain and Tissue Banks for Developmental Disorders at the University of Maryland and used under the approval of the University's Institutional Review Board. Adult human heart and intestinal tissues were utilized for comparative analysis. Tissues were washed with buffer D (20 $\text{mmol}\cdot\text{L}^{-1}$ Tris-HCl, 20 $\text{mmol}\cdot\text{L}^{-1}$ EDTA, 250 $\text{mmol}\cdot\text{L}^{-1}$ sucrose, pH 7.5), homogenized in buffer E (buffer D containing 5 $\text{mg}\cdot\text{L}^{-1}$ leupeptin, 2 $\text{mg}\cdot\text{L}^{-1}$ aprotinin, 1 $\text{mg}\cdot\text{L}^{-1}$ pepstatin, 10 $\text{mg}\cdot\text{L}^{-1}$ phenylmethylsulfonyl fluoride (PMSF), and centrifuged at 5 000 $\times g$, 4°C for 10 min. Supernatants were centrifuged at 12 000 $\times g$, 4°C for 45 min. Precipitates were discarded and supernatants were centrifuged at 30 000 $\times g$, 4°C for an additional 90 min. Precipitates were dissolved in buffer E with 5 $\text{g}\cdot\text{L}^{-1}$ 3[(3-cholamidopropyl) dimethylammonio]-1-propanesulfonate (CHAPS), sitting on ice for 60 min with gentle mixing every five minutes.

Affinity purification of his-Zot binding proteins

Membrane preparations obtained from human brain were loaded on an AminoLink plus -Zot affinity column, washed, and equilibrated with PBS at room temperature containing 1 $\text{g}\cdot\text{L}^{-1}$ Triton X-100. The columns were incubated for 90 min at room temperature, washed with 8 volumes of PBS containing 1 $\text{g}\cdot\text{L}^{-1}$ Triton X-100, and eluted with PBS containing 1 $\text{g}\cdot\text{L}^{-1}$ Triton X-100 with 0.1 $\text{mol}\cdot\text{L}^{-1}$ NaCl, 0.3 $\text{mol}\cdot\text{L}^{-1}$ NaCl, 0.5 $\text{mol}\cdot\text{L}^{-1}$ NaCl, 0.8 $\text{mol}\cdot\text{L}^{-1}$ NaCl and 1.0 $\text{mol}\cdot\text{L}^{-1}$ NaCl, respectively. Fractions were collected and subjected to SDS-PAGE. N-terminal amino acid sequence analysis.

N-terminal amino acid sequence analysis

The fractions of human tissue lysates containing Zot binding proteins were resolved by 50 $\text{g}\cdot\text{L}^{-1}$

150 g·L⁻¹ gradient SDS-PAGE and transferred onto PVDF membranes using CAPS buffer [10mmol·L⁻¹ 3-(cyclohexylamino)-1 propanesulfonic acid and 100 mL·L⁻¹ methanol]. The protein bands were excised and subjected to N-terminal sequencing using a Perkin-Elmer Applied Biosystems Apparatus Model 494.

Microtubule binding assay

Spin-Down assay kit (Cytoskeleton) was used in the experiments according to the *manufacturer's* recommendations. MT (20 nmol·L⁻¹ final concentration) were obtained by mixing an aliquate of tubulin (20 µL, 5 g/L) and 2 µL, 200 mmol·L⁻¹ taxol in G-PEM buffer (80mmol·L⁻¹ Pipes pH 6.8, 1mmol·L⁻¹ MgCl₂, 1mmol·L⁻¹ EGTA and 1mmol·L⁻¹ GTP). One µg of Zot was incubated with 20 nmol·L⁻¹ microtubule at room temperature for 20 min, while MT-associated protein MAP2 and bovine serum albumin (BSA) were used as positive and negative control, respectively. Proteins attached to MT and unbound proteins were separated by centrifugation. Each reaction product was carefully placed on the top of a cushion (G-PEM buffer plus 400 g·L⁻¹ glycerol) in Ultraclear TM ultracentrifuge tube. Following centrifugation, supernants and pellets were carefully removed and supernants were mixed with 1/20th volum of 500 g·L⁻¹ TCA solution for precipitation protein using centrifuge. Both supernants and pellets of the preparations containing the tested proteins were analyzed by either SDS-PAGE (MAP2 and BSA) or western blotting (Zot).

RESULTS

Isolation of Zot binding proteins from human brain

His-Zot was successfully immobilized to AminoLink Plus gel with immobilization yields of 89%-95%, as established by the protein assay (Bio-Rad detergent-compatible protein assay). Plasma membrane preparations from human brain loaded on the Zot affinity column contained two major Zot-binding proteins with apparent molecular masses of approximately 45kU and 55kU, respectively (Figure 1, lane 2).

N-terminal sequencing of the Zot binding proteins from human brain

The N-terminal sequences of the two Zot/zonulin binding proteins are shown in Table 1. The two proteins were also compared to other protein sequences by Blast search analysis. The N-terminal sequence of the 55kU protein was 100% identical to the N-terminal sequence of tubulin (Table 1) whereas the -45kU protein band resulted 72% identical to the N-terminus of calprotectin, a

calcium binding protein associated to chronic inflammatory processes^[14] and the cystic fibrosis antigen (CFA)^[15]. This second protein resulted to be the Zot/zonulin brain receptor^[16].

Western immunoblotting experiments

To investigate whether Zot and tau (a well characterized MAP) are immunologically related, cross immunoscreening experiments were performed. As shown in Figure 2, both proteins were recognized by either anti-Zot antibodies (left panel) or anti-tau antibodies (right panel). These results suggest that Zot and tau are immunologically related.

Microtubule binding assay

To confirm that Zot possesses MT binding properties, an *in vitro* binding assay was performed. As shown in Figure 3, we observed that Zot co-precipitated with MT as shown by Western immunoblotting analysis, while no Zot was found unbound. BSA lacking MT-binding properties was present only in the supernant. MAP2, a well defined MT associated protein, co-precipitated with MT and was not present in the supernant. These results confirmed the Zot ability to bind to MT.

Table 1 N-terminal amino acid sequences of Zot binding protein (55kU), β -tubulin, Zot binding protein (45kU), calprotectin (MRP-8), and cystic fibrosis antigen

Sample	N-terminus	Identity(%)
Zot binding protein-55kU	MREIVHIQAGQAGNQIGAKF	100
β -tubulin	MREIVHIQAGQAGNQIGAKF	
Zot binding protein-45kU	LTELEKALNXGGGVGHKY	77
Calprotectin (MRP-8)	LTELEKALNSIIDVYHKY	
Cystic fibrosis antigen	LTELEKALNSIIDVYHKY	77

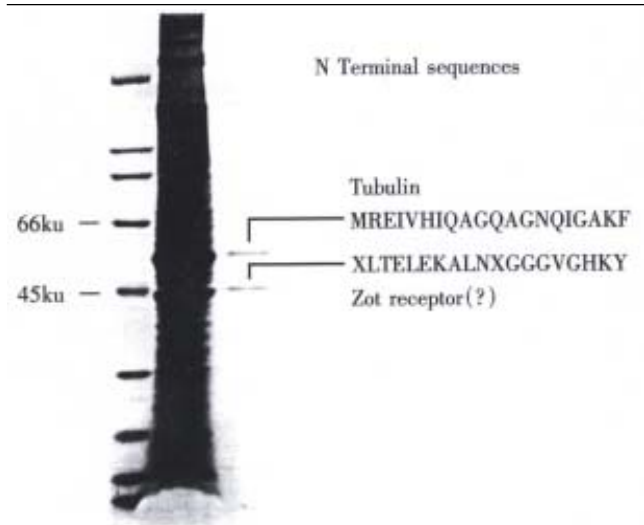


Figure 1 SDS-PAGE of Zot binding proteins isolated by affinity column chromatography from human brain cortex plasma membrane preparations. Lane 1, molecular mass standards; Lane 2, whole-plasma membrane lysate; lane 3, eluate with 0.5 mol·L⁻¹ NaCl in PBS containing 1 g·L⁻¹ Triton X-100.

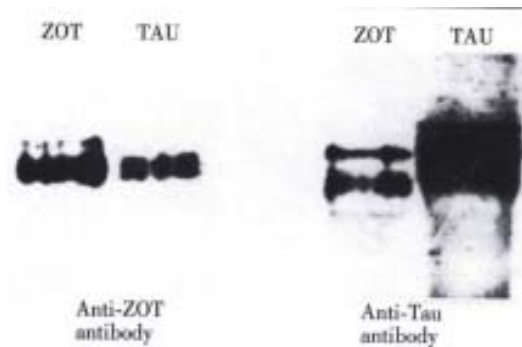


Figure 2 Western immunoblotting of Zot and tau using either anti-Zot antibodies (left panel) or anti-tau antibodies (right panel). Zot and tau were recognized by both antibodies.

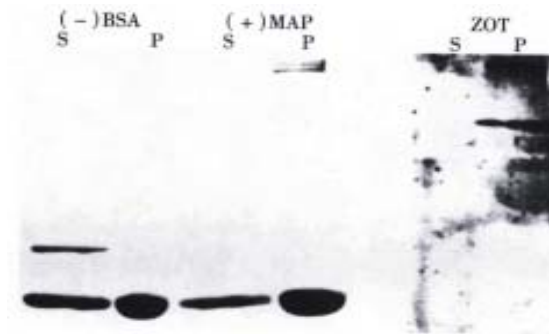


Figure 3 Microtubule binding assay. BSA (negative control) and MAP2 (positive control) were visualized by Coomassie staining (left panel) while Zot was visualized by immunoblotting (right panel). The bottom protein bands in the left panel are tubulins. As anticipated, BSA remained in the supernatant (S), while MAP2 was entirely precipitated in the pellet (P). Zot also appeared confined in the pellet, confirming that it bound to MT.

DISCUSSION

Tj is the hallmark of absorptive and secretory epithelia. As a barrier between apical and basolateral compartments, the tj selectively controls the paracellular passage of water, solutes and immune cells between epithelial and endothelial cells. Variations in transepithelial conductance can usually be attributed to changes in the permeability of the paracellular pathway, since the resistances of eukaryotic cells plasma membrane are relatively high^[17]. Tj represent the major barrier in this paracellular pathway and the electrical resistance of epithelial and endothelial tissues seems to depend on the number of transmembrane protein strands and their complexity as observed by freeze-fracture electron microscopy^[18]. It has become abundantly clear that, in the presence of Ca^{2+} , assembly of the tj is the result of cellular interactions that trigger a complex cascade of biochemical events that ultimately lead to the formation and modulation of an organized network of tj elements, the composition of which has been only partially characterized^[19].

Identification and characterization of Zot, a toxin produced by *Vibrio cholerae*, has provided

new information on the regulation of intercellular tj^[5,7,20-22]. After binding to its surface receptor, Zot is internalized^[23], and subsequently triggers a series of intracellular events including phospholipase C and PKC α -dependent actin polymerization which leads to the opening of tj^[7]. However, the complete cascade of the intracellular events activated by Zot, particularly concerning the early steps, remains undefined. There is now a large body of evidence that protein phosphorylation plays a major role in tj development^[24] and cytoskeleton rearrangement^[25]. In eukaryotic cells, junctional complex proteins, actin filaments, microtubules, and intermediate filaments interact to form the cytoskeleton network involved in determination of cell architecture, intracellular transport, modulation of surface receptors, paracellular permeability, mitosis, cell motility, and differentiation^[26]. We have previously demonstrated that there are two Zot binding proteins in the cell lysates of Zot-sensitive tissues^[16]. One has been characterized as the Zot/zonulin receptor. With this paper we showed that tubulin is the second Zot-binding protein. Based on these results, it is possible to hypothesize that Zot affects the actin filament network by binding to MT. The association of Zot to MT could be responsible of the effects of Zot on cell uptake and intracellular trafficking of molecules^[10,11] as well as the changes of tj structure and permeability. Alterations of intestinal tj occur in a variety of clinical conditions affecting the gastrointestinal system, including food allergies, malabsorption syndromes, and inflammatory bowel diseases. The knowledge that can eventually be acquired by studying the regulation of tj may have a tremendous impact on our understanding of the pathogenesis of these disease. It would not be surprising if the modification of tj structure and function by these pathological conditions would be an extension of normal physiologic regulation of tj.

However, several questions remain unanswered: what is the role of Zot-MT interaction on rearrangement of actin filament? Does this interaction affect the permeability of tj? Are MT-dependent cell functions, such as redistribution of organelles and the polarized distribution of membrane proteins, influenced by the MT-Zot binding? Experiments aimed at addressing these questions are presently in progress in our laboratory.

REFERENCES

- Colombo MM, Mastrandrea S, Santona A, de Andrade AP, Uzzau S, Rubino S, Cappuccinelli P. Distribution of the ace, zot, and ctxA Foxin genes in clinical and environmental *Vibrio cholerae* [letter]. *J Infect Dis*, 1994;170:750-751
- Johnson JA, Morris Jr JG, Kaper JB. Gene encoding zonula occludens toxin (zot) does not occur independently from cholera enterotoxin genes (ctx) in *Vibrio cholerae*. *J Clin Microbiol*, 1993; 31:732-733
- Karasawa T, Mihara T, Kurazono H, Nair GB, Garg S, Ramamurthy T, Takeda Y. Distribution of the zot (zonula occludens toxin) gene among strains of *Vibrio cholerae* O1 and non-O1. *FEMS Microbiol*

- Lett, 1993;106:143-145
- 4 Kurazono H, Pal A, Bag PK, Nair GB, Karasawa T, Mihara T, Takeda Y. Distribution of genes encoding cholera toxin, zonula occludens toxin, accessory cholera toxin, and El Tor hemolysin in *Vibrio cholerae* of diverse origins. *Microb Pathog*, 1995;18:231-235
 - 5 Fasano A, Baudry B, Pumplin DW, Wasserman SS, Tall BD, Ketley JM, Kaper JB. *Vibrio cholerae* produces a second enterotoxin, which affects intestinal tight junctions. *Proc Natl Acad Sci USA*, 1991;88:5242-5246
 - 6 Trucksis M, Galen JE, Michalski J, Fasano A, Kaper JB. Accessory cholera enterotoxin (Ace), the third toxin of a *Vibrio cholerae* virulence cassette. *Proc Natl Acad Sci USA*, 1993;90:5267-5271
 - 7 Fasano A, Fiorentini C, Donelli G, Uzzau S, Kaper JB, Margaretten K, Ding X, Guandalini S, Comstock L, Goldblum S. Zonula occludens toxin modulates tight junctions through protein kinase C-dependent actin reorganization, *in vitro*. *J Clin Invest*, 1995;96:710-720
 - 8 Murphy DB, Johnson KA, Borisy GG. Role of tubulin-associated proteins in microtubule nucleation and elongation. *J Mol Biol*, 1977;117:33-52
 - 9 Sloboda RD, Dentler WL, Rosenbaum JL. Microtubule-associated proteins and the stimulation of tubulin assembly *in vitro*. *Biochemistry*, 1976;15:4497-4505
 - 10 Goodson HV, Valetti C, Kreis TE. Motors and membrane traffic. *Curr Opin Cell Biol*, 1997;9:18-28
 - 11 Cole NB, Lippincott-Schwartz J. Organization of organelles and membrane traffic by microtubules. *Curr Opin Cell Biol*, 1995;7:55-64
 - 12 Fuchs E, Yang Y. Crossroads on cytoskeletal highways. *Cell*, 1999; 98:547-550
 - 13 Danowski BA. Fibroblast contractility and actin organization are stimulated by microtubule inhibitors. *J Cell Sci*, 1989;93(Pt 2): 255-266
 - 14 Odink K, Cerletti N, Bruggen J, Clerc RG, Tarcsay L, Zwadlo G, Gerhards G, Schlegel R, Sorg C. Two calcium-binding proteins in infiltrate macrophages of rheumatoid arthritis. *Nature*, 1987;330:80-82
 - 15 Dorin JR, Novak M, Hill RE, Brock DJ, Secher DS, van Heyningen V, Dorin JR. A clue to the basic defect in cystic fibrosis from cloning the CF antigen gene. *Nature*, 1987;326:614-617
 - 16 Lu R, Wang W, Uzzau S, Vigorito R, Zielke HR, Fasano A. Affinity purification and partial characterization of the zonulin/ zonula occludens toxin (Zot) receptor from human brain [in Process Citation]. *J Neurochem*, 2000;74:320-326
 - 17 Diamond JM. Twenty-first Bowditch lecture. The epithelial junction: bridge gate, and fence. *Physiologist*, 1977;20:10-18
 - 18 Madara JL. Loosening tight junctions. Lessons from the intestine. *J Clin Invest*, 1989;83:1089-1094
 - 19 Denker BM, Nigam SK. Molecular structure and assembly of the tight junction. *Am J Physiol*, 1998;274(1 Pt 2):F1-9
 - 20 Baudry B, Fasano A, Ketley J, Kaper JB. Cloning of a gene (zot) encoding a new toxin produced by *Vibrio cholerae*. *Infect Immun*, 1992;60:428-434
 - 21 Fasano A, Uzzau S. Modulation of intestinal tight junctions by Zonula occludens toxin permits enteral administration of insulin and other macromolecules in an animal model. *J Clin Invest*, 1997; 99:1158-1164
 - 22 Fasano A, Uzzau S, Fiore C, Margaretten K. The enterotoxic effect of zonula occludens toxin on rabbit small intestine involves the paracellular pathway. *Gastroenterology*, 1997;112:839-846
 - 23 Fasano A. Modulation of intestinal permeability: an innovative method of oral drug delivery for the treatment of inherited and acquired human diseases. *Mol Genet Metab*, 1998;64:12-18
 - 24 Madara JL. Maintenance of the macromolecular barrier at cell extrusion sites in intestinal epithelium: physiological rearrangement of tight junctions. *J Membr Biol*, 1990;116:177-184
 - 25 Tang DG, Timar J, Grossi IM, Renaud C, Kimler VA, Diglio CA, Taylor JD, Honn KV. The lipoxigenase metabolite, 12(S)- HETE, induces a protein kinase C-dependent cytoskeletal rearrangement and retraction of microvascular endothelial cells. *Exp Cell Res*, 1993;207:361-375
 - 26 MacRae TH. Towards an understanding of microtubule function and cell organization: an overview. *Biochem Cell Biol*, 1992;70: 835-841

Edited by Pan BR
proofread by Ma JY

Anticipation phenomenon in familial adenomatous polyposis: an analysis of its origin

Takeo Iwama¹ and Joji Utsunomiya²

Subject headings familial adenomatous apolyposis (FAP); anticipation phenomenon; intergenerational bias; child generations; hereditary disorder; mortality

Iwama T, Utsunomiya J. Anticipation phenomenon in familial adenomatous polyposis: an analysis of its origin. *World J Gastroentero*, 2000;6(3):335-338

Abstract

AIM To analyze the origin of the anticipation phenomenon, which means earlier death in successive generation in familial adenomatous polyposis.

METHODS The study subjects were 2161 patients with familial adenomatous polyposis and their 7465 first-degree relatives who were members of 750 families registered at our Polyposis Registry. The ages at death and cumulative mortality rates in the parent, the proband, and the child generations were compared for both all subjects and the patients alone.

RESULTS In the patients over 5 years of age, the mean age at death was 50.9 years for the parent, 42.3 years for the proband, and 33.3 years for the child generations, respectively ($P < 0.001$). The deceased rates in the three generations were 90.7%, 51.3% and 23.1% of the patients, respectively, and this difference was the main cause of the anticipation measured by parent-child pairing method. The cumulative mortality rates for all subjects failed to show anticipation, however the cumulative mortality rates for the patients showed the anticipation. The anticipation phenomenon was shown by any parent-child pairing methods for the deceased patients. Other important causes of the anticipation were different proportion of causes of death between generations ($P < 0.001$), and a low proportion of detected or deceased patients

($P < 0.001$) in the child generation.

CONCLUSION Anticipation in familial adenomatous polyposis may be caused by parent-child pairing methods as well as several intergenerational biases.

INTRODUCTION

The earlier onset of a hereditary disorder in successive generations, often with increased severity or early death, is known as anticipation [1,2]. Despite the development of medical care over generations, this phenomenon is commonly encountered in human dominant type hereditary disorders including familial adenomatous polyposis (FAP) clinically. The anticipation was evaluated by Penrose [1] in myotonic dystrophy and by Veale [2] in FAP using parent-child pairs. They attributed the apparent anticipation to ascertainment biases and the general variability in age of onset in the parent-child pairs. They assumed that the modifying allelic gene might be the cause of the lack of the parent-child correlation. Of these two conditions, the cause of the anticipation in myotonic dystrophy was proved to expand trinucleotide repeats in the causative gene [3-9].

However, a mutation of the APC gene is stable, and the site of mutation determines the severity or associated features of FAP with strong parent-child correlation [10-13]. If the anticipation is the biological phenomenon in FAP, not only we need to investigate the cause of the anticipation in the APC gene, but also it has a considerable clinical meaning because colorectal cancer must be prevented by an early detection and treatment. Consequently, it has aroused our interest to study whether the anticipation phenomenon in FAP is a biological fact.

MATERIALS AND METHODS

Between January 1975 and December 1995, data were collected from 750 families from 1198 FAP patients registered at our Polyposis Registry [14]. These FAP cases fulfilled the diagnostic criteria by Bussey [15]. Turcot syndrome was excluded. Histories of their family members were obtained from their doctors who registered patients, death

¹Department of Surgery, Kyoundo Hospital, Sasaki Institute Kanda-Surugadai 1-8, Chiyoda-Ku, Tokyo 101-0062, Japan

²Institute for Advanced Medical Sciences, Hyogo Medical College Mukogawa 1-1, Nisinomiya, Hyogo 663-8131, Japan

Correspondence to: Takeo Iwama, Department of Surgery, Kyoundo Hospital Kanda-Surugadai 1-8, Chiyoda-Ku, Tokyo 101-0062, Japan
Tel. 0081-3-3292-2051, Fax. 0081-3-3292-3376
Email. iwamata@msn.com

Received 2000-04-03 Accepted 2000-04-28

certificates and the National Family Registry^[16]. All first-degree relatives of proved FAP patients were recruited and no selection was made in these collections. Among the families of 9626 members (4991 men, and 4635 women), 2161 were FAP patients with colorectal cancer, and 7465 were their first-degree family members. Their births and deaths were certified by the National Family Registry or from the documents of the registry, and causes of death were ascertained by death certificates or by inquiring the doctors. The 9626 members were divided into three generations. They were 2958 individuals in the generation of the index patients (the proband generation), 4273 in the generation of their parents (the parent generation), and 2395 in the child generation of the indicated patients (the child generation). The ages at death, causes of death, and cumulative mortality rates of the three generations were compared to evaluate the features of anticipation. The cumulative mortality rates were calculated for both the entire group and the FAP patients by the Kaplan-Meier method. Chi-square test was used for comparison of occurrence rate in pairs of groups, and *t* test was used for the comparison of age.

RESULTS

There were a total of 3891 deceased individuals in the entire group. The proportion of deceased individuals in each generation was 66.0% in the parent generation, 39.5% in the proband generation, and only 10.5% in the child generation ($P<0.001$, Table 1). The mean age at death was 41.6 ± 26.2 years in the parent generation, 26.3 ± 22.3 years in the proband generation, and 15.8 ± 16.8 years in the child generation. These low age and large standard deviation in the age at death were the result of early childhood death occurring before five years of age, accounting for 18.4% of all deaths in the parent generation, 33.4% in the proband generation, and 47.2% in the child generation (Table 1). We examined the causes of death in each generation and their age at death (Table 2). The death from unknown causes in the parent generation (0.84 to FAP deaths) was almost five times higher than that in the other two generations ($P<0.001$). In this generation, the mean age at death (36.7 ± 19.8 years) from unknown causes was significantly lower than that at death from other causes ($P<0.05$).

The number of FAP patients was 508 (17.2%) in the parent generation, 1316 (30.8%) in the proband generation, and 337 (14.1%) in the child generation (Table 3). Among them, the number of deceased FAP patients was 460 (90.6% of 508) in the parent generation, 675 (51.3% of 1316) in the proband generation, and 78 (23.1% of 337) in the

child generation. There were significant differences among the groups in the FAP death rate ($P<0.001$). The age at death of FAP patients in each generation was 50.9 ± 12.4 years, 42.3 ± 12.3 years, and 33.3 ± 8.8 years, respectively, and the differences among the generations were significant ($P<0.001$). These results showed that any random selection of deceased intergenerational pairing in FAP patients would produce anticipation caused by these differences between the generations.

The cumulative mortality rates of the FAP patients gave us a few clues to the anticipation (Figure 1). The generation included less young FAP patients, and the start of death was delayed as compared to other generations. It may be said pseudo-anticipation. Between the child and proband generations, the acceleration of death was observed in the age between 22 and 40 years. Both a low detection rate of FAP patients (14.1%, Table 3) in the child generation, and a low portion of deceased FAP patients (23.1%) among them may cause this situation because many FAP patients were remained undiagnosed. This suggests a comparatively short observation period in the child generation. The incidence of colorectal cancer increased rapidly between 20 to 40 years of age, and this period might be overestimated in this generation.

In order to minimize these intergenerational biases in FAP patients, we calculated the cumulative mortality rates for the entire members as well as for the FAP patients to evaluate the anticipation. The cumulative mortality rates for the all subjects were plotted on Weibull's probability paper according to each generation (Figure 2). If the mortality curve of a descendant shifts to the left, it means earlier death or anticipation, and if a mortality curve shifts downside, it means the improvement of the general health condition of the group. The cumulative mortalities for both the parent and the proband generations were almost the same and parallel, while there was a slight vertical shift in these two curves, no horizontal shift was observed. This calculation method revealed no anticipation between the parent and the proband generations. The mortality rate of the child generation differed from those of the other generations; the overall cumulative mortality rate was low because of the lower infantile mortality in this generation. Although the mortality curve for the child generation showed a steeper slope line than those for the other two generations, the starting point of the steep slope, just after 20 years of age, was common to all the generations.

Table 1 Deceased subjects in each generation, *n* (%)

Generation	Total	Deceased	Age at death ($\bar{x} \pm s$, years)	Early childhood death [*] (% of the deceased cases)
Parent	2958	1952(66.0) ^b	41.6 ± 26.2	359(18.4)
Proband	4273	1687(39.5) ^b	26.3 ± 22.3	563(33.4)
Child	2395	252(10.5) ^b	15.8 ± 16.8	119(47.2)

^b $P<0.001$, among the generations; ^{*}Death before the age of five years.

Table 2 The proportion of causes of death in each generation and their mean age at death (each number of deaths is shown as a proportion to the number of FAP deaths)

Generation	FAP	Extra colonic malignancies	Other diseases	Unknown cause	Death in childhood
Parent <i>n</i> = 1952	1.00 [*] (50.9 ± 12.4)	0.37 (57.6 ± 14.4)	1.24 (58.2 ± 19.6)	0.84 ^b (36.7 ± 19.8) ^a	0.78
Proband <i>n</i> = 1687	1.00 (42.3 ± 12.3)	0.11 (46.2 ± 15.8)	0.37 (36.7 ± 19.0)	0.19 (22.7 ± 16.7)	0.84
Child <i>n</i> = 252	1.00 (33.3 ± 8.8)	0.13 (26.2 ± 16.3)	0.44 (22.9 ± 14.2)	0.14 (21.9 ± 14.2)	1.53

FAP: Death from familial adenomatous polyposis and colorectal cancer.
^{*}n: Total number of deaths.

^{*}: Deaths from FAP were calculated as 1.00. ($\bar{x} \pm s$, years): Age at death.

^a*P* < 0.05, vs other causes of death; ^b*P* < 0.001, vs other two generations.

Table 3 Age at death in the FAP patients, *n*(%)

Generation	Total number of subjects	Patients with FAP [*]	Deceased FAP patients	Age at death ($\bar{x} \pm s$, years)
Parent	2958	508(17.2)	460(90.6)	50.9 ± 12.4 ^b
Proband	4273	1316(30.8)	675(51.3)	42.3 ± 12.3 ^b
Child	2395	337(14.1)	78(23.1)	33.3 ± 8.8 ^b

^b*P* < 0.001, among the generations

FAP: familial adenomatous polyposis.

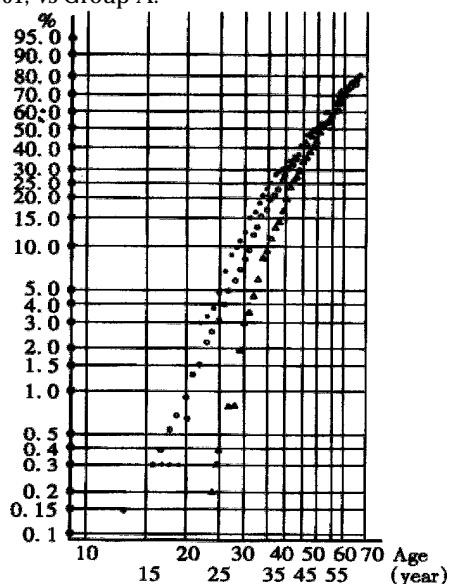
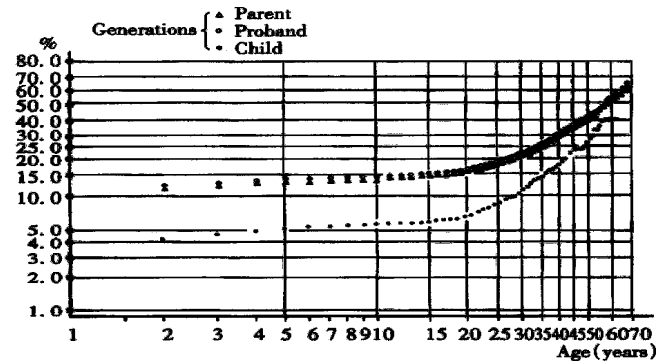
^{*}FAP patients and patients with colorectal cancer.

Table 4 Deceased parent-child pairs of FAP patients classified by the parental status of the child, and the anticipation

Age at death	Group A	Group B ^b
Parent > child	184	93
Parent ≤ child	57	5

Group A: Parent-child pairs in which the child had become a parent.
 Group B: Parent-child pairs in which the child had not had any child.

^b*P* < 0.01, vs Group A.

**Figure 1** Age specific cumulative mortalities of FAP patients. Circles: the proband generation; Triangles: the parent generation; Black dots: the child generation**Figure 2** Age specific cumulative mortalities of all subjects, including FAP patients and their first-degree relatives.

DISCUSSION

The anticipation phenomenon is so powerful that it surmounts the improvement of medical standards over years, and it is easily detected in hereditary diseases^[1,2,17-19]. Comparison of the age at death or onset in affected parent-child pairs is a conventional method in the study of the anticipation phenomenon^[1,2,17,18]. McInnis *et al*^[18] and Imamura *et al*^[19] applied the life-table analysis or random pairs method only to diagnosed patients and excluded other family members. If this method was applied to our FAP patients, the mean age at death in the proband generation was 8.5 years lower than that in the parent generation, and that in the child generation was 9 years lower than that in the proband generation. These figures exceed a standard period of 5 years to calculate postoperative survival of patients with colorectal cancer. This apparent anticipation was well correlated to the proportion of deceased cases in these three generations. This indicates that any fair pairing method will produce the anticipation. Veale^[2] estimated that a lack of parent-child correlation in onset of FAP was a major cause of sampling bias in his study over a limited period of time. He also concluded that the lack of correlation was due to the allele of the APC gene. Although his suggestions have not been denied as a contributor to the anticipation, some recent reports^[10-12] have suggested an apparent relationship between the site of the APC gene mutation and colorectal polyp density and retinal pigments in FAP patients. In addition, the comparison of the age at onset or death in parent-child pairs inevitably has two selection biases besides the intergenerational biases. One is that the parent has already been selected because he or she has already had at least one child, and this child must necessarily have already developed a symptom or died in order to make a parent-child pair. The other one is that a patient with a severe condition is difficult to gain a child, and this patient cannot be treated as a parent. We

confirmed the effect of selection bias in analysis of our 339 deceased parent-child pairs with FAP (Table 4). When the pairs were classified according to whether the child of the pair had become a parent or not, the childless group showed a significantly higher incidence of the anticipation phenomenon.

Recent reports have revealed that the elongation of trinucleotide repeat sizes is correlated with the increased severity of several hereditary neurological diseases such as myotonic dystrophy^[4], fragile X syndrome^[5], Huntington's disease^[6,7], and spinal and bulbar muscular atrophy^[8]. Although it is proved that the meiotic elongation of trinucleotide repeats accelerates these diseases, it does not necessarily mean that the elongation is inevitable in the meiosis. If we take parent-child pairs, it may seem as if the meiosis in these diseases constantly increases the length of trinucleotide repeats as the cause of the anticipation. The anticipation is such a powerful phenomenon as Ashizawa *et al*^[20] noted in 48% of 56 parent-child pairs that showed contractions of CTG repeat. Because anticipation is commonly encountered in clinical practice, its mechanism must be rather general. It is necessary to approach the elucidation of this phenomenon using some methods other than parent-child pair comparisons^[21]. We studied not only the FAP patients but also their first-degree relatives in our calculations of life tables. In this kind of studies, the change of medical environment among generations may influence the pattern of mortality. Besides its difficulty in taking the recent improvement of medical care in count, we have several reasons for not calculating this influence. ① parent-child pairing method in this series showed an apparent anticipation phenomenon; ② overall improvement of mortality in colorectal cancer was not so substantial as the anticipation phenomenon was diminished; and ③ proportion of early detection and preventive treatment in FAP patients was comparably small^[14]. Bias was minimized by our method because the effect of deaths of undiagnosed FAP patients in the parent generation was taken into account. In the parent generation, inherent bias was present in the form of deceased but undiagnosed young FAP patients. In the child generation, the bias was present mainly in the form of premature observation period and unidentified FAP patients, picking up only young deaths.

As the anticipation phenomenon is observed only in the conditions that threat their life and reproductive ability, one of the methods to avoid these biases is to examine the anticipation phenomenon on the FAP specific phenotypes that do not affect the life of FAP patients. For example, congenital hypertrophy of the retinal pigment epithelium is specific to FAP, and it has no influence on optical function. Our experience did not show apparent anticipation phenomenon in number of the pigment areas^[22]. Despite these

results it will be wise to watch FAP patients for colorectal cancer before the age at which their parents had cancer.

ACKNOWLEDGEMENT We thank doctors who registered FAP cases that were the clue of this research. This work was supported by Foundation for Promotion of Cancer Research in Japan, Grant in Aid from the Ministry of Health and Welfare, and Japanese Society for Cancer of the Colon and Rectum. We are also grateful to Dr. Yoshiyuki Hashimoto for his important advice.

REFERENCES

- 1 Penrose LS. The problem of anticipation in pedigrees of dystrophia myotonica. *Ann Eug*, 1948;14:125-132
- 2 Veale AMO. Intestinal polyposis. *Eug Lab Memoir*, 1965;60:1-101
- 3 Howeler CJ, Busch HFM, Geaerts JPM, Niermeijer MF, Stall A. Anticipation in myotonic dystrophy: fact or fiction. *Brain*, 1989;112:779-797
- 4 Brook JD, Mc Currach, Harley HG, Buckler AJ, Church D, Aburatani H, Hunter K, Stanton VP, Thirion J-P, Hudson T, Sohn R, Zemelman B, Snell RG, Rundle SA, Crow S, Davies J, Shelbourne P, Buxton J, Johnson K, Harper PS, Shaw DJ, Housman DE. Molecular bases of myotonic dystrophy: expansion of a trinucleotide (CGT) repeats at the 3' end of a transcript encoding a protein kinase family member. *Cell*, 1992;68:799-808
- 5 Taylor AK, Safanda JF, Fall MZ, Quince C, Lang KA, Hull CE, Carpenter I, Staley LW, Hagelman RJ. Molecular predictors of cognitive involvement in female carriers of fragile X syndrome. *JAMA*, 1994;271:507-514
- 6 Ashizawa T, Wong LJC, Richards CS, Caskey CT, Jankovic J. CAG repeat size and clinical presentation in Huntington's disease. *Neurology*, 1994;44:1137-1143
- 7 Tottier Y, Biancalana V, Mandel JL. Instability of CAG repeats in Huntington's disease: relation to parental transmission and age of onset. *J Med Genet*, 1994;31:377-382
- 8 La Spada AR, Roling DB, ZHarding AE, Warner CL, Spiegel R, Hausmanowa Petrusiewicz I, Yee WC, Fishbeck KH. Meiotic stability and genotype phenotype correlation of the trinucleotide repeats in X-linked spinal and bulbar muscular atrophy. *Nature Genetics*, 1992;2:301-304
- 9 Teisberg P. The genetic background of anticipation. *J Roy Soc Med*, 1995; 88:185-187
- 10 Nagase H, Miyoshi Y, Horii A, Aoki T, Ogawa M, Utsunomiya J, Baba S, Sasazuki T, Nakamura Y. Correlation between the location of germ line mutation in the APC gene and the number of colorectal polyps in familial adenomatous polyposis patients. *Cancer Res*, 1992;52:4055-4057
- 11 Spirio R, Olschwang S, Groden J, Robertson M, Samowitz W, Joslyn G, Gelbert L, Thliveris A, Carlson M, Otterud B, Lynch H, Watson P, Lynch P, Laurent Puig P, Burt R, Hughes JP, Thomas G, Leppert M, White R. Alleles of the APC gene: an attenuated form of familial polyposis. *Cell*, 1993;75:951-957
- 12 Olschwang S, Turet A, Laurent-Puig P, Mureris M, Parc R, Thomas G. Restriction of ocular fundus lesions to a specific subgroup of APC mutations in adenomatous polyposis coli. *Cell*, 1993;75:959-968
- 13 Young J, Simms LA, Tarish J, Buttenshaw R, Knight N, Anderson GJ, Bell A, Leggett B. A family with attenuated familial adenomatous polyposis due to a mutation in the alternatively spliced region of APC exon 9. *Human Mutation*, 1998;11:450-455
- 14 Iwama T, Mishima Y, Utsunomiya J. Current status of the registration of familial adenomatous polyposis at the Polyposis Center in Japan. In: Utsunomiya J, Lynch HT, eds. Hereditary colorectal cancer. Tokyo: Springer Verlag, 1990:63-69
- 15 Bussey HJR. Familial polyposis coli. Baltimore: Johns Hopkins University Press, 1975:2-8
- 16 Utsunomiya J. Pathological and genetic aspects of adenomatosis coli in Japan. In: Takebe H, Utsunomiya J, eds. Genetics of human tumors in Japan. Tokyo: Japan Scientific Societies Press, 1988:45-62
- 17 Ashizawa T, Dunne CR, Dubel JR, Perryman MB, Epstein HF, Boerwinkel E, Hejtmancik JF. Anticipation in myotonic dystrophy. I. Statistical verification based on clinical and haplotype findings. *Neurology*, 1992;42:1871-1877
- 18 McInnis MG, McMahon FI, Chase GA, Simpson SG, Ross CA, DePaulo JR. Anticipation in bipolar affective disorder. *Am J Hum Genet*, 1993;53:385-390
- 19 Imamura A, Honda S, Nakane Y, Okazaki Y. Anticipation in Japanese families with schizophrenia. *J Hum Genet*, 1998;43:217-223
- 20 Ashizawa T, Anvert M, Baignet M, Barcelo JM, Brunner H, Cobo AM, Dallapiccola B, Fenwick RG Jr, Grandell U, Harley H, Junien C, Koch MC, Korneluk RG, Lavedan C, Miki T, Mulley JC, Lopez de Munai A, Novelli G, Roses AD, Seltzer WK, Shaw DJ, Smeets H, Sutherland GR, Yamagata H, Harper PS. Characteristics of intergenerational contractions of the CTG repeat in myotonic dystrophy. *Am J Hum Genet*, 1994;54:414-423
- 21 Bormann Hassenbach MB, Albus M, Scherer J, Dreikorn B. Age at onset anticipation in familial schizophrenia. Does the phenomenon even exist. *Schizophr Res*, 1999;40:55-65
- 22 Iwama T, Mishima Y, Okamoto N, Inoue J. Association of congenital hypertrophy of the retinal pigment epithelium with familial adenomatous polyposis. *Br J Surg*, 1990;77:273-276

Review of 336 patients with hepatocellular carcinoma at Songklanagarind Hospital

Pasiri Sithinamsuwan¹, Teerha Piratvisuth¹, Wiwatana Tanomkiat², Nualta Apakupakul³ and Surat Tongyoo¹

Subject headings hepatoma/therapy; biopsy; neoplasm staging; survival analysis; neoplasms metastasis; prognosis; drug therapy

Sithinamsuwan P, Piratvisuth T, Tanomkiat W, Apakupakul N, Tongyoo S. Review of 336 patients with hepatocellular carcinoma at Songklanagarind Hospital. *World J Gastroentero*, 2000;6(3):339-343

Abstract

AIM To determine the clinical presentations, survival and prognostic factors of hepatocellular carcinoma (HCC) in Southern Thailand.

METHODS Retrospective analysis was performed on the 336 hepatocellular carcinoma patients treated at Songklanagarind hospital between 1 January 1991 and 31 January 1999.

RESULTS Of these 336 patients, 276 were males and 60 were females. The mean age was 54.4 years. The common symptoms and signs were abdominal pain and hepatomegaly. The most common presentation of tumor was a dominant mass with daughter nodules. Portal vein involvement was found in 50% of total. Extra hepatic metastasis was found in 13%, and the lung was the most common site. There were 65.4% with evidence of cirrhosis and half of them were in Child's class B. HBsAg was positive in 72.6%. Regarding Okuda's tumor staging, 15%, 61% and 24% were stage I, II and III, respectively. Overall median survival was 2.1 months (11.5, 2.6 and 0.7 months for stage I, II and III respectively). Treatments of HCC improved patient survival (5.5 months vs 1.6 months for untreated patients). Most common causes of death were hepatic failure. Using multivariate analysis, the prognostic

factors identified were tumor staging, alpha-fetoprotein level above 10 000 $\mu\text{g}\cdot\text{L}^{-1}$, extrahepatic metastasis, portal vein thrombosis and treatment.

CONCLUSION HCC in Thailand is a fatal disease with poor outcome due to late presentation and high prevalence of liver cirrhosis. Early detection and proper management may improve outcome.

INTRODUCTION

Hepatocellular carcinoma (HCC) is the most common form of primary liver cancer and is the leading cause of cancer death especially among males in South-East Asia including Thailand^[1,2]. This may be related to high prevalence of chronic hepatitis B infection (8%-15% in Asia and Africa, and 8%-12% in Thailand)^[3-7]. Though many types of treatment have been tried, HCC is still a fatal disease possibly associated with the advanced stage at which the disease is usually diagnosed^[2,8-11]. Thus, it remains a serious medical problem in this part of the world. There were many reports of the natural history of HCC in Japan, Mainland China, Southern Africa, Alaskan Eskimos, Taiwan, Italy, Spain and North America, but little information has been published from South-East Asia^[9-24]. Therefore, we reviewed 336 HCC patients at Songklanagarind Hospital to describe the clinical presentations and history of known risk factors and determine the survival rate, prognostic factors and the benefit of treatments.

MATERIALS AND METHODS

Patients

The medical records of 336 HCC patients admitted at Songklanagarind hospital between January 1, 1991 and January 31, 1999 were reviewed retrospectively. The diagnosis of HCC was made by liver biopsy or elevated serum alpha-fetoprotein level above 500 $\mu\text{g}\cdot\text{L}^{-1}$ with radiologic findings suggestive of HCC in patients whose liver biopsy was not available^[25]. Data from medical records, including patient demographic, known risk factors, clinical manifestation, abnormal physical findings, laboratory data (complete blood count, coagulogram, renal function test, liver function

¹Department of Medicine, Prince of Songkla University, Hat Yai, Songkhla, Thailand

²Department of Radiology, Prince of Songkla University, Hat Yai, Songkhla, Thailand

³Department of Epidemiology, Prince of Songkla University, Hat Yai, Songkhla, Thailand

Pasiri Sithinamsuwan M.D., graduated from Siriraj Hospital (First Class Honor in raining in Internal Medicine at Songklanagarind University Hospital, Thailand. Presented at The 5th Asia-Pacific Conference, American Gastroenterological Association and The 40th Annual Conference, The Gastroenterological Association of Thailand [Digestive Disease Week (DDW) Thailand 1999], Lotus Pang Suang Kaew Hotel, Chiang Mai Thailand, December 14th 1999.

Correspondence to: Pasiri Sithinamsuwan M.D., Department of Medicine, Songklanakarind Hospital, Hat Yai, Songkhla 90110, Thailand Fax. 0066-74-429385

Email. Pasiri@Kichimail. Com

Received 2000-03-20 Accepted 2000-05-15

tests, viral hepatitis serology, serum alpha-fetoprotein level, chest X-ray, ultrasonography, CT scan, liver biopsy and other tissue biopsy if suggested metastasis), survival and treatments modality, were used for analysis. The known risk factors include alcohol drinking, history of blood transfusion and history of jaundice or viral hepatitis infection or known cases of cirrhosis. Patients were classified into 6 groups based on their clinical presentation: group 1, mass-related symptoms (abdominal pain or fullness, dyspepsia, palpable mass); group 2, cirrhosis-related symptoms (jaundice, GI bleeding, edema, abdominal enlargement, hepatic encephalopathy); group 3, liver abscess-like symptoms (high fever with abdominal pain and tenderness); group 4, non-specific symptoms (anorexia, nausea, vomiting, malaise, weight loss and anemia); group 5, metastasis symptoms (dyspnea, cough, bone pain and palpable lymph node); and group 6, asymptomatic cases (accidental finding by routine check-up or complain of other unrelated disease). The abnormal physical findings included anemia, jaundice, fever, hepatomegaly, splenomegaly, ascites and sign of chronic liver stigmata such as palmar erythema, spider nevi, gynecomastia and superficial dilated vein. A test of viral marker for hepatitis B (HBsAg) was done in most of patients but that for hepatitis C (anti-HCV) was not available until 1996. Tumor volume was calculated from ultrasonography or CT scan of the liver by a radiologist. Tumor volume or sum of tumors in instances multiple nodules were expressed as fraction of total liver and subsequently classified into two groups (tumor size $\leq 50\%$, $>50\%$ of the whole liver). Staging of HCC was made according to Okuda's^[9]. Cirrhosis was confirmed by liver biopsy or ultrasonography or CT scan and classified by Child-Pugh's (Class A, B or C)^[26]. The extrahepatic metastasis was confirmed by histology (incisional biopsy, excisional biopsy, necropsy or autopsy).

Therapy

The treatment of HCC ranged from no treatment, transhepatic artery oily chemoembolization (TOCE), percutaneous ethanol intralesional injection (PEI), hepatectomy, systemic chemotherapy and multimodality combination chemotherapy.

For systemic chemotherapy before 1995, we used intravenous adriamycin and/or 5-FU injection. Later this was changed to PIAF regimen (cisplatin $80 \text{ mg} \cdot \text{m}^{-2}$ body surface area (BSA) and adriamycin $40 \text{ mg} \cdot \text{m}^{-2}$ BSA at d1, followed by 5-FU $500 \text{ mg} \cdot \text{m}^{-2}$ infusion over 24 h for the following 3 d, with alpha-Interferon $5 \text{ mU} \cdot \text{m}^{-2}$, iv, 3 h after cisplatin and 5-FU every day).

TOCE was performed monthly by super-selective insertion of catheter to the right or left hepatic artery branch feeding the tumor then injection adriamycin 50 mg, lipiodol 8 mL and gelfoam. PEI was performed by using 10 mL of absolute ethanol injected percutaneously under CT-scan guide.

Multimodality combination therapy comprised a combination of several treatments depending on the tumor staging and complication, such as the patients who presented with advanced HCC and had portal vein involvement with lung metastasis, the treatment was started with systemic chemotherapy (PIAF regimen) until no evidence of extrahepatic metastasis remained and was then followed by TOCE and/or intralesional ethanol injection (PEI). Because of the limitation of retrospective study, we were unable to determine the exact outcome or improvement of general condition after treatments, so we determined the outcome by survival analysis.

In patients who were lost to follow-up, we determined the date and cause of death from the population register and personal contact with the family. Patient status was unable to determine in 20% of the patients. For statistical analysis these patients were considered as censored at the date of last contact.

Survival profiles were constructed using the Kaplan-Meier method. Prognostic factors were identified using Cox proportional hazards regression. P value <0.05 was considered statistically significant.

RESULTS

Of the 336 patients, 276 (82%) were male with a male to female ratio of 4.6:1. The mean age was 54.4 (a range of 20-89) years (54.3 years in male and 55 years in female) (Table 1). Diagnosis was confirmed histologically in 273 (72.3%) cases and 63 (18.7%) cases were diagnosed by a combination of elevated serum alpha-fetoprotein level above $500 \mu\text{g} \cdot \text{L}^{-1}$ and imaging such as ultrasound or CT scan showing a lesion compatible with HCC.

The most common symptom was mass-related such as abdominal pain, abdominal discomfort, dyspepsia and palpable mass (Table 2). Mean duration of symptoms was 49 d (range <1 day -1 year). Among the abnormal physical findings hepatomegaly was the most common, followed by fever and jaundice (Table 2).

Elevation of alkaline phosphatase and serum aspartate aminotransferase (AST) was the most common abnormal finding in the liver function test. Serum bilirubin above $51.3 \mu\text{mol} \cdot \text{L}^{-1}$ was found in 30%. The most common radiologic finding was a solitary mass with or without daughter nodules (73%, Table 1). The tumor was located most frequently in the right lobe (53%) followed by both

lobes (37%) and left lobe (10%). Tumor volume larger than half of the total liver was found in 71% and portal vein thrombosis or portal vein involvement in 50%. Portal vein thrombosis or involvement was significantly associated with increased tumor volume ($P = 0.0005$). The mean serum alpha-fetoprotein level was 145 110 (range 2-7 990 000 $\mu\text{g}\cdot\text{L}^{-1}$) and values above 500 $\mu\text{g}\cdot\text{L}^{-1}$ (the cut point for diagnosing HCC) occurred in 64% (Table 1).

Table 1 HCC patient characteristics

Patient characters		<i>n</i>	%	Mean	Range
Age(years)	All			54.4	20-89
	Male			54.3	20-89
	Female			55.0	20-81
Sex	Male	276	82.0		
	Female	60	18.0		
Risk factors	Alcohol drinking	126	38.0		
	HBsAg positive (299 sample)	217	72.6		
	anti-HCV positive (135 sample)	10	7.4		
	Cirrhosis	219	65.2		
Liver function test	Total bilirubin ($\mu\text{mol}\cdot\text{L}^{-1}$)			63.8	3.4-752.4
	Direct bilirubin ($\mu\text{mol}\cdot\text{L}^{-1}$)			38.8	0.5-581.4
	Aspartate aminotransferase ($\text{U}\cdot\text{L}^{-1}$)			225	17-3890
	Alanine aminotransferase ($\text{U}\cdot\text{L}^{-1}$)			97	4-3370
	Alkaline phosphatase ($\text{U}\cdot\text{L}^{-1}$)			304	8-2080
	Albumin ($\text{g}\cdot\text{L}^{-1}$)			35.6	20-52
	Globulin ($\text{g}\cdot\text{L}^{-1}$)			38.2	18-78
Radiologic finding (<i>n</i> = 329)	Solitary type (total)	240	73.0		
	with daughter nodules	144	43.8		
	without daughter nodules	96	29.2		
	Multinodular type	47	14.3		
	Diffuse or infiltrative type	42	12.7		
Alpha fetoprotein ($\mu\text{g}\cdot\text{L}^{-1}$) (<i>n</i> = 295)				145 110	2-7990 000
	<10	38	13.0		
	10-99	36	12.0		
	100-499	33	11.0		
	≥ 500	188	64.0		
Okuda's staging	Stage I	51	15.0		
	Stage II	205	61.0		
	Stage III	80	24.0		

The most common risk factor was chronic hepatitis B infection (72.6%), and 65.2% showed evidences of liver cirrhosis (Table 1). Patients with cirrhosis were classified into Child A, B and C in 20%, 55.3% and 24.7% respectively. Cirrhosis was found in 76.2% of alcoholic patients, 66.4% of HBV infected patients and 90% of HCV infected patients. Okuda's staging distribution was 15%, 61% and 24% for stage I, II and III respectively (Table 1). Spontaneous rupture of HCC was found 11% (4%, 9.3% and 20% in stage I, II and III). At the time of diagnosis, extrahepatic metastasis occurred in 43 cases (13.1%), 13.7%, 10.7% and 18.8% of stage I, II and III respectively. The metastatic sites were lung (76%), lymph node (16%) and bone (7%).

Overall median survival was 2.1 months (Stage I, 11.5 months; Stage II, 2.6 months; and Stage III, 0.7 months) (Table 3, Figure 1). The 1 and 2-year survival rates were 15% and 8% respectively. Treatment of HCC was associated with improvement of patient survival (5.5 vs 1.6 months

in non-treated group; $P = 0.011$) (Table 3, Figure 2). In the non-treated group ($n = 245$) median survival was 1.6 months (7.7, 1.8 and 0.6 months for stages I, II and III respectively, Table 3, Figure 3). Regarding treatment, patients treated with TOCE, intravenous chemotherapy, multimodality combination therapy and Tamoxifen administration had median survival times of 6.3, 5.33, 17.1 and 3 months, respectively (Table 3). Compared to the non-treated group, patients treated with TOCE, intravenous chemotherapy or combination therapy had significantly better survival ($P = 0.0005$, 0.011 and 0.007 respectively) whereas survival of the patients treated with Tamoxifen was not significantly different from non-treated ($P = 0.86$) patients.

Table 2 Presenting symptoms and abnormal physical findings of patients

Presenting symptoms	<i>n</i>	%
Mass-related symptoms (Abdominal pain or fullness, dyspepsia, palpable mass)	188	56
Cirrhosis-related symptoms (Jaundice, GI bleeding, edema, abdominal enlargement, encephalopathy)	59	17.6
Liver abscess-like symptoms (High fever with acute abdominal pain and tenderness)	45	13.4
Non-specific symptoms (Anorexia, nausea, vomiting, malaise, weight loss, chronic anemia)	26	7.7
Metastasis symptoms (Dyspnea, cough, bone pain, palpable lymph node)	11	3.2
Asymptomatic (Routine checked up or other unrelated disease)	7	2.1
Abnormal physical findings		
Hepatomegaly	282	83.9
Fever	185	50.5
Jaundice	143	42.6
Anemia	138	41.1
Ascites	123	36.6
Cachexia	86	25.6
Chronic liver stigmata	86	25.6
Edema	59	17.6
Splenomegaly	42	12.5

Table 3 Median survival

Group of patients	<i>n</i>	Median survival (months)
All	336	2.1
Stage I	51	11.5
Stage II	205	2.6
Stage III	80	0.73
Untreated	245	1.6
Stage I	26	7.7
Stage II	146	1.8
Stage III	73	0.63
Treated	91	5.5
Stage I	25	13.7
Stage II	59	4.2
Stage III	7	1.7
TOCE	44	6.3
Stage I	11	24.3
Stage II	29	5.5
Stage III	4	1.4
Chemotherapy (adriamycin and/or 5-FU)	16	5.2
Multimodality therapy (PIAF/iv, chemotherapy \pm TOCE \pm PEI)	12	17.1
Tamoxifen	9	3.0
PIAF regimen chemotherapy	5	-
Hepatectomy	4	-
PEI	1	-

*Data of PIAF regimen chemotherapy is not completely finished. †It were too small number of patients to evaluated.

The most common causes of hospital death ($n = 54$) were hepatic failure, GI bleeding and rupture of tumor (59.2%, 20.4% and 20.4% respectively). Among cases with hepatic failure, sepsis was the most common complication leading to death. Cox proportional hazards model reviewed the following, prognostic factors: Okuda's stage II ($P = 0.014$, hazard ratio 2.05), stage III ($P = 0.001$, hazard ratio 3.79), AFP level above $10\,000\ \mu\text{g}\cdot\text{L}^{-1}$ ($P = 0.001$, hazard ratio 2.03), lung metastasis ($P = 0.01$, hazard ratio 1.93), lymph node metastasis ($P = 0.015$, hazard ratio 3.76), portal vein involvement or thrombosis ($P = 0.0005$, hazard ratio 1.79) and treatment ($P = 0.011$, hazard ratio 0.91).

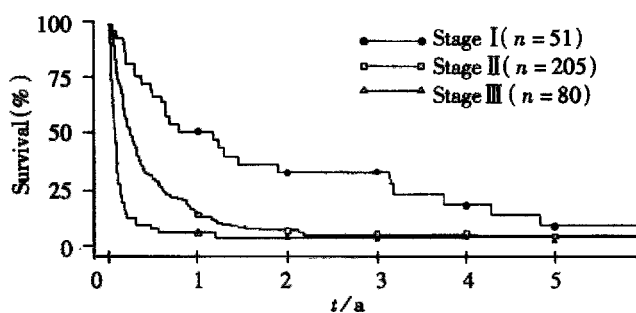


Figure 1 Kaplan-Meier survival curve for overall patients. Total ($n = 336$) median survival of 2.1 months; Okuda's stage I ($n = 51$), median survival of 11.5 months; Okuda's stage II ($n = 205$), median survival of 2.6 months; Okuda's stage III ($n = 80$), median survival of 0.7 months ($P = 0.014$ and 0.001 respectively).

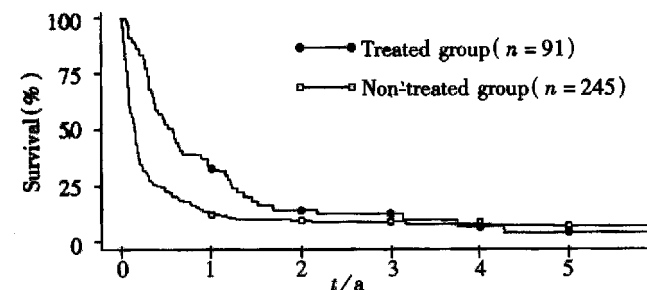


Figure 2 Kaplan-Meier survival curve in relation to treatment or non-treatment. Treated group ($n = 91$), median survival of 5.5 months; non-treated group ($n = 245$), median survival of 1.6 months ($P = 0.011$).

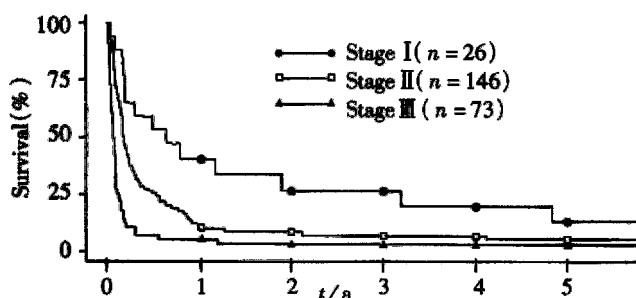


Figure 3 Kaplan-Meier survival curve in non-treated group. Total ($n = 245$), median survival of 1.6 months, Okuda's stage I ($n = 26$), median survival of 7.7 months; Okuda's stage II ($n = 146$), median survival of 1.8 months; Okuda's stage III ($n = 73$), median survival of 0.6 months.

DISCUSSION

Similar to other studies, we found that HCC was more common in males (a male to female ratio of 4.6:1) because the risk factors such as cirrhosis, chronic HBV infection and alcoholic are more frequently seen in males than females^[2,8,12-19,27,28]. In our study, the most common risk factor was chronic HBV infection (72.6%) as HBV is endemic in South-East Asia^[5]. The common symptoms were non-specific and included abdominal pain, dyspepsia, jaundice, hepatomegaly, anorexia and weight loss. Clinical jaundice was found in 42.6% and mainly caused by failure of hepatic function due to cirrhosis. The most common type of tumor in our patients was dominant mass with daughter nodules whereas multiple nodules or diffuse lesion are common in Western patients^[15,17,18]. The difference in risk factors may explain the variation in tumor characters as chronic HBV infection is the most important risk factors in our region while chronic HCV infection and alcohol drinking are the largest risk factors in Japan and Western countries^[3,8,13-18,27,29]. Cirrhosis was found in 65% of our patients and 80% of them were classified as Child's B or C. These may be associated with poor prognosis. In our study, hepatectomy and TOCE were not suitable in more than half of the patients due to portal vein involvement (50%) and advanced liver cirrhosis (24.7%). Extrahepatic metastasis was found in 13% and most of them were located in the lung, probably because of direct drainage into the right heart via the hepatic vein. Elevated serum alpha-fetoprotein above $500\ \mu\text{g}\cdot\text{L}^{-1}$ was found in only 64% of patients, so this tumor marker was not very sensitive for diagnosis of HCC in our country. Most our patients had advanced HCC (61% and 24% were stage II and III respectively). The overall median survival in our patients was 2.1 months because majority of our patients had advanced disease with significant liver cirrhosis. In treatment of HCC, hepatectomy and TOCE could improve survival^[9,13], but could not be performed because of liver cirrhosis and portal vein involvement. Systemic chemotherapy, arterial infusion and Tamoxifen administration could not improve survival^[9,20,24,30-32], whereas data of PIAF regimen chemotherapy showed complete pathological remission, but survival analysis did not^[33]. In our study, TOCE and multimodality therapy could improve survival, particularly in patients with stage I and stage II disease as compared with the non-treatment group (24.3% vs 7.7 months in stage I and 5.5 vs 1.8 months in stage II receiving TOCE and 17.1 months vs 0.63 months in patients receiving multimodality therapy). However, our study is only a retrospective study that had its limitation in comparing survival rate between different groups. The most of our patients died of hepatic failure (60%) as a majority of them had

advanced HCC and liver cirrhosis. By multivariate analysis, poor prognosis was associated with advanced stage of the tumor, serum alpha-fetoprotein level $>10\,000\,\mu\text{g}\cdot\text{L}^{-1}$, extrahepatic metastasis and portal vein involvement.

ACKNOWLEDGEMENTS The authors acknowledge the cooperation of the staff of the Registration Unit of Songklanagarind Hospital and of the Official Register of Population for providing patient data and Dr. Allan Geater for English advice.

REFERENCES

- 1 Srivatanakul P, Sontipong S. Incidence of liver cancer in Thailand 1979. *Thai Cancer J*, 1979;8:127-134
- 2 Kassianides C, Kew MC. The clinical manifestations and natural history of hepatocellular carcinoma. *Gastroenterol Clin N Am*, 1987;16:553-562
- 3 Srivatanakul P, Burke DS, Thanasombutt S, Tan ngarmtrong D. Serum markers of hepatitis A and B virus infection in Thai patients with primary hepatocellular carcinoma. *Thai Cancer J*, 1983;9:113-118
- 4 Kane MA. Progress on the control of hepatitis B infection through immunisation. *Gut*, 1993;34(Suppl):S10-12
- 5 Perrillo RP. Hepatitis B: transmission and natural history. *Gut*, 1993;34(Suppl):S48-49
- 6 Beasley RP. Hepatitis B virus as the etiologic agent in hepatocellular carcinoma epidemiologic considerations. *Hepatology*, 1982;2(Suppl):S21
- 7 Beasley RP, Hwang LY, Lin CC, Chien CS. Hepatocellular carcinoma and hepatitis B virus. A prospective study of 22,707 men in Taiwan. *Lancet*, 1981;2:1129-1132
- 8 Bisceglie AM, Rustgi VK, Hoofnagle JH, Dusheiko GM, Lotze MT. Hepatocellular carcinoma: NIH conference. *Ann Intern Med*, 1988;108:390-401
- 9 Okuda K, Ohtsuki T, Obata H, Tomimatsu M, Okazaki N, Hasegawa H, Nakajima Y, Ohnishi K. Natural history of hepatocellular carcinoma and prognosis in relation to treatment: study of 850 patients. *Cancer*, 1985;56:918-928
- 10 Kew MC, Geddes EW. Hepatocellular carcinoma in rural southern African blacks. *Medicine*, 1982;61:98-108
- 11 Okuda K, Nakashima T. Primary carcinomas of the liver. 4th ed. In: Berk Bockus Gastroenterology. Philadelphia: WB Saunders, 1985:335-3376
- 12 Cong WM, Wu MC. Primary hepatocellular carcinoma in women of Mainland China: a clinicopathologic analysis of 104 patients. *Cancer*, 1993;71:2941-2945
- 13 Stuart KE, Anand AJ, Jenkins RL. Hepatocellular carcinoma in the United States: prognostic features, treatment outcome, and survival. *Cancer*, 1996;77:2217-2222
- 14 Chlebowski RT, Tong M, Weissman J, Block JB, Ramming KP, Weiner JM, Bateman JR, Chlebowski JS. Hepatocellular carcinoma: diagnostic and prognostic features in North American patients. *Cancer*, 1984;53:2701-2706
- 15 Calvet X, Bruix J, Gines P, Bru C, Sole M, Vilana R, Rodes J. Prognostic factors of hepatocellular carcinoma in the West: a multivariate analysis in 206 patients. *Hepatology*, 1990;12:753-760
- 16 Ebara M, Ohto M, Shinagawa T, Sugiura N, Kimura K, Matsutani S, Morita M, Saisho H, Tsuchiya Y, Okuda K. Natural history of minute hepatocellular carcinoma smaller than three centimeters complicating cirrhosis: a study in 22 patients. *Gastroenterology*, 1986;90:289-298
- 17 Llovet JM, Bustamante J, Castells A, Vilana R, Ayuso MDC, Sala M, Bru C, Rodes J, Bruix J. Natural history of untreated nonsurgical hepatocellular carcinoma: rationale for the design and evaluation of therapeutic trials. *Hepatology*, 1999;29:62-67
- 18 Colombo M. The natural history of hepatocellular carcinoma in Western countries. *Hepatogastroenterol*, 1998;45:1221-1225
- 19 Nagasue N, Yukaya H, Hamada T, Hirose S, Kanashima R, Inokuchi K. The natural history of hepatocellular carcinoma: a study of 100 untreated cases. *Cancer*, 1984;54:1461-1465
- 20 Okuda K. Primary liver cancer: Quadrennial review lecture. *Dig Dis Sci*, 1986;31(Suppl):S133-146
- 21 Heyward WL, Lanier AP, McMahon BJ, Bender TR, Francis DP, Maynard JE. Serological markers of hepatitis B virus and Alpha Fetoprotein levels preceding primary hepatocellular carcinoma in Alaskan Eskimos. *Lancet*, 1982;23:889-891
- 22 Ebara M, Hatano R, Fukuda H, Yoshikawa M, Sugiura N, Saisho H. Natural course of small hepatocellular carcinoma with underlying cirrhosis. A study of 30 patients. *Hepatogastroenterol*, 1998;45:1214-1220
- 23 Nomura F, Ohnishi K, Tanabe Y. Clinical features and prognosis of hepatocellular carcinoma with reference to serum Alpha-Fetoprotein levels: analysis of 606 patients. *Cancer*, 1989;64:1700-1707
- 24 Group d'Etude et de traitement du carcinoma hepatocellulaire. A comparison of Lipiodol chemoembolization and conservative treatment for unresectable hepatocellular carcinoma. *N Engl J Med*, 1995;332:1256-1261
- 25 Jones DB, Koorey DJ. Screening studies and markers: hepatic carcinoma. *Gastroenterol Clin N Am*, 1987;16:563-573
- 26 Pugh RMH, Murray-Lyon IM, Dawson JL, Pierroni MC, Williams R. Transection of the esophagus for bleeding esophageal varices. *Br J Surg*, 1973;60:646-664
- 27 Dusheiko G. Hepatocellular carcinoma: molecular biology, etiology and animal models. *Gastroenterol Clin N Am*, 1987;16:575-590
- 28 Sutton FM, Russell NC, Guinee VF, Alpert E. Factors affecting the prognosis of primary liver carcinoma. *J Clin Oncol*, 1988;6:321-328
- 29 Okada S, Okazaki N, Nose H, Yoshimori M, Aoki K. Prognostic factors in patients with hepatocellular carcinoma receiving systemic chemotherapy. *Hepatology*, 1992;16:112-117
- 30 Yamashita Y, Takahashi M, Koga Y, Saito R, Nanakawa S, Hatanaka Y, Nobuyuki S, Nakashima K, Urata O, Yoshizumi K, Ito K, Sumi S, Kan M. Prognostic factors in the treatment of hepatocellular carcinoma with transcatheter arterial embolization and arterial infusion. *Cancer*, 1991;67:385-391
- 31 Bruix J, Llovet JM, Castells A, Montana X, Bru C, Ayuso MDC, Vilana R, Rodes J. Transarterial embolization versus symptomatic treatment in patients with advanced hepatocellular carcinoma: results of a randomized controlled trial in a single institution. *Hepatology*, 1998;27:1578-1583
- 32 Castells A, Bruix J, Bru C, Ayuso C, Roca M, Boix L, Vilana R, Rodes J. Treatment of hepatocellular carcinoma with Tamoxifen: a double blind placebo-controlled trial in 120 patients. *Gastroenterology*, 1995;109:917-922
- 33 Leung TWT, Patt YZ, Lau WY, Ho SKW, Yu SCH, Chan ATC, Mok TSK, Yeo W, Liew C, Leung NWY, Tang AMY, Johnson PJ. Complete pathological remission is possible with systemic combination chemotherapy for inoperable hepatocellular carcinoma. *Clin Cancer Res*, 1999;5:1676-1681

Edited by Ma JY and Pan BR

Three-dimensional image of hepatocellular carcinoma under confocal laser scanning microscope

Wang Hai Zhang¹, Shi Neng Zhu², Shi Lun Lu², Ya Lin Huang³ and Peng Zhao³

Subject headings HCC; nucleus, three-dimensional reconstruction; microscopy, confocal laser scanning

Zhang WH, Zhu SN, Lu SL, Huang YL, Zhao P. Three-dimensional image of hepatocellular carcinoma under confocal laser scanning microscope. *World J Gastroentero*, 2000;6(3):344-347

Abstract

AIM To investigate the application of confocal laser scanning microscopy (CLSM) in tumor pathology and three-dimensional (3-D) reconstruction by CLSM in pathologic specimens of hepatocellular carcinoma (HCC).

METHODS The 30 μm thick sections were cut from the paraffin-embedded tissues of HCC, hyperplasia and normal liver, stained with DNA fluorescent probe YOYO-1 iodide and examined by CLSM to collect optical sections of nuclei and 3-D images reconstructed.

RESULTS HCC displayed chaotic arrangement of carcinoma cell nuclei, marked pleomorphism, indented and irregular nuclear surface, and irregular and coarse chromatin texture.

CONCLUSION The serial optical tomograms of CLSM can be used to create 3-D reconstruction of cancer cell nuclei. Such 3-D impressions might be helpful or even essential in making an accurate diagnosis.

INTRODUCTION

Under conventional light microscope, *histopathologists* often use plane image to evaluate the three-dimensional (3-D) cellular characteristics. Three-D configuration may be reconstructed by using serial mechanical sectioning, but its axis definition is not good, image is blur and tiny structure can't be shown clearly, and the specimen might be damaged. Using the serial optical tomograms and 3-D reconstruction function, confocal laser scanning microscopy (CLSM) can provide a much better quality 3-D image than conventional light microscope, and lead the observer into a brand-new 3-D world. Although CLSM has been used extensively in cell biology^[1], few applications were reported in routine clinical pathology such as three-dimensional DNA image cytometry by CLSM in thick tissue blocks of prostatic lesions and 3-D reconstruction by CLSM in routine pathologic specimens of benign and malignant lesions of human breast^[2-4]. In this study, 3-D reconstruction was performed on routine formalin-fixed, paraffin-embedded tissues of normal, and hyperplastic tissues of liver and hepatocellular carcinoma by using computer-assisted CLSM together with 3-D reconstruction. The goals of our study were to present 3-D morphologic characteristics of benign and malignant specimens of the liver and to attempt to demonstrate the usefulness of CLSM in routinely obtained surgical pathologic tissues.

MATERIALS AND METHODS

Two cases of normal liver tissue were selected from autopsy specimens collected in the Department of Pathology of Shanghai Medical University, six cases of hepatocellular carcinoma including adjacent liver tissue were routine clinical specimens collected in 1996 from the Liver Cancer Institute of Zhongshan Hospital affiliated to Shanghai Medical University.

All tissues were fixed in 10% formalin, embedded in paraffin, serial sections were cut at 5 μm and 30 μm . The 5 μm slices were stained with hematoxylin and eosin for conventional light microscopic observation. The 30 μm slices were stained with DNA fluorescent probe, YOYO-1 iodide (Molecular Probes, Eugene, Ore., USA).

¹Division of Pathology, Zhongshan Hospital, Shanghai Medical University, Shanghai 200032, China

²Department of Pathology, Shanghai Medical University, Shanghai 200032, China

³National Laboratory of Medical Neurobiology, Shanghai Medical University, Shanghai 200032, China

Dr. Wang Hai Zhang, graduated from Shanghai Medical University as a Ph.D. in 1999, majoring in surgical pathology and molecular pathology, having 10 papers published.

Correspondence to: Dr. Wang Hai Zhang, Division of Pathology, Zhongshan Hospital, Shanghai Medical University, Shanghai 200032, China

Tel. 0086-21-64041990 Ext.2732

Email. whzhangsh@hotmail.com

Received 2000-03-19 **Accepted** 2000-04-28

The sections were deparaffinized with xylene (10 min \times 2) and dehydrated with 100%, 95%, and 70% ethanol (5 min \times 2) and rinsed in distilled water for 2 min \times 5. The specimens were then fixed with 10% neutral buffered formalin for 30 min and washed with tap water. After rinsing with distilled water and 0.01M phosphate buffer 5 min \times 2, nuclear RNA was removed by incubating the sections for 30 min at 37°C in 200 μ L of ribonuclease A (RNAase; Sigma, USA) at a concentration of 160 g/L in PBS. DNA was next hydrolyzed with 2N HCl for 25 min at 27.5°C. After rinsing with distilled water for 2 min \times 5, the sections were covered with 200 μ L of YOYO-1 iodide diluted into 1:2000 with PBS. The PBS was diluted 1:5 with distilled water to reduce the salt concentration. To this 200 μ L working solution of YOYO-1 iodide, 20 μ L of 0.1N HCl was added and the final solution was stored in the dark at 4°C for use. Homogeneous fluorescence intensity of nuclei at different depths of the confocal slices was obtained by agitating the YOYO-1 iodide for 1 h in the dark. Afterwards, the sections were rinsed with distilled water, covered with buffered glycerol, and the glass cover slip were sealed with finger nail polish. Sections were stored at 4°C in the dark until CLSM examination.

A Leica TCS-NT confocal laser scanning microscope equipped with epifluorescence optics and an appropriate combination of filters to visualize and digitize the images of the different specimens. An argon laser with an excitation wavelength of 488 nm was used to activate the green fluorescence of the YOYO-1 iodide-stained nuclear DNA (maximal absorption 491 nm and emission 509 nm). A 16 \times objective (numerical aperture of 1.30) was used to observe the specificity of the staining, and a 100 \times water objective (numerical aperture of 1.30) was used to study the details of chromatin pattern. Optical sections were collected throughout the entire stained thickness of the paraffin sections with a Z-step interval of 0.3 μ m or 0.6 μ m. The 3-D image processing was performed on a Leica computer with the original 3-D interactive visualization software. The collected confocal optical sections and the 3-D reconstructed images were printed with a Panasonic color video dye-sublimation copy processor.

RESULTS

Three-D morphologic features of normal liver cells

A microscopic field of view was selected from the normal liver specimen and comparison of the images taken under transmission conventional light microscope and CLSM is illustrated in Figure 1. The transmission conventional light microscopic image

was shown on the right side and the out-of-focus signals were visible. The out-of-focus blur reduced the contrast and sharpness of the final image. In the confocal image (left) the out-of-focus signals were cut off and only signals in focus were clearly visible. Optical sections (planes 1-60) were taken from the surface to the bottom of normal liver specimen with a Z-step interval of 0.5 μ m. Figure 2 shows the 10th, 20th, 30th, 40th, 50th and 60th plane digital images of Z-series. The confocal images were taken at 5, 10, 15, 20, 25 and 30 μ m depths, respectively. In the confocal images some nuclei appeared or disappeared depending on their orientation in space. The 60 2-D optical sections were computer focused on a plane (deep-focusing) to analyze the fine structure of chromatin patterns inside the nucleus and reconstructed 3-D images to display the 3-D detailed arrangement of nucleus. Figure 3 shows normal liver cells with similar round or ovoid nuclei, homogeneous intensity of YOYO-1 iodide fluorescence as well. Three-dimensional view was shown in Figure 4. The nuclear surface appeared smooth with homogeneous fluorescence intensity.

Three-D morphologic features of atypical hyperplasia of liver cells

Optical sections (planes 1-50) were taken from the surface to the bottom of atypical hyperplasia of liver specimen with a Z-step interval of 0.6 μ m. The structure of chromatin patterns inside the nucleus with homogeneous fluorescence intensity is shown with deep-focusing in Figure 5. Three-dimensional view is shown in Figure 6. The nuclear surface appeared smooth with homogeneous fluorescence intensity. But the volume of nucleus of atypical hyperplasia liver cell was bigger than that of normal liver cell.

Three-D morphologic features of hepatocellular carcinoma cells

Optical sections (planes 1-50) were taken from the surface to the bottom of hepatocellular carcinoma specimen with a Z-step interval of 0.6 μ m. The deep-focusing images were shown in Figure 7 and Figure 8. The structure of chromatin patterns inside the nucleus with heterogeneous karyotheca thickness, irregular and coarse chromatin texture, chromatin underside the karyotheca mainly. Three-dimensional view is shown in Figure 9 and Figure 10. HCC displayed remarkably different features in 3-D morphology, including: indented, molding, and irregular nuclear surface; marked pleomorphism; chaotic arrangement of tumor cell nuclei.

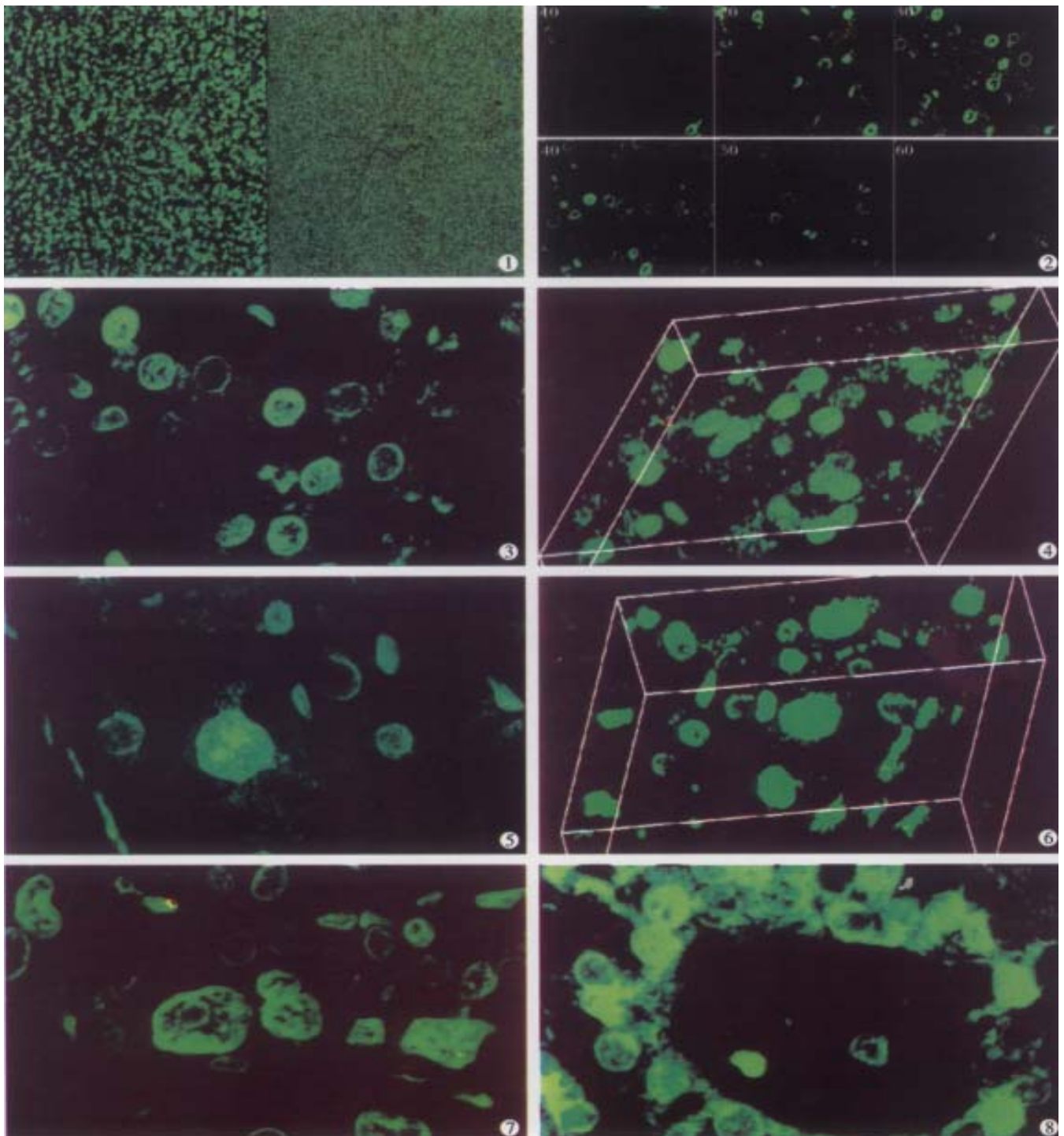


Figure 1 The transmission conventional light microscopical image was shown on the right side. The out-of-focus blur reduced the contrast and sharpness of the image. In the confocal image (left) the out-of-focus signals were cut off and only signals in focus were clearly visible. $\times 160$

Figure 2 The 10th, 20th, 30th, 40th, 50th and 60th plane digital images of Z-series. In the normal liver tissues of the confocal images some nuclei appeared or disappeared depending on their orientation in space. $\times 1000$

Figure 3 Deep-focusing image showed the normal liver cells with similar round or ovoid nuclei, similar in size and homogeneous intensity of YOYO-1 iodide fluorescence as well. $\times 1000$

Figure 4 Three-dimensional view of normal liver cells, the nuclear surface appeared smooth with homogeneous fluorescence intensity. $\times 1000$

Figure 5 Deep-focusing image of atypical hyperplasia liver cells, the structure of chromatin patterns inside the nucleus with homogeneous fluorescence intensity. $\times 1000$

Figure 6 Three-dimensional view of atypical hyperplasia liver cells. $\times 1000$

Figure 7 Deep-focusing image of HCC cells, the structure of chromatin patterns inside the nucleus with heterogeneous karyotheca thickness, irregular and coarse chromatin texture, chromatin underside the karyotheca mainly. $\times 1000$

Figure 8 Deep-focusing image of highly differentiated HCC chromatin texture. $\times 1000$

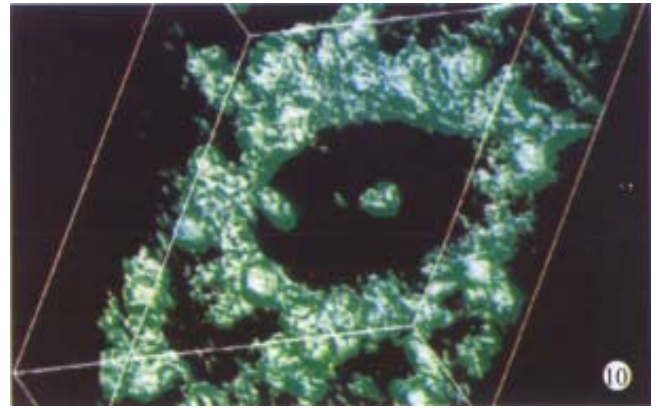
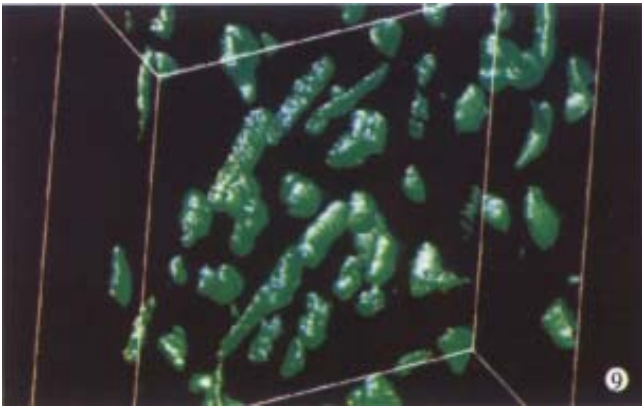


Figure 9 Three-dimensional view of spindle cell HCC. $\times 1000$

Figure 10 Three-dimensional view of tubular adenocarcinoma of HCC. $\times 1000$

DISCUSSION

The area, volume, shape, DNA content, and chromatin pattern of nuclei may be important for the diagnosis and prognosis of cancer. *Histopathologists* often use $4\text{ }\mu\text{m}$ to $6\text{ }\mu\text{m}$ thick paraffin sections to obtain representative and diagnostically relevant images. Due to the very limited section thickness in comparison with the size of the tissue, and the images are nearly two-dimensional, focusing up and down at high magnification provides a rough idea of the 3-D cellular characteristics, and such 3-D impression may be helpful or even essential in arriving at a certain diagnosis, especially for borderline lesions or tumors. However, in spite of the usefulness of such 3-D information about nuclei, conventional light microscopy is not always the ideal tool for 3D evaluation due to the interference of out-of-focus structures with the images of the focus plane studied. Much of the light emitted from the regions of specimen above and below the focal plane contributes to the out-of-focus blur, which seriously reduces the contrast and sharpness of the final image. Confocal laser scanning microscope allows the acquisition of optical sections from a thick specimen and out-of-focus blur can be reduced considerably and thus much sharper and clearer images will be obtained. CLSM has become an exciting new instrument in biomedical research because of its increased resolution over conventional light microscope and its utility for subsequent 3-D-reconstruction analysis^[5,6].

In this paper, the 3-D reconstruction have demonstrated 3-D contour of representative characteristics of normal liver cells, atypical hyperplasia liver cells, and HCC cells and the spatial relationship of nuclei, as well as the subtle structure of chromatin texture inside nuclei. This

paper emphasized the practical feasibility of CLSM and 3-D reconstruction from routine surgical histopathologic materials. To obtain desirable quality 3-D image from formalin-fixed, paraffin-embedded specimens, YOYO-1 iodide, a highly specific and sensitive (picogram sensitivity)^[7] DNA probe was utilized. Intense and homogeneous fluorescence was obtained by incubating the YOYO-1 iodide for 1h with agitation in the dark. To reveal subtle details of nuclear structure, RNA was removed by RNase predigestion, since nuclear RNA was stained by YOYO-1 iodide as well.

CLSM combines the three most advanced and important elements of our era, the microscope, the laser and the computer in one, moreover it is non-invasive and can be used on archival paraffin blocks. We anticipate that, in the future, pathologists may utilize these new techniques to make more precise diagnosis.

REFERENCES

- 1 Minsky M. Memoir on inventing the confocal scanning microscope. *Scanning*, 1988;10:128-138
- 2 Boon ME, Schut JJ, Suurmeijer AJ, Benita EM, Hut PK, Kok LP. Confocal microscopy of false-negative breast aspirates. *Diagn Cytopathol*, 1995;12:42-48
- 3 Liu S, Weaver DL, Taatjes DJ. Three-dimensional reconstruction by confocal laser scanning microscopy in routine pathologic specimens of benign and malignant lesions of the human breast. *Histochem Cell Biol*, 1997;107:267-278
- 4 Beil M, Irinopoulou T, Vassy J, Rigaut JP. Chromatin texture analysis in three-dimensional images from confocal scanning laser microscopy. *Anal Quant Cytol Histol*, 1995;17:323-331
- 5 White JG, Amos WB, Fordham M. An evaluation of confocal versus conventional imaging of biological structures by fluorescence light microscopy. *J Cell Biol*, 1987;105:41-48
- 6 Shotton DM. Electronic light microscopy: present capabilities and future prospects. *Histochem Cell Biol*, 1995;104:97-137
- 7 Tekola P, Baak JP, Belien JA, Brugghe J. Highly sensitive, specific, and stable new fluorescent DNA stains for confocal laser microscopy and image processing of normal paraffin sections. *Cytometry*, 1994;17:191-195

Direct technetium-99m labeling of anti-hepatoma monoclonal antibody fragment: a radioimmunoconjugate for hepatocellular carcinoma imaging

Hui Jie Bian¹, Zhi Nan Chen¹ and Jing Lan Deng²

Subject headings antibody, monoclonal; antibody fragments; technetium-99m; hepatocellular carcinoma; liver neoplasms; radioimmunoimaging

Bian HJ, Chen ZN, Deng JL. Direct technetium-99m labeling of anti-hepatoma monoclonal antibody fragment: a radioimmunoconjugate for hepatocellular carcinoma imaging. *World J Gastroentero*, 2000;6(3):348-352

Abstract

AIM To directly radiolabel an anti-hepatoma mAb fragment HAb18 F(ab')₂ with ^{99m}Tc by stannous-reduced method, and assess the stability, biodistribution and radioimmunoimaging (RII). **METHODS** Immunoreactive fraction was determined according to Lindmo's method. Ellman's reagent was used to determine the number of thiols in the reduced F(ab')₂. Labeling efficiency and homogeneity were measured by paper chromatography, sodium dodecylsulphate polyacrylamide gel electrophoresis (SDS-PAGE) and autoradiography. Challenge assay involved the incubation of aliquots of labeled antibody in ethylenediaminetetraacetate (EDTA) and L-cysteine (L-cys) solutions with different molar ratio at 37°C for 1 h, respectively. Investigations *in vivo* utilized nude mice bearing human hepatocellular carcinoma (HHCC) xenografts with gamma camera imaging and tissue biodistribution studies at regular intervals. **RESULTS** The labeling procedure was finished within 1.5 h compared with the "pretinning" method which would take at least 21 h. *In vitro* studies demonstrated that the radiolabeled mAb fragment was homogeneous and retained its immunoreactivity. Challenge studies indicated that ^{99m}Tc-labeled HAb18 F(ab')₂ in EDTA is more stable than in L-cys. Imaging and biodistribution

showed a significant tumor uptake at 24 h post-injection of ^{99m}Tc-labeled HAb18 F(ab')₂. The blood, kidney, liver and tumor uptakes at 24 h were 0.56 ± 0.09, 56.45 ± 11.36, 1.43 ± 0.27 and 6.57 ± 3.01 (%ID/g), respectively. **CONCLUSION** ^{99m}Tc-HAb18 F(ab')₂ conjugate prepared by this direct method appears to be an effective way to detect hepatoma in nude mice model.

INTRODUCTION

The introduction of mAbs as targeting devices in nuclear medicine is well developed and many different antibodies which labeled with a variety of isotopes have been reported in cancer diagnosis. It seemed that ^{99m}Tc is the most popular radionuclide for nuclear medicine imaging because of its favorable physical characteristics, low cost, and ready availability. ^{99m}Tc labeled mAb fragments should be superior to other big molecule radioimmunoconjugates for use in tumor RII. A number of methods have been proposed for ^{99m}Tc labeling proteins, and mAbs in particular. In general, these methodologies can be divided into two categories: indirect and direct methods^[1]. In indirect method the protein was modified with a technetium binding ligand and then reacted with a technetium complex. Several bifunctional chelating agents have been synthesized and used, such as diethylenetriaminepentaacetic acid (DTPA)^[2], diamide dimercaptide N₂S₂ ligands, and hydrazino nicotinamide analog^[3]. Although it is said that the indirect method can lead to loss of immunoreactivity, Joiris *et al.* have tested that the derivatization of antibody or fragment by iminothiolane does not split the protein and keeps the immunoreactivity^[4]. By direct method, ^{99m}Tc metal ion binds directly to endogenous donor groups on the antibody. The method is simple to perform and compatible with practical clinical use. However, direct labeling of mAbs with ^{99m}Tc was reported to be unstable due to non-specific binding (low and high-affinity)^[5,6], but some reports suggest an improved labeling of proteins with ^{99m}Tc.

¹Cell Engineering Research Center, Basic Medical Department, Fourth Military Medical University, Xi'an 710032, Shaanxi Province, China

²Department of Clinical Nuclear Medicine, Xijing Hospital, Xi'an 710033, Shaanxi Province, China

Supported by National Natural Science Foundation of China, No.39700175

Correspondence to: Prof. Zhi Nan Chen, Cell Engineering Research Center, Basic Medical Department, Fourth Military Medical University, Xi'an 710032, Shaanxi Province, China
Tel. 0086-29-3374545, Fax. 0086-29-3293906
Email. Chercr1@fmmu.edu.cn

Received 2000-02-03 Accepted 2000-04-28

In the Schwarz and Steinstrasser procedure, as modified by Mather and Ellison^[7], disulfide bridges in the mAb are reduced with 2-mercaptoethanol (2-ME). After purification, the resulting reduced antibody can be stored frozen until required for use. Labeling is accomplished by addition of stannous ion from a bone-scanning kit and pertechnetate. In addition to using regular reducing agents, such as 2-ME, stannous ions^[8], borohydride^[9], ascorbic acid^[10], dithionite^[11], or glutathione^[12] to generate sulphhydryl groups, other peculiar approaches also appeared recently. Direct ^{99m}Tc labeling of mAbs were finished by reduction of antibodies using photoactivation and insoluble macromolecular Sn (II) complex^[13,14]. With the development of direct method, there have been a few reports of successful use of this technique in colorectal, breast, and ovarian cancer imaging^[15-17].

In this report, we describe a direct method for radiolabeling anti-hepatoma monoclonal antibody fragment HAb 18F (ab')₂ with ^{99m}Tc . The stability and homogeneity of ^{99m}Tc -HAb18 F(ab')₂ were evaluated. The biodistribution and tumor localization in nude mice bearing a HHCC xenograft were studied.

MATERIALS AND METHODS

Monoclonal antibody

The mAb HAb18 is of murine IgG₁ isotype and was developed by our laboratory^[18]. F(ab')₂ fragment of HAb18 was generated by papain digestion with a molecular weight of 96 000 dalton^[19].

Tumors

Hepatocellular carcinoma grown in Balb/c mice was used as a prototype tumor model. Approximately 10⁷ HHCC cells obtained from Shanghai Cell Institute of Chinese Academy of Sciences were implanted in the left thigh of the animals and the tumors were allowed to grow for 8-10 days to approximately 1cm in diameter.

Antibody reduction

The antibody concentrated to 8 g/L in neutral PBS was reduced by reaction with a molar excess of stannous/glucoseheptonate (Sn/GH) ranging from 10:1 to 50:1 (Sn/GH: MAb) at 37°C for 15 min-30 min. The Sn/GH with a mass ratio of 1:100 was dissolved in 50mM acetate-buffered saline (ABS), pH 5.3 purged with nitrogen. The reduced antibody was isolated from reductant through a PD-10 column (Pharmacia) equilibrated with 0.05 mol/L ABS. The number of resulting free sulphhydryl groups was assayed with Ellman's reagent 5, 5'-dithio-bis (2-nitrobenzoic acid), (DTNB, Sigma Chemical Co., USA)^[20]. One hundred μL of sample was mixed with 20 μL of 0.01 mol/L-DTNB and diluted to

3 mL with 0.05 mol/L Tris-HCl buffer pH 8.4. The mixture was incubated at room temperature for 15 min and coloration measured with an UV/VIS spectrophotometer at 412 nm. The number of thiols was obtained by comparison with a series of L-cysteine (L-cys) standards ranging from 0.312 mg/L to 10 mg/L.

The integrity of the reduced F(ab')₂ was determined by non-reduced SDS-PAGE with 100 g/L gel using Vertical Gel Electrophoresis System (Bio-Rad). The gel was stained with Coomassie brilliant blue R250. Control experiments were run using unreduced mAb F(ab')₂.

Radiolabeling

For labeling, 160 μg of reduced HAb18 F(ab')₂ was mixed with a 10 μL -20 μL of diluted Sn/GH solution (0.2 g/L), and pertechnetium solution (0.2 mL, 74MBq), (Chinese Academy of Atomic Energy) was injected into the mixture. The Sn/GH solution was freshly prepared each time by dissolving 100 mg GH and 1mg SnCl₂·2H₂O in 5 mL of saline purged with nitrogen. The reaction mixture was incubated for 0.5 h-1 h at 37°C before it was analyzed by Whatman 3MM paper chromatography which was then developed in acetone or 100 g/L trichloroacetic acid (TCA). R-f values for acetone are: mAb 0.0, ^{99m}Tc -GH 0.0, and $^{99m}\text{TcO}_4$ -0.9-1.0. R-f values for 100 g/L TCA are: mAb 0.0, ^{99m}Tc GH 0, and $^{99m}\text{TcO}_4$ - 0.7. Labeled mAb was differentiated from ^{99m}Tc colloid by the method of Thrall *et al.*^[21]. The same strips impregnated with 10g/L-20g/L human serum albumin before development with 5:2:1, water: ethanol: 5N NH₄OH. Colloid remained on the bottom of the strip while mAb-bound isotope migrated with the solvent front.

The integrity of the labeled F(ab')₂ was assayed using the same non-reduced SDS-PAGE as described above. The gel was autoradiographed on x-ray film before stained with Coomassie brilliant blue R250.

Immunoreactivity assessment

The *in vitro* immunoreactivity of the radiolabeled HAb18 F(ab')₂ was evaluated by a live cell assay^[22]. Briefly, HHCC cells 5 × 10⁹/L were centrifuged (1 000r/min) for 5 min and washed twice with 1% bovine serum albumin (BSA) in PBS, then 5 serial 1:2 dilutions were made in 10 g/L BSA in Eppendorf tubes precoated with BSA. Radiolabeled HAb18 F(ab')₂ at a concentration of 40 ng/mL in 10 g/L BSA was added using a volume equal to half the volume of cell suspension. The total volume of cell-binding assay solution was 0.3 mL. After incubation for 2 h at 37°C, the total as well as the cell-bound radioactivity were counted in a gamma counter.

In Vitro stability studies

The stability was analyzed by using two different challenging agents, EDTA and L-cys. An aliquot of 50 μL $^{99\text{m}}\text{Tc}$ -HAb 18 F(ab')₂ solution was incubated with EDTA or L-cys at 37°C for 1 h. The molar ratio of mAb to challenging agent was at a maximum of 10 000:1. Dissociation ratio was analyzed on paper chromatography.

Biodistribution and imaging

Balb/c mice bearing HHCC were divided into three groups. Each group consisted of three animals and each animal received approximately 15 μg antibody with about 7.4MBq through a lateral tail vein. At time intervals of 4, 10 and 24 h postinjection, three groups of mice were killed, and imaged on a SPECT (Starcam 3 000, UK). Data were collected 100 000 counts per image and peak energy settings at the 140 keV (20%) window for $^{99\text{m}}\text{Tc}$. The blood and other organs of interest were collected. Tissues were washed, blotted, weighed and counted in a gamma counter. For each mouse, data are expressed as percent of injected dose per gram of tissue (%ID/g) after physical decay corrected.

RESULTS

Figure 1 represents the calibration curve for the determination of sulphhydryl groups using L-cys standards over a range of 0.312 to 10 mg/L, by plotting optical density at 412 nm versus L-cys standard concentrations after subtraction of the background due to Ellman's reagent. Linear regression was used and correlation coefficient 0.999 was obtained. Table 1 shows the influence of the reduction conditions on the number of free sulphhydryl groups detected by this thiol assay. As expected, increasing the molar ratio of Sn/GH to antibody in the reaction mixture does increase the number of apparent -SH groups per antibody, and increase the labeling efficiency correspondingly, which results in the labeling efficiency at a maximum of 84.2%. The free $^{99\text{m}}\text{TcO}_4^-$ and colloid amounts determined by Whatman 3MM paper using different developing systems were also showed in Table 1. In control experiments, labeling efficiency was 2% when unreduced HAb18 F(ab')₂ was used. SDS-PAGE by both staining and autoradiography showed that the radioactivity co-migrated with the proteins and that there were almost no protein fragments present within the 60:1 of molar ratio of Sn/GH to mAb (Figure 2). However, another SDS-PAGE in Figure 3 illustrates that fragmentation occurred during the reduction procedure when the molar ratio of Sn/GH to mAb was at 500:1.

As shown in Figure 4, the immunoreactive fraction, 0.84 was determined by plotting the inverse of the bound fraction compared with the inverse of the cell concentration, which is based on

the assumption that the total antigen concentration (cell concentration) is a good enough approximation for the free antigen concentration.

Challenging with EDTA did not remove $^{99\text{m}}\text{Tc}$ from the labeling conjugate remarkably, while L-cys at a molar ratio of 625:1 remove approximately one-tenth of the label (Figure 5).

Biodistribution of radioactivity in blood and excised tissues are displayed in Table 2. The preparation localized at the tumors was more than at any organ examined at both 10 h and 24 h after injection, except the kidneys. The lower radioactivity in blood at 24 h suggested fast blood clearance. The imaging results in Figure 6 showed significant tumor uptake at 24 h post-injection.

Table 1 Effect of molar ratio (Sn/GH: mAb) on quantity of -SH, free $^{99\text{m}}\text{TcO}_4^-$ and colloid and labeling efficiency (%), $n = 3$

Molar ratio (Sn/GH: mAb)	-SH groups /mAb	$^{99\text{m}}\text{TcO}_4^-$	colloid	labeling efficiency
Control	0 \pm 0	62.1 \pm 4.5	1.1 \pm 1.2	2.0 \pm 0.9
10:1	0.43 \pm 0.04	3.0 \pm 1.4	1.4 \pm 1.14	4.6 \pm 3.8
20:1	1.25 \pm 0.10	2.9 \pm 1.1	1.4 \pm 0.77	2.8 \pm 5.1
30:1	2.46 \pm 0.08	2.0 \pm 0.9	3.2 \pm 1.47	8.6 \pm 3.2
40:1	3.34 \pm 0.09	1.8 \pm 1.2	2.8 \pm 1.38	4.2 \pm 2.8
50:1	3.61 \pm 0.12	2.1 \pm 0.8	3.6 \pm 1.58	4.4 \pm 3.4

Table 2 Biodistribution of $^{99\text{m}}\text{Tc}$ -HAb 18F(ab')₂ in nude mice bearing hepatoma ($\bar{x} \pm s$, %ID/g)

Organ	Time after injection (h)		
	4	10	24
Blood	2.21 \pm 0.24	1.45 \pm 0.15	0.56 \pm 0.09
Kidney	72.38 \pm 4.37	70.47 \pm 15.23	56.45 \pm 11.36
Liver	1.82 \pm 0.48	1.59 \pm 0.31	1.43 \pm 0.27
Lung	1.62 \pm 0.34	1.40 \pm 0.17	0.75 \pm 0.21
Stomach	1.37 \pm 0.39	1.05 \pm 0.28	0.50 \pm 0.29
Spleen	2.35 \pm 0.81	2.11 \pm 0.75	1.82 \pm 0.85
Large intestine	1.16 \pm 0.34	1.42 \pm 0.39	0.94 \pm 0.32
Small intestine	0.97 \pm 0.31	0.95 \pm 0.18	0.62 \pm 0.24
Heart	2.04 \pm 0.55	1.83 \pm 0.48	1.17 \pm 0.42
Muscle	1.15 \pm 0.20	0.77 \pm 0.28	0.51 \pm 0.25
Brain	0.18 \pm 0.02	0.07 \pm 0.04	0.02 \pm 0.01
Tumor	5.14 \pm 2.26	5.84 \pm 2.98	6.57 \pm 3.01

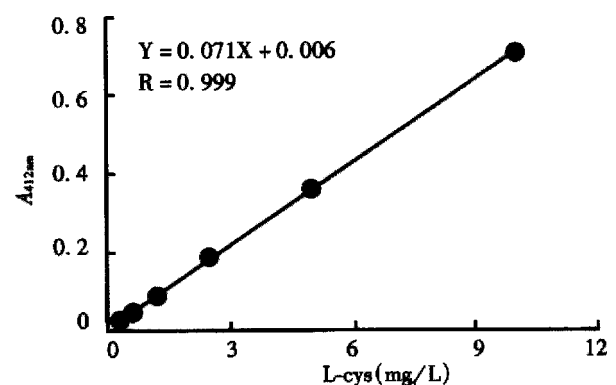


Figure 1 L-cysteine standard curve for sulphhydryl determination using Ellman reaction.

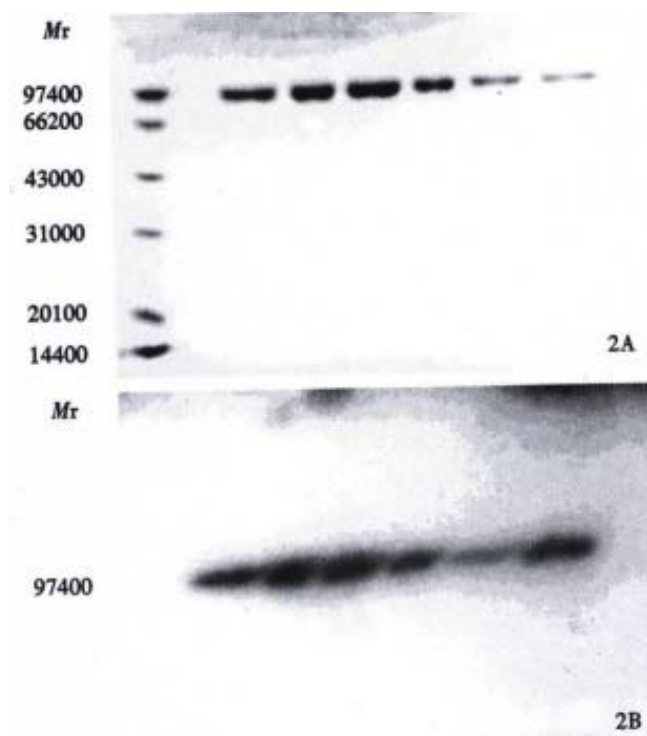


Figure 2 Effect of reduction on integrity of ^{99m}Tc -labeled HAb18 F(ab')₂ as monitored by SDS-PAGE. Vertical lanes represent molar ratios of Sn/2GH to HAb18 F(ab')₂: 1, 10:1; 2, 20:1; 3, 30:1; 4, 40:1; 5, 50:1; 6, 60:1. (A) Coomassie brilliant blue R250 staining. Molecular weight (kD) is indicated at the left. (B) autoradiography.

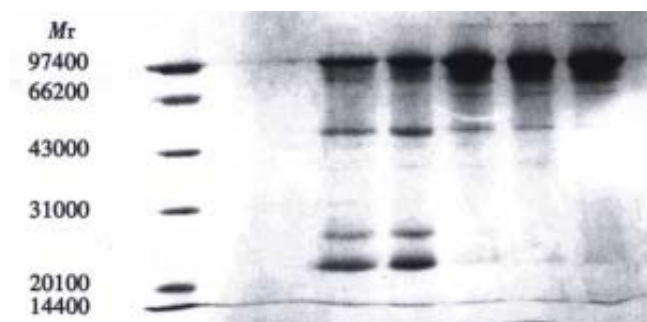


Figure 3 Effect of reduction on integrity of HAb18 F(ab')₂ as monitored by SDS-PAGE. Molecular weights (kD) are indicated at the left. Vertical lanes represent molar ratios of Sn/GH to HAb18 F(ab')₂: 1, 1000:1; 2, 500:1; 3, 50:1; 4, 10:1; 5, unreduced F(ab')₂.

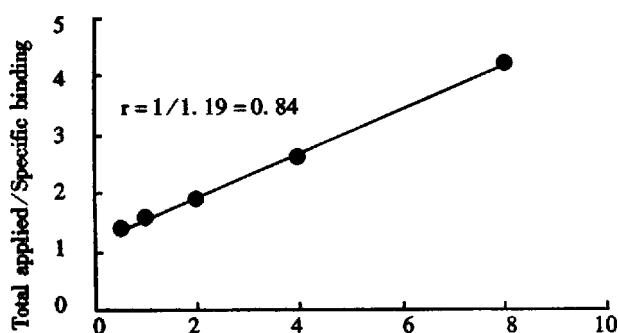


Figure 4 Binding assay for the determination of the immunoreactive fraction of ^{99m}Tc -labeled HAb18 F(ab')₂.

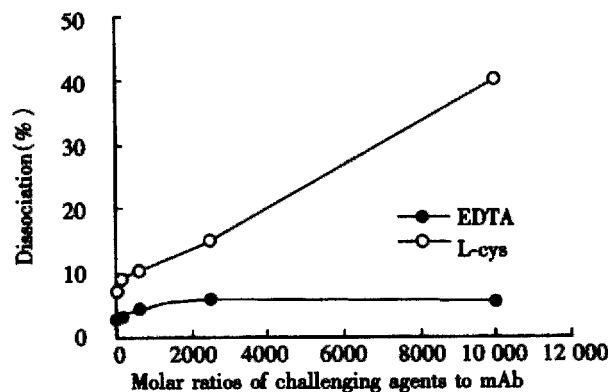


Figure 5 Dissociation of ^{99m}Tc -labeled HAb18 F(ab')₂ with increasing molar ratio of EDTA to mAb (●) and L-cys to mAb (○).

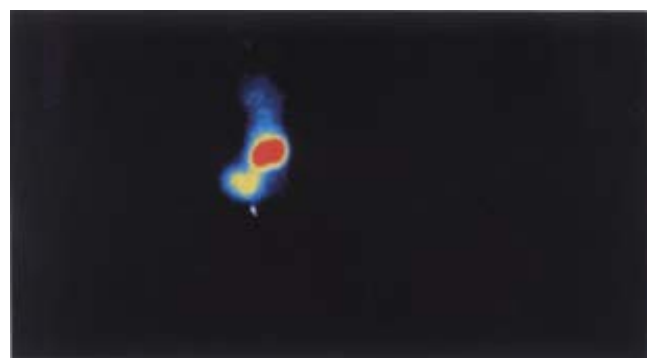


Figure 6 Images of nude mice bearing human hepatocellular carcinoma with ^{99m}Tc -HAb18 F(ab')₂ at 24 h.

DISCUSSION

Great efforts have been made to develop a method that can be used for the direct labeling of mAbs with ^{99m}Tc ^[16]. Earlier studies involved the incubation of mAbs with stannous phthalate tartrate solution for up to 21 h at room temperature, which was named “pretinning” method. Clinical success with this method has been claimed by the author^[23].

One aim of our study was to further evaluate the role of stannous as a reducing agent in the direct labeling of mAb F(ab')₂-2 with ^{99m}Tc . The difference between the “pretinning” method and this method is that we use GH instead of phthalate-tartrate as transfer ligand and stabilizer to avoid Sn or Tc-colloid formation. To do this, we investigated the effect of the quantity of Sn/GH on the labeling time and efficiency. When the molar ratio of Sn/GH to mAb F(ab')₂ was constant, we found that there was no obvious difference on the number of-SH between the reduction time of 20 min and 30 min or even longer^[24]. The whole labeling process can be accomplished within 1.5h. Hnatowich *et al.* reported that labeling efficiency in the case of the stannous ion-reduced antibodies was generally in excess of 70%^[12], however, in our method molar ratio of Sn/GH to mAb was an important parameter to obtain good labeling results, and molar ratio of 40:1 or higher were needed to get labeling

efficiency of more than 80% (Table 1). The low percentage of free $^{99m}\text{TcO}_4$ and radiocolloid in each sample implied that pH 5.3 and GH are the optimal pH value and transfer ligand. Under this condition, the labeled mAb HAb18 F(ab')₂ keeps its immunoreactivity. Autoradiography of SDS-PAGE had only one migration of component identical to that of native HAb18 F(ab')₂ determination by staining with Coomassie brilliant blue R250 (Figure 2), which demonstrated that Sn/GH reduction is mild and does not destroy interchain bridges in mAbs. Labeling efficiency of 2% in control experiments using unreduced HAb18 F(ab')₂ indicated that there was no exchange with the low affinity sites and also demonstrated that reduction of disulfides is a necessary initial step in ^{99m}Tc direct labeling of antibodies. The bond between ^{32}S H and Tc is stronger than that of N-Tc or O-Tc which was verified by the challenge assay of ^{99m}Tc -HAb18 F(ab')₂ in the presence of EDTA. We found that EDTA even at a molar ratio of 10 000:1 failed to remove a significant amount of ^{99m}Tc , this is in agreement with the results of Rhodes *et al*^[8]. But L-cys at 625 Å remove one-tenth of the label (Figure 5). Despite such instability of the label, there was no *in vivo* evidence of release of pertechnetate due to no thyroid imaging observed in the whole imaging process (Figure 7). Tumor localization of ^{99m}Tc -HAb18 F(ab')₂ was successfully demonstrated in a human tumor/nude mouse xenograft model. Biodistribution and imaging results showed the highest tumor uptake at 24 h post-injection. Where as kidney levels were found to be higher in the whole process. Accumulation of radioactivity in the kidney may be the result of retention of this metallic radionuclide by the kidney proximal tubule^[25], the possible release of ^{99m}Tc -labeled cysteine and glutathione^[26] stemming from the radioimmunoconjugate catabolism, and the relative amount of ^{99m}Tc -GH. A technique has been used in patients to block renal tubule uptake of ^{99m}Tc -anti-CEA Fab' fragments by amino acid infusion^[27].

In conclusion, a radioimmunoimaging conjugate for hepatoma detection was prepared by direct labeling mAb HAb18 F(ab')₂-with ^{99m}Tc using stannous/glucoheptonate as reducing agent. Although the labeling efficiency is not satisfactory to some degree, it has several advantages: simple, easy and quick, besides, the labeled mAb fragment retains its immunoreactivity. Biodistribution and imaging studies reveal that this conjugate is useful for the detection of hepatoma.

ACKNOWLEDGMENTS The authors are grateful to Dr. Wang Jing for mice imaging and the Department of Nuclear Medicine of Shaanxi People's Hospital for their support of this project.

REFERENCES

- Rhodes BA. Direct labeling of proteins with ^{99m}Tc . *Nucl Med Biol*, 1991; 18:667-676
- Childs RL, Hnatowich DJ. Optimum condition for labeling of DTPA coupled antibodies with Technetium-99m. *J Nucl Med*, 1985;26:293-299
- Ultee ME, Bridger GJ, Abrams MJ, Longley CB, Burton CA, Larsen SK, Henson GW, Padmanabhan S, Gaul FE, Schwartz DA. Tumor imaging with technetium-99m-labeled hydrazinonicotinamide-Fab' conjugates. *J Nucl Med*, 1997;38:133-138
- Joris E, Bastin B, Thomback JR. A new method for labeling of monoclonal antibodies and their fragments with technetium-99m. *Nucl Med Biol*, 1991;18:353-356
- Eckelman WC, Meinken G, Richards P. ^{99m}Tc -human serum albumin. *J Nucl Med*, 1971;12:707-710
- John E, Thakur ML, Wilder S, Alauddin MM, Epstein AL. Technetium-99m-labeled monoclonal antibodies: influence of technetium-99m binding sites. *J Nucl Med*, 1994;35:876-881
- Mather SJ, Ellison D. Reduction-mediated technetium-99m labeling of monoclonal antibodies. *J Nucl Med*, 1990;31:692-697
- Rhodes BA, Zamora PO, Newell KD, Valdez EF. Technetium-99m labeling of murine monoclonal antibody fragments. *J Nucl Med*, 1986;27:685-693
- Pauwels EKJ, Welling MM, Feitsma RIJ, Atsma DE, Nieuwenhuizen W. The labeling of proteins and LDL with ^{99m}Tc : a new direct method employing KBH₄ and stannous chloride. *Nucl Med Biol*, 1993;20:825-833
- Schwarz SW, Connett JM, Anderson CJ, Rocque PA, Philpott GW, Guo LW, Welch MJ. Evaluation of a direct method for technetium labeling intact and F(ab')₂ 1A3, an anticolorectal monoclonal antibody. *Nucl Med Biol*, 1994;21:619-626
- Qi P, Muddukrishna SN, Both RT, Rahn J, Chen A. Direct ^{99m}Tc -labeling of antibodies by sodium dithionite reduction, and role of ascorbate as a stabilizer in cysteine challenge. *Nucl Med Biol*, 1996;23:827-835
- Hnatowich DJ, Virzi F, Fogarasi M, Rusckowski M, Winnard-JR P. Can a cysteine challenge assay predict the *in vivo* behavior of ^{99m}Tc -labeled antibodies. *Nucl Med Biol*, 1994;21:1035-1044
- Sykes TR, Woo TK, Baum RP, Qi P, Noujaim AA. Direct labeling of monoclonal antibodies with technetium 99m by photoactivation. *J Nucl Med*, 1995;36:1913-1922
- Nakayama M, Wada M, Araki N, Ginoza Y, Terahara T, Harada K, Sugh A, Tomiguchi S, Kojima A, Hara M, Takahashi M. Direct ^{99m}Tc labeling of human immunoglobulin with an insoluble macromolecular Sn (II) complex. *Nucl Med Biol*, 1995;22:795-802
- Rosenzweig HS, Ranadive GN, Seskey T, Epperly MW, Bloomer WD. A novel method for the non-chromatographic purification of technetium-99m-labeled monoclonal antibodies: a study with B72.3 monoclonal antibody. *Nucl Med Biol*, 1994;21:171-178
- Alauddin MM, Khawli LA, Epstein AL. An improved method of direct labeling monoclonal antibodies with ^{99m}Tc . *Nucl Med Biol*, 1992;19:445-454
- Gooden CSR, Snook DE, Maraveyas A, Rowlinson BG, Peters AM, Epenetos AA. Direct technetium 99m labeling of three anticancer monoclonal antibodies: stability, pharmacokinetics and imaging. *J Nucl Med*, 1995;36:842-849
- Chen ZN, Liu YF, Yang JZ. Anti human hepatocellular carcinoma monoclonal antibody and immunohistochemical location of associated antigen P60. *Dankelong Kangti Tongxun*, 1989;2:33-36
- Qiu K, Chen ZN, Liu ZG, Wang Q, He FC, Qu P, Mi L, Sui YF, Liu YF. Preparation of anti hepatoma mAb HAb18 F(ab')₂ and Fab fragments by papain digestions in different conditions. *Disi Junyi Daxue Xuebao*, 1995; 16:414-417
- Ellman GL. Tissue sulphydryl groups. *Arch Biochem Biophys*, 1959;82:70-77
- Thrall JH, Freitas JE, Swanson D, Rogers WL, Clare JM, Brown ML, Pitt B. Clinical comparison of cardiac blood pool visualization with technetium-99m red blood cells labeled *in vivo* and with technetium-99m human serum albumin. *J Nucl Med*, 1978;19:796-803
- Lindmo T, Boven E, Cuttitta F, Fedorko J, Bunn-Jr PA. Determination of the immunoreactive fraction of radiolabeled monoclonal antibodies by linear extrapolation to binding at infinite antigen excess. *J Immun Med*, 1984;72:77-89
- Morrison RT, Lyster DM, Alcorn L, Rhodes BA, Breslow K, Burchiel SW. Radioimmunoimaging with ^{99m}Tc monoclonal antibodies: clinical studies. *Int J Nucl Med Biol*, 1984;11:184-188
- Bian HJ, Chen ZN, Deng JL, Duan XD, Mi L, Yu XL, Xu LQ. Direct labeling of anti hepatoma monoclonal antibody fragment with ^{99m}Tc by an improved pretinning method. *Tongweisu*, 1999;12:90-94
- Granowska M, Mather SJ, Britton KE, Bentley S, Richman P, Phillips RKS, Northover JMA. ^{99m}Tc radioimmunosintigraphy of colorectal cancer. *Br J Cancer*, 1990;62(Suppl X):30-33
- Hnatowich DJ, Mardrossian G, Rusckowski M, Fogarasi M, Virzi F, Winnard-Jr P. Directly and indirectly technetium-99m-labeled antibodies-a comparison of *in vitro* and animal *in vivo* properties. *J Nucl Med*, 1993;34:109-119
- Behr TM, Becker WS, Sharkey RM, Juweid ME, Dunn RM, Bair HJ, Wolf FG, Goldenberg DM. Reduction of renal uptake of monoclonal antibody fragments by amino acid infusion. *J Nucl Med*, 1996;37:829-833

Effect of intestinal ischemia-reperfusion on expressions of endogenous basic fibroblast growth factor and transforming growth factor β in lung and its relation with lung repair

Xiao Bing Fu, Yin Hui Yang, Tong Zhu Sun, Xiao Man Gu, Li Xian Jiang, Xiao Qing Sun and Zhi Yong Sheng

Subject headings lung; intestinal ischemia-reperfusion injury; basic fibroblast growth factor; transforming growth factor β

Fu XB, Yang YH, Sun TZ, Gu XM, Jiang LX, Sun XQ, Sheng ZY. Effect of intestinal ischemia-reperfusion on expressions of endogenous basic fibroblast growth factor and transforming growth factor β in lung and its relation with lung repair. *World J Gastroentero*, 2000;6(3):353-355

Abstract

AIM To study the changes of endogenous transforming growth factor β (TGF β) and basic fibroblast growth factor (bFGF) in lung following intestinal ischemia and reperfusion injury and their effects on lung injury and repair.

METHODS Sixty Wistar rats were divided into five groups, which underwent sham-operation, ischemia (45 minutes), and reperfusion (6, 24 and 48 hours, respectively) after ischemia (45 minutes). Immunohistochemical method was used to observe the localization and amounts of both growth factors.

RESULTS Positive signals of both growth factors could be found in normal lung, mainly in alveolar cells and endothelial cells of vein. After ischemia and reperfusion insult, expressions of both growth factors were increased and their amounts at 6 hours were larger than those of normal control or of 24 and 48 hours after insult.

CONCLUSION The endogenous bFGF and TGF β expression appears to be up-regulated in the lung following intestinal ischemia and reperfusion, suggesting that both growth factors may be involved in the process of lung injury and repair.

INTRODUCTION

Our previous investigations have shown that basic fibroblast growth factor (bFGF) and transforming growth factor β (TGF β) play important roles in organ injury and repair after ischemia and reperfusion insult, and that there was a significant relationship between gene expression of bFGF or TGF β and lung repair^[1,2]. Because many growth factors are involved in wound repair by their mitogenic and non-mitogenic effects, we have further investigated the alteration of endogenous bFGF and TGF β in the lung tissue following intestinal ischemia-reperfusion injury and explored their effects on lung repair as well.

MATERIALS AND METHODS

Animal model and tissue preparation

Sixty male, pathogen-free Wistar rats, weighing 250 g \pm 10 g were used in this study. They were divided into 5 groups, which underwent sham-operation, ischemia for 45 minutes, and reperfusion for 6 hours, 24 hours and 48 hours after ischemia for 45 minutes, respectively. Anesthesia was induced by administration of 30 mg/kg of pentobarbital sodium. Following midline laparotomy, intestinal ischemia was achieved by complete occlusion of the superior mesenteric artery (SMA) with a non-crushing microvascular clip. Reperfusion was performed by removal of the microvascular clip after 45 minutes SMA occlusion. All animals were killed by exsanguination at designated times. The samples from right base of lung were obtained immediately and fixed in 10% formalin for analysis. All procedures but SMA clip were done in animals of sham-operated control group.

Immunohistochemical detection for bFGF and TGF β

Immunohistochemical detection was made using polyclonal anti-bFGF or TGF β antibody (Santa Cruz Co. and Zymed Co., respectively) by an indirect streptavidin/peroxidase (SP) technique. Experiments were performed following the manufacturer's recommendation. Paraffin-embedded sections were incubated with polyclonal anti-rat bFGF or TGF β antibody for 12 hours at 4°C

Research Laboratory, 304th Hospital of PLA, Beijing 100037, China
Dr. Xiao Bing Fu, graduated from the Third Military Medical University as a Master of Medicine in 1988 and University of Madrid, Spain as a Doctor of Medicine, professor and head of research laboratory, majoring in wound healing, multiple organ injury and biology of growth factors, having 160 papers and 3 books published.

Project supported by the National Grant for Outstanding Young Researchers of China, No.39525024

Correspondence to: Dr. Xiao Bing Fu, 304th Hospital, 51 Fu Cheng Road, Beijing 100037, China
Tel. 0086-10-66867396, Fax. 0086-10-88416390
Email. FuXB@cgw.net.cn

Received 2000-01-15 **Accepted** 2000-03-01

after antigen repair. Biotinylated IgG was added as second antibody. Horseradish peroxidase labeled streptomycin-avidin complex was used to detect second antibody. Slides were stained with diaminobenzidine, and examined under light microscope. The brown or dark brown stained cytoplasm and/or cell membrane was considered as positive. The phosphate-buffered saline (PBS) solution was used as negative control.

Statistical analysis

The slides from 5 animals in each group were used for observation and statistical analysis. One visual field in each slide was randomly selected and observed under light microscope with 400-fold magnification. The percentage of positive immunohistochemical staining cells was expressed as mean \pm SD. Statistical analyses were performed using paired *Student's t* test. $P < 0.05$ was considered significant.

RESULTS

Pathological alternations of lung tissue

The histological structure of alveolar and mesenchymal cells was normal in healthy lungs, while the lung tissues from ischemia and reperfusion rats were significantly damaged, with pulmonary edema and inflammatory cell infiltration.

Expression of bFGF and TGF β

Both bFGF and TGF β were expressed in alveolar epithelial cells and microvascular endothelial cells of normal lung tissues. The positive signals were of immunohistochemical staining in brown or dark brown color and localized in cytoplasm and/or membrane when observed under light microscopy (Figure 1A and B). After ischemia, the expressions of both bFGF and TGF β were increased, especially in the area of alveolar epithelial cells and capillary endothelial cells (Figure 2A and B). At 6 hours postinjury, the expression of bFGF was the same as that in the early injury, while that of TGF β was increased significantly. Many positive cells were type I alveolar cells (Figure 3A and B). Up to 24 hours and 48 hours postinjury, the expression of both growth factors returned to basal levels. By quantitative analysis, the expressions of both bFGF and TGF β were quite different in the early injury when compared with those of control group ($P < 0.01$, Table 1).

Table 1 Expression of bFGF and TGF β in lung following ischemia-reperfusion injury ($\bar{x} \pm s$)

Groups	Animals	bFGF	TGF β
Sham-operated	5	15.4 \pm 3.4	20.0 \pm 5.1
Ischemia 45min	5	61.8 \pm 7.5 ^b	63.4 \pm 7.0 ^b
Reperfusion 6h	5	42.4 \pm 10.1 ^b	50.6 \pm 7.1 ^b
Reperfusion 24h	5	29.0 \pm 5.5 ^b	32.8 \pm 8.7 ^a
Reperfusion 48h	5	15.6 \pm 3.3	19.4 \pm 7.1

^a $P < 0.05$, ^b $P < 0.01$, vs sham-operated.

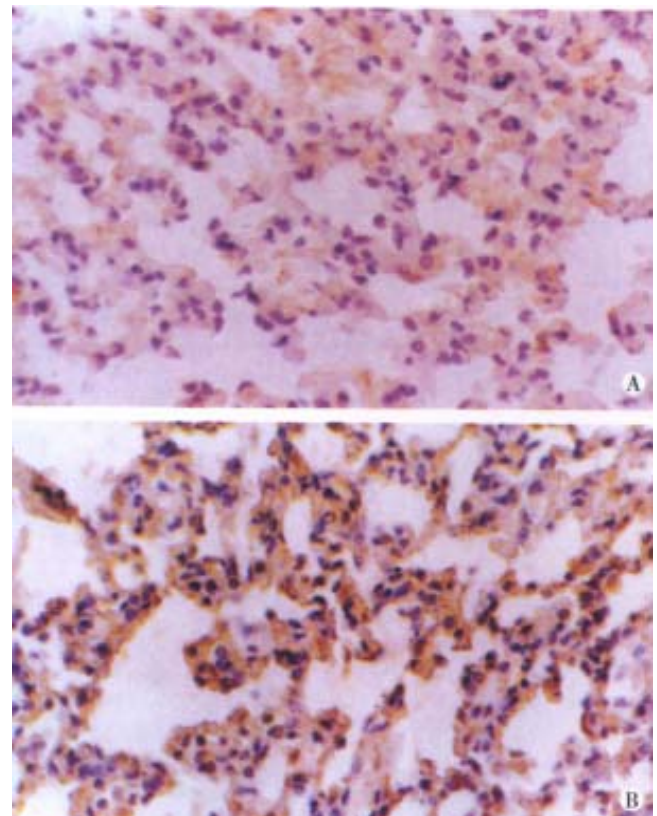


Figure 1 The expressions of bFGF and TGF β in normal lung. The weakly positive signal could be found in alveolar epithelial cells and microvascular endothelial cells. SP stain $\times 400$

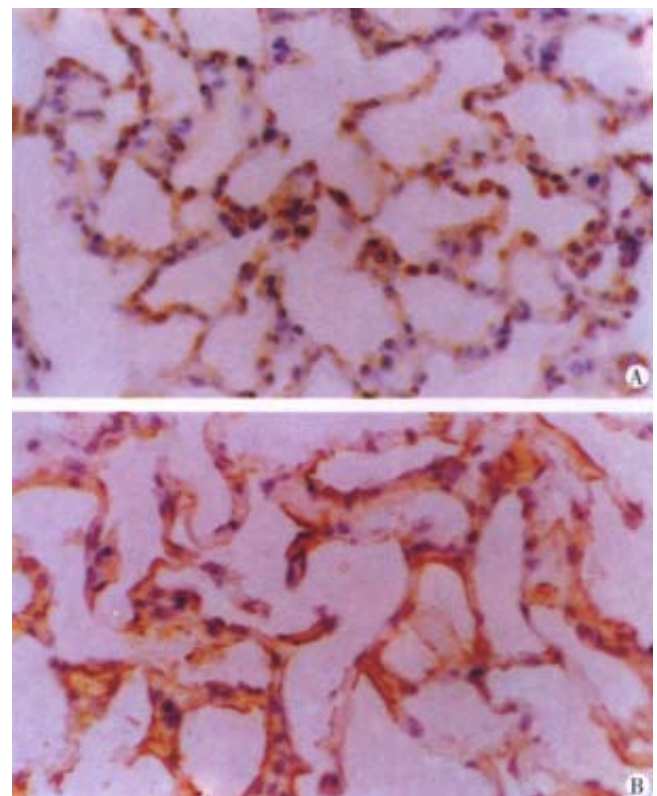


Figure 2 The expressions of bFGF and TGF β in damaged lung following ischemia (45 minutes) and reperfusion (6 hours). Deep staining of both growth factors could be found in alveolar epithelial cells and microvascular endothelial cells. SP stain $\times 400$

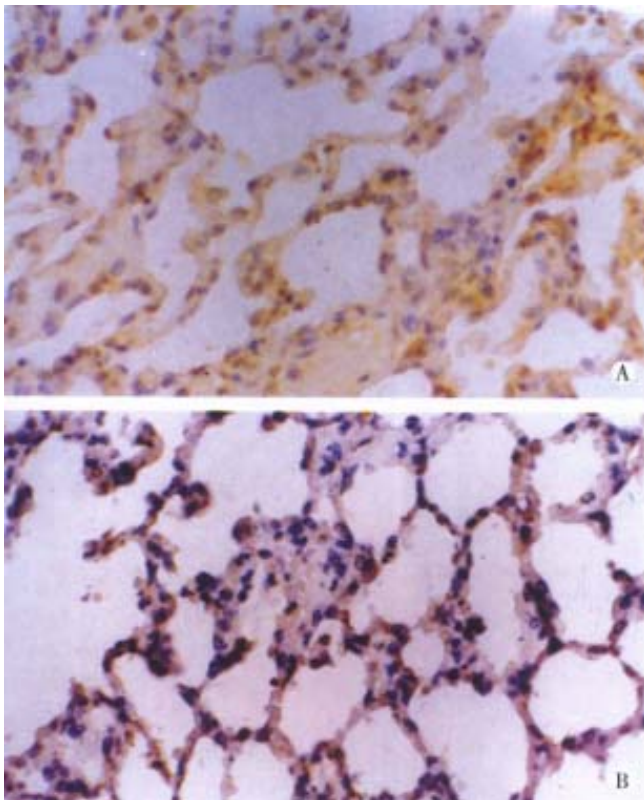


Figure 3 The expressions of bFGF and TGF β in damaged lung following ischemia (45 minutes) and reperfusion (24 hours). The staining of both growth factors could be found in alveolar epithelial cells and microvascular endothelial cells and the expression returned to normal levels. SP stain $\times 400$

DISCUSSION

The lung is one of the very important target organs in multiple organ dysfunction syndrome (MODS) or multiple system organ failure (MOSF) caused by severe injury^[3]. It has been found that in addition to the direct trauma, the lung could also be damaged by indirect injury such as shock, gut ischemia, reperfusion insult, etc. Under the condition of an inadequate mucosal blood flow, the gut barrier function can be progressively impaired and invaded by bacteria or endogenous endotoxin. This process is associated with activation of systemic inflammatory mediators including bacteriotoxin, inflammatory mediators, such as tumor necrosis factor (TNF) and interleukin (IL) and immunocytokines. The tissue damage was manifested as increased inflammatory reaction, low content of ATP in tissue, alveolar endothelial cell damage, enhanced permeability of microcirculation, etc.^[4]. In severe cases, the animal would die of pulmonary failure. But most commonly, these changes are maintained brief because the lung has the ability of self-repair. Recent studies demonstrated that one of the important mechanisms of self-protection and self-repair was the effect of endogenous growth factor and/or nitric oxide synthetase^[2,5]. Therefore, the

localization and quantitation of endogenous growth factors play important roles in lung repair.

Both bFGF and TGF β are important growth factors involved in tissue repair. They are involved in dermal and epidermal wound healing via their chemotactic effects for inflammatory cells and mitogenic effects for tissue cells, such as epidermal cells, fibroblasts and endothelial cells. Normally, TGF β is stored and released from platelets and macrophages, while bFGF combined with heparin is stored in endothelial cells in an inactive form. Both the growth factors are involved in the process of capillary reconstruction and tissue regeneration by their mitogenic and non-mitogenic effects. At the same time, they can also be relieved from injured tissues^[6,7]. Our previous researches have indicated that severe trauma results in histological damage, further decreasing the endogenous growth factors. Thus, it is necessary to supply exogenous growth factors to promote internal organ repair. We have also found that slight ischemia can induce the expression of endogenous factors, and these growth factors participate in the process of wound healing^[8,9]. We also investigated the gene expression of both growth factors in the same animal model, and found that the changes of these gene expressions were consistent with the changes of their proteins. On the basis of these studies, we came to a conclusion that there is a positive relationship between growth factors and tissue repair, and induction of endogenous bFGF and TGF β by ischemia is necessary for tissue repair. By the end of tissue repair, they are restored in tissue again. This result demonstrates that growth factors are involved in organ repair by their increased synthesis or released from damage cells after ischemia-reperfusion insult.

REFERENCES

- 1 Fu XB. Treatment of internal organ damage by growth factors. *Xin Xiaohuabingxue Zazhi*, 1997;5:663-664
- 2 Yang YH, Fu XB, Sun TZ, Wang YP, Sheng ZY. bFGF and TGF β gene expression in rat lung after ischemia reperfusion. *Jiefangjun Yixue Zazhi*, 1998;23:405-409
- 3 Guan J, Jin DD, Jin LJ. [JP2]Apoptosis in rat lung after shock caused by multiple injuries. *Zhongguo Weizhongbing Jijiu Yixue*, 1998;10:479-483
- 4 Turnage RH, Guice KS, Oldham KT. Endotoxemia and remote organ injury following intestinal reperfusion. *J Surg Res*, 1994; 56:571-578
- 5 Turnage RH, Kadesky KM, Bartula L. Intestinal reperfusion injury up regulates inducible nitric oxide synthase activity within the lung. *Surgery*, 95;118:288-293
- 6 Muthukrishnan L, Warder E, McNeil PL. Basic fibroblast growth factor is efficiently released from a cytosolic storage site through plasma membrane disruptions of endothelial cells. *J Cell Physiol*, 1991;148:1-6
- 7 Sporn MB, Roberts AB. Transforming growth factor-beta: recent progress and new challenges. *J Cell Biol*, 1992;199:1017-1021
- 8 Fu XB, Cuevas P, Gimenez-Gallego G, Tian HM, Sheng ZY. Ischemia and reperfusion reduce the endogenous basic fibroblast growth factor in rat skeletal muscles: an immunohistochemical study. *Wound Rep Reg*, 1996;4:381-385
- 9 Fu XB, Yang YH, Li XK, Sun TZ, Wang YP, Sheng ZY. Ischemia and reperfusion impair the gene expression of endogenous basic fibroblast growth factor (bFGF) in rat skeletal muscles. *J Surg Res*, 1998;80:88-93

Analysis of *in vivo* patterns of caspase 3 gene expression in primary hepatocellular carcinoma and its relationship to *p21^{WAF1}* expression and hepatic apoptosis

Bao Hua Sun, Jun Zhang, Bao J¹ Wang, Xi Ping Zhao, You Kun Wang, Zhi Qun Yu, Dong Liang Yang and Lian Jie Hao

Subject headings carcinoma, hepatocellular; caspase 3; apoptosis; liver neoplasms; gene expression

Sun BH, Zhang J, Wang BJ, Zhao XP, Wang YK, Yu ZQ, Yang DL, Hao LJ. Analysis of *in vivo* patterns of caspase 3 gene expression in primary hepatocellular carcinoma and its relationship to *p21^{WAF1}* expression and hepatic apoptosis. *World J Gastroentero*, 2000;6(3): 356-360

Abstract

AIM To detect the expression of caspase 3 gene in primary human hepatocellular carcinoma (HCC) and investigate its relationship to *p21^{WAF1}* gene expression and HCC apoptosis.

METHODS *In situ* hybridization was employed to determine caspase 3 and *p21^{WAF1}* expression in HCC. *In situ* end-labeling was used to detect hepatocytic apoptosis in HCC.

RESULTS Twenty-one of 39 (53.8%) cases of HCC were found to express caspase 3 transcripts, while 46.2% of HCC failed to express caspase 3. Non-cancerous adjacent liver tissues showed more positive caspase 3 (87.5%, 7/8) as compared with HCC ($P < 0.05$). The expression of caspase 3 is correlated with HCC differentiation, 72.2% (13/18) of moderately to highly differentiated HCC showed caspase 3 transcripts positive, while only 38.1% of poorly differentiated HCC harbored caspase 3 transcripts ($P < 0.05$). No relationship was found between caspase 3 expression and tumor size or grade or metastasis, although 62.5% (5/8) of HCC with metastasis were caspase 3 positive and a little higher than that with no metastasis (51.6%, $P > 0.05$). Expression of

caspase 3 alone did not affect the apoptosis index (AI) of HCC. The AI was 7.12% in caspase 3-positive tumors ($n = 21$), while in caspase 3-negative cases ($n = 18$) 6.59% ($P > 0.05$). Expression of caspase 3 clearly segregated with *p21^{WAF1}* positive tumors as compared with *p21^{WAF1}* negative cases (16 of 23, 69.6% versus 5 of 16, 31.3%) with statistical significance ($P = 0.017$). In the cases with positive caspase 3 and negative *p21^{WAF1}*, the AI was found slightly higher, but with no statistical significance, than that with expression of *p21^{WAF1}* and caspase 3 (7.21% vs 6.98%, $P > 0.05$).

CONCLUSION Loss of caspase 3 expression may contribute to HCC carcinogenesis, although the expression of caspase 3 does not correlate well with cell apoptosis in HCC. *p21^{WAF1}* may be merely one of the inhibitors which can reduce caspase 3 mediated cell apoptosis in HCCs.

INTRODUCTION

Hepatocellular carcinoma (HCC), representing 80%-90% of the primary liver cancer, is one of the leading causes of cancer morbidity and mortality on a global scale. More than 80% of liver cancer cases occur in the developing world, especially in China, where HCC is the second cause of cancer death and responsible for 130 000 deaths every year^[1]. Despite dramatic advances in basic and clinical research in the past decades, the exact molecular mechanism for hepatocarcinogenesis is unclear. Gene expression changes have been demonstrated in accordance with cell growth, differentiation and carcinogenesis^[2]. Tumor formation can result from a decrease in cell death, as well as an increase in cell proliferation. In addition to altered expression of cell cycle-related gene, dysregulation of apoptosis (programmed cell death) is thought to contribute to cancer by aberrantly extending cell viability and favoring the accumulation of transforming mutations^[3].

Department of Clinical Immunology, Tongji Hospital, Tongji Medical University, Wuhan 430030, Hubei Province, China

Dr. Bao Hua Sun, graduated from the Department of Pathology of Tongji Medical University in 1997, Postdoctor, currently engaged in apoptosis research of hepatocellular carcinoma, having 17 papers published.

Correspondence to: Dr. Dong Liang Yang, Department of Clinical Immunology, Tongji Hospital, Tongji Medical University, Wuhan 430030, Hubei Province, China

Tel. 0086-27-83662570

Email. bhsun@yahoo.com

Received 2000-01-01 Accepted 2000-01-15

Caspase is a large family which contains at least 14 members. It has been shown that caspase play an important role in regulating cancer cell death both induced by activated lymphocytes through Fas/FasL pathway and by chemotherapy agents^[4]. Caspase 3 or cpp32 is the key member of effector caspases. Caspase 3 had overexpression in B-cell chronic lymphocytic leukemia (B-CLL)^[5], acute myelogenous leukemia (AML)^[6], follicular small cleaved cell non-Hodgkin's B-cell lymphomas^[7,8], human breast cancer cell lines and primary breast tumors^[9] and neuroblastomas^[10]. Caspase 3 is a potent protease which can cleave a large scale of substrate, including cell-cycle related genes such as p21^{WAF1}^[4]. p21^{WAF1} is a cyclin-dependent kinase inhibitor and plays an important role in DNA damage-induced growth arrest. p21^{WAF1} overexpression can cause G₁ cell cycle arrest and further interrupt the apoptotic process at a point upstream from caspase 3 activation^[11]. In this study, we investigated the expression of caspase 3 in primary human HCC and its potential impact on tumor cell apoptosis and its relationship to p21^{WAF1} expression.

MATERIALS AND METHODS

Patients and samples

The surgically resected specimens employed in this study were obtained from consecutive patients with primary HCC who had undergone potentially curative tumor resection at the Department of General and Hepato-Biliary Surgery, Tongji Hospital during 1996-1997. A cohort of 39 cases was involved in this study. All cases were selected on the basis of availability of frozen material for study and on the absence of extensive chemotherapy-induced tumor necrosis. Materials were composed of 3 cases of grade I, 18 cases of grade II, 11 cases of grade III, the remaining 7 cases were grade IV according to TNM system (1987). The tumor lesions analyzed here included 21 poor, 9 moderate and 9 well differentiations. There were 34 males and 5 females, and the age ranged from 24 to 71 years with an average of 46.1 (SD, 12.5). Eight cases of non-cancerous adjacent liver tissues were also included in the study. Routinely processed 40 g/L paraformaldehyde-fixed, paraffin-embedded blocks containing principal tumor were selected. Serial sections of 5 μ m were prepared from the cut surface of blocks at the maximum cross-section of the tumor.

In situ hybridization staining for caspase 3 and p21^{WAF1} and scoring methods for its expression

The plasmid pET21b-cpp32 containing caspase 3 (cpp32) cDNA probe was kindly provided by Dr. JC. Reed (La Jolla, USA). After digestion with *Xho*I and *Nde*I, the fragment was separated by

electrophoresis through an agarose gel and recovered by QIA quick gel extraction kit (QIAGEN) using a micro-centrifuge according to the manufacturer's protocol. The p21^{WAF1} cDNA probe was kindly provided by Dr. SJ Elledge (Houston, USA). Preparation of p21^{WAF1} probe was described previously^[12]. The probes were labeled and detected using a Dig DNA labeling and detection kit (Boehringer Mannheim Biochemica, Germany). Briefly, 40g/L paraformaldehyde-fixed paraffin embedded samples were cut at 5 μ m and adhered to APES-treated slides. After deparaffinized and rehydrated through a graded series of ethanol, the sections were immersed in a 0.01 mol/L DEPC-treated PBS (pH 7.4) two times each for 5min, and then, in PBS containing 100 mmol/L glycine and PBS containing 3 mL/L Triton X-100 for 5 min in turns. Sections were permeabilized for 30 min at 37°C with TE buffer (100 mmol/L Tris-HCl, 50 mmol/L EDTA, pH 8.0) containing 10 mg/L RNase-free proteinase K and washed with DEPC-treated PBS, then incubated at 42°C for 2 h with pre-hybridization buffer. Hybridization solution (400 mL/L deionized formamide, 500 g/L dextra sulfate, 1 \times Dehardt's reagent, 4 \times SSC, 10 mmol/L DTT, 1 g/L yeast tRNA, 1 g/L denatured salmon sperm DNA) containing 2 mg/L probe overlay each section after deprive prehybridization buffer from slides and hybridize at 42°C for 36 h in a humid chamber. The sections were washed in a shaking water bath at 37°C in 2 \times SSC, 1 \times SSC, 0.1 \times SSC for 15 min each, then washed with buffer I (100mmol/L Tris-HCl, pH 7.5, 150 mmol/L NaCl) for 20 min and with blocking solution (buffer I containing 20 mL/L normal sheep serum) for 30 min, and added sheep anti-Dig-alkaline phosphates (diluted at 1:800 in buffer I) and incubated for another 1h before development by NBT at 37°C for 3 h in the dark. Hybridization buffer containing no probe was used for negative control for each staining. Scoring method for caspase 3 and p21^{WAF1} expression was described by Kawasaki^[13]. Positive tumor cells were quantified by two independent observers, and the average percentage of positive tumor cells was determined in at least 5 areas at \times 400 and assigned to one of five categories: (a) 0, <1%; (b) 1, 1%-25%; (c) 2, 25%-50%; (d) 3, 50%-75% and (e) 4, >75%. The ISH staining intensity was scored as (a) weak 1+; (b) moderate, 2+; and intense, 3+. For tumors showing heterogeneous staining, the predominant pattern was taken into account for scoring. The percentage of positive tumor cells and staining intensity were multiplied to produce a weighted score for each case. Cases with weighted scores <1 were defined as negative, otherwise were defined as positive.

Histochemical detection of apoptosis and

determination of the AI

Tumor cell apoptosis was identified by DNA fragmentation detection kit (QIA33-kit, Calbiochem). Briefly, deparaffinized and rehydrated sections were permeated with proteinase K (20 mg/L in 10 mmol/L Tris, pH 8.0) for 20 min at room temperature and washed with $1 \times$ TBS (20 mmol/L Tris pH 7.6, 140 mmol/L NaCl). After endogenous peroxidases were inactivated by using 30 mL/L hydrogen peroxide for 5 min and washed with $1 \times$ TBS, equilibration buffer was added to each section and incubated at room temperature for 20 min. Terminal deoxynucleotidyl transferase (TDT) enzyme in TDT labeling reaction mix at a 1:20 dilution was pipetted onto the sections, followed by 1.5 h incubation at 37°C. After the reaction was terminated by immersing sections into stop solution and washed with blocking buffer for 10 min at room temperature, the anti-digoxigenin-peroxidase was added to the sections. DAB solution was used for color development. Sections were counterstained by methyl green. A positive control generated covering specimen with DNase I (1 mg/L) for the first procedure. Specific positive tissue sections were used for negative control by substituting distilled water for the TDT in the reaction mixture. The AI was expressed as the ratio of positively stained tumor cells and bodies to all tumor cells, given a percentage for each case. A minimum of 1 000 cells was counted under a 400-fold magnification. Positively staining tumor cells with morphological characteristics of apoptosis were identified using standard criteria, including chromatin condensation, nuclear disintegration and formation of crescentic caps of condensed chromatin at the nuclear periphery.

Statistical analysis

Variables associated with caspase 3 expression as well as the relationship between caspase 3 and p21^{WAF1} were analyzed by χ^2 test. Differences in the tumor cell AI for groups dichotomized according to caspase 3 expression were checked by independent *t* test.

RESULTS

Expression of caspase 3 gene in HCCs

By ISH staining, caspase 3 transcripts was detected predominantly in cytoplasm (Figure 1). Consistent with the presence of caspase 3 protein in human biopsy liver samples, expression of caspase 3 in non-cancerous adjacent liver tissue was also observed in 87.5% (7/8) of cases. The intensity of caspase 3 staining was heterogeneous within a case detected. The tumor cells positively stained by ISH range from 10% to 90%, depending on the cases

examined. After multiplying the weighted caspase 3 score, 21 cases of HCC in the present study were defined as positive (53.8%), with weighted caspase 3 score from 1 to 12.

The expression of caspase 3 and its association with clinicopathological variables

A clinicopathological analysis of caspase 3 positive cases is shown in Table 1. No statistical significance was observed in the prognostic parameters, including tumor size, metastasis, TNM grade, analyzed in the present study except for differentiation. The expression of caspase 3 is correlated with HCC differentiation. It was found that as high as 72.2% (13/18) of moderately to highly differentiated HCC showed caspase 3 transcripts positive, while only 38.1% of poorly differentiated HCC harbored caspase 3 transcripts ($P < 0.05$).

Relationship between caspase 3 and p21^{WAF1}

Twenty-three cases were detected expression p21^{WAF1} transcripts. Positive signal was predominantly located in cytoplasm with a heterogeneous distribution of positive tumor cells. The significance of p21^{WAF1} gene expression was discussed in our previous study^[12]. Expression of caspase 3 clearly segregated with p21^{WAF1} positive tumors as compared with p21^{WAF1} negative cases (16 of 23, 69.6% vs 5 of 16, 31.3%) with statistical significance ($P < 0.05$).

Table 1 Correlation between clinicopathological parameters and expression of caspase 3 in HCCs

	No. Caspase 3 expression (%)		P
Samples			
Non-cancerous adjacent liver	8	7(87.5)	<0.05
HCC	39	21(53.8)	
Age(year)			
<60	28	15(53.6)	NS
>60	11	6(54.5)	
Sex			
Male	34	18(52.9)	NS
Female	5	3(60.0)	
Tumor size (cm)			
>5.0	27	15(55.6)	NS
<5.0	12	6(50.0)	
Differentiation			
Well-moderate	18	13(72.2)	<0.05
Poor	21	8(38.1)	
TNM grade			
I-II	21	12(57.1)	NS
III-IV	18	9(50.0)	
Metastasis			
Negative	31	16(51.6)	NS
Positive	8	5(62.5)	
p21 ^{WAF1}			
Positive	23	16(69.6)	<0.05
Negative	16	5(31.3)	

NS: no statistic significance

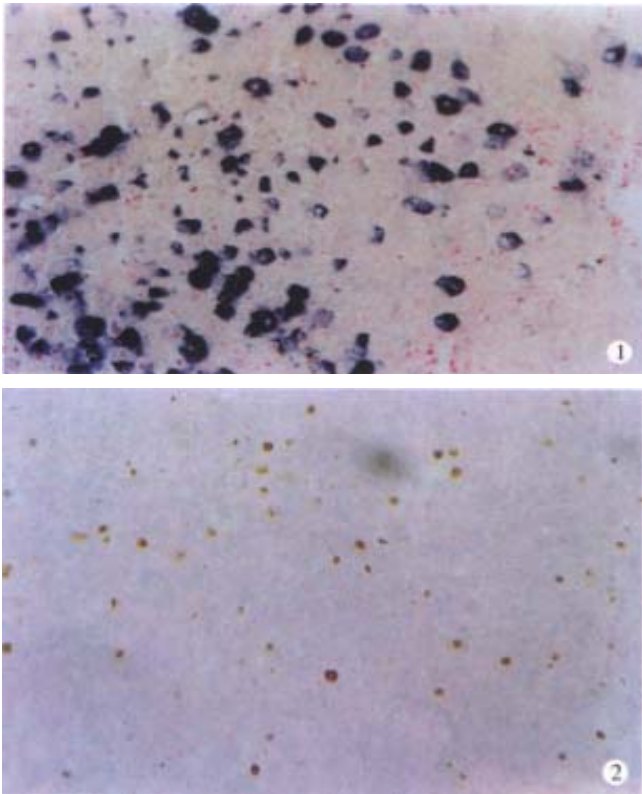


Figure 1 Caspase 3 transcripts were detected predominantly in cytoplasm by ISH (×200)

Figure 2 Apoptotic cells were determined by criteria as described in materials and methods. Arrow shows fragmented nucleus (×200)

Relationship between tumor cell apoptosis and caspase 3 expression

Apoptotic cells and apoptotic bodies were found in all cases of HCCs examined by *in situ* end-labeling (Figure 2). The mean AI of all tumors cases was 6.82‰ (s, 3.36‰; range 0.87‰-17.3‰). No significant association was observed between AI and tumor stage. The mean AI for caspase 3-positive tumors ($n = 21$) was 7.12‰ (s, 3.75‰), while in caspase 3-negative cases ($n = 18$) the AI was 6.59‰ (s, 2.98‰), no statistical significance was found between the two groups ($P > 0.05$). In the cases with co-expression of p21^{WAF1} and caspase 3, the AI was found lower, but with no significance, than that of cases with positive caspase 3 and negative p21^{WAF1} (6.98‰ vs 7.21‰).

DISCUSSION

In this study, we have shown that caspase 3 was expressed in most of HCC cases. In our opinion, we are the first to describe the cyp32 expression in human primary HCCs. Like the result of human biopsy and autopsy liver materials^[14], the non-cancerous adjacent liver tissue showed strong caspase 3 expression. As high as 46.2% of human primary HCCs failed to show caspase 3 expression.

In the 21 cases which express caspase 3, the expression showed heterogeneous pattern with a weighted score from 1 to 12. Because caspase 3 is the effector caspase in the apoptosis pathways, we think that loss of caspase 3 expression may play an important role in HCC carcinogenesis. Caspase 3 expression had no relationship with clinicopathological features except for tumor differentiation (Table 1). The result suggests that the expression of caspase 3 is correlated with tumor differentiation in HCC. It was reported that 33.1% cases of gastric carcinoma were caspase 3 positive^[7]. Two of 3 breast carcinoma tissues expressed caspase 3, the immunointensity was generally higher in invasive cancers^[8]. It raised the possibility that expression of caspase 3 in tumors showed tissue specificity. It was observed in this study that the apoptosis index (AI) was not associated with the expression of caspase 3 in HCC (7.12‰ in cyp32-positive cases versus 6.59‰ in cyp32-negative group). In the non-cancerous adjacent liver tissues more than 50% of the cells showed positive caspase 3, the AI was not increased as compared with HCC, no matter caspase 3 was positive or negative. This suggests that other factor(s) may exist in regulating normal cell apoptosis.

p21^{WAF1} was first reported as a universal inhibitor of cyclin-dependent kinase, which is required for G₁ to S transition^[15]. Previous studies demonstrated that p21^{WAF1} can interrupt the apoptotic process at a point upstream from caspase-3 activation, because serum starvation, which also synchronized cells in G₁ but did not induce p21^{WAF1}, did not protect cells from apoptosis, while restoring a late G₁ checkpoint by inducing p21^{WAF1} expression can protect cells from DNA damage induced apoptosis^[16]. p21^{WAF1} can bind procaspase-3 but not activate caspase 3. On the other hand, activated caspase 3 can cleave p21^{WAF1}. P21 cleavage by the activated cyp32 specifically abolished its interaction with PCNA and may interfere with normal PCNA-dependent repair^[15]. The presence of p21^{WAF1} in human HCCs was reported previously in our paper^[12]. In this context, the expression of p21^{WAF1} was also determined together with caspase 3 in an attempt to find whether there is relationship between them. We found that expression of caspase 3 was strongly associated with p21^{WAF1} in 16 cases of HCC. There was no significant difference in AI between p21^{WAF1}(+)/cyp32(+) and p21^{WAF1}(-) / cyp32(+) (6.98‰ vs 7.21‰). The results indicated that p21^{WAF1} may be merely one of the inhibitors which can reduce caspase 3 mediated cell apoptosis in HCCs. In fact, some other caspase 3 inhibitors, for example survivin, were reported to have overexpression in human tumors, including gastric and colorectal cancer^[17,18]. Survivin is

believed to bind activated caspase 3 and further inhibit cell apoptosis. It was reported that XIAP can interrupt caspase 3 mediated apoptosis via the same way as p21^{WAF1}. So, further investigation on other caspase 3 regulating protein is needed to find the regulation mechanism of caspase 3 mediated apoptosis in human HCCs.

REFERENCES

- 1 Tang ZY, Yu YQ, Zhou XD, Ma ZC, Wu ZQ. Progress and prospects in hepatocellular carcinoma surgery. *Ann Chir*, 1998;52: 558-563
- 2 Kokura K, Nakadai T, Kishimoto T, Makino Y, Muramatsu M, Tamura T. Gene expression in hepatomas. *J Gastroenterol Hepatol*, 1998;13(Suppl):S132-141
- 3 Wyllie AH. Apoptosis and carcinogenesis. *Europ J Cell Biology*, 1997;73:189-197
- 4 Kidd VJ. Proteolytic activities that mediate apoptosis. *Annu Rev Physiol*, 1998;60:533-573
- 5 Kitada S, Andersen J, Akar S, Zapata JM, Takayama S, Krajewski S, Wang HG, Zhang X, Bullrich F, Croce CM, Rai K, Hines J, Reed JC. Expression of apoptosis-regulating proteins in chronic lymphocytic leukemia: correlations with *in vitro* and *in vivo* chemoresponses. *Blood*, 1998;91: 3379-3389
- 6 Estrov Z, Thall PF, Talpaz M, Estey EH, Kantarjian HM, Andreeff M, Harris D, Van Q, Walterscheid M, Kornblau SM. Caspase 2 and caspase 3 protein levels as predictors of survival in acute myelogenous leukemia. *Blood*, 1998;92:3090-3097
- 7 Krajewski S, Gascoyne RD, Zapata JM, Krajewska M, Kitada S, Chhanabhai M, Horsman D, Berean K, Piro LD, Fugier-Vivier I, Liu YJ, Wang HG, Reed JC. Immunolocalization of the ICE/Ced-3-family protease, CPP32 (Caspase-3), in non-Hodgkin's lymphomas, chronic lymphocytic leukemias, and reactive lymph nodes. *Blood*, 1997;89:3817-3825
- 8 Chhanabhai M, Krajewski S, Krajewska M, Wang HG, Reed JC, Gascoyne RD. Immunohistochemical analysis of interleukin-1 β -converting enzyme/Ced-3 family protease, CPP32/Yama/Caspase-3, in Hodgkin's disease. *Blood*, 1997;90:2451-2455
- 9 Zapata JM, Krajewska M, Krajewski S, Huang RP, Takayama S, Wang HG, Adamson E, Reed JC. Expression of multiple apoptosis-regulatory genes in human breast cancer cell lines and primary tumors. *Breast Cancer Res Treat*, 1998;47:129-140
- 10 Nakagawara A, Nakamura Y, Ikeda H, Hiwasa T, Kuida K, Su MS, Zhao H, Cnaan A, Sakiyama S. High levels of expression and nuclear localization of interleukin-1 beta converting enzyme (ICE) and CPP32 in favorable human neuroblastomas. *Cancer Res*, 1997; 57:4578-4584
- 11 Suzuki A, Tsutomi Y, Akahane K, Araki T, Miura M. Resistance to Fas-mediated apoptosis: activation of caspase 3 is regulated by cell cycle regulator p21WAF1 and IAP gene family ILP. *Oncogene*, 1998;17:931-939
- 12 Sun BH, Wu ZB, Ruan YB, Yang ML, Liu B. p21WAF1/Cip1 gene expression in primary human hepatocellular carcinoma and its relationship with p53 gene mutation. *J Tongji Medical University*, 1999;19:1-5
- 13 Kawasaki H, Altieri DC, Lu CD, Toyoda M, Tenjo T, Tanigawa N. Inhibition of apoptosis by survivin predicts shorter survival rates in colorectal cancer. *Cancer Res*, 1998;58:5071-5074
- 14 Krajewska M, Wang HG, Krajewski S, Zapata JM, Shabaik A, Gascoyne R, Reed JC. Immunohistochemical analysis of *in vivo* patterns of expression of CPP32 (caspase 3), a cell death protease. *Cancer Res*, 1997;57:1605-1613
- 15 Li R, Waga S, Hannon GJ, Beach D, Stillman B. Differential effects by the p21 CDK inhibitor on PCNA dependent DNA replication and repair. *Nature*, 1994;371:534-537
- 16 Bissonnette N, Hunting DJ. p21-induced cycle arrest in G1 protects cells from apoptosis induced by UV irradiation or RNA polymerase II blockage. *Oncogene*, 1998;16:3461-3469
- 17 Lu CD, Altieri DC, Tanigawa N. Expression of a novel antiapoptosis gene, survivin, correlated with tumor cell apoptosis and p53 accumulation in gastric carcinomas. *Cancer Res*, 1998; 58:1808-1812
- 18 LaCasse EC, Baird S, Korneluk RG, Mackenzie AE. The inhibitors of apoptosis (IAPs) and their emerging role in cancer. *Oncogene*, 1998; 17:3247-3259

Edited by Ma JY
proofread by Sun SM

Effects of salvianolic acid-A on NIH/3T3 fibroblast proliferation, collagen synthesis and gene expression

Cheng Hai Liu, Yi Yang Hu, Xiao Ling Wang, Ping Liu and Lie Ming Xu

Subject headings salvianolic acid-A, NIH/3T3 fibroblast, cell viability, cell proliferation, collagen, gene expression

Liu CH, Hu YY, Wang XL, Liu P, Xu LM. Effects of salvianolic acid-A on NIH/3T3 fibroblast proliferation, collagen synthesis and gene expression. *World J Gastroenterol*, 2000;6(3):361-364

Abstract

AIM To investigate the mechanisms of salvianolic acid A (SA-A) against liver fibrosis *in vitro*.

METHODS NIH/3T3 fibroblasts were cultured routinely, and incubated with 10^{-4} mol/L- 10^{-7} mol/L SA-A for 22 h. The cell viability was assayed by [3 H]proline incorporation, cell proliferation by [3 H]TdR incorporation, cell collagen synthetic rate was measured with [3 H]proline impulse and collagenase digestion method. The total RNA was prepared from the control cells and the drug treated cells respectively, and α (1) I pro-collagen mRNA expression was semi-quantitatively analyzed with RT-PCR.

RESULTS 10^{-4} mol/L SA-A decreased cell viability and exerted some cytotoxicity, while 10^{-5} mol/L- 10^{-7} mol/L SA-A did not affect cell viability, but inhibited cell proliferation significantly, and 10^{-6} mol/L SA-A had the best effect on cell viability among these concentrations of drugs. 10^{-5} mol/L- 10^{-6} mol/L SA-A inhibited intracellular collagen synthetic rate, but no significant influence on extracellular collagen secretion. Both 10^{-5} mol/L and 10^{-6} mol/L SA-A could decrease α (1) I pro-collagen mRNA expression remarkably.

CONCLUSION SA-A had potent action against liver fibrosis. It inhibited NIH/3T3 fibroblast proliferation, intracellular collagen synthetic rate and type I pro-collagen gene expression, which may be one of the main mechanisms of the drug.

Institute of Liver Diseases, Shanghai University of Traditional Chinese Medicine, Shanghai 200032, China

Dr. Cheng Hai Liu, graduated from Shanghai University of Traditional Chinese Medicine as Ph.D. in 1996, associate professor, majoring in hepatology, having 20 papers and 4 books published.

Supported by Shanghai Educational Committee Grant, No. 96CJ04, 95SG26

Correspondence to: Dr. Cheng Hai Liu, No 530, Lingling Road, Institute of Liver Diseases, Shanghai University of Traditional Chinese Medicine, Shanghai, 200032, China

Tel. 0086-21-54231109, Fax. 0086-21-64036889

Email. Liuliver@online.sh.cn

Received 2000-01-13 Accepted 2000-02-28

INTRODUCTION

Radix salviae miltiorrhizae, one of the most frequently used Chinese herbs, is regarded to have effects on both blood production and circulation by traditional Chinese medicine, and is widely applied in clinical therapy for liver diseases, such as chronic hepatitis, hepatic cirrhosis, etc. Salvianolic Acid-A is one of the water soluble components from *Radix salviae miltiorrhizae*. It was reported to have good actions on peroxidation^[1]. Lipid peroxidation could stimulate hepatic stellate cell (HSC) transformed into myofibroblast like cell (MFBC) and collagen gene expression *in vivo* and *in vitro*, and played an important role in liver fibrogenesis^[2]. In our previous work^[3], it was found that SA-A could protect hepatic lipid peroxidation, and had marked effects against liver injury and fibrosis in carbon tetrachloride induced fibrotic rats. In order to investigate the mechanism by which SA-A protects against liver fibrosis, we observed the effects of SA-A on NIH/3T3 fibroblast proliferation, collagen protein production and procollagen gene expression.

MATERIALS AND METHODS

Drug

SA-A, molecular formula as $C_{26}H_{22}O_{10}$, molecular structure as shown in Figure 1, molecular weight 494, was extracted and identified by Shanghai Institute of Materia Medica, Chinese Academy of Sciences.

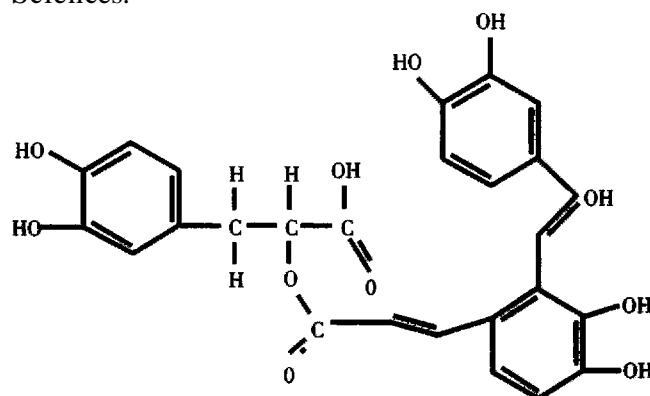


Figure 1 SA-A molecular structure.

Main reagents and solutions

PRMI-1640 Medium and Duboccal modified Eagle Medium (DMEM) were purchased from Gibco BRL

Co., new brown serum (NBS) from Shanghai Sino-American Co., purified type III collagenase (specific activity, 960U/mg), N-ethylmaleimide (NEM) and β -aminopropionitrile from Sigma Co. [^3H]proline ([^3H]Pro) from Amersham Co. methyl-[^3H] thymidine (TdR) from Shanghai Institute of Atomic Energy, guanidium thiocyanate from Serva Co. Access RT-PCR System Kit, PCR marker from Promega Co., Diethylpyrocarbonate, saturated phenol/chloroform mix and agarose from Shanghai Sangon Biotech Co. Other reagents all were of analytical grade.

The non-homogeneous scintillation liquid was dimethylbenzene solution containing 5 g/L 2,5-diphenyloxazol (PPO) and 0.5 g/L 1,4-bis[5-phenyloxazol-2]benzene (POPOP), the homogeneous scintillation liquid was dimethylbenzene solution containing 7 g/L PPO, 0.5 g/L POPOP, 100 g/L naphthalene and 400 mL/L₂-ethoxy-ethanol.

Cell line

Mouse NIH/3T3 fibroblasts were purchased from Shanghai Institute of Cell Biology, Chinese Academy of Sciences, and cultured with PRMI-1640 medium containing 100 g/L NBS, 100KU/L penicillin and 100 mg/L streptomycin. After the cell growth became confluent, they were digested with trypsin-EDTA and subcultured.

PCR Primers

The PCR primers for pro-collagen $\alpha 2(\text{I})$ and β -actin were designed according to the published sequences and references in Table 1^[4], and were synthesized by Gibco BRL Co.

Table 1 PCR primer sequences and expected size of amplified products

Primers	Sequence	Size
$\alpha 2(\text{I})$ collagen upstream	5'TGT TCG TGG TTC TCA GGG TAG3'	254 bp
$\alpha 2(\text{I})$ collagen downstream	5'TTG TCG TAG CAG GGT TCT TTC3'	
β -actin upstream	5'ACA TCT GCT GGA AGG TGG AC3'	163 bp
β -actin downstream	5'GGT ACC ACC ATG TAC CCA GG3'	

Cell proliferation assay

Confluent NIH/3T3 fibroblasts in 24 well plates were incubated with 10^{-4}mol/L - 10^{-7}mol/L SA-A diluted in PRMI-1640 medium containing 100 mL/L NBS for 22 h, and [^3H]TdR (55.5KBq/well) was impu lused in the last 16 h. Then cells were harvested with trypsin digestion and collected on the filtration membrane, then sample radioactivity (cpm) in the non-homogeneous scintillation liquid was measured by Backman Wallac 1410 Scintillator. All tests were repeated 3 times.

Cell viability assay

According to *Mallat's* method^[5], confluent

NIH/3T3 fibroblast s in 24-well plates were incubated with 10^{-4}mol/L - 10^{-7}mol/L SA-A dissolved in PRMI-1640 medium without NBS for 22 h, and [^3H]Pro (55.5KB q/well) was impu lused in the last 16 h. Then cells were collected and the cpm was measured as above.

Assay of cell collagen synthetic rate

According to Greets' method^[6], confluent NIH/3T3 fibroblasts in 6 well plates were incubated with 10^{-5}mol/L - 10^{-6}mol/L SA-A diluted in PRMI-1640 without NBS for 22 h, during the later 16h the culture media were changed to DMEM containing 185 KBq/mL [^3H]Pro, 100 mg/L- β -aminopropionitrile, 50 mg/L ascorbic acid as well as the same drugs. Then the culture media and cell layer extract were collected respectively, dialyzed thoroughly and reacted with collagenase, etc. The total radioactivity in the samples (cpm_t), radioactivity in the samples treated with collagenase (cpm_c) and not treated with collagenase (cpm_b) were counted in the homogeneous scintillation liquid by Backman Wallac 1410 Scintillator. The new collagen that cell produced, i.e. the fraction of collagenous protein expressed as percentage of total radiolabeled protein, was calculated using the formula:

$$\% \text{ of collagen} = 100 \div \left(5.4 \times \frac{\text{cpm}_t - \text{cpm}_c}{\text{cpm}_c - \text{cpm}_b} + 1 \right)$$

RNA extraction and RT-PCR (reverse transcription and polymerase chain reaction)

The total RNA was extracted from the control cells and SA-A incubated cells by the acid guanidium thiocyanate-phenol-chloroform method^[7]. The RNA quantity was determined by absorption at 260 nm, its purity was confirmed with A_{260}/A_{280} spectrophotometer readings that ranged from 1.6 to 1.9, and its integrity was checked by 9 g/L agarose gel electrophoresis with ethidium bromide (EB) staining of 18S and 28S ribosomal RNA (Figure 2). With Access RT-PCR system kit, the cDNA synthesis and amplification was done in one tube following the manufacturer's instructions. In brief, 1 μg RNA, 50 pmol/L primers for $\alpha 2(\text{I})$ pro-collagen or β -actin were added to each reaction mixture respectively, which included 10 mmol/L dNTPs 1 μL , 25 mmol/L MgSO_4 2 μL , AMV reverse transcriptase 5U, Tfl DNA polymerase 5U, AMV/Tfl-5 \times buffer 10 μL . The reaction final volume was 50 μL and was covered with 20 μL mineraloil. Then with PCR Touchdown thermal cycler (Hyaid, England), RT-PCR reaction was run in the following procedures: ① 48°C for 45 min, 1 circle. ② 94°C for 2 min, 1 circle. ③ 94°C for 30s, 60°C for 1 min, 38°C for 2 min, 30 circles. ④ 68°C for 7 min, 1 circle. Five μL PCR product was run on 15 g/L agarose gel and observed by EB

staining under UV light, the electrophoresis image was transformed into computer, and $\alpha 1$ (I) pro-collagen intensity was analyzed with MPIAS500 image system, while the β -actin band intensity was subtracted as an internal standard.

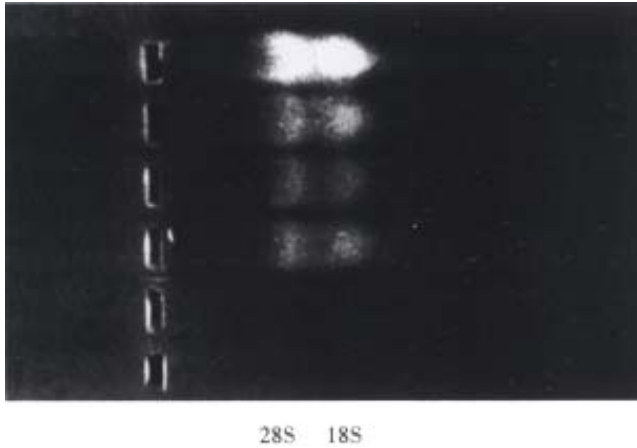


Figure 2 Total RNA gel electrophoresis photograph. 28S and 18S of total RNA run on 9 g/L agarose gel stained with EB.

Statistical analysis

Data were analyzed by *Student's t* test.

RESULTS

Effects on cell morphology and viability

10^{-5} mol/L- 10^{-7} mol/L SA-A had no marked effects on cell morphology, but 10^{-4} mol/L SA-A led to shrinkage and detachment of some cells, showing cytotoxicity to some degree. 10^{-4} mol/L- 10^{-7} mol/L SA-A did not decrease intercellular [3 H] Pro incorporation, while 10^{-6} mol/L SA-A could increase [3 H]Pro impulse ($P < 0.05$) and enhance cell viability (Table 2).

Effects on cell proliferation

10^{-4} mol/L- 10^{-6} mol/L SA-A remarkably decreased intercellular [3 H]TdR incorporation and inhibited cell proliferation ($P < 0.05$), 10^{-4} mol/L SA-A showed more significant effect ($P < 0.01$), but it induced some cell death, which may be associated with its cytotoxic action. 10^{-7} mol/L SA-A had no obvious effect on cell [3 H] TdR incorporation (Table 2).

Table 2 Effects of SA-A on cell intracellular [3 H]TdR and [3 H] Pro incorporation (cpm/well, $\bar{x} \pm s$, $n = 4$)

Group	[3 H]TdR	[3 H]Pro
Control	1482 \pm 486	21018 \pm 5473
10^{-4} mol/L SA-A	675 \pm 201 ^b	18659 \pm 2363
10^{-5} mol/L SA-A	969 \pm 183 ^a	23761 \pm 5430
10^{-6} mol/L SA-A	868 \pm 183 ^a	31408 \pm 4981 ^a
10^{-7} mol/L SA-A	1056 \pm 187	26080 \pm 4504

^a $P < 0.05$, ^b $P < 0.01$, vs control.

Effects on cell collagen synthetic rates

10^{-5} mol/L- 10^{-6} mol/L SA-A could inhibit intracellular collagen synthetic rate significantly ($P < 0.01$), but did not influence extracellular synthetic rate (Table 3).

Table 3 Effects of SA-A on NIH/3T3 fibroblast collagen synthetic rates (% , $\bar{x} \pm s$, $n = 4$)

Group	Intracellular	Extracellular
Control	0.78 \pm 0.03	2.57 \pm 0.37
10^{-5} mol/L	0.48 \pm 0.24 ^b	2.54 \pm 0.91
10^{-6} mol/L	0.43 \pm 0.26 ^b	3.02 \pm 0.69

^b $P < 0.01$, vs control.

Effects on procollagen $\alpha 2$ (I) mRNA expression

Both 10^{-5} mol/L and 10^{-6} mol/L SA-A decreased procollagen $\alpha 1$ (I) mRNA expression significantly ($P < 0.05$), but there was no difference between the two different concentration groups (Table 4, Figure 3).

Table 4 The relative expression amount of $\alpha 2$ (I) procollagen mRNA ($\bar{x} \pm s$, % of β -actin)

Group	<i>n</i>	Col $\alpha 1$ (I) mRNA
Control	3	98.71 \pm 9.96
10^{-5} mol/L SA-A	3	76.23 \pm 12.02 ^a
10^{-6} mol/L SA-A	3	68.44 \pm 8.06 ^a

^a $P < 0.05$, vs control.

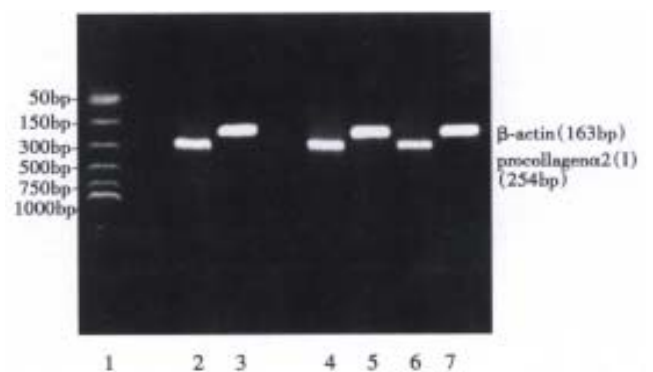


Figure 3 RT-PCR product gel electrophoresis photograph. Five μ L RT-PCR products of procollagen $\alpha 2$ (I) and β -actin run on 1.5% agarose gel stained with EB. Lane 1 as PCR marker, lane 2 and 3 as the control for procollagen $\alpha 2$ (I) and β -actin respectively, lane 4 and 5 SA-A 10^{-6} mol/L for procollagen $\alpha 2$ (I) and β -actin respectively, lane 6 and 7 as SA-A 10^{-5} mol/L for procollagen $\alpha 2$ (I) and β -actin respectively.

DISCUSSION

Hepatic fibrosis, a precursor of cirrhosis, is a common and important pathological feature of chronic liver diseases, which involves the abnormal accumulation of extracellular matrix (ECM)

proteins, particularly collagen^[8]. In fibrotic liver, ECM components are mainly produced by HSC and fibroblasts. It is known that during fibrogenesis, HSC undergoes a process of activation, developing a myofibroblast-like phenotype associated with increased proliferation and ECM production, especially type I collagen synthesis. The mouse NIH/3T3 fibroblast also shared the features that active HSC (MFBC) presented, such as remarkable proliferation and substantial production of collagen, and stable cell line. In practice, NIH/3T3 fibroblast is often used as a desirable cell model for investigation of antifibrotic drugs.

In order to rule out the possibility of SA-A cytotoxic influence *in vitro*, the intracellular [³H] Pro incorporation was measured, and inverted microscopic observation was done. It was found that only 10⁻⁴ mol/L SA-A caused some cell detachment, decreased [³H] Pro incorporation, and showed cytotoxicity to some extents. 10⁻⁵ mol/L-10⁻⁷ mol/L SA-A did not influence cell morphology or inhibit cell viability. However, 10⁻⁶ mol/L SA-A enhanced cell viability. Both 10⁻⁵ mol/L-10⁻⁶ mol/L SA-A could inhibit intracellular [³H] TdR impulse that NBS stimulated. It is suggested that SA-A had an effective action against NIH/3T3 fibroblast proliferation.

Type I collagen is the predominant component of ECM during liver fibrosis. Its production involves two processes: the first is intracellular synthesis, including gene transcription, translation and modification to form procollagen, then procollagen alpha chains are secreted to the outside of the cell to form helix collagen by sorting and alignment etc. In the study, it was found that SA-A downregulated procollagen α 2(I) steady-state mRNA expression, and intracellular collagen synthetic rate, but exerted no effect on extracellular synthetic rate. It is suggested that SA-A influence on collagen production through the intracellular synthetic

process. The fibrogenic cells have two predominant features: one is active in cell proliferation, which led to increase in cell number, another is strong fibrogenic ability per cell, which led to accumulation of ECM. In the study, SA-A not only inhibited NIH/3T3 fibroblast proliferation, but also decreased collagen synthesis, showing a good action against liver fibrosis.

Salvianolic acid is widely used as an important component in Chinese herbal formulas for the treatment of chronic liver diseases. Salvianolic Acid-A, one of water-soluble ingredients from Salvianolic acid, had effective actions on hepatic peroxidation and fibrosis *in vivo*^[3]. In the paper, it is for the first time found that SA-A has the potential action against hepatic fibrosis *in vitro*, and its main mechanisms of antifibrotic action perhaps was associated with the inhibition of fibrogenic cell proliferation, collagen gene expression and protein synthesis.

REFERENCES

- 1 Lin TJ, Liu GT. Protective effect of salvianolic acid A on heart and liver mitochondria injury induced by oxygen radicals in rats. *Zhongguo Yaolixue Yu Dulixuebao*, 1991;5:276-281
- 2 Olaso E, Friedman SL. Molecular regulation of hepatic fibrogenesis. *J Hepatol*, 1998;29:836-847
- 3 Hu YY, Liu P, Liu C, Xu LM, Liu CH, Zhu DY, Huang MF. Actions of salvianolic acid A on CCl₄ poisoned liver injury and fibrosis in rats. *Zhongguo Yaoli Xuebao*, 1997;18:478-480
- 4 Mallat A, Preaux AM, Blazejewski S, Rosenbaum J, Dhumeaux D, Mavrier P. Interferon alpha and gamma inhibit proliferation and collagen synthesis of human Ito cells in culture. *Hepatology*, 1995; 21:1003-1010
- 5 Power WJ, Kaufman AH, Merayo-Lioves J, Arrunategui-Correa V, Foster CS. Expression of collagens I, III, IV and V mRNA in excimer wounded rat cornea: analysis by semi quantitative PCR. *Curr Eye Res*, 1995;14:879- 886
- 6 Greets A, Vrijssen R, Rauterberg J, Burt A, Schellinck P, Wisse E. In vitro differentiation of fat-storing cells parallels marked increase of collagen synthesis and secretion. *J Hepatol*, 1989;9:59-68
- 7 Chomczynski P, Sacchi N. Single step method of RNA isolation by acid guanidinium thiocyanate phenol-chloroform extraction. *Anal Biochem*, 1987;162:156-159
- 8 Friedman SL. The cellular basis of hepatic fibrosis: mechanisms and treatment strategies. *New Eng J Med*, 1993;328:1828-1836

Edited by Zhu LH
proofread by Sun SM

Primary porcine hepatocytes with portal vein serum cultured on microcarriers or in spheroidal aggregates

Yi Gao, Huan Zhang Hu, Ke Chen and Ji Zhen Yang

Subject headings porcine hepatocytes; microcarriers; cell culture; spheroidal aggregate culture; portal vein serum

Gao Y, Hu HZ, Chen K, Yang JZ. Primary porcine hepatocytes with portal vein serum cultured on microcarriers or in spheroidal aggregates. *World J Gastroentero*, 2000;6(3):365-370

Abstract

AIM To develop a culture mode providing durable biomaterials with high yields and activities used in bioartificial liver.

METHODS Hepatocytes were isolated from a whole pig liver by Seglen's method of orthotopic perfusion with collagenase. In culture on microcarriers, primary porcine hepatocytes were inoculated at a concentration of $5 \times 10^7/\text{mL}$ into the static culture systems containing 2 g/L Cytodex-3, then supplemented with 100 mL/L fetal calf serum (FCS) or 100 mL/L porcine portal vein serum (PPVS) respectively. In spheroidal aggregate culture hepatocytes were inoculated into 100 mL siliconized flasks at a concentration of $5.0 \times 10^6/\text{mL}$.

RESULTS In culture on microcarriers hepatocytes tended to aggregate on Cytodex-3 obviously after being inoculated. Typical multicellular aggregated spheroids could be found in the two systems 24 h-48 h after hepatocytes were cultured. The morphological characteristics and synthetic functions were maintained for 5 wk in FCS culture system and 8 wk in PPVS culture system. In spheroidal aggregate culture about 80%-90% isolated hepatocytes became aggregated spheroids 24 h after cultured in suspension and mean diameter of the spheroids was 100 μm . The relationship among the hepatocytes resembled that in the liver *in vivo*. Synthetic functions of albumin and urea of the

spheroids were twice those of hepatocytes cultured on monolayers.

CONCLUSION As high-yields and high-activity modes of culture on microcarriers or in spheroidal aggregate culture with portal vein serum are promising to provide biomaterials for bioartificial liver (BAL) efficiently.

INTRODUCTION

Great attention was paid world-wide to the bioartificial liver (BAL) aiming to release the clinical symptoms of severe acute liver diseases or liver injuries and act as a transitional bridge for liver transplantation. Modern BAL is mainly characterized by its multiple biofunctions resembling those of liver *in vivo* and such functions may be completely derived from the biomaterials in BAL. Years of researches at home and abroad showed that primary hepatocytes were the most ideal biomaterial of BAL. But for the morphological and functional changes of primary hepatocytes cultivated *in vitro* occurred obviously in short time, it was deadly restrained to use them as the biomaterial in BAL. To probe into this question, together with our proceeding researches on this subject^[1], we took the method of two-step orthotopic collagenase perfusion to isolate hepatocytes and cultured them on microcarriers Cytodex-3 statically in flasks in the systems supplemented with FCS or PPVS respectively, and also cultured them in the matrix DMEM containing porcine portal vein serum at a concentration of 100 mL/L through the way of spheroidal aggregating, then estimated the possibility of such hepatocytes acting as the biomaterial in BAL in view of their morphology and biofunctions.

MATERIALS AND METHODS

Materials

The experimental animals were five native sex-unlimited pigs aged 1 mo-2 mo and weighed 10 kg-15 kg from the experiment animal center of SUN Yat-Sen Medical University. Insulin, glucagon, transferrin, collagenase IV, tyran and microcarrier Cytodex-3 were purchased from Sigma (USA). Solution of 50 g/L methyl silicon resin ethyl acetate

Department of Hepatobiliary Surgery, Zhujiang Hospital, First Military Medical University, Guangzhou 510282, Guangdong Province, China
Dr. Yi Gao, graduated from Second Military Medical University as M.D. in 1992, associate professor of hepatobiliary surgery, mentor of postgraduate.

Supported by the National Natural Science Foundation of China, No.39570212

Correspondence to: Dr. Yi Gao, Department of Hepatobiliary Surgery, Zhujiang Hospital, First Military Medical University, Guangzhou 510282, Guangdong Province, China

Tel. 0086-20-85143556

Received 2000-01-10 Accepted 2000-03-02

was confected by ourselves. Ten g/L osmic acid, 20 g/L pentanal and gradient acetone solutions were provided by the Department of Electron microscope of First Military Medical University. S-450 electron scanning microscope was from Japan. PPVS was collected in the experiment. The liver perfusion solution was prepared according to Table 1.

Methods

Isolation of porcine hepatocytes The experimental pig was kept fasting for 12 h preoperatively and anaesthetized with 30 g/L sodium barbiturate ip. After the abdominal skin being prepared and disinfected, celiotomy was performed, then portal vein and inferior caval vein below the liver exposed and 0.25 mg (125 IU) heparin injected into the inferior caval vein. After being dissected, the portal vein and the inferior caval vein were ligated at the distal end and intubated at the proximal end respectively. When the inferior caval vein above the liver ligated at the superior end of liver vein, successive perfusing solutions I and II pre-warmed in 37°C water bath were perfused along the circuit via portal vein to inferior caval vein. Perfusing speed was about 50 mL/min-60 mL/min for 20 min. Perfusion was ended until the liver became pallor or yellow in color. Then the well digested liver were taken out, tore off the liver sheath and the isolated hepatocytes delivered into solution III pre-warmed in 37°C water bath. After being filtered by 150 µm, 100 µm and 80 µm sieve, the hepatocytes were suspended in solution and centrifuged at a speed of 1 000r/min for 3 min-5 min repeated three times. The deposited hepatocytes were added into solution IV to prepare the hepatocyte suspension for use. Portal vein blood was gathered from the distal end of the ligated portal vein and in a total amount of 1 300 mL from 5 pigs. It was centrifuged at a 2 000r/min to isolate the portal vein serum, and the very serum centrifuged three times more to prepare the refined serum which finally amounted to 714 mL. The refined serum was filtered to be excluded from bacteria and preserved separately for use. Sample from the suspension was observed under light microscope to calculate the yielding rate of hepatocytes and stained by typran for determination of their activity.

Static culture of hepatocytes on microcarriers in flasks

Porcine hepatocyte suspension was divided randomly into two halves, then one half was cultured on microcarriers in FCS system and the other in PPVS system. Five pigs were done separately and by the same method. ① Culture of hepatocytes in FCS system: five flasks were prepared and each one added with 2 mL-3 mL 50 g/L sterile methyl silicon resin ethyl acetate solution. After the flasks being shaken mildly and equably, the remained

solution was discarded. The flasks were parched in 60°C electric oven for use. 20 mg-30 mg Cytodex-3 was deposited into the siliconized flasks and rinsed with 40 mL Ca^{2+} and Mg^{2+} free phosphate buffer solution (PBS) for three times, then dipped in PBS over night. After being sterilized at 15 pounds for 30 min, the microcarriers were dipped in DMEM matrix over 10 h for use. Hepatocytes were inoculated into the flasks at the concentration of $5 \times 10^6/\text{mL}$ and DMEM matrix containing 100 mL/L FCS, 100 µg/L glucagon, 100 µg/L transferrin, 200 µg/L hydrocortisone, 100 µg/L insulin and 200 µg/L fortum added up to the total volume, 50 mL. Then the flasks were deposited into an incubator with 100% humidified atmosphere containing 5% CO_2 at 37°C and shaken reelingly once every 15 min-30 min at the first 4 h, once every 2 h after 4 h and laid quietly after 8 h without further shaking. Ten mL supernatant fluid of the culture matrix was changed after 24 h and once every 2 d from then on. The supernatant fluid was centrifuged at 1 000r/min for discarding the cell fragments. Synthesized albumin and urea were determined. ② Culture of hepatocytes in PPVS system: 100 mL/L refined PPVS was added into the culture system instead of FCS, and the other demands were the same as those of the FCS culture.

Spheroidal aggregate culture of primary porcine hepatocytes

Five flasks were prepared and each one added with 2 mL-3 mL 50 g/L sterile methyl silicon resin ethyl acetate solution. After the flasks being shaken mildly and equably, the residual solution was discarded. The flasks were parched in 60°C electric oven for use. Hepatocytes were inoculated into the flasks at the concentration of $5 \times 10^6/\text{mL}$ and DMEM matrix containing 100 mL/L porcine portal vein serum, 100 µg/L glucagon, 100 µg/L transferrin, 200 µg/L hydrocortisone, 100 µg/L insulin and 200 µg/L fortum added up to a total volume, 50 mL. Then the flasks were deposited into the incubator with 100% humidified atmosphere containing 5% CO_2 at 37°C and shaken reelingly once every 15 min-30 min at the first 4 h, once every 2 h after 4 h and laid quietly after 8 h without further shaking. 10 mL supernatant fluid of the culture matrix was changed after 24 h and once every 2 d from then on. The supernatant fluid was centrifuged at 1 000r/min for discarding the cell fragments. Syntheses of albumin and urea were determined.

Morphological observation and counting of hepatocytes

The porcine hepatocytes cultured on microcarriers and those cultured as aggregated spheroids were observed under phase-contrast light microscope and photographed on an automatic microscopic photographing device successively (Olympus, Japan). In culture on microcarriers 1 mL samples

were collected every day to calculate the amount of cells in the culture system by means of trypan blau. On d7, cell sample was taken at a well-distributed state, culture matrix discarded, rinsed with PBS, then fixed for 0.5 h with 2 mL 20 g/L pentanal, rinsed with PBS again, fixed for 0.5 h with 10 g/L osmic acid, and next dehydrated gradientially for 10 min each stage, exchanged with acetic isopental ester for 4 hours, dried by CO₂ drier (Hitachi HCP₂, Japan), and finally splashed with ionic platinum in vacuum. Growth of the cells was observed on S-450 electron scanning microscope (Japan). In spheroidal aggregate culture, 1 mL samples were taken well-distributedly from the matrix for cell calculation on the d7 and d12.

Determination of albumin and urea syntheses

When the culture matrix was changed, samples of supernatant fluid were obtained from the culture on microcarriers and spheroidal aggregate culture to determine the contents of albumin and urea through an automatic biochemical analyzer (Beckman, USA).

RESULTS

Isolation of porcine hepatocytes

We successfully took the improved *Seglen's* two-step orthotopic perfusion method with collagenase to isolate the porcine hepatocytes. About 2.82×10^{10} hepatocytes were obtained and the survival rate 91.2%. Each gram pig liver offered 7.01×10^7 hepatocytes.

Cultivation of porcine hepatocytes

In culture on microcarriers, the amount of hepatocytes on the d7 in the two systems is shown in Table 2. Hepatocytes growth curve (Figure 1) was drawn on the basis of Table 2. On d18 hepatocytes in FCS culture system amounted to $(1.1 \pm 0.53) \times 10^7$ and those in PPVS system $(3.1 \pm 0.71) \times 10^8$. In spheroidal aggregate culture the amount of hepatocytes on d7 was $(3.12 \pm 0.26) \times 10^7$ and that on d10 $(1.39 \pm 0.51) \times 10^8$.

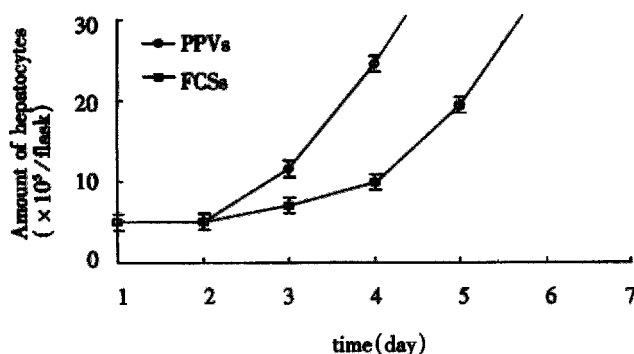


Figure 1 Hepatocytes growth curve in different culture systems on microcarriers.

Morphological observation of hepatocytes cultured on microcarriers

Observation under phase-contrast light microscope Four hours after inoculation microcarriers were observed to be adhered with hepatocytes and the hepatocytes were beginning to expand. The phenomenon of bridge-link could be observed between microcarriers (Figure 2), i. e. the microcarriers were linked with each other through hepatocytes and arranged as slices or a string of beads (Figure 3). There was "snowball" effect between some microcarriers and hepatocytes. Twenty-four hours after culture over 1/3 microcarriers were covered with cells. The hepatocytes adhering to microcarriers was in irregular polygonal shape and thereafter these cells were observed to expand and grow. Forty-eight hours after culture most vivid hepatocytes were attached to microcarriers directly or indirectly. Growth of hepatocytes on microcarriers resembled that of monolayer growth in flasks. In FCS system hepatocytes began to adhere to microcarriers and expanded 2 h after inoculation. Double-nucleus hepatocytes could be observed and some linked to others in insular configuration. Twenty-four hours later about 60%-70% hepatocytes were attached. Three days after inoculation they began to proliferate and there were anile hepatocytes 6 days later. About 22 days later microcarriers were covered fully with hepatocytes. Five weeks after inoculation hepatocytes tended to become rough and blurry-edged. Granules and vacuoles could be observed in most of them. About 2 days later hepatocytes began to detach from microcarriers and died. Morphology of hepatocytes in PPVS system resembled that in FCS system at the first 24 h except that there were more double-nucleus hepatocytes in PPVS system. Three days after inoculation most microcarriers were covered with neonatal hepatocytes and they linked to others in spheroidal or trabecular conformation. Eighteen days later microcarriers were covered fully with hepatocytes and such condition could be maintained to the d52. Fifty-four days later hepatocytes could be observed to begin falling off from microcarriers and completed on the d56.

Observation under electron microscope On d18 of culture, the electron microscope showed that the hepatocytes adhering firmly to the microcarriers in semi-spherical form. The microvilli on the surfaces of hepatocytes could be observed clearly. The amount of hepatocytes adhering to the microcarriers varied and they were distributed unevenly. Some microcarriers aggregated with others through cell-bridge as shown in Figure 4.

Morphological observation of spheroidal aggregated hepatocytes

When successively observing the normal primary porcine hepatocytes cultured in spheroidal-aggregates under the phase-contrast microscope, we found that: about 80%-90% hepatocytes began to aggregate spheroidally 24 h after being inoculated and diameters of the spheroids ranged from 62 μm to 134 μm . Each spheroid contained 10-20 hepatocytes. The hepatocytes at this time linked with each other loosely and were likely to be

dispersed. When observed under light microscope, they looked like “cell flowers” (Figure 5). On the d7 they were hyperplastic and linked with others tightly and looked like “cell spheroids” (Figure 6). On d10 they took the shapes of spheroid and irregular column as “algoid plant” (Figure 7). On the d20, the algoid hepatocytes began to atrophy and vacuolous granules appeared in them, the nuclei began to lyse and the hepatocytes ended in falling off and dying. On the d23, all of the spheroidal aggregating hepatocytes died.

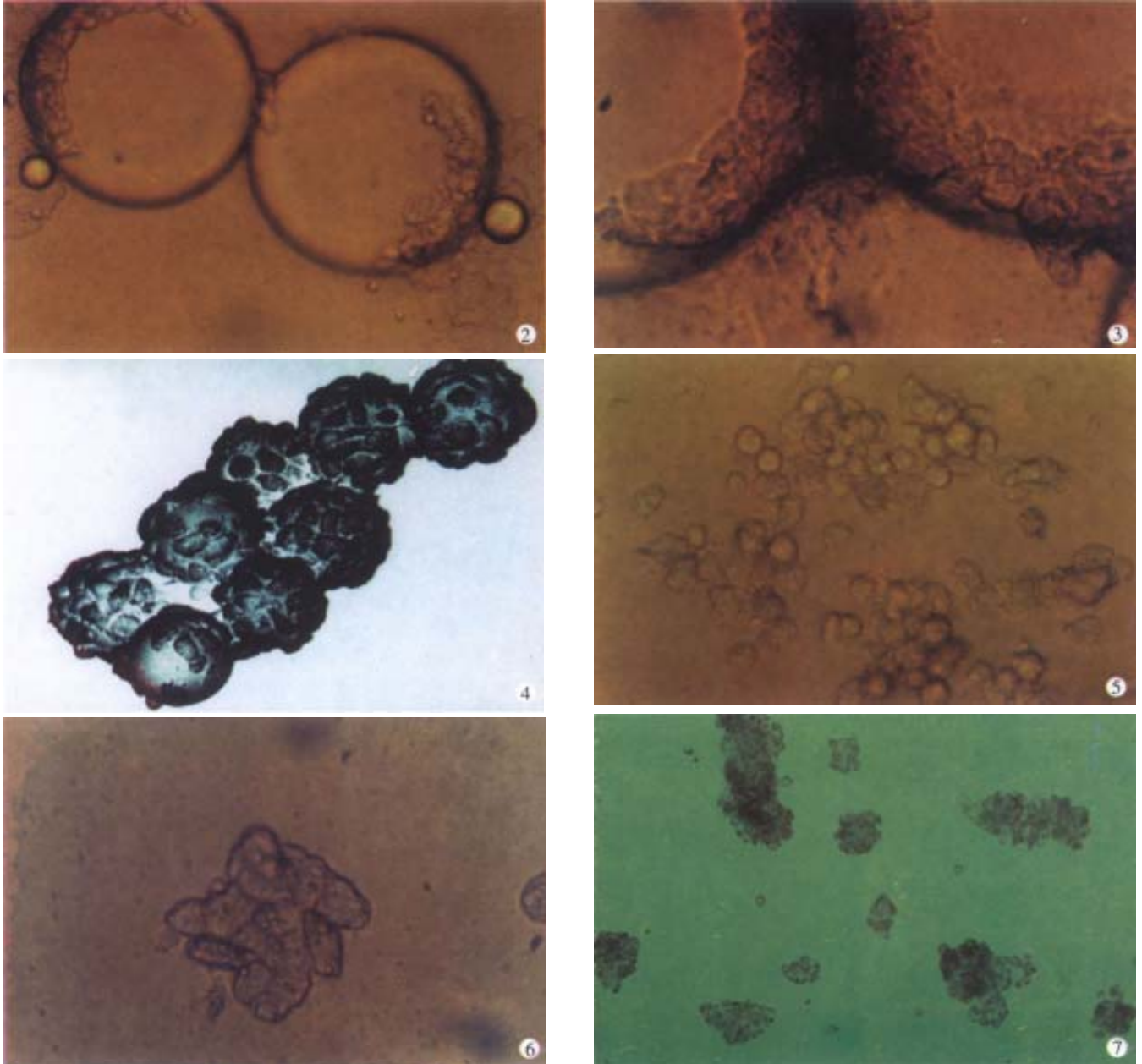


Figure 2 Four hours after inoculation cell-bridge could be observed between microcarriers (under phase-contrast microscope $\times 200$).

Figure 3 Microcarriers were arranged as a string of beads by adhered hepatocytes (under phase-contrast microscope $\times 400$).

Figure 4 Stringed microcarriers with adhered hepatocytes (under phase contrast microscope $\times 730$).

Figure 5 Hepatocytes looked like “cell flowers” 24 h after being cultivated in suspension and aggregated spheroids (under phase contrast microscope $\times 400$).

Figure 6 On the d7 hepatocytes aggregated into “cell spheroids” (under phase contrast microscope $\times 400$).

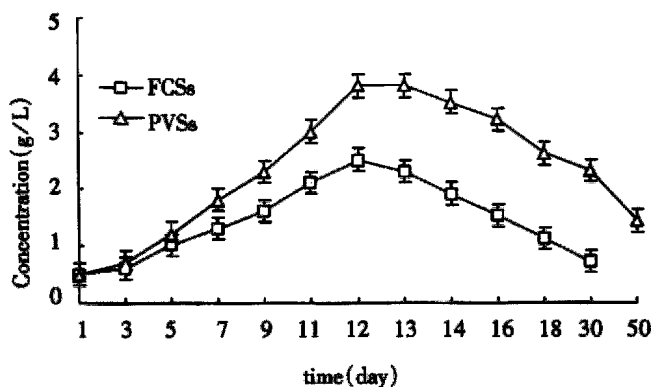
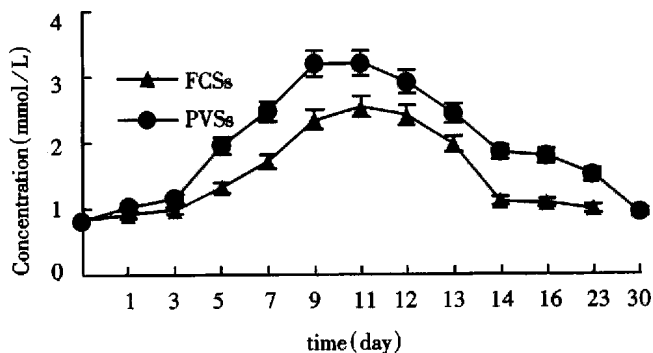
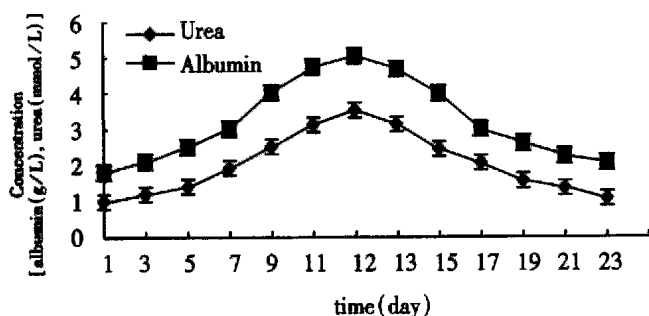
Figure 7 On the d10 hepatocytes in the forms of algoid plants (under phase contrast microscope $\times 200$).

Table 1 Ingredients of different liver-perfusing solutions (g/L)

	NaCl	KCl	NaOH	CaCl ₂	MgCl ₂	Na ₂ SO ₄	HEPES	Collagen ase(IV)	Tricine	Tes	pH
I	8.3	0.5	0.22				2.4				7.4
II	3.9	0.5	2.6	0.53			24	0.5			7.4-7.6
III	4.0	0.4	2.1	0.136	0.13	0.1	7.2		6.5	6.9	7.4
IV	8.3	0.5	0.11	0.136			2.4				7.4

Table 2 Amounts of hepatocytes at various time in different culture systems on microcarriers ($\bar{x} \pm s$, $\times 10^5/\text{pore}$)

	1st	2nd	3rd	4th	5th	6th	7th(day)
FCSs	5.0 \pm 0.4	5.0 \pm 0.1	6.9 \pm 0.2	9.8 \pm 0.6	19.3 \pm 0.2	34.3 \pm 0.3	58.6 \pm 0.7
PPVSs	5.0 \pm 1.2	5.0 \pm 0.4	11.4 \pm 0.5 ^a	24.3 \pm 0.1 ^a	40.4 \pm 0.4 ^a	70.7 \pm 0.7 ^a	136.1 \pm 0.1 ^a

^a $P < 0.05$ (compared with FCSs group)**Figure 8** Changes of albumin synthesis in hepatocytes from different culture systems on microcarriers.**Figure 9** Changes of urea secretion in hepatocytes from different culture systems on microcarriers.**Figure 10** Dynamic changes of albumin and urea in the supernatant fluid.

Determination of albumin and urea syntheses

By using the automatic biochemical analyzer (Beckman, U.S.A.) we determined the contents of albumin and urea in the supernatant fluid at different times successively. In the two culture systems on microcarriers the values were kept in high levels from the d7 to d14 and got the summit on the d11 to d12 (Figures 8 and 9). As Figures 8 and 9 showed, functions of hepatocytes in PPVS system 3-5 days after inoculation were obviously higher than those in FCS system. Hepatocytes in PPVS can maintain their activity for about 50 days. In spheroidal aggregate culture the values were kept in high levels from d7 to d14 and got the summit on d10. From then on, the values degraded gradually and finally the hepatocytes lost their biofunctions on d23 (Figure 10).

DISCUSSION

Years of researches at home and abroad showed that primary hepatocytes were the most ideal biomaterial for BAL. But for the morphological and functional changes of primary hepatocytes cultivated *in vitro* occurred obviously in short time, it was deadly restrained to use them as biomaterial in BAL. The specific functions of hepatocytes lost in *in vitro* culture accounted for the lack of some *in vivo* elements. Then it was proposed that syntheses of albumin and urea could be promoted by adding some nutritional factors and hormones into the monolayer culture system. By now some improvements has been achieved in searching for a new effective system to cultivate primary hepatocytes *in vitro* by the following methods: ① adding hormonal agents such as insulin, glucagon, transferrin and hydrocortisone into the basal culture medium^[1]; ② adding extracellular biological matrix into the culture system^[2-4]; ③ enriching the culture system with hepatocytes growth stimulating factors such as hepatocytes growth factor and epithelial cell growth factor etc^[5,6]; ④ co-culturing with other endodermal and mesodermal cells; ⑤ three-

dimensional cultivation such as microcapsular and macrocapsular culture, spheroid aggregate, microcarrier culture and hollow fiber culture^[7,8]; ⑥ adding several amino acids and nutritional substances into the culture system; and ⑦ adding penetrating-inducer such as pentobarbiturate to the culture system^[9]. The above measures all aimed to make a circumstance mimic to the *in vivo* environment for the hepatocytes.

It is well-known that about 70% blood supply of liver comes from portal vein system. The growth of liver and maintenance of its functions depend mainly on the nutritional circumstance provided by the portal vein system, that is, hepatocytes *in vivo* are nourished by the contents of portal vein blood. The later provides various amino acids, energy substances and several growth factors. Our experiments were based on this very point and PPVS was added into the culture matrix. The results showed that hepatocytes in this system could durably survive and maintain their biofunctions. This fluid was the ideal circumstance to cultivate the biomaterial for BAL.

Microcarriers Cytodex-3 were used to provide three-dimensional space for adhering and suspending hepatocytes so as to bring benefit from fully utilizing of the nutritional components in the culture system. Our proceeding studies had proved that Cytodex-3 was the best microcarrier for primary hepatocytes^[3]. Hepatocytes on Cytodex-3 were readily to shape the microstructure similar to that of liver so they could grow and function well.

Landry^[10] *et al* found that when no adhering agent in the spheroidal-aggregate culture system the isolated hepatocytes tended to be changed less in morphology and could survive and maintain their activities for 4 wk-6 wk due to the resemblance of the structure between the aggregating spheroids and normal liver. Clayton^[11,12] *et al* found that the specific transcription gene of hepatocyte in little masses of liver could be kept well than that of isolated hepatocytes and obviously the three-dimension structure of hepatocytes is of great importance in maintaining their specific functions. Relationship between cell skeleton and specific proteins reflected the influences of morphology to functions, that is, cell functions directly related with levels of mRNA and specific proteins, and inversely related with levels of actin and canalicular protein. Sakai^[13] *et al* found that the inoculation concentration was of great influence to the formation of hepatocyte spheroids in the

suspending spheroidal aggregate culture system. When hepatocytes being inoculated at a high concentration it often occurred that pH of culture matrix declined, cell-to-cell and spheroid to spheroid relationships changed and multiple necrotic foci could be observed in hepatocyte spheroids. When hepatocytes being inoculated at a low concentration they were difficult to aggregate into spheroids. Sakai *et al* considered $5.0 \times 10^6/\text{mL}$ to be the optimal inoculation concentration in suspending spheroid aggregate culture system of hepatocytes.

On view of the above factors, we concluded that primary porcine hepatocytes cultured on Cytodex-3 in PPVS system or in spheroidal-aggregate were promising to act as the biomaterial of BAL. Still there is much to be desired to promote the density, function and surviving time of hepatocytes for clinical use.

REFERENCES

- 1 Chen K, Gao Y, Pan YX, Yang JZ. An effective system for culturing primary porcine hepatocytes. *Shijie Huaren Xiaohua Zazhi*, 1999;7:206-209
- 2 Kimura M, Ogihara M. Proliferation of adult rat hepatocytes in primary culture induced by insulin is potentiated by cAMP-elevating agents. *Eur J Pharmacol*, 1997;327:87-95
- 3 Kono Y, Yang S, Roberts EA. Extended primary culture of human hepatocytes in a collagen gel sandwich system. *In Vitro Cell Dev Biol Anim*, 1997;33:467-472
- 4 Taguchi K, Matsushita M, Takahashi M, Uchino J. Development of a bioartificial liver with sandwiched-cultured hepatocytes between two collagen gel layers. *Artif Organs*, 1996;20:178-185
- 5 Koike M, Matsushita M, Taguchi K, Uchino J. Function of culturing monolayer hepatocytes by collagen gel coating and co-culture with nonparenchymal cells. *Artif Organs*, 1996;20:186-192
- 6 Schuppan D, Schmid M, Somasundaram R, Ackermann R, Ruehl M, Nakamura T, Riecken EO. Collagens in the liver extracellular matrix bind hepatocyte growth factor. *Gastroenterology*, 1998;114:139-152
- 7 Hu MY, Cipolle M, Sielaff T, Lovdahl MJ, Mann HJ, Rimmel RP, Cerra FB. Effect of hepatocytes growth factor on viability and biotransformation function of hepatocytes in gel-entrapped and monolayer culture. *Crit Care Med*, 1995;23:1237-1242
- 8 Flendrig LM, Te Velde AA, Chamuleau RA. Semipermeable hollow fiber membranes in hepatocyte bioreactors a prerequisite for a successful bioartificial liver. *Artif Organs*, 1997;21:1177-1181
- 9 Sielaff TD, Myberg SL, Rollins MD, Hu MY, Amiot B, Lee A, Wu FJ, Hu WS, Cerra FB. Characterization of the three compartment gel entrapment porcine hepatocytes bioartificial liver. *Cell Biol Toxicol*, 1997;13:357-364
- 10 Landry J, Bernier D, Ouellet C, Goyette R, Marceau N. Spheroidal aggregate culture of rat liver cells: histotypic reorganization, biomatrix deposition and maintenance of functional activities. *J Cell Biol*, 1985;101:914-923
- 11 Clayton DF, Harrelson AL, Darnell JE Jr. Dependence of liver specific transcription on tissue organization. *Mol Cell Biol*, 1985;5:2623-2632
- 12 Sawamoto K, Takahashi N. Modulation of hepatocyte function by changing the cell shape in primary culture. *In Vitro Cell Dev Biol Anim*, 1997;33:569-574
- 13 Sakai Y, Naruse K, Nagashima I, Muto T, Suzuki M. Large-scale preparation and function of porcine hepatocytes spheroids. *Int J Artif Organs*, 1996;19:294-301

Edited by You DY
proofread by Sun SM

Relationship between insulin A chain regions and insulin biological activities

Shi Zhen Yang, Yi Ding Huang, Xin Feng Jie, You Min Feng and Jing Yi Niu

Subject headings insulin/chemistry; biological activities; A chain analogues

Yang SZ, Huang YD, Jie XF, Feng YM, Niu JY. Relationship between insulin A chain regions and insulin biological activities. *World J Gastroentero*, 2000;6(3):371-373

Abstract

AIM To study the relationship between insulin A chain regions and insulin biological activities, we designed a series of insulin analogues with changes at A21, A12-18 of C-terminal helical region and A8-10 located in the region of A6-A11 intra-chain disulphide bond. **METHODS** Insulin A-chain analogues were prepared by stepwise Fmoc solid-phase manual synthesis and then combined with natural B-chain of porcine insulin to yield corresponding insulin analogues. Their biological activities were tested by receptor binding, mouse convulsion and immunological assay.

RESULTS [A21Ala]Ins retains 70.3% receptor binding capacity and 60% *in vivo* biological activity. [DesA13-14, A21Ala]Ins and [DesA12-13-14-15, A21Ala]Ins still have definite biological activity, 7.9% and 4.0% receptor binding, and 6.2% and 3.3% *in vivo* biological activity respectively. [A15Asn, A17Pro, A21Ala]Ins maintains 10.4% receptor binding and 10% *in vivo* biological activity. [A8His, A9Arg, A10Pro, A21Ala]Ins, [A8His, A9Lys, A10Pro, A21Ala]Ins and [A8His, A9Lys, A10Arg, A21Ala]Ins have 51.9%, 44.3% and 32.1% receptor binding respectively, 50%, 40% and 30% *in vivo* biological activity respectively, and 28.8%, 29.6% and 15.4% immunological activity respectively.

CONCLUSION A21Asn can be replaced by simple amino acid residues. The A chains with gradually damaged structural integrity in A12-18 helical region and the demolition of the A12-18 helical region by the substitution of Pro and Asn for A17Glu and A15Gln respectively can combine with the B chain and the combination products show definite biological activity, the helical structure of A12-18 is essential for biological activities of insulin. A8-10 is not much concerned with biological activities, but is much more important antigenically in binding to its antibodies, these results may help us design a new type of insulin analogue molecule.

INTRODUCTION

To elucidate the multi-functions of insulin molecule, hundreds of insulin analogues with changes involving 90% of the constituting 51 amino acid residues at various parts of insulin molecule have been prepared by either chemical modification or synthesis during the past two decades. In this communication we report the influences of three different regions of insulin A chain, especially the secondary structure region, i.e. A12-18 helical region, on insulin biological activities. Recently, thorough studies of insulin analogues with deletion of fragments of the molecule were also undertaken, but restricted mostly to changes in the C-terminal part of the B chain^[1,2], presumably due to its location outside the disulfide linkage and therefore ease of splitting off a tryptic or peptic fragment and recombining with a modified or shortened fragment by chemical or enzymatic semi-synthesis. No such enzymatic site was found in A chain, and most of its amino acid residues are confined inside disulfide linkages. Chemical synthesis might be a better choice for making analogues with modification or deletion in part of the A chain, which constitutes the main feature of this communication.

To obtain insulin analogues, we first set up the semisynthesis strategy of insulin. Insulin A chain was synthesized by the Fmoc solid phase synthesis strategy, and then synthetic A chain S-sulphonate was combined with porcine insulin B chain S-sulphonate forming crystalline insulin^[3]. Based on these experiences, the following insulin analogues

Shanghai Institute of Biochemistry, Chinese Academy of Sciences, Shanghai 200031, China

Dr. Shi Zhen Yang, graduated from Beijing Scientific and Technical College, Academia Sinica, in 1964, associate researcher, majoring in peptide synthesis, having 40 papers published.

Supported by the Eighth Five Year Plan Key Research Project, No. KS 852017 and National Natural Science Foundation of China. No. 3880193, No.39270157, No.39700028 and Chinese Academy of Sciences, KJ951-B1-606.

Correspondence to: Dr. Shi Zhen Yang, Shanghai Institute of Biochemistry, Chinese Academy of Sciences, 320 Yueyanglu, Shanghai 200031, China

Tel. 0086-21-64374430, Fax. 0086-21-64338357

Email: Yangsz@Sunm. Shenc. ac. cn

Received 2000-01-03 Accepted 2000-02-29

were semisynthesized. They are [A21Ala]Ins^[4], where A21Asn is replaced by Ala, and its derivatives with deletions in the A12-18 helical region, [DesA13-14, A21Ala] Ins^[4] and [DesA12-13-14-15, A21Ala]Ins^[4], and [A15Asn, A17Pro, A21Ala]Ins, where the helical structure of A12-18 was also demolished by the substitutions of Pro for A17Glu and Asn for A15Gln predicted by Chou-Fasman method, and [A8His, A9Arg, A10Pro, A21Ala]Ins^[5], and [A8His, A9Lys, A10Pro, A21Ala]Ins^[5], and [A8His, A9Lys, A10Arg, A21Ala]Ins^[5], in which His reminiscent A8 of chicken insulin with high biological activity took the place of A8Thr and Arg, Lys, Pro replaced A9Ser and A10Ile to examine the influences of these alterations on receptor binding and antigenicity of insulin. The sequences of insulin A chain analogues are as follows (Figure 1).

	1	5	10	15	20
Insulin A Chain	G.I.V.E.Q.C.C.T.S.I.C.S.L.Y.Q.L.E.N.Y.C.N				
1	G.I.V.E.Q.C.C.T.S.I.C.S.L.Y.Q.L.E.N.Y.C.A				
2	G.I.V.E.Q.C.C.T.S.I.C.S.....Q.L.E.N.Y.C.A				
3	G.I.V.E.Q.C.C.T.S.I.C.....L.E.N.Y.C.A				
4	G.I.V.E.Q.C.C.T.S.I.C.S.L.Y.N.L.P.N.Y.C.A				
5	G.I.V.E.Q.C.C.H.R.P.C.S.L.Y.Q.L.E.N.Y.C.A				
6	G.I.V.E.Q.C.C.H.K.P.C.S.L.Y.Q.L.E.N.Y.C.A				
7	G.I.V.E.Q.C.C.H.K.R.C.S.L.Y.Q.L.E.N.Y.C.A				

Figure 1 Insulin A chain analogue sequence.

MATERIALS AND METHODS

Materials

Porcine insulin (26.4U/mg), Shanghai Biochemical Plant; Sephadex G-15, G-50, Sepharose CL-6B, Pharmacia; Fmoc amino acid, prepared in the laboratory; DCC, acetonitrile, trimethylsilyl trifluoromethane sulfonate (TMSOTf), thioanisole, Fluka Co. trifluoroacetic acid (TFA) Merck Co.; DTT, Serva Co.

Methods

Peptide synthesis Base labile N-Fmoc protected amino acid was coupled by DCC-HOBt to the 2% cross linked α -alkoxybenzyl alcohol resin. The functional side chain groups were protected by tBu for Cys, Glu, Tyr and Ser. Scheme of manipulation was the same as reported^[6]. The peptide chain was detached from the resin support with simultaneous removal of all tBu protecting groups by TFA except S-tBu of cysteine. S-tBu was deprotected by M TMSOTf-thioanisole-TFA system^[5] and transformed to S-sulphonate by tetrathionate and sulfite with the procedure as reported^[7].

Isolation and purification of ASSO₃⁻ Crude ASSO₃⁻ fractions were purified by HPLC with gradient elution (A: 0.1% TFA, B: 60% CH₃CN, 0.125%

TFA).

Recombination with the natural (porcine) BSSO₃⁻ and purification This was carried out according to modified Chance's procedure^[4]. The crude product was purified by HPLC using the same procedure as that for ASSO₃⁻.

Receptor binding, *in vivo* activities and RIA The receptor-binding of insulin and analogues was determined by the displacement of labelled insulin from the insulin receptor on the human placental membrane according to Feng's^[8] procedure. The *in vivo* activity was estimated semiquantitatively by mouse convulsion assay. RIA kit produced by the Shanghai Biological Product Institute was used for RIA of insulin and analogues.

RESULTS

Peptide synthesis

Insulin A chain analogues were prepared starting from 300 mg-500 mg each of Fmoc-alanyl resin and products obtained from each step and the final overall yield is given in Table 1.

Table 1 Data on the synthesis of A chain analogues

A Chain analogues	FmocAla-resin mg(mmol)	Target peptide-resin(mg)	After HPLC(mg)	Overall yield(%)
1	500(0.19)	769	62.1	12.3
2	500(0.19)	749	54.6	12.0
3	500(0.19)	724	45.4	12.4
4	500(0.32)	865	20.0	4.5
5	300(0.135)	657	39.6	10.6
6	300(0.135)	648	40.1	11.2
7	300(0.135)	660	41.3	11.1

Reconstitution of A and B chain and purification of the products

According to the modified Chance's procedure, insulin analogues were obtained by purification of the crude reconstituted products. The identifications of amino acid analysis and HPLC indicated homogeneous products of insulin analogues.

Biological activities

The receptor-binding capacities calculated from the receptor binding curve, *in vivo* activities and immunological activities are shown in Table 2.

Table 2 Biological activities of insulin analogues (%)

Sample	Receptor binding	Mouse convulsion	Immunological activity
Ins	100	100	100
1B	70.3	60	
2B	7.9	6.2	
3B	4.0	3.3	
4B	10.4	10	
5B	51.9	50	28.8
6B	44.3	40	29.6
7B	33.1	30	15.4

DISCUSSION

A21Asn was considered to be a key amino acid of the insulin molecule in regard to its receptor binding. It has been very conservative in the evolutionary process, and when replaced the analogues showed remarkable diminution of biological activity. Our results showed that the analogue with the A21 Asn replaced by Ala exhibited substantial activity *in vivo* and especially higher level of receptor binding, indicating the non-essentiality of A21Asn in receptor binding and biological activity as well. It could well be replaced by other amino acid residues with good retention of biological activities. Better results were observed when the side chain of the A21 amino acid is smaller or not present (Gly)^[9]. However, deletion of the A21 residue is fatal as the activity of desA21 insulin showed only less than 1% of the activity. Apparently, like some non-essential amino acid residues in the insulin molecule, A21 is important in maintaining the specified spatial configuration of insulin required for its biological activities.

It is generally accepted that during the reconstitution of A and B chain to insulin A6-11 disulfide bond formed first and this led to the formation of right natural conformation by self adjustment. When the B chain was getting in touch with the intrachain disulfide, A6-11, a hydrophobic nucleus was formed to enhance the proper pairing of two Cys in both ends of the B chain to corresponding Cys of the A chain^[10]. The success of our reconstitution with deleted A chain supports to a certain extent this suggestion. It showed that the C-terminal helical region in the A chain of insulin was not as important as the N-terminal helical region in reconstitution with the B chain. The biological activities of insulin analogues with gradually damaged structural integrity in A12-18 helical region were similar to that of insulin analogue with the demolition of the A12-18 helical region by the substitution of Pro and Asn for A17Glu and A15Gln respectively. The observations suggested that the helical structure of A12-18 is essential for biological activities of insulin.

It was generally suggested that the enhanced activities of [A8His]Ins^[11], chicken and turkey insulins were ascribed to the His at A8^[12-14], which should account for the higher affinity for insulin receptor. Our results showed that the presence of His at A8 apparently did not enhance the receptor binding. The receptor binding of [A8His] Ins should lie at the range of about 50%. The enhanced

potency of these insulins containing His at A8 may not result solely from an apparent and direct effect due to the presence of A8His. A8His and A10Arg signify a higher influence on insulin antigenicity. A8His will enhance the binding activity to the anti-insulin serum^[11], while A10Arg will decrease this binding, but amino acid at A9 had very little to do with antigenic activity. In addition to studies on how to elucidate the action of an insulin molecule to its receptor and express the physiological activity that follows such action, the purpose of studies on the structure activity relationship of insulin will rely more on how to get a better analogue with high potency but low antigenicity. We hope that the information provided in this study will be beneficial to the development of a new type insulin analogue with those qualities through design of an appropriate architecture of this important hormone.

REFERENCES

- 1 Shanghai Insulin Research Group. Structural studies on despentapeptide (B26-30)insulin. *Zhongguo Kexue*, 1976;4: 351-356
- 2 Chen LT, Huang CM, Zhang M, Yang ZR, Hu MH. Purification and characterization of Des-terpeptide of C-terminal (B28-30) human insulin. *Shengwu Huaxue Zazhi*, 1996;12:187-195
- 3 Yang SZ, Niu JY. Solid phase synthesis of the A-chain of insulin and its recombination with the B-chain to crystalline insulin. *Shengwu Huaxue Yu Shengwu Wuli Xuebao*, 1992;24:497-502
- 4 Yang SZ, Huang YD, Feng YM, Niu JY. Insulin analogues with deletions at the helical region of the A chain. *Shengwu Huaxue Yu Shengwu Wuli Xuebao*, 1994;26:49-55
- 5 Yang SZ, Lin W, Huang YD, Feng YM, Niu JY. Insulin analogues with alteration at A8-10. *Acta Biochemi Biophys Sin*, 1995;27: 329-334
- 6 Yang SZ, Niu JY. Solid phase synthesis of serum thymic factor and preparation of its antiserum. *Shengwu Huaxue Zazhi*, 1991;7: 349-354
- 7 Paynovich RC, Carpenter FH. Oxidation of the sulfhydryl forms of insulin A-chain and B chain. *Int J Peptide Protein Res*, 1979; 13:113-121
- 8 Feng YM, Zhu JH, Zhang XT, Zhang YS. Studies on the mechanism of insulin action. *Acta Biochemi Biophys Sin*, 1982;14:137-143
- 9 Markussen J, Diers I, Hougaard P, Langkjaer L, Norris K, Snel L, Sørensen AR, Sørensen E, Voigt HO. Soluble prolonged acting insulin derivatives. III. Degree of protraction, crystallizability and chemical stability of insulins substituted in positions A21, B13, B23, B27 and B30. *Protein Engineering*, 1988;2:157-166
- 10 Peking Insulin Structure Research Group. Studies on the insulin crystal structure: the molecule at 1.8 Å resolution. *Zhongguo Kexue*, 1974;2:752-761
- 11 Marki F, Gasparo MD, Eisler K, Kamber B, Riniker B, Rittel W, Sieber P. Synthesis and biological activity of seventeen analogues of human insulin. *Hoppe-seyler's Z Physiol Chem*, 1979; 360:1619-1632
- 12 Pullen RA, Lindsay DG, Wood SP, Tickle IJ, Blundell TL, Wollmer A, Krail G, Brandenburg D, Zahn H, Gliemann J, Gammeltoft S. Receptor binding region of insulin. *Nature*, 1976;259:369-373
- 13 Weitzel G, Renner R, Kemmler W, Rager K. Struktur und erhöhte aktivität des insulin vom truthuhn (melleagris gallopavo). *Hoppe-seyler's Z Physiol Chem*, 1972;353:980-986
- 14 Simon J, Freychet P, Rosselin G. Chicken insulin: Radioimmunological characterization and enhanced activity in rat fat cells and liver plasma membranes. *Endocrinology*, 1974;95: 439-1445

Edited by You DY and Zhu LH
proofread by Sun SM

Helicobacter pylori infection and risk of gastric cancer in Changle County, Fujian Province, China

Lin Cai¹, Shun Zhang Yu² and Zuo Feng Zhang³

Subject headings Helicobacter pylori; stomach neoplasm; risk factors; case control studies

Cai L, Yu SZ, Zhang ZF. Helicobacter pylori infection and risk of gastric cancer in Changle County, Fujian Province, China. *World J Gastroentero*, 2000;6(3):374-376

Abstract

AIM To evaluate the effects of *Helicobacter pylori* infection and other environmental factors on the development of gastric cancer.

METHODS A population-based case-control study was conducted in Changle County, Fujian Province. The primary gastric cancer cases were histologically confirmed or diagnosed by surgery between January 1996 and March 1998. Healthy controls were randomly selected and matched by age, sex, and neighborhood of residence. A total of 101 pairs were included in the study. Specially trained interviewers conducted face-to-face interviews with the subjects according to a standardized questionnaire. *Helicobacter pylori* infections were measured by serum IgG antibody to *Helicobacter pylori*. Conditional Logistic Regression analysis was used.

RESULTS The presence of IgG antibody to *Helicobacter pylori* was 63.7% in study subjects, 56.0% in patients with cardiac cancer, and 60.5% in patients with non-cardiac gastric cancer. The risk factors of gastric cancer in Changle County were identified such as low educational level [OR=3.864; 95% confidence interval (95%CI) 1.604-9.311], low consumption of fresh vegetables (OR=4.925; 95% CI 1.356-17.885), high intake of fish sauce (OR = 10.587; 95% CI 2.821-39.738), unscheduled meals (OR = 4.254; 95% CI 1.445-

12.552), and *Helicobacter pylori* infection (OR = 3.453; 95% CI 0.901-13.224).

CONCLUSION *Helicobacter pylori* infection may be important in the etiology of gastric cancer, but major risk factors other than *Helicobacter pylori* are responsible for the high gastric morbidity in Changle County.

INTRODUCTION

Helicobacter pylori (*H. pylori*) infection is associated with gastric cancer^[1-4]. However, only a small proportion of individuals developed gastric cancer in comparison with the relatively high prevalence of *H. pylori* infection in the general population. In this study we evaluated the effects of *H. pylori* infection and other environmental risk factors on the development of gastric cancer in Changle County, one of the areas with highest morbidity of gastric cancer in the world.

MATERIALS AND METHODS

Study subjects

One hundred and one gastric cancer patients (87 males and 14 females) and the same number of normal controls, individually matched with region, sex and age (± 3 years) were included in the study. The studied subjects must have resided in Changle County for more than 20 years. The primary gastric cancer patients were histologically confirmed or diagnosed by operation during January 1996 - March 1998. Those who have ever been diagnosed as having gastric diseases in the past 3 years were not eligible as controls.

Data collection

Trained interviewers interviewed the patients and controls. A standardized questionnaire was used to obtain information on basic demographic characteristics (gender, race, year and place of birth, and education), dietary habits, personal habits (smoking and drinking), medical history and so on.

H. pylori assay

The presence of anti-*H. pylori* - IgG was assessed using the commercially available high-molecular-weight cell-associated protein *H. pylori* -immuno-

¹Department of Epidemiology, Fujian Medical University, Fuzhou 350004, Fujian Province, China

²Department of Epidemiology, Shanghai Medical University, Shanghai 200032, China

³Department of Epidemiology, UCLA School of Public Health, Los Angeles California, USA

Dr. Lin Cai, graduated from Shanghai Medical University in 1983, received Ph. D. degree from Shanghai Medical University in 1999, associated professor, majoring in gastric cancer epidemiology, having 30 papers published.

Project supported by the Natural Science Foundation of Fujian Province, China, No. K98031

Correspondence to: Lin Cai, Department of Epidemiology, Fujian Medical University, Fuzhou 350004, Fujian Province, China
Tel. 0086-591-3357231

Received 2000-01-03 Accepted 2000-02-06

assay (Enteric Products Inc, Westbury, New York). The assay was done in 96-well microtiter plates. Sera diluted 1:101 were added, and peroxidase conjugated anti-human IgG was used as the detector. The absorbance of the solution was measured at 450 nm.

Statistical analysis

Data were handled by Epi-info. Odds ratios (OR) and 95% confidence intervals (95% CI) were calculated by Conditional Logistic Regression using STATA software

RESULTS

A total of 101 pairs were included in the study. They were all Han nationality. The age of the patients ranged from 32 years to 78 years, averaging 58.93 years. The educational level was higher in controls than in the patients. The serum samples of 101 patients and 100 controls were tested for antibodies against *H. pylori*. Among them, 128(63.68%) were *H. pylori* positive. The prevalence of *H. pylori* infection was not significantly different in different age (above 30 years) and sex groups. The demographic characteristics as well as the distributions of prevalence of *H. pylori* infection in different sex and age groups are presented in Table 1 and Table 2.

Table 1 Demographic characteristics as well as *Helicobacter pylori* infection in patients and controls

	Patients		Controls		P value
	n	%	n	%	
Age (years)					
30-39	4	(4.0)	5	(5.0)	
40-49	18	(17.8)	18	(17.8)	
50-59	25	(24.8)	22	(21.8)	
60-69	34	(33.7)	38	(37.6)	
≥70	20	(19.8)	18	(17.8)	0.9597
Gender					
Males	87	(86.1)	87	(86.1)	
Females	14	(13.9)	14	(13.9)	1.0 000
Education					
College	1	(1.0)	1	(1.0)	
High school	17	(16.8)	68	(67.3)	
Elementary school	65	(64.4)	24	(23.8)	
Illiterate	18	(17.8)	8	(7.9)	0.0 000
<i>H. pylori</i>					
Positive	60	(59.4)	68	(68.0)	
Negative	41	(40.6)	32	(32.0)	0.2 064

Table 2 *Helicobacter pylori* infection in study subjects

Age group (years)	Men			Women		
	n	Hp(+)	%	n	Hp(+)	%
30-39	7	7	(100.0)	2	2	(100.0)
40-49	29	18	(62.1)	7	5	(71.4)
50-59	46	28	(60.9)	1	1	(100.0)
60-69	58	39	(67.2)	13	6	(46.2)
≥70	33	18	(54.6)	5	4	(80.0)
Total	173	110	(63.6)	28	18	(64.3)

$\chi^2 = 5.68$, $P = 0.2241$; $\chi^2 = 4.22$, $P = 0.3769$

No statistical difference was found in respect to presence of IgG antibody to *H. pylori* between patients and controls (Table 3). No significant difference was observed in anatomic distribution, although the prevalence of *H. pylori* infection was higher in non-cardiac gastric cancer (60.5%) than in cardiac cancer (56.0%), (Table 4).

Table 3 *Helicobacter pylori* infection and gastric cancer

Controls	Patients		Pairs
	Hp(+)	Hp(-)	
Hp(+)	39	29	68
Hp(-)	20	12	3
Pairs	59	41	100

$c^2 = 1.31$, $P = 0.25$

Table 4 *Helicobacter pylori* infection in gastric cancer cases

Gastric cancer	n	<i>H. pylori</i> infection	
		n	%
Cardiac	25	14	56.0
Non-cardiac	76	46	60.5

$\chi^2 = 0.04$, $P = 0.8395$

Further analysis was conducted using Conditional Logistic Regression. The results showed the risk factors of gastric cancer in Changle County were fish sauce intake, low consumption of fresh vegetables, unscheduled meals, low educational level and *H. pylori* infection (Table 5).

Table 5 The results of multivariate Conditional Logistic Regression analysis

Factors	β	S_x	OR	95%CI
Low educational level	1.3 517	0.4 487	3.864	1.604-9.311
Low consumption of vegetables	1.5944	0.6580	4.925	1.356-17.885
High intake of fish sauce	2.3596	0.6748	10.587	2.821-39.738
Unscheduled meals	1.4479	0.5508	4.254	1.445-12.552
<i>H. pylori</i> infection	1.2392	0.6852	3.453	0.901-13.224

DISCUSSION

Changle County is a hyperendemic area of gastric cancer^[5]. Chronic *H. pylori* infection has been identified as the most important risk factor of gastric cancer^[6]. The results of our study showed that residents in Changle County had a high prevalence of *H. pylori* infection. This coincided with the concept of high prevalence of *H. pylori* infection in the high risk area of gastric cancer. However, no statistical significant difference was found in respect to presence of *H. pylori* infection between patients and controls. The lack of association in this study may be due to the high prevalence of *H. pylori* in Changle County. *H. pylori* infection can initiate a sequence of histological alterations in the mucosa that may finally result in the development of gastric cancer,

but not all infected subjects will eventually develop gastric cancer. *H. pylori* alone cannot account for development of gastric cancer. Apart from *H. pylori* infection, other factors may play important roles in carcinogenesis.

The development of gastric cancer is believed to be a multistep and multifactorial process. In the Correa model of gastric carcinogenesis, environmental factors are related to the evolution from normal gastric tissue through superficial gastritis, atrophic gastritis, intestinal metaplasia and dysplasia to carcinoma^[7]. Environmental co-factors other than microbial agents may play roles in initiation, promotion or progression of gastric cancer.

The results of this study suggest that dietary factors, such as high intake of fish sauce and low consumption of fresh vegetables possibly increase the risk of gastric cancer. Fish sauce is a kind of traditional sauce consumed daily by Changle residents. It is usually produced from several kinds of sea fishes after long fermentation processes. The mutagenicity of fish sauce has been reported by several experimental studies^[8,9]. There was a large amount of important precursors of N-nitrosamines detected in fish sauce. High intake of fish sauce was an important risk factor involved in the etiology of gastric cancer. However, consumption of diets high in vegetables is the most effective means in preventing gastric cancer. Vegetables contain many biologically active compounds that may be responsible for an anticarcinogenic effect against gastric cancer^[10]. Additionally, unscheduled meals may cause injuries of gastric mucosa and potentiate the effects of carcinogens. Our study indicated that unscheduled meals might be one of the etiological factors for gastric cancer. In this study the educational level was higher in controls than in patients.

This supported the results of previous studies that socioeconomic status is a risk factor for gastric cancer, which in turn is related to diet and education.

These findings indicate that primary prevention should be focused in Changle County on reducing the etiological factors: fish sauce intake, deficiency in fresh vegetables, and *H. pylori* infection. Further elucidation of these risk factors for stomach cancer in Changle and assessment of the interaction between these risk factors and *H. pylori* infection are important for investigating the possible mechanisms of gastric carcinogenesis.

REFERENCES

- 1 The Eurogast study group. An international association between *Helicobacter pylori* infection and gastric cancer. *Lancet*, 1993; 341:1359-1362
- 2 Tatsuta M, Lishi H, Okuda S, Taniguchi H, Yokota Y. The association of *Helicobacter pylori* with differentiated type early gastric cancer. *Cancer*, 1993;72:1841-1845
- 3 Miehke S, Hackelsberger A, Meining A, Arnim U vom, Müller P, Ochsenkühn T, Lehn N, Malfertheiner P, Stolte M, Bayerdorffer E. Histological diagnosis of *Helicobacter pylori* gastritis is predictive of a high risk of gastric carcinoma. *Int J Cancer*, 1997;73: 837-839
- 4 Blasser MJ. Hypotheses on the pathogenesis and natural history of *Helicobacter pylori* induced inflammation. *Gastroenterology*, 1992;102:720-727
- 5 Cai L, Yi YN, Liu YY. A case control study of stomach cancer in Changle, Fujian Province by the risk state analysis. *Zhonghua Liuxingbingxue Zazhi*, 1991;1:15-18
- 6 Forman D, Newell DG, Fullerton F, Yarnell JW, Stacey AR, Wald N, Sitas F. Association between infection with *Helicobacter pylori* and risk of gastric cancer: evidence from a prospective investigation. *Br Med J*, 1991;302:1302-1305
- 7 Correa P. Human gastric carcinogenesis: a multistep and multifactorial process: first American cancer society award lecture on cancer epidemiology and prevention. *Cancer Res*, 1992;52:6735-6740
- 8 Zhang RF, Deng DJ, Chen Y, Chen CS, Fan ZH. Analysis of precursors of N-nitroso compounds in fish sauce from gastric cancer high risk area. *Aizheng*, 1993;12:395-398
- 9 Deng DJ, Zhang RF, Chen Y, Chen CS, Jin S, Zhu SX. Mutagenicity and carcinogenicity of fish sauce from a county with the high risk for gastric cancer in China. *Aibian Jibian Tubian*, 1991;3:18-23
- 10 Zhang HM, Wakisaka N, Maeda O, Yamamoto T. Vitamin C inhibits the growth of a bacterial risk factor for gastric carcinoma: *Helicobacter pylori*. *Cancer*, 1997;80:1897-1903

Edited by You DY and Zhu LH
proofread by Sun SM

Construction of HBV-specific ribozyme and its recombinant with HDV and their cleavage activity *in vitro*

Shu Juan Wen¹, Kai Jun Xiang², Zhen Hua Huang¹, Rong Zhou¹ and Xue Zhong Qi¹

Subject headings hepatitis B virus; hepatitis D virus; ribozyme gene; recombinant DVRZ

Wen SJ, Xiang KJ, Huang ZH, Zhou R, Qi XZ. Construction of HBV-specific ribozyme and its recombinant with HDV and their cleavage activity *in vitro*. *World J Gastroentero*, 2000;6(3):377-380

Abstract

AIM To construct the recombinant of HDV cDNA and HBV-specific ribozyme gene by recombinant PCR in order to use HDV as a transporting vector carrying HBV-specific ribozyme into liver cells for inhibiting the replication of HBV.

METHODS We separately cloned the ribozyme (RZ) gene and recombinant DVRZ (comprising HDV cDNA and HBV-specific ribozyme gene) into the downstream of T7 promoter of pTAdv-T vector and studied the *in vitro* cleavage activity of their transcripts (rRZ, rDVRZ) on target RNA (rBVCF) from *in vitro* transcription of HBV C gene fragment (BVCF).

RESULTS Both the simple (rRZ) and the recombinant ribozyme rDVRZ could efficiently catalyze the cleavage of target RNA (rBVCF) under different temperatures (37°C, 42°C and 55°C) and Mg²⁺ concentrations (10 mmol/L, 15 mmol/L and 20 mmol/L) and their catalytic activity tended to increase as the temperature was rising. But the activity of rRZ was evidently higher than that of rDVRZ.

CONCLUSION The recombinant of HDV cDNA and ribozyme gene had the potential of being further explored and used in gene therapy of HBV infection.

INTRODUCTION

Hepatitis B virus (HBV) can cause acute and chronic B-type hepatitis in man. The conventional ways available for curing this disease have not been very efficient. This promotes people to explore novel genetic therapeutical ways. Hammerhead ribozyme is a kind of antisense RNA which can specifically cleave the target RNA^[1,2]. In the light of this, people have developed many effective genetic vectors containing ribozyme genes, the transcripts of which showed catalytic activity *in vitro* and *in vivo*^[3-5]. But how to improve the stability and efficiency of ribozyme and specifically carry ribozyme gene into only target cells or tissues has been a tackling problem. HDV, a human hepatitis agent, is a defective RNA virus, the replication cycle of which relies on the infection of HBV^[6]. So HDV can be developed as a specific transporting and replicating vector *in vivo* for ribozyme to reach liver^[7]. In this study, we constructed HBV-specific hammerhead ribozyme gene (RZ) and the recombinant (DVRZ) of HDV cDNA (DV) and ribozyme gene (RZ) and made a careful investigation of their *in vitro* catalytic activity under various conditions. The positive results encouraged us to further explore the feasibility of using HDV as a vector carrying ribozyme for inhibiting the replication of HBV *in vivo*.

MATERIALS AND METHODS

Plasmids

The plasmid pSVC-D3 (containing HDV cDNA) as one of two templates of recombinant PCR was kindly offered by Prof. Taylor of American. pTAdv-T vector used for cloning was purchased from Clontech Corporation.

Major reagents

RiboMax transcription kit, acrylamide, bisactylamide, dNTP, rNTP and Taq polymerase were purchased from Promega. [α -³²P]UTP from Beijing Yuhui Corporation. Advantage-TM PCR pure kit (gel purification kit) from Clontech. X-film from Kodak. DNA polymerase I from Biolabs. T7/Sp6 sequencing kit from Pharmacia.

PCR primers

Primers P1 and P2 covered the whole sequence of designed HBV-specific hammerhead ribozyme gene (RZ) and were used to amplify ribozyme gene (53bp) because of 9nt base-pairing of their 3' ends.

¹Gene Center of Nanfang Hospital, First Military Medical University, Guangzhou 510515, Guangdong Province, China

²School of Life Sciences, University of Science and Technology of China, Hefei 230027, Anhui Province, China

Shu Juan Wen, graduated from First Military Medical University in 1985, major in gene diagnosis, having 6 papers published.

Supported by Natural Science Foundation of Guangdong Province, No.940311.

Correspondence to: Shu Juan Wen, Gene Center of Nanfang Hospital, First Military Medical University, Guangzhou 510515, Guangdong Province, China

Tel. 0086-20-85141044, Fax. 0086-20-87730347

Email. zhou@fimmu.edu.cn

Received 2000-01-11 Accepted 2000-02-18

The sequence of HBV-specific hammerhead ribozyme was designed according to the requirement of domains of ribozyme^[1] and the sequence of HBV C gene fragment.

The ribozyme gene (RZ: 53bp) was also used as one of two templates for recombinant PCR to construct the recombinant (DVRZ) of HDV cDNA and ribozyme gene (mentioned below).

P3, P4 were both recombinant primers, each of which was composed of partial sequences of ribozyme and HDV in order to replace the sequence (17-67) of near 5'-end of HDV with ribozyme by recombinant PCR. P5 was the 3'-end sequence of HDV cDNA.

P3, P4, P5 were used to construct the recombinant (DVRZ) of HDV cDNA (DV) and HBV-specific ribozyme gene (RZ) by one-tube recombinant PCR^[8].

P6, P7 were used to amplify HBV C gene fragment (BVCF), which was the transcription template of target RNA (rBVCF). T7 was partial sequence of T7 promoter region of pTAdV-T vector and was used for sequencing (with Sp6) and identifying (with P2, P5, P7) whether 5'-end of foreign fragment forwardly inserted the downstream of T7 promoter.

The sequencing of all gene fragments was performed on ABI391 automatic sequencer (Pharmacia). The sequences and positions of these primers are listed in Table 1.

Table 1 The sequences and positions of primers

Primer name	Sequences	Positions
P1	5'-AACATTGACATAGCTCTGATGAGTCCGTGAG-3'	RZ:1-31
P2	5'-TCCAGGGAATTAGTACTTTTGCTCCTCACGGAC-3'	RZ:53-23
P3	5'-AGCAAGCTTGAGCCAAAACATTGACATAGCTCT-3'	HDV:1-16, RZ:53-37
P4	5'-CTCCGACGTTCCAATGCTCCAGGGAATTAGTACT-3'	HDV:84-68, RZ:53-37
P5	5'-GTCGAATTCGGGCTCGGGCGCGATCCAGCAGTC-3'	HDV:1680-1647
P6	5'-GATAAGCTTTTACATAGAGGACTCTTGG-3'	HBV:1650-1677
P7	5'-CTGGAATTCGGCGAGGGAGTTCTTCTTAG-3'	HBV:2480-2450

Construction and cloning of HBV-specific ribozyme gene(RZ)

Because of 9nt base-pairing between 3'ends of P1 and P2, direct PCR could produce complete 53bp ribozyme gene (Figure 1). After gel-purification (according to Advantage-TM PCR pure kit, Clontech Corporation), the PCR product (RZ) was directly cloned into the downstream of T7 promoter of pTAdV-T vector and so the resulting recombinant plasmid pTA-RZ was obtained. PCR with T7/P2 as primers and pTA-RZ as template could produce about 100 bp DNA fragment if 5'-end of ribozyme gene was forwardly inserted in to the downstream of T7 promoter of pTAdV-T vector and so could be used to identify the recombinant plasmid pTA-RZ of forward insert. The preparation of competent DH5α cells and transformation of plasmids were performed according to the reference^[9]. The cloned ribozyme gene was finally verified by sequencing with T7/Sp6 primers.

Construction, cloning and sequencing of the recombinant (DVRZ) of HDV cDNA and HBV-specific ribozyme gene

Thirty μL PCR reaction system was established^[8]: 20 mmol/L Tris-HCl (pH 8.3), 50 mmol/L KCl, 2 mmol/L MgCl₂, each dNTP 200 μmol/L; Primers P3, P4, P5 were separately 0.05 μmol/L, 0.005 μmol/L, 0.05 μmol/L. The two templates were recombinant plasmids pTA-RZ (containing ribozyme gene) and pSVC-D3 (containing HDV cDNA), each 10 ng. Taq polymerase 2 μL, denaturation at 92 °C-50s; annealing at 53 °C-50s; elongation at 70 °C-120s; 33cycles; the final elongation at 70 °C lasted 5 min. PCR product (DVRZ, 1.7kb) was identified by agarose-gel (1.5%) electrophoresis and then purified with Advantage-TM PCR pure kit. The obtained DNA fragment (DVRZ) was directly cloned into the downstream of T7 promoter of pTAdV-T vector. The resulting recombinant plasmid pTA-DVRZ (positive clones on Ampr & white-blue plate) was verified by PCR with primers T7/P5 and sequencing with Sp6/T7 primers. PCR with primers T7/P5 could produce about 1.7kb-1.8kb DNA fragment and was used to identify the forward insertion of 5'-end of DVRZ. Sequencing was performed on ABI 391 automatic sequencer (Pharmacia).

Cloning and isolation of target gene fragment (HBV C gene fragment-BVCF)

PCR with primers P6, P7 was performed to amplify HBV C gene fragment from serum of HBV. Extraction of sample DNA and PCR reaction were performed according to the reference^[10]. PCR product (BVCF) was directly cloned into the downstream of T7 promoter of pTAdV-T vector and the resulting recombinant plasmid pTA-BVCF (positive clones on Ampr & blue-white plate) was verified by PCR with T7/P7 and bidirectional sequencing with T7/Sp6 primers. PCR with primers T7/P7 was utilized to identify the forward-direction insertion of 5'-end of BVCF.

Linearization of recombinant plasmids pTA-RZ, pTA-DVRZ and pTA-BVCF

These plasmids were separately digested with BamHI and then filled with Klenow fragment for *in vitro* transcription of inserted gene fragments (RZ, DVRZ, BVCF).

In vitro transcription of linearized plasmids pTA-RZ and pTA-DVRZ

³²P-UTP-labeled transcription of the two plasmids was first carried out in order to test the effect of transcription. But the plasmids' transcripts (rRZ, rDVRZ) used for catalyzing the cleavage of target RNA (rBVCF-transcript of plasmid pTA-BVCF containing HBV C gene fragment-BVCF) were not ³²P-labeled. In vitro transcription was performed with T7 RNA polymerase according to RiboMax Transcription kit and the reference^[11]. The

transcripts (rRZ, rDVRZ) would additionally contain 100nt partial sequence of pTAdV-T vector at their both ends. rRZ and rDVRZ were extracted by phenol/chloroform/iso-propyl alcohol (25:24:1), precipitated with ethanol and resuspended with H₂O (RNase-free). The latter was the recombinant of HDV and ribozyme.

Preparation of ³²P-UTP-labeled target RNA (rBVCF)

Linearized plasmid pTA-BVCF (containing HBV C gene fragment) was *in vitro* transcribed and the target RNA (rBVCF) was produced. 20 μ L transcription system was so established: ATP, CTP, GTP each 2.5 mmol/L and UTP 0.1 μ mol/L, 0.5 μ Ci/ μ L [α -³²P]UTP, 2 μ g linearized plasmid pTA-BVCF, T7 RNA polymerase 20U, RNasin 10U, 37°C-60 min. The product was loaded for 5% PAGE-7M urea autoradiographed electrophoresis. Gel-band of 1cm length and 0.5 cm breadth was cutted off from the position of target RNA and soaked overnight with NES buffer (0.5 mol/L NH₄Ac, 1 mmol/L EDTA, 0.1% SDS) and extracted with phenol/chloroform/iso-propyl alcohol (25:24:1). The supernate was precipitated with ethanol and then the pellet was harvested and resuspended with H₂O (RNase-free). rBVCF(831+100nt) contained also 100nt partial sequence of pTAdV-T vector at its two ends.

Cleavage reaction

Ten μ L reaction system was established: 0.1 mol/L Tris-HCl (pH 8.0), 20 mmol/L MgCl₂, rRZ or rDVRZ and their target RNA (rBVCF) each 2 μ L, mixed and incubated under different temperatures (37°C, 42°C, 55°C) for 1h. Negative control with ³²P-labeled rBVCF incubated at 55°C without rRZ & rDVRZ was performed. In the meantime, rRZ and rDVRZ were separately incubated with target RNA (rBVCF) at 37°C under different Mg²⁺ concentrations (10mmol/L, 15mmol/L). In the end, 10 μ L ion-free formamide and 1 μ L loading buffer (50% glycerol, 1mmol/L EDTA, 0.04% bromophenol blue) were added to terminate the reaction. Then after incubated at 65°C for 10 min, 5 μ L reaction sample was loaded for 5% PAGE-7M urea electrophoresis.

RESULTS

Construction and cloning of ribozyme gene

53bp DNA fragment was obtained by PCR with primers P1/P2 (Figure 1). This was in accordance with the size of anticipated ribozyme gene. PCR using T7/P2 as primers and plasmid pTA-RZ as the template amplified a DNA fragment of about 100 bp, which identified forward-direction insertion of ribozyme gene into the downstream of T7 promoter of pTAdV-T vector. Sequencing verified the HBV-specific ribozyme gene. The sequence of ribozyme gene was as follows: 5'-AACATTGACATAGCTCTGATGAGTCCG-TGAGGACAACTACTAATTCCTGGA-3'

Construction, cloning and sequencing of the recombinant (DVRZ) of HDV cDNA(DV) and HBV-specific ribozyme gene(RZ)

About 1.7kb DNA was amplified by recombinant PCR, which indicated the anticipated recombinant DNA molecule DVRZ (Figure 1). After DVRZ's cloning into pTAdV-T vector and transforming into DH5 α on Ampr & white-blue plate, PCR with primers T7/P5 produced about 1.8 kb-DNA fragment and identified the positive recombinant plasmid pTA-DVRZ of correct DVRZ's insertion direction. Sequencing of DVRZ with primers T7/Sp6 (pTA-DVRZ as template) confirmed the construct DVRZ.

Cloning and isolation of target gene fragment (HBV C gene fragment-BVCF)

Anticipated 831bp target DNA fragment was amplified by PCR from the serum of HBV (Figure 1). After its cloning into pTAdV-T vector and then transformed into DH5 α , PCR with primers T7/P7 produced an about 0.9 kb DNA fragment and so identified the positive recombinant plasmid pTA-BVCF of BVCF's correct insertion direction. Finally, sequencing with primers T7/Sp6 confirmed the inserted BVCF.

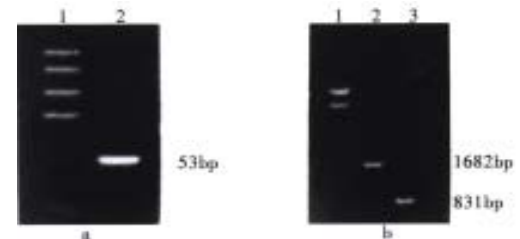


Figure 1 Construction of HBV-specific ribozyme gene (RZ), its recombinant with HDV cDNA (DVRZ) and target DNA (BVCF) by PCR. a: Lane 1-PCR marker, Lane 2-ribozyme gene RZ (53bp). b: Lane 1- λ DNA/-Hind III+*Eco* RI marker, Lane 2-recombinant DVRZ (1682bp) Lane 3-target gene BVCF (831bp).

In vitro transcription of linearized recombinant plasmids pTA-BVCF, pTA-RZ and pTA-DVRZ

Target RNA (rBVCF) of 931nt was transcribed from pTA-BVCF. HBV-specific ribozyme (rRZ) of 153nt was transcribed from pTA-RZ.

HBV-specific recombinant ribozyme (rDVRZ, containing HDV) of 1782nt was transcribed from pTA-DVRZ (Figure 2). All these transcripts (rBVCF, rRZ, rDVRZ) contained the same partial sequence of pTAdV-T vector at their both ends after transcription with T7 RNA polymerase.

Cleavage reaction

Ribozymes rRZ and rDVRZ without ³²P-label were separately incubated with target RNA (³²P-labeled rBVCF) under different temperatures (37°C, 42°C, 55°C) and Mg²⁺ concentrations. The results from autoradiographed electrophoresis showed that under these temperatures and Mg²⁺ concentrations, both

rRZ and rDVRZ could catalyze the cleavage of target rBVCF into two RNA fragments (721nt, 210nt) and their catalytic activity tended to increase with the rising of temperature. Comparatively, the catalytic activity of rRZ was higher than that of rDVRZ. But it seemed that Mg^{2+} from 10 mmol/L to 20 mmol/L had no obvious effect on their cleavage activity (Figure 3).

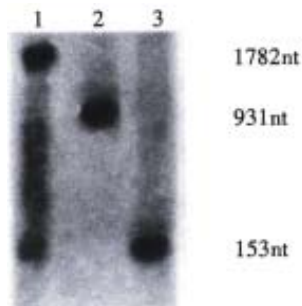


Figure 2 *In vitro* transcription of linearized pTA-RZ, pTA-DVRZ and pTA-BVCF (Lane 1-rDVRZ,1782nt. Lane 2-rBVCF,931nt. Lane 3-rRZ,153nt).

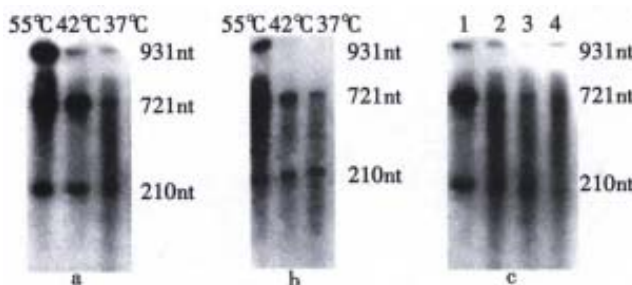


Figure 3 Cleavage of target RNA(rBVCF) catalyzed by rRZ and rDVRZ. a: Cleavage of target RNA (rBVCF) by rRZ under 37°C, 42°C and 55°C with 20 mmol/L Mg^{2+} . b: Cleavage of target RNA (rBVCF) by rDVRZ under 37°C, 42°C and 55°C with 20 mmol/L Mg^{2+} . c: Cleavage of target RNA (rBVCF) separately by rRZ and rDVRZ at 37°C under different Mg^{2+} concentrations (10 mmol/L, 15 mmol/L) (Lane 1,2-cleavage by rRZ separately under 10 and 15 mmol/L Mg^{2+} ; Lane 3,4-cleavage by rDVRZ separately under 10 and 15 mmol/L Mg^{2+})

DISCUSSION

Hammerhead ribozyme is a kind of antisense RNA with specific catalytic activity, which can catalyze the specific cleavage of target RNA^[1-3]. So far, many specific ribozyme constructs have demonstrated their catalytic activity both *in vitro* and *in vivo*^[12-15]. HDV, is a defective RNA virus, the replication cycle of which must be dependent on the infection of HBV^[6]. In view of the characteristics of hammerhead ribozyme and HDV, we constructed the recombinant(rDVRZ) of HDV and ribozyme by one-tube recombinant PCR with 3 primers and intended to have HBV-specific ribozyme carried into liver cells by using HDV as a transporting vector. As the first step, we studied the *in vitro* cleavage activity of HBV-specific ribozymes-rRZ and rDVRZ. The results showed that both rRZ and rDVRZ had the ability of catalyzing the specific cleavage of target RNA (rBVCF-*in vitro* transcript of HBV C gene fragment) into two RNA fragments (721nt, 210nt).

The activity of ribozyme rRZ (without containing HDV) was much higher than that of recombinant rDVRZ, which in part cleaved the target RNA. One possible reason is that rDVRZ has much longer two arms outside its base-pairing region and can easily form a complex secondary or tertiary structure, an obstacle to subsequent base-pairing with target RNA (rBVCF). Its three-dimensional structure simulated by computer (not presented here) supports this conclusion. However, we could conclude that the post-transcripted hammerhead ribozyme should not be too long though we are unsure how long ribozyme and its target RNA are optimal to their interaction.

We found that with the temperature rising, the ribozyme activity increased, possibly because higher temperature helped transit the complex tertiary structure into comparatively extended state and so partially delete the structural obstacle to base-pairing. We also found that the requirement of ribozyme for Mg^{2+} was not strict. It appeared that different Mg^{2+} concentrations from 10 mmol/L to 20 mmol/L could meet the ribozymes' activity. But overhigh Mg^{2+} seemed to cause the non-specific cleavage of target RNA (not presented). The reason for this was unclear. Presently, we are studying the activity of the recombinant ribozyme *in vivo* and its repressive effect on HBV replication.

REFERENCES

- 1 Cech TR. The chemistry of self-splicing RNA and RNA enzymes. *Science*, 1987;236:1532-1539
- 2 Hutchins CJ, Rathjen PD, Forster AC, Symons RH. Self-cleavage of plus and minus RNA transcripts of avocado sunblotch viroid. *Nucl Acids Res*, 1986;14:3627-3640
- 3 von Weizsacker F, Blum HE, Wands JR. Cleavage of hepatitis B virus RNA by three ribozymes transcribed from a single DNA template. *Biochem Biophys Res Commun*, 1992;189:743-748
- 4 Funato T, Ishii T, Kanbe M, Scanlon KJ, Sasaki T. Reversal of cisplatin resistance *in vivo* by an anti-fos ribozyme. *In Vivo*, 1997;11:217-220
- 5 Kim YK, Junn E, Park I, Lee Y, Kang C, Ahn JK. Repression of hepatitis B virus X gene expression by hammerhead ribozymes. *Biochem Biophys Res Commun*, 1999;257:759-765
- 6 Karayiannis P. Hepatitis D virus. *Rev Med Virol*, 1998;8:13-24
- 7 Hsieh SY, Taylor J. Delta virus as a vector for the delivery of biologically active RNAs: possibly a ribozyme specific for chronic hepatitis B virus infection. *Adv Exp Med Biol*, 1992;312:125-128
- 8 Marini F, Naeem A, Lapeyre JN. An efficient 1-tube PCR method for internal site directed mutagenesis of large amplified molecules. *Nucl Acid Res*, 1993;21:2277-2278
- 9 Sambrook J, Fritsch EF, Maniatis T. Molecular cloning laboratory manual, 2nd. New York: Cold Spring Harbor Laboratory Press, 1989
- 10 Bruce AW. PCR Protocols: current methods and applications. New Jersey, Human Press, 1993
- 11 Xu ZK, Anzola JV, Nalin CM, Nuss DL. The 3' terminal sequence of a wound tumor virus transcript can influence conformational and functional properties associated with the 5' terminus. *Virology*, 1989;170:511-522
- 12 Beck J, Nassal M. Efficient hammerhead ribozyme-mediated cleavage of the structured hepatitis B virus encapsidation signal *in vitro* and in cell extracts, but not in intact cells. *Nucl Acid Res*, 1995;23:4954-4962
- 13 Zern MA, Ozaki I, Duan L, Pomerantz R, Liu SL, Strayer DS. A novel SV40-based vector successfully transduces and expresses an alpha 1-antitrypsin ribozyme in a human hepatoma-derived cell line. *Gene Ther*, 1999;6:114-120
- 14 Wands JR, Geissler M, Putlitz JZ, Blum H, Weizsacker FV, Mohr L, Yoon SK, Melegari M, Scaglioni PP. Nucleic acid-based antiviral and gene therapy of chronic hepatitis B infection. *J Gastroenterol Hepatol*, 1997;12:s354-369
- 15 Albuquerque-Silva J, Milican F, Bollen A, Houard S. Ribozyme mediated decrease in mumps virus nucleocapsid mRNA level and progeny in infected vero cells. *Anti Nucleic Acid Drug Dev*, 1999;9:279-288

A 12-year cohort study on the efficacy of plasma-derived hepatitis B vaccine in rural newborns

Hong Bin Liu¹, Zong Da Meng¹, Jing Chen Ma², Chang Quan Han², Ying Lin Zhang², Zhan Chun Xing², Yu Wei Zhang², Yu Zhong Liu² and Hui Lin Cao³

Subject headings hepatitis B vaccine; HBsAg; vaccination; rural newborn; cohort study

Liu HB, Meng ZD, Ma JC, Han CQ, Zhang YL, Xing ZC, Zhang YW, Liu YZ, Cao HL. A 12-year cohort study on the efficacy of plasma-derived hepatitis B vaccine in rural newborns. *World J Gastroentero*, 2000;6(3):381-383

Abstract

AIM To understand the anti-HBs persistence and the long-term preventive efficacy in rural newborns after vaccination with plasma-derived hepatitis B vaccine.

METHODS In the time of expanded program on immunization (EPI), the newborns were vaccinated with $10\ \mu\text{g} \times 3$ doses of hepatitis B vaccine and 762 newborns who were HBsAg negative after primary immunization were selected for cohort observation from 1986 to 1998. Their serum samples were detected qualitatively and quantitatively for hepatitis B infecting markers, including HBsAg, anti-HBs and anti-HBc by SPRIA Kits. The annual HBsAg positive conversion rate was counted by life-table method.

RESULTS ① The anti-HBs positive rate was 94.44% for the babies born to HBsAg negative mothers and 84.21% for those born to HBsAg positive mothers in the 1st year after immunization, and dropped to 51.31% and 52.50% in the 12th year respectively. GMT value was dropped from 31.62 to 3.13 and 23.99 to 3.65 in the 2nd to the 12th year respectively. There was a marked drop in GMT at the 3rd to the 5th year, and in anti-HBs positive rate at the 9th to the 10th year. ② In the period of 12 years observation, the person-year HBsAg positive

conversion rates were 0.12% (5/4150.0) in newborns born to HBsAg negative mothers and 0.20% (1/508.0) in those born to HBsAg positive mothers, and none of the HBsAg positive converted children became HBsAg chronic carriers. Compared with the baseline before immunization, the protective rates were 97.19% and 95.32% respectively.

CONCLUSION The protective efficacy of plasma-derived hepatitis B vaccine persisted at least 12 years, and a booster dose seems not necessary within at least 12 years after the primary three-doses immunization to newborns born to HBsAg negative mothers.

INTRODUCTION

In recent years, many studies on the efficacy of hepatitis B plasma-derived vaccine demonstrated that the anti-HBs antibodies were declined gradually, but the protective rate for children vaccinated with three-doses hepatitis B vaccine was still more than 80%^[1,2]. To understand the anti-HBs persistence and long-term efficacy in newborn, a 1-12 year experimental study on hepatitis B plasma-derived vaccine was carried out among newborns vaccinated with three doses $10\ \text{mg/L}$ vaccine in rural area.

MATERIALS AND METHODS

Objects

Newborn infants from one township in Zhengding County, Hebei Province, were vaccinated during 1986-1989. A total of 762 infants who were HBsAg negative after primary vaccination were selected for cohort observation, of them 688 born to HBsAg-negative mothers, and 74 to HBsAg carrier mothers. The annual HBsAg positive conversion rate for newborn infants was 4.72% before immunization.

Vaccine and immunization

Hepatitis B plasma-derived vaccine was produced by Beijing Institute of Biological Product. The newborns were immunized with three doses vaccine at 0mo, 1mo and 6mos of age by well-trained

¹Virology Department of Hebei Provincial Sanitary and Anti-Epidemic Station, Baoding 071000, Hebei Province, China

²Department of Hepatitis, Zhengding county Sanitary and Anti-Epidemic Station, Zhengding 070800, Shijiazhuang, Hebei Province, China

³Department of Hepatitis, Institute of Virology, Chinese Academy of Preventive Medicine, Beijing 100052, China

Dr. Hong Bin Liu, graduated from Hebei Medical University as a postgraduate in 1998, associate professor of epidemiology, majoring in epidemiology, having 15 papers published.

Supported by the National "95" Scientific Foundation, No. 96-906-03-02

Correspondence to: Dr. Hong Bin Liu, Virology Department of Hebei Provincial Sanitary and Anti-Epidemic Station, 36 Hongqilu, Baoding 071000, Hebei Province, China

Tel. 0086-312-5061472, Fax. 0086-312-5063123

Received 2000-01-18 Accepted 2000-01-28

nurses between 1986-1989 under the rural area immunization program launched in 1986. The first dose was vaccinated at 2.7 mo-0.3 mo (95% CI). The coverage rate of vaccination with a complete course of 3-dose hepatitis B vaccine was 91.5%.

Blood collection and laboratory study

Blood samples were collected from infants by venipuncture at intervals of one or two years. Serum HBsAg, anti-HBs and anti-HBc were tested by RIAs from Beijing Institute of Biological Product. Those who showed HBsAg (S/N value ≥ 2.1), anti-HBc (CO/S value ≥ 2.0) or both were defined as HBV infection, and anti-HBs (S/N value ≥ 2.1) as immunity.

RESULTS

Persistence of anti-HBs after vaccination

The 688 new born babies were born to HBsAg negative mothers, and 74 were born to HBsAg positive mothers. Anti-HBs positive rate was gradually dropped from 94.44% to 51.31% and 84.21% to 52.50% in the 1st-12th year respectively. GMT value was dropped from 31.62 to

3.13 and 23.99 to 3.65 in the 2nd-12th year respectively. There was a marked drop in GMT value at the 3rd-5th year, and in anti-HBs positive rate at the 9th-10th year. Compared with infants born to HBsAg negative mothers, GMT value was lower in infants born to HBsAg positive mothers (Table 1).

HBsAg annual positive conversion rate for vaccinated children

In the period of 12 years follow-up, 5 children born to HBsAg-negative mothers became HBsAg positively converted. Two of them occurred at the 5th year and the rest occurred at the 9th-10th year. The person-year HBsAg positive conversion rate was 0.12% (5/4150.0). One child born to HBsAg positive mothers became HBsAg positively converted, and it occurred at the 5th year. The person-year HBsAg positive conversion rate was 0.20% (1/508.0). None of 6 HBsAg positive converted children became HBsAg chronic carriers (Table 2). Compared with the baseline before immunization, the protective rates were 97.19% and 95.32% respectively (Table 3).

Table 1 Dynamic change of anti-HBs positive rate and GMT after vaccination

Years vaccinated	Mothers HBsAg (-)			Mothers HBsAg (+)		
	No. tested	Positive rate (%)	GMT (S/N)	No. tested	Positive rate (%)	GMT (S/N)
1	18	94.44	26.30	19	84.21	15.14
2	134	89.55	31.62	48	95.83	23.99
3	232	89.22	26.30	51	92.16	22.91
4	344	85.17	18.62	51	73.33	6.46
6	296	79.39	9.77	54	79.63	8.71
7	608	80.76	9.33	58	86.21	7.78
8	599	78.30	6.17	56	75.00	5.25
9	517	57.79	4.17	48	60.24	3.47
10	412	50.24	3.09	23	34.78	2.51
11	173	51.80	2.86	30	56.00	2.91
12	424	51.30	3.13	20	52.50	3.65
χ^2 m-h		226.12			338.58	
P value		P<0.001			P<0.001	

Table 2 HBsAg person-year positive conversion for immunized children

Follow-up (year)	Mother HBsAg (-)			Mother HBsAg (+)		
	No. person year	No. positively converted	Annual positive conversion rate	No. person year	No. positively converted	Annual positive conversion rate
1	9.0	0	0.00	9.5	0	0.00
2	76.0	0	0.00	33.5	0	0.00
3	183.0	0	0.00	49.5	0	0.00
4	288.0	0	0.00	51.0	0	0.00
5	454.0	2	0.44	55.5	1	1.80
6	428.0	0	0.00	57.0	0	0.00
7	450.0	0	0.00	56.0	0	0.00
8	602.0	0	0.00	57.0	0	0.00
9	482.0	2	0.34	52.0	0	0.00
10	486.0	1	0.20	35.5	0	0.00
11	292.5	0	0.00	26.5	0	0.00
12	298.5	0	0.00	25.0	0	0.00
Total	4150.0	5	0.12	508.0	1	0.20

Table 3 Protective rate to vaccinated neonates

Mother HBsAg	Observed numbers	Person year numbers	HBsAg positive conversion numbers	Annual Positive conversion rate	Effective protective rate
Negative(-)	688	4150.0	5	0.12	97.19
Positive (+)	74	508.0	1	0.20	95.32
Total	762	4658.0	6	0.13	96.96
Baseline	562	1124.0	48	4.27	

DISCUSSION

The ultimate strategy for newborn vaccination with hepatitis B vaccine is controlling and eliminating hepatitis B. Many specialists think that newborns should be vaccinated within 24 hours which is more effective for preventing HBV mother-infant transmission. In recent studies, some reports say that the risk of HBV infection should increase with the decline of anti-HBs positive rate and GMT value after vaccination of hepatitis B vaccine^[2,3]. Thus, a booster of hepatitis B vaccine should be given. In this study, anti-HBs positive rate declined with age, so was GMT value. The anti-HBs positive rate declined markedly from the 9th to the 10th year, and maintained 50% or so at the 10th-12th year. GMT value declined markedly from the 3rd to the 5th year. Therefore, if we only analyze anti-HBs positive rate and GMT value, it is the best schedule to revaccinate at 3-5 years of age after the primary 3-doses regimen.

With the long-term observation of hepatitis B vaccine, more and more scholars think that the protective efficacy for immune responder could persist several years, even if anti-HBs may have declined to undetectable levels. This may be due to the good memory response to hepatitis B vaccination. The higher anti-HBs level after booster immunization dropped quickly with time, and at the end of 3-5 years dropped to the level of children who had not received booster immunization^[4,5]. The evaluation of the immune efficacy of hepatitis B vaccine should induce antibody level, but the dynamic of HBsAg and the chronic carrier rate during ten years of immunization. Cao *et al*^[6] reported that anti-HBs level declined with years after vaccination and HBsAg positive conversion had not been detected among children born to HBsAg negative mothers in Hunan. Our study indicated that none of children born to HBsAg negative mother became HBsAg chronic carrier within 12 years after vaccination with hepatitis B vaccine, although a few children were infected with HBV and positive for HBsAg. The protective rate

to those newborns born to HBsAg negative mother was still more than 95% within 12 years. We believed that long-term efficacy of hepatitis B vaccine was better and the children would have benefited from life-long hepatitis B vaccine. A booster dose seems unnecessary for children born to HBsAg negative mothers within 12 years after primary 3-dose regimen. It was reported by Cao *et al*^[7] that HBsAg positive conversion children born to HBsAg carrier mothers may become HBsAg chronic carriers after vaccination with hepatitis B vaccine, and most of them occurred at 2-3 years of age. In our study, only 1 of 74 children born to HBsAg carrier mother became HBsAg positively converted, but did not become HBsAg chronic carrier within 12 years after vaccination. In order to improve the immune efficacy for those children born to HBsAg positive mothers, the dynamic of HBsAg carrier rate should be observed further in vaccinated children on a large scale.

REFERENCES

- 1 Yuan JD. Observation on efficacy of health children immunized with China hepatitis B vaccine. *Shandong Weisheng Fangyi*, 1987; 2:27-30
- 2 Maupas P, Chiron JP, Barin F, Coursaget P, Goudeau A, Perrin J, Denis F, Diop-Mar I. Efficacy of hepatitis B vaccine in prevention of early HBsAg carrier state in children. Controlled trial in an endemic area (Senegal). *Lancet*, 1981;1:289-292
- 3 Coursaget P, Yvonnet B, Chotard J, Sarr M, Vincelot P, N'doye R, Diop-Mar I, Chiron JP. Seven-year study of hepatitis B vaccine efficacy in infants from an endemic area (Senegal). *Lancet*, 1986; ii:1143-1145
- 4 Jilg W, Schmidt M, Deinhardt F. Immune response to hepatitis B revaccination. *J Med Virol*, 1988;24:377-384
- 5 Yang JY, Wang SS, Li RC, Li YP, Gong J, Nong Y, Chen XR, Cao HL, Liu CB, Xu ZY. The efficacy of HB vaccine and reactivation of anti-HBs by booster at 7th year after neonates vaccination. *Zhonghua Shiyan He Linchuang Bingduxue Zazhi*, 1995;9(Suppl): 47-50
- 6 Cao HL, Liu CB, Xia GL, Yan TQ, Ma JC, Li RC, Ou-Yang PY, Liu YX, Zhang MT, Wang JJ, Gong J. A cohort study on immune persistence and preventive efficacy of hepatitis B vaccine II: the dynamic change of anti-HBs levels in immunized children. *Zhonghua Shiyan He Linchuang Bingduxue Zazhi*, 1995;9(Suppl): 10-12
- 7 Cao HL, Xu ZY, Liu CB, Xia GL, Yan TQ, Ma JC, Li RC, Liu YX, Zhang MT, Wang JJ, Yang JY, Sun YD, Zhu QR. A cohort study of immune persistence and preventive efficacy in children after hepatitis B vaccination I: the dynamic observation of HBsAg positive conversion in neonates after HB vaccine immunization. *Zhonghua Shiyan He Linchuang Bingduxue Zazhi*, 1995;9(Suppl):5-9

Pharmacokinetics of traditional Chinese syndrome and recipe: a hypothesis and its verification (I)

Xi Huang¹, Ping Ren¹, Ai Dong Wen², Li Li Wang¹, Li Zhang¹ and Feng Gao³

Subject headings traditional Chinese syndrome/recipe; Chinese medicine; pharmacokinetics; blood stasis; spleen deficiency; hypothesis

Huang X, Ren P, Wen AD, Wang LL, Zhang L, Gao F. Pharmacokinetics of traditional Chinese syndrome and recipe: a hypothesis and its verification (I). *World J Gastroentero*, 2000;6(3):384-391

Abstract

AIM To propose a hypothesis defining the absorption, distribution, metabolism and elimination of traditional Chinese recipe (TCR) component in blood of healthy subjects and patients, and estimate its correctness. **METHODS** The pharmacokinetics (PK) of same dose of drug was studied in the animal model of traditional Chinese syndrome (S) and healthy animals. The classification, terminology, concept and significance of the hypothesis were set forth with evidence provided in the present study. The hypotheses consisted of traditional Chinese syndrome PK (S-PK) and traditional Chinese recipe PK (R-PK). Firstly, the observed tetramethylpyrazine (TMP) PK in healthy, chronically reserpinized rats (rat model of spleen deficiency syndrome, RMSDS) and RMSDS treated with Sijunzi decoction (SJZD) for confirmation were used to verify S-PK; secondly, the ferulic acid (FA) PK in healthy and high molecular weight dextran (HMWD)-induced rabbit model with blood

stasis syndrome (RDBSS) was also used to verify S-PK; and lastly, TMP PK parameters in serum of healthy rats afterorally taken - *Ligusticum wallichii* (LW), LW and *Salvia miltiorrhiza* (LW&SM) decoctions were compared to verify R-PK.

RESULTS The apparent first-order absorption [K_a , $(13.61 \pm 2.56)h^{-1}$], area under the blood drug concentration-time curve [AUC, $(24.88 \pm 9.76) \mu g \cdot h^{-1} mL^{-1}$], maximum drug concentration [C_{max} , $(4.82 \pm 1.23) \mu g \cdot mL^{-1}$] of serum TMP in RMSDS were increased markedly ($P < 0.05$) compared with those [$K_a = (5.41 \pm 1.91)h^{-1}$, AUC = $(5.20 \pm 2.57) \mu g \cdot h^{-1} \cdot mL^{-1}$, $C_{max} = (2.33 \pm 1.77) \mu g \cdot mL^{-1}$] of healthy rats (HR). The apparent first-order rate constant for α and β distribution phase [$\alpha = (0.38 \pm 0.09)h^{-1}$, $\beta = (0.06 \pm 0.03)h^{-1}$], the apparent first-order intercom partmental transfer rate constants [$K_{10} = (0.24 \pm 0.07)h^{-1}$, $K_{12} = (0.11 \pm 0.02)h^{-1}$, $K_{21} = (0.11 \pm 0.02)h^{-1}$] of serum TMP in RMSDS were decreased significantly ($P < 0.01$) compared with those [$K_{10} = (0.88 \pm 0.20)h^{-1}$, $K_{12} = (1.45 \pm 0.47)h^{-1}$, $K_{21} = (0.72 \pm 0.22)h^{-1}$] of HR. However, no apparent differences occurred between HR and RMSDS treated with SJZD. The serum FA concentration and its AUC [$(5.6690 \pm 2.3541) \mu g \cdot h^{-1} \cdot mL^{-1}$] in RMBSS were also higher than those [AUC = $(2.7566 \pm 0.8232) \mu g \cdot h^{-1} \cdot mL^{-1}$] of healthy rabbits ($P < 0.05$). The K_a $(11.51 \pm 2.82)h^{-1}$, AUC $(0.84 \pm 0.17) \mu g \cdot h^{-1} \cdot mL^{-1}$ of LW & SM-derived TMP in serum were much lower ($P < 0.05$) than those [$K_a = (19.58 \pm 4.14)h^{-1}$, AUC = $(1.27 \pm 0.26) \mu g \cdot h^{-1} \cdot mL^{-1}$] of LW-derived TMP in serum after oral decoctions.

CONCLUSION The SDS and blood stasis syndrome state could affect significantly the pharmacokinetic parameters of drugs and the abnormal SDS pharmacokinetic parameters could be normalized by SJZD. The combination of Chinese medicine in TCR could reciprocally affect the pharmacokinetic parameters of other components absorbed into the systemic circulation. These results support the S and R-PK hypothesis.

¹Laboratory of Clinical Pharmacology of Chinese Medicine, Xijing Hospital, The Fourth Military Medical University, Xi'an 710032, Shaanxi Province, China

²Department of Pharmacy, Xijing Hospital, The Fourth Military Medical University, Xi'an 710032, Shaanxi Province, China

³Department of Physiology, The Fourth Military Medical University, Xi'an 710032, Shaanxi Province, China

Xi Huang M.D. & Ph.D. graduated from Fourth Military Medical University as a postgraduate in 1995, worked as a postdoctoral research fellow in Laboratory of Cardiovascular Disease, Xiyuan Hospital, China Academy of Traditional Chinese Medicine from 1996 to 1998, now professor and director in Laboratory of Clinical Pharmacology of Chinese Medicine, majoring clinical pharmacology of Chinese medicine, having 50 papers published.

Supported by National Natural Science Foundation of China, No.39870932; 39670865; 39570870 and 39100139.

Correspondence to: Dr. Xi Huang, Laboratory of Clinical Pharmacology of Chinese Medicine, Xijing Hospital, The Fourth Military Medical University, Xi'an 710032, Shaanxi Province, China
Tel. 0086-29-3373914, Fax. 0086-29-3224474
Email. tcmwsh@fmmu.edu.cn

Received 2000-01-05 Accepted 2000-01-22

INTRODUCTION

Three progresses in the related subjects arouse us to propose hypotheses defining the traditional Chinese syndrome (S) and recipe PK (S-PK and R-PK)^[1-6]. Firstly, in the field of traditional Chinese medicine (TCM), their characteristic PK has not developed as a consequence of what are the chemical components absorbed into the circulation after administering traditional Chinese recipe (TCR) is not clear yet. Then, the progresses in successful detection of TCR-derived component in serum from 1985 to 1989 supported the concept of above hypothesis^[7,8]. Finally, the theoretical and practical achievements of chronopharmacokinetics are not only an example but also enhanced our intention of presenting the hypothesis^[9-11].

The investigation of TCR-derived compound *in vivo* affords a sound basis for advancing the hypothesis of S and R-PK^[2-8,12,13] and the inspiration from the theory and practice of chronopharmacokinetics greatly encourages^[9-11]. The knowledge dealing with the rhythmic changes of pharmacokinetic phenomenon in living organisms is called chronopharmacokinetics^[14], in which, PK of administering drug at different time is not constant and is related to its therapeutic and toxic effects^[14]. Similarly, are there possible differences of serum drug concentration and its pharmacokinetic parameters between different TCS and different Chinese medicines of TCR? In other words, does TCS state and the drugs combination in TCR affect significantly the blood drug concentration and their pharmacokinetic parameters after oral administration? We have postulated the above positive differences in the previously published hypotheses^[11-6].

The four applications according to above concepts have been supported by National Natural Science Foundation of China since 1991. Under the support of grants, we choose *Ligusticum wallichii* (LW) prescriptions and its chemical components as the examples to verify the above hypotheses.

MATERIALS AND METHODS

Drugs, chemicals and reagents

Tetramethylpyrazine phosphorus (TMPP) intravenous infusion in 2 mL ampule (25 g/L, lot No. 90101) and sodium ferulate (SF) were purchased from Guangdong Limin Pharmaceutical Factory (Shaoguang, China); reserpine injection solution in 1 mL (1mg, lot No. 901008) was purchased from Red-Flag Pharmaceutical Factory of Shanghai Medical University (Shanghai, China).

LW was purchased from Dujiangyan City Pharmaceutical Company (Sichuan, China) which was identified by Professor Hu ZH (the Department of Botany, Northwest University, Xi'an, China). *Salvia miltiorrhiza* (SM), *Panax ginseng* C.A.Mey,

Atractylodes macrocephala Koidz, *Poria cocos* (Schw.) Wolf, *Glycyrrhiza uralensis* Fisch were purchased from Xi'an Pharmaceutical Company (Xi'an, China). All organic reagents were bought from Xi'an Chemical Reagent Factory. All chemicals were of analytical reagent grade unless otherwise stated. Methaqualonum (internal standard) was presented by Institute of Materia Medica, Beijing Medical University (Beijing, China). Coumarin (internal standard) was purchased from Sigma. High molecular weight dextran (HMWD) (M_w 500 000) was bought from Tianjin Air Force hospital (Tianjin, China).

Instruments

The following main instruments were used in the experiment: Shimadzu LC-6A HPLC system; SPD-6A ultraviolet detector; shimadzu QP-1000 gas chromatography-mass spectrometer. 7650 infrared spectrometer. RH-90 NMR meter.

Definitions of S and R-PK hypotheses^[1-6]

The S-PK hypothesis indicates that the pharmacokinetic differences between the different TCS have statistical significance and R-PK hypothesis means that one of TCM could influence markedly the pharmacokinetic parameters of other TCM-derived components in blood when administered together in same TCR. The above two pharmacokinetic characteristics are related to the therapeutic, toxic responses and theory of TCM.

The verification of S-PK

The preparation of SJZD (TCR): it consists of *Panax ginseng* C.A.Mey, *Atractylodes macrocephala* Koidz, *Poria cocos* (Schw.) Wolf and *Glycyrrhiza uralensis* Fisch (2:2:2:1). The 7000 g of SJZD drugs were divided into 7 parts. Each part of 1000g was macerated with 7000 mL of distilled water (drug: water=1:7, v/v) at room temperature for 1 h and then boiled for 40 min. The residues were boiled by same volume of water for 40 min once again. Firstly, the two boiled water extracts were mixed, then filtered through several layers of cotton gauze to remove the coarse particles and concentrated by evaporation, repeated preparation of the other parts of SJZD in the same way. The mixture of the seven parts of extraction gives the final concentration of 3 g·mL⁻¹.

Serum TMP and FA PK in healthy and modeled animals were studied to verify the hypotheses. Healthy animals and animal models were divided into five groups and the latter included rat model of spleen deficiency syndrome (RMSDS) treated with SJZD; and rabbit model with blood stasis syndrome (RMBSS). Group 1 (HR-1, *n* = 72): healthy male Wistar rats weighing 240 g ± 20 g afforded from the Experimental Animal Center, the Fourth Military Medical University were injected ip with normal

saline ($0.1 \text{ mL} \cdot \text{kg}^{-1} \cdot \text{d}^{-1}$, 14d). Group 2 (RMSDS, $n = 72$): healthy Wistar rats were injected ip with reserpine ($0.5 \text{ mg} \cdot \text{kg}^{-1} \cdot \text{d}^{-1}$, 14d). Group 3 (RMSDS treated by SJZD, $n = 72$): healthy Wistar rats were prepared the same as Group 2 and treated with intragastric administration of SJZD ($30 \text{ g} \cdot \text{kg}^{-1} \cdot \text{d}^{-1}$, 14 d). The above three groups were given *po* $10 \text{ mg} \cdot \text{kg}^{-1}$ of TMPP 24 h after the final injection of normal saline or reserpine. Group 4 (HR-2, $n = 6$): healthy male New Zealand white rabbits afforded from the Animal Center of our university were injected intravenously with normal saline ($15 \text{ mL} \cdot \text{kg}^{-1}$). Group 5 (RMBS, $n = 6$): rabbits were prepared by intravenous injection of 100 g/L HMWD in normal saline ($15 \text{ mL} \cdot \text{kg}^{-1}$). FA was injected intravenously of $5 \text{ mg} \cdot \text{kg}^{-1}$ 30 min after the end of injection of normal saline or HMWD. Rats and rabbits were fasted 12 h before administration.

The 0.5 mL of serum samples of rats were obtained by decapitation after a single oral TMPP at 0.083 h , 0.5 h , 1.0 h , 3 h , 5 h , 8 h , 12 h and 24 h , respectively. At each time point, 6 samples were obtained. The rabbit blood sample of 0.5 mL was directly withdrawn and collected from the ear vein at 2 min , 5 min , 10 min , 20 min , 30 min , 45 min , 60 min , 90 min , 120 min , 150 min and 180 min after intravenous FA. The blood samples were centrifuged ($3000 \text{ r} \cdot \text{min}^{-1}$, 5 min), and 0.2 mL of the resulting serum was used.

Chromatographic condition

Determination of serum TMP concentration^[15-17]: the chromatographic system (Shimadzu LC-6A, Japan) consisted of two pumps (LC-6A), a sample injector (Rheodyne, model 7125), a SPD-6AV detector (Shimadzu) and a C-R3A data processor (Shimadzu). A Shim-Pach CLC-ODS column (particles $5 \mu\text{m}$, $150 \text{ mm} \times 4.6 \text{ mm ID}$) was used for quantitative analysis; AUFs was 0.04 , the flow rate was 1 mL/min , the paper speed was 3 mm/min , column temperature was 38°C , the detection wavelength was 280 nm , the mobile phase consisted of methanol and water ($72:28 \text{ v/v}$). The serum concentration data of HR-1 and RMSDS were analyzed by the 3P87 (Chinese Pharmacological Association) software.

Determination of serum FA concentration^[18]: the detector was set at 320 nm (AUFs: 0.01); the mobile phase was acetonitrile $0.1 \text{ mL} \cdot \text{min}^{-1}$ phosphoric acid ($\text{pH } 2.5$) ($3:7, \text{ v/v}$); the other chromatographic conditions were the same as those in determining serum TMP concentration.

Sample preparation

Serum sample contained TMP: internal standard of Methaqualonium (428 ng) was added to 5 mL of

ground conical centrifuge tube containing $100 \mu\text{L}$ of methanol. The mixture was oscillated on vortex mixer and evaporated to dryness at 48°C on water bath under the stream of nitrogen. Successively added 0.2 mL of blank rat serum, the different amount of TMPP ($0.044 \mu\text{g} \cdot \text{mL}^{-1}$, $0.087 \mu\text{g} \cdot \text{mL}^{-1}$, $0.168 \mu\text{g} \cdot \text{mL}^{-1}$, $0.336 \mu\text{g} \cdot \text{mL}^{-1}$, $0.671 \mu\text{g} \cdot \text{mL}^{-1}$ and $1.342 \mu\text{g} \cdot \text{mL}^{-1}$), $0.2 \text{ mL } 0.05 \text{ mol/L}$ of NaOH solution and 2 mL of trichloromethane to the above centrifugate. After the mixture was vortex mixed again for 15 s , it was centrifuged at $3000 \text{ r} \cdot \text{min}^{-1}$ for 10 min . The organic layer was transferred into another 5 mL ground conical centrifuge tube contained $100 \mu\text{L}$ of 1 mol/L hydrochloric acid-methanol solution (50 mL/L) and evaporated again to dryness on water bath at 48°C under a stream of nitrogen. The residue was dissolved with $100 \mu\text{L}$ of methanol solution and then $20 \mu\text{L}$ was determined by HPLC each time^[15].

Serum sample contained FA: to 0.2 mL of rabbit serum added 0.4 mL of acetonitrile contained $1.5 \mu\text{g}$ of coumarin internal standard. The mixture was vortex mixed and then the deproteinized precipitate was separated by centrifugation ($3000 \text{ r} \cdot \text{min}^{-1}$, 5 min). The supernatant was evaporated at 60°C water bath under a stream of nitrogen. The residue was dissolved in $60 \mu\text{L}$ acetonitrile and $20 \mu\text{L}$ of solution was directly injected into HPLC system for determination. To each 0.2 mL of rabbit blank sera 20 to $800 \mu\text{g} \cdot \text{L}^{-1}$ of FA were added respectively. Their serum samples were analyzed separately by the corresponding method described above^[18].

The verification of R-PK

The preparation of LW decoction, LW&SM (LW: SM=3:1) decoction: the dried roots of them were pounded to about $2 \text{ mm} \times 4 \text{ mm} \times 4 \text{ mm}$ pieces. The other procedure was the same as those for preparing SJZD. The final concentration of LW decoction and LW&SM decoction were $3 \text{ g} \cdot \text{mL}^{-1}$ and $4 \text{ g} \cdot \text{mL}^{-1}$, respectively. TMP content of LW and LW&SM decoctions were determined before administration^[17].

Only healthy rats were used to verify R-PK. Twelve Wistar rats were divided into two groups. LW decoction ($30 \text{ g} \cdot \text{kg}^{-1}$) was given intragastrically to one group ($n = 6$) and LW&SM decoction ($40 \text{ g} \cdot \text{kg}^{-1}$) was given to another group ($n = 6$). The blood samples of 0.2 mL each were obtained by cutting the animal tails at 0.083 h , 0.25 h , 0.50 h , 0.75 h , 1.00 h , 1.50 h , 2.00 h , 3.00 h and 5.00 h after oral TCR.

Analytical method: all quantitative but qualitative detections of TMP were the same as those described above. Chromatographic

conditions: Shim-Pach CLC-ODS column (particles 5 μm , 150 mm \times 4.6 mm ID) was also used for quantitative analysis; the half-preparative column (particles 10 μm , 250 mm \times 10 mm ID) was used for the separation and purification of LW decoction components in serum; Nebulizer and vaporizer temperatures were 250 $^{\circ}\text{C}$. The drift voltage was 70eV.

The identification of LW-derived component in serum^[17]: the related component was firstly separated, purified, enriched and then identified by 3-dimensional HPLC, mass spectrum, and NMR. Calibration curve and statistical analysis were the same as the correspondings described above.

Statistical analysis

The results are expressed as $\bar{x} \pm s$. Comparison of serum drug concentration and pharmacokinetic parameters between controls and studied model of LW and LW&SM decoctions were made by *t* test for paired samples. Differences were considered significant when $P < 0.05$.

RESULTS

The methodological results

One of the chemical components in serum after oral administration of LW extract to rats was identified as TMP by three-dimensional HPLC, UV, IR, MS and NMR (data not shown)^[17].

The chromatographic retention time of TMP, methaqualone (internal standard), FA and coumarin (internal standard) were 3.992 min, 6.223 min, 3.82 min and 7.68 min, respectively (Figure 1, A-B)^[17,18]. They were separated well under their own chromatographic conditions. The ratios between the peak areas of the TMP and methaqualone (internal standard) in serum of rat, and of the FA and coumarin (internal standard) in serum of rabbit were calculated to make the calibration curves and the good linearity over the range (220-6710) $\mu\text{g} \cdot \text{mL}^{-1}$ (TMP, $r = 0.9990$, $n = 6$) and (20-800) $\mu\text{g} \cdot \text{mL}^{-1}$ (FA, $r = 0.9986$, $n = 6$) were obtained. Their equation of the curves were $Y = 0.1889 + 0.0440X$ (TMP) and $Y = 0.5826X + 0.1718$ (FA). If the concentration of FA was above 800 $\mu\text{g} \cdot \text{mL}^{-1}$, the sample was diluted. The detection limit of TMP and FA in sera were 68 $\text{mg} \cdot \text{L}^{-1}$ and 15 $\text{mg} \cdot \text{L}^{-1}$ respectively with a signal-to-noise ratio at 3.

The recoveries of TMP and FA contents from sera of rat and rabbit were determined. Their results are shown in Table 1.

The precision in sera with three levels (0.22 $\mu\text{g} \cdot \text{mL}^{-1}$, 0.8388 $\mu\text{g} \cdot \text{mL}^{-1}$ and 6.7100 $\mu\text{g} \cdot \text{mL}^{-1}$) of TMP and (0.030 $\mu\text{g} \cdot \text{mL}^{-1}$, 0.450 $\mu\text{g} \cdot \text{mL}^{-1}$ and 0.700 $\mu\text{g} \cdot \text{mL}^{-1}$) of FA was detected (Table 2).

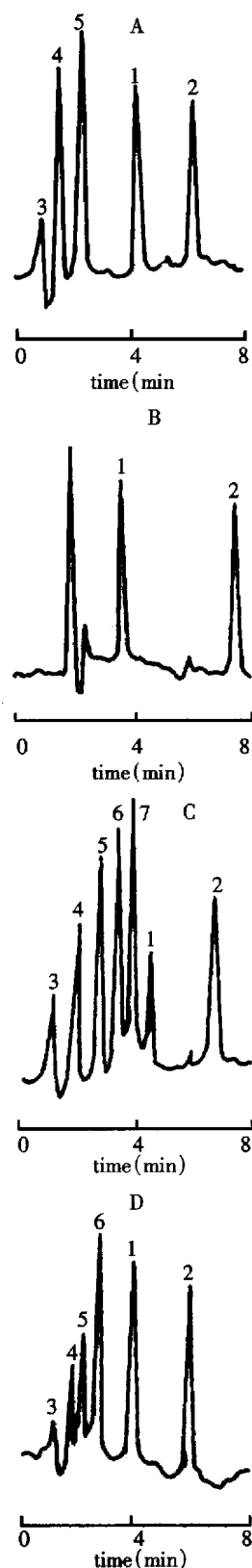


Figure 1 HPLC chromatography of A. TMP (methaqualone, IS) added to rat serum; B. FA (coumarin, IS) in rabbit serum 1. FA (t_R : 3.82 min), 2. coumarin (t_R : 7.68 min); C. serum sample after oral administration of LW&SM extracts in rats; D. sample serum after oral administration of TMPP. 1: TMP (t_R : 3.992 min). 2. coumarin (t_R : 6.233 min). 3. methanol (t_R : 1.017); 4,5: impurities in serum (t_R : 1.725 min and t_R : 2.467 min); 6,7: unknown components (t_R : 3.000 min and t_R : 3.201 min)

Table 1 Recovery of TMP added to rat serum and ferulic acid added to rabbit serum

Drug	Added(mg/L)	Found+SD(mg/L)	Recovery+RSD(%)
TMP	0.2200	0.2126 ± 0.0081	96.64 ± 3.18
TMP	0.8388	0.8294 ± 0.0181	98.99 ± 2.18
TMP	6.7100	0.6657 ± 0.1973	99.34 ± 2.96
FA	0.0300	0.0280 ± 0.0009	95.00 ± 1.60
FA	0.4500	0.43804 ± 0.0043	97.40 ± 1.00
FA	0.7000	0.6883 ± 0.0053	98.30 ± 0.80

Table 2 Precision of tetramethylpyrazine from rat serum and ferulic acid from rabbit serum

Drug	Amount added(mg/L)	Interday cv(%)	Intraday cv(%)
TMP	0.2200	2.45	5.57
TMP	0.8388	1.25	5.67
TMP	6.7100	1.44	4.72
FA	0.030	5.5	6.1
FA	0.450	3.2	4.3
FA	0.700	2.1	3.8

The results of verifying S-PK

RMSDS: Four days after ip injection of reserpine, RMSDS showed decrease in activity, severe muscular hypotonia, palpebral ptosis and diarrhea, which were similar to those reported in our previously paper^[15] and accorded with the published diagnostic standard of spleen deficiency syndrome by Chinese Association of Integrated Traditional and Western Medicine^[19]. In RMSDS, the body weights of rats were reduced by 40% (242 g ± 22 g vs 145 g ± 20 g), and in RMSDS treated with SJZD, they had not shown any significant changes (results not shown).

The above analytical method of TMP was used to study TMP PK following oral TMPP. The pharmacokinetic profiles of oral TMPP in HR-1, RMSDS and SJZD treated RMSDS were the 2-compartment models according to the calculation of serum TMPP concentration-time data (Figure 2), which was in agreement with the results obtained from human and rats^[20,21]. The serum concentrations of TMP in RMSDS were higher than those in HR-1 ($P < 0.01$, Figure 2). The pharmacokinetic parameters of TMPP in RMSDS (Table 3) with the exception of $V/F(C)$ and T peak were significantly different from those in HR-1 ($P < 0.01$); k_a , $T_{1/2\alpha}$, AUC , absorption of TMPP; α , β , $T_{1/2\beta}$, $T_{1/2\alpha}$, CLs , K_{12} , and K_{10} demonstrated that RMSDS decreased the rate of the distribution, transportation and clearance of TMPP ($P < 0.01$). The state of the syndrome in RMSDS affected obviously the absorption, distribution, metabolism and excretion of TMPP.

Table 3 Pharmacokinetic parameters of TMP in serum after oral administration of TMPP (10 mg/kg) to healthy rats and RMSDS with or without SJZD treatment

Parameter	Healthy rat	RMSDS	SJZD
$\alpha(h^{-1})$	2.83 ± 0.70	0.38 ± 0.09 ^b	2.33 ± 0.65
$\beta(h^{-1})$	0.22 ± 0.02	0.06 ± 0.30 ^b	0.24 ± 0.05
$K_a(h^{-1})$	5.41 ± 1.91	13.61 ± 2.56	5.28 ± 1.39
$K_{10}(h^{-1})$	0.88 ± 0.20	0.24 ± 0.07 ^b	0.82 ± 0.11
$K_{12}(h^{-1})$	1.45 ± 0.47	0.11 ± 0.02 ^b	1.39 ± 0.68
$K_{21}(h^{-1})$	0.72 ± 0.22	0.11 ± 0.02 ^b	0.77 ± 0.18
$t_{1/2\alpha}(h)$	0.14 ± 0.09	0.05 ± 0.04 ^b	0.16 ± 0.10
$t_{1/2\alpha}(h)$	0.27 ± 0.11	1.92 ± 0.44 ^b	0.31 ± 0.09
$t_{1/2\beta}(h)$	3.19 ± 0.39	13.35 ± 5.92 ^b	3.21 ± 0.28
$AUC(\mu g \cdot h \cdot mL^{-1})$	5.20 ± 2.57	24.88 ± 9.76 ^b	5.11 ± 6.81
$T_p(h)$	0.30 ± 0.05	0.34 ± 0.03	0.33 ± 0.02
$C_{max}(\mu g/mL)$	2.33 ± 1.17	4.82 ± 1.23 ^b	2.18 ± 1.14
$V_{FC}(\mu g/mL)$	2.81 ± 1.30	2.03 ± 0.58	2.19 ± 0.98

^a $P < 0.01$ vs healthy rabbit.

RMBSS: the above method of detecting FA used to study PK in healthy rabbit and FA serum concentration in RMBSS compartment model was fitted and then pharmacokinetic parameters were calculated with a MCPKP program on a COMPAQ 80-386 computer. Compartmental analysis yielded a two-compartment open model. A rapid distribution phase followed by a slower elimination phase was observed. The mean pharmacokinetic parameters are given in Table 4 and serum concentration-time data in Figure 3.

The results of verifying R-PK

The results of detecting TMP concentrations in LW and LW&SM decoctions were 574.50 g·kg⁻¹·L⁻¹ and 463.02 g·kg⁻¹·L⁻¹, respectively.

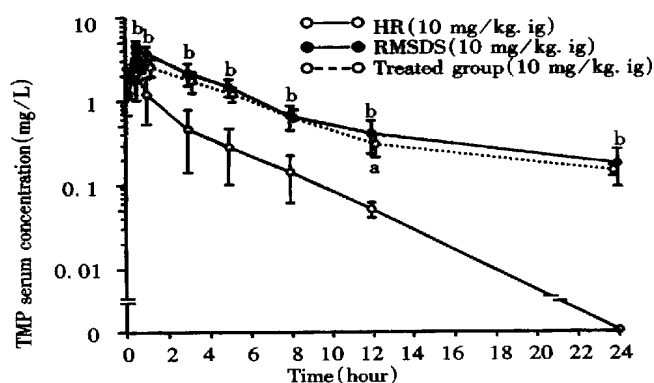
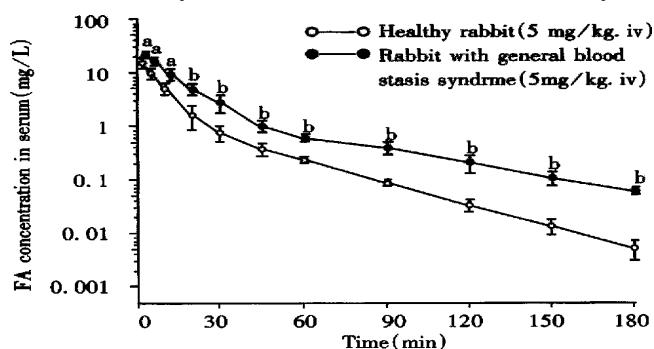
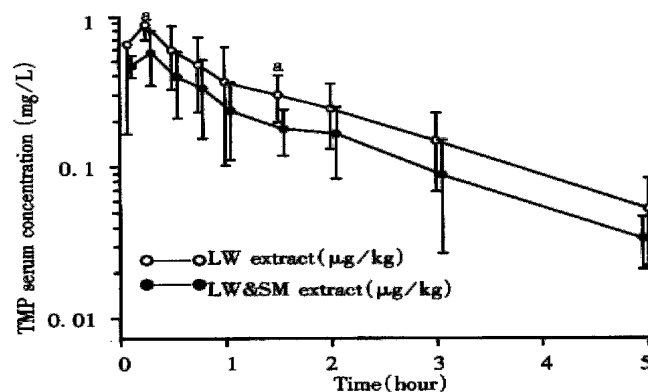
The chromatograms of TMP and methaqualonum, the latter was added into serum, and then extracted, were the same as shown in Figure 1A, 1B. The serum TMP chromatogram after administration of LW or LW&SM decoctions was different from that of TMP and of IS added to blank serum (Figure 1A) as well as that of post-administrative TMPP injection solution (Figure 1D). There were two more peaks of unknown significance in Figure 1C than that in Figure 1A and one more unknown peak than that in Figure 1D. The serum TCR-derived component parameters of 4 spectra of UV, IR, MS and NMR (data not shown) are similar to that of TMP standard substance and the reference value. Thus it gives an evidence to reveal that this TCR-derived component is undoubtedly TMP. The TMP PK were calculated by 3P87 program (Chinese Pharmacological Association). The fitted figures from two compartment open model and their parameters are indicated in Table 5.

Table 4 Pharmacokinetic parameters of FA in serum after intravenous administration of sodium ferulate (5 mg/kg) in healthy rabbit and rabbit with general blood stasis syndrome ($\bar{x} \pm s$, $n = 6$)

Parameter	RMBSS	Healthy rabbit
$K_{12}(h^{-1})$	1.01 ± 0.86	1.62 ± 1.18
$K_{21}(h^{-1})$	1.45 ± 0.99	2.47 ± 0.99
$K_{el}(min^{-1})$	4.49 ± 1.10^a	7.37 ± 1.40
$T_{1/2}\alpha(h)$	0.12 ± 0.10	0.07 ± 0.02
$T_{1/2}\beta(h)$	0.62 ± 0.12^b	0.36 ± 0.09
$AUC(\mu g \cdot h \cdot mL^{-1})$	5.67 ± 2.35^b	2.76 ± 0.82
$Cl(L \cdot kg^{-1})$	0.88 ± 0.55	1.81 ± 0.95
$V_{FC}(L/kg)$	0.71 ± 0.03	0.95 ± 0.22

^a $P < 0.05$; ^b $P < 0.01$ vs healthy rabbit. Mean \pm SEM, $n = 6$ **Table 5** Pharmacokinetic parameters of TMP in serum after oral administration of LW or LW&SM extracts to rats mean \pm SEM ($n = 6$)

Parameter	LW	LW&SW
$\alpha(h^{-1})$	1.928 ± 0.719	2.328 ± 0.719
$\beta(h^{-1})$	0.479 ± 0.205	0.479 ± 0.289
$K_a(h^{-1})$	19.58 ± 4.139	11.508 ± 2.821^a
$K_{10}(h^{-1})$	1.090 ± 0.502	0.788 ± 0.255
$K_{12}(h^{-1})$	0.470 ± 0.160	0.205 ± 0.092
$T_{1/2}\alpha(h^{-1})$	0.354 ± 0.101	0.298 ± 0.223
$T_{1/2}\beta(h^{-1})$	1.448 ± 0.880	1.447 ± 0.901
$AUC(\mu g \cdot h \cdot mL^{-1})$	1.273 ± 0.255	0.836 ± 0.168^b
$V_{C/F}(L/kg)$	9.665 ± 1.810	7.390 ± 1.089^a

^a $P < 0.05$; ^b $P < 0.01$ vs LW.**Figure 2** TMP concentration-time curve in serum after oral administration of TMPP in healthy rat ($n = 6$), RMSDS ($n = 6$) and RMSDS treated by SJZD ($n = 6$), ^a $P < 0.05$ vs; ^b $P < 0.01$ vs healthy rat.**Figure 3** FA concentration-time curve in serum after intravenous administration of sodium ferulate (5 mg/kg). ^a $P < 0.05$; ^b $P < 0.01$ vs healthy rabbit.**Figure 4** TMP concentration-time curve in serum after oral administration of boiled water extract to rats. ^a $P < 0.05$ vs LW extract.

DISCUSSION

Hypothesis

The concept, terminology, essentials and significance, especially scientific evidences, of S- and R-PK hypothesis were firstly reported and theoretically elaborated in our previous papers^[1-6]. These ideas were exclusively cited^[22-26]. Besides the definition described in above method, we summarized the main elements as follows: ① TCR-derived components *in vivo* are possibly to be detected; ② their number are relatively restricted; ③ they could represent the therapeutic effect of the parent recipe; ④ their concentration and PK could be affected by the combination of TCM in TCR; ⑤ effects of new bioactive components related with those of their parent TCR; and ⑥ the syndrome state could affect their PK significantly. All the ideas of S- and R-PK exhibited the characteristics of combination of TCM theory and PK. The other two published papers only concerned the element 1^[1-6]. So far, over 20 evidences in the available published literatures^[2-8,12,13] supported the element 1.

Methodology

It is necessary to develop scientific analytical method, mainly chromatography, for verifying the hypothesis of S- and R-PK. In general, western drug component (single chemical substance) in blood is only identified by the consistency of retention time of peak in chromatograms as compared with its standard substance derived from the national and international authorized unit^[27-29]. However, this method is not sufficient in analysing the serum TCR-derived component because the coherence of retention time may result from two possibilities, i.e., only a single component peak or an overlap of two or more component peaks according to the theory of chromatography^[17].

We developed the above HPLC method, to determine the serum TMP PK after the administration of TMPP or TCR-LW. When TMPP

solution (Figure 1D) was administered, determination of TMP qualitatively and quantitatively by HPLC is enough corresponding to the method for determining ordinary western drug^[27-29]. As orally administering LW or LW&SM decoctions, the structure of TMP was firstly identified by HPLC in combining with UV, IR, MS and NMR (Figure 1C) and then its concentration and pharmacokinetic value were determined by HPLC. Thus, it is likely to avoid the analytical errors in serum TMP derived from LW or LW & SM in our present experiments^[15-17]. Tables 1 and 2 indicated that these methods for the determinations of serum TMP and FA concentrations were simple, rapid, sensitive, accurate, specific and reduplicable, with high recoveries. All these indexes were sufficient in studying S- and R-PK.

The verification of S-PK

S-PK hypothesis was advanced according to the theories of TCM and PK^[1-6]. To verify this hypothesis, the animal models of spleen deficiency and blood stasis were chosen and their pharmacokinetic characteristics of TMP and FA were studied. One of these models, RMSDS, was induced by injecting reserpine, which had been used as an animal model for "spleen deficiency syndrome" (SDS) in TCM^[30,31] because its physical signs were similar to those seen in the SDS.

The "spleen" digests food, transports, distributes and transforms nutrients and replenishes qi^[32]. We inferred from the above "spleen theory" that the "spleen" should be also responsible for the absorption and disposal of drugs. So, syndrome state of "spleen" is likely to affect the PK. The aim described in the S-PK hypothesis is to demonstrate the pharmacokinetic differences between syndrome and non-syndrome. Our experimental design from S-PK hypothesis is that the poor absorption of drug in SDS state would decrease its blood concentration and bioavailability. On the contrary, Figure 2 and Table 3 show the results of the increases in TMP serum concentration and AUC in RMSDS. Moreover, the parameters of the distribution and elimination of TMP in RMSDS (Table 3) were slowish. The SDS state could markedly affect the absorption, distribution, metabolism and elimination of TMPP in rat, and the observed results from Figure 2 and Table 3 show that SJZD could restore the above abnormal PK of TMPP in SDS model rats. All these TMP pharmacokinetic characteristics in RMSDS and the normalizing effect of SJZD on PK of TMP in RMSDS provided evidences for S-PK.

The mechanism of forming TMP pharmacokinetic characteristics in RMSDS is unknown. It was reported that the gastric and intestinal motility^[33] and the absorptivity of D-xylose^[34] were all decreased in reserpine-induced RMSDS and the patients with SDS. These

observations are paradoxical to the increased serum TMP concentration in RMSDS. This confusion should be settled by further studies. Figure 3 shows that at corresponding time points the FA concentration in RMBSS increased markedly ($P<0.05$) as compared with normal rabbits. From Table 4 we also found that in RMBSS both the total volume of distribution (V_B) and total elimination rate (CL_B) decreased significantly while FA elimination half-life time ($t_{1/2\beta}$) and AUC increased significantly. This phenomenon may be due to the impairment of microcirculation induced by HMWD infusion. HMWD can lead to abnormal blood rheology (dense, sticky, aggregative, coagulative). So, it is impossible for FA to be metabolized quickly and distributed widely. In conclusion, through this experiment we found a significant difference in the pharmacokinetic parameters between healthy rabbits and RMBSS. This result coincides with S-PK hypothesis^[18].

The verification of R-PK hypothesis

So far, the orthodox academic society has thought that TCR-derived chemical components *in vivo* and their PK are not detectable and enable to study because they or their components are too complicated, trace in quantity or unable to represent curative effect of their parent TCR^[35-38]. Therefore, the article related to above problem is rarely seen in recent years, and resulted in hard to explore the basic pharmacodynamic substance of TCR. The R-PK hypothesis emerged in literature since 1991 holds the idea that TCR-derived chemical components *in vivo* and their PK are possibly to be determined^[1-6]. However, the qualitative and quantitative analysis of LW and LW&SM-derived TMP *in vivo* from Figure 1(C) and its PK from Figure 4 and Table 5 supported the R-PK hypothesis. Similarly, the determinations of over 20 TCR-derived chemical components in blood/urine and their PK^[2-8,12,13,39] in published papers are consistent with the viewpoint of R-PK hypothesis. All these achievements help elucidate the pharmacology of TCM and TCR^[39].

From the results provided in Figure 4 and Table 5 we found that the absorption (K_a), transport (K_{21}) and distribution (V_c/F) of LW&SM-derived TMP in rat serum were decreased significantly compared with those of LW-derived TMP. In Figure 4 and Table 5 it also shows that the concentration and AUC of LW&SM-derived TMP in rat serum were lower than those of LW-derived TMP, which could explain why LW and SM are rarely used alone in a TCR. This viewpoint supported the hypothesis that the combination of drugs in TCR could affect pharmacokinetic parameters of TCR-derived component *in vivo*. It is extremely urgent to explore which component play an important role in the field of interaction of LW or LW&SM derived components *in vivo*.

REFERENCES

- Huang X, Ma Y, Jiang YP, Xia T, Ren P. The scientific evidence and prospect of traditional Chinese syndrome and recipe pharmacokinetics hypothesis. In: Chen KJ. March of integration of TCM and WM towards 21st century. Beijing: China Medicine Pharmaceutics Science-technology Publisher, 1991:207-216 (in Chinese)
- Huang X, Jiang YP, Wen AD, Zang YM, Niu GB. Is it possible to study the pharmacokinetics of chemical component of herbal recipe. *Chin J Intern Med*, 1995;1:297-300
- Huang X. The concepts of recipe-derived component spectrum and target component *in vivo*/serum and their significance. *Disi Junyi Daxue Xuebao*, 1999;20:277-279 (in Chinese with English abstract)
- Huang X, Zang YM, Xia T, Ren P. The hypothesis of traditional Chinese syndrome and recipe pharmacokinetics. *Zhongyao Yaoli Yu Linchuang*, 1994;10:43-44 (in Chinese)
- Huang X, Ren P. The difficulty and breakthrough point on prevention and treatment of hypertension and coronary heart disease therapeutic drug control of recipe. *Zhongguo Zhongxiyi Jiehe Zazhi*, 1997;17:515-518 (in Chinese)
- Huang X, Chen KJ. The theory and practice of traditional Chinese syndrome and recipe hypothesis. *Zhongyi Zazhi*, 1997;38:745-747 (in Chinese)
- Tanaka S, Ihoko O, Shinichi T. Establishment of methods evaluating the "shyo" and effectiveness of Kampo formulae by measuring their blood concentration. *J Med Pharmaceut Society for Wakan Yaku*, 1986;3:276-277
- Kano Y, Sakurai T, Saito K. Pharmacological properties of Galenical preparation XII. Components of Chinese traditional prescription "Kanzobusito" in rat portal blood after oral administration. *Shoyakugaku Zasshi*, 1989;43:199-203
- Lemmer B. The cardiovascular system and daily variation in response to antihypertensive and antianginal drugs: recent advances. *Pharmacol Ther*, 1991;51:269-274
- Eradiri O, Midha KK. Comparison of diltiazem bioavailability from 3 marketed extended-release products for once-daily administration: implications of chronopharmacokinetics and dynamics. *Int J Clin Pharmacol Ther*, 1997;35:369-373
- Gries JM, Benowitz N, Verotta D. Importance of chronopharmacokinetics in design and evaluation of transdermal drug delivery systems. *J Pharmacol Exp Ther*, 1998;285:457-463
- Nishioka Y, Kyotani S, Miyamura M, Kusunose M. Influence of time of administration of a shosaiko to extract granule on blood concentration of its active constituents. *Chem Pharm Bull*, 1992;40:1335-1337
- Homma M, Oka K, Taniguchi C, Niitsuma T, Hayashi T. Systematic analysis of post administrative saiboku to urine by liquid chromatography to determine pharmacokinetics of traditional Chinese medicine. *Biomed Chromatogr*, 1997;11:125-131
- Ritschel WA, Forusz H. Chronopharmacology: a review of drugs studied. *Methods Find Exp Clin Pharmacol*, 1994;16:57-75
- Huang X, Ren P, Wen AD, Xia T, Zang YM, Song L, Niu GB. Pharmacokinetic Characteristics of tetramethylpyrazine and study on hemorheology in rat model of spleen deficiency syndrome. *Zhongguo Zhongxiyi Jiehe Zazhi*, 1994;14:159-161 (in Chinese with English abstract)
- Huang X, Wen AD, Jiang YP, Ren P, Zang YM. Determination of tetramethylpyrazine in serum by RP-HPLC after oral administration of boiled water extracts of Ligusticum chuansong to rats. *Zhong Yao Cai*, 1995;18:305-307 (in Chinese with English)
- Huang X, Xia T, Ren P, Ma Y, Wen AD, Jiang YP. Influence of combined Salvia Miltiorrhiza and Ligusticum wallichii on pharmacokinetics of tetramethylpyrazine in rats. *Zhongguo Zhongxiyi Jiehe Zazhi*, 1994;14:288-291 (in Chinese with English abstract)
- Wen AD, Huang, Jiang YP, Fan YX. High-Performance liquid chromatographic determination of free ferulic acid in serum of rabbits with blood stasis. *Yaoxue Xuebao*, 1995;30:762-767
- Shen ZY, Wang WJ. The reference standards of differential diagnosis of deficiency syndrome of traditional Chinese medicine. *Zhongguo Zhongxiyi Jiehe Zazhi*, 1986;6:598 (in Chinese)
- Liu XQ, Lou YC, Shi WZ. Study on the relationship between pharmacokinetics and pharmacodynamics of tetramethylpyrazine and effects of acute hepatic poisoning on its pharmacokinetics in rats. *Beijing Yike Daxue Xuebao*, 1991;23:185-189 (in Chinese with English abstract)
- Liu XQ, Lou YC, Chen QT. The clinical pharmacokinetics studies of tetramethylpyrazine hydrochloride in normal volunteers and patients with acute cerebral ischemia disease (CID). *Zhongguo Linchuang Yaoli Zazhi*, 1991;7:32-36 (in Chinese with English abstract)
- Zhang WH, Zha LL. Review and prospect of making blood stasis animal model. *Zhongguo Zhongxiyi Jiehe Zazhi*, 1996;16:184-186 (in Chinese with English abstract)
- Song DM, Su H, Wu MH, Huang XM. Effect of tetramethylpyrazine and radix salviae miltiorrhizae on collagen synthesis and proliferation of cardiac fibroblasts. *Zhongguo Zhongxiyi Jiehe Zazhi*, 1998;18:423-425 (in Chinese with English abstract)
- Li M, Du LJ, Sun H. Survey of studies on pharmacokinetics of Chinese herbal combination. *Zhongguo Zhongxiyi Jiehe Zazhi*, 1998;18:637-639 (in Chinese with English abstract)
- Ma W, Wang JH. A hypothesis of syndrome and treatment toxicology of Chinese materia medica. *Zhongyao Xinyao Yu Linchuang Yaoli*, 1999;10:116-118 (in Chinese)
- Pan GY, Liu XD. The methods and prospects of studies on the recipe-pharmacokinetics of Chinese materia medica. *Zhong Cao Yao*, 1998;29:642-644 (in Chinese)
- Marzo A, Dal Bo L. Chromatography as an analytical tool for selected antibiotic classes: a reappraisal addressed to pharmacokinetic applications. *J Chromatogr A*, 1998;812:17-34
- Pehourcq F, Jarry C. Determination of third-generation cephalosporins by high performance liquid chromatography in connection with pharmacokinetic studies. *J Chromatogr A*, 1998;812:159-178
- Tyrrell CJ, Denis L, Newling D, Soloway M, Channer K, Cockshott ID. Casodex™ 10mg-200mg daily, used as monotherapy for the treatment of patients with advanced prostate cancer. An overview of the efficacy, tolerability and pharmacokinetics from three phase II dose-ranging studies. Casodex Study Group. *Eur Urol*, 1998;33:39-53
- Ren P, Song GZ, Xia T, Huang X, Zhang ZB, Hu JL. Relationship between diarrhea with spleen deficiency and motilin of plasma and intestinal tissue. *Zhongguo Zhongxiyi Jiehe Zazhi*, 1994;14(Suppl): 25-27 (in Chinese with English abstract)
- Shen H, Guan CF. Description and application of an enzyme-linked immunosorbent assay for the detection of protein tyrosine kinase activity and the study on spleen deficiency syndrome. *Zhongguo Zhongxiyi Jiehe Zazhi*, 1998;18(Suppl):243-245 (in Chinese with English abstract)
- Xie ZF, Liao JZ. Traditional Chinese Internal Medicine. Foreign Languages Press, Beijing, 1993:37-39
- Ren P, Huang X, Jiang YP, Wen AD, Song GZ. Effect of Sijunzi, decoction on motilin pharmacokinetic characteristics of tetramethylpyrazine in rat model of spleen deficiency syndrome. *Zhongguo Zhongxiyi Jiehe Zazhi*, 1997;17:45-47 (in Chinese with English abstract)
- Xiong DX. Surveying of bacteroides in human lower intestine. *Weishengwu Xuebao*, 1985;25:69-72 (in Chinese with English abstract)
- Huang JC. Studies of the metabolism and pharmacetics of active principles isolated from Chinese herb medicine since the foundation of the people's republic of China. *Yaoyue Xuebao*, 1987;22:553-560 (in Chinese)
- Ammon HPT, Wahl MA. Pharmacology of curcuma longa. *lanta Med*, 1991;57:1-7
- Yano H, Mizoguchi A, Fukuda K, Haramaki M, Ogasawara S, Momosaki S, Kojiro M. The herbal medicine Shosaiko-to inhibits proliferation of cancer cell lines by inducing apoptosis and arrest at the G0/G1 phase. *Cancer Res*, 1994;54:448-454
- Chan K. Progress in traditional Chinese medicine. *TIPS*, 1995;16: 182-187
- Huang X, Jiang YP, Zang YM, Niu GB. Advances in the study of metabolism and pharmacokinetics of chemical components in decoction of traditional Chinese medicine. *Zhongcaoyao*, 1995;26:546-549 (in Chinese)

Brief Reports

Research on optimal immunization strategies for hepatitis B in different endemic areas in China

Hui Li¹, Lu Wang¹, Shu Sheng Wang², Jian Gong², Xian Jia Zeng¹, Rong Cheng Li², Yi Nong², Yue Kui Huang², Xiu Rong Chen² and Zhao Neng Huang²

Subject headings hepatitis B vaccine; immunization strategy; cost-benefit analysis; china

Li H, Wang L, Wang SS, Gong J, Zeng XJ, Li RC, Nong Y, Huang YK, Chen XR, Huang ZN. Research on optimal immunization strategies for hepatitis B in different endemic areas in China. *World J Gastroentero*, 2000;6(3):392-394

INTRODUCTION

At present hepatitis B vaccine immunization is an unique effective measure for controlling hepatitis B. It is important to determine optimal immunization strategy for controlling HB and to rationally allocate health resources. From the angle of health economics, cost-effective analysis (CBA) is used for the evaluation of economic benefit of the immunization strategies implemented in different endemic areas of HB in China in order to provide the evidences for decision-making and revision of the current HB immunization strategy.

MATERIALS AND METHODS

Basic data

The data for low and medium endemic areas of HB, involving morbidity and mortality of HB and liver cancer, cost of HB vaccine administration, overage personal income, GNP, and expenses for medical treatment of patients with acute, chronic hepatitis B and hepatocellular carcinoma, were collected from the medical literature^[1,2]. The corresponding data related to heavy endemic area were obtained from the survey.

Definition of immunization strategies and protective effectiveness

The principal immunization strategies currently

¹Institute of Basic Medical Sciences, CAMS and PUMC, Beijing 100005, China

²Guangxi Anti-Epidemic & Hygiene Center, Nanning 530021, Guangxi Zhuang Autonomous Region, China

Professor Hui Li, M.D., M.P.H., graduated from Beijing Medical University in 1970 and from Peking Union Medical College as a postgraduate in 1982, professor, majoring methodology of epidemiology, hepatitis B control, and etiology on cardiovascular diseases, having 33 papers and 7 books published.

Supported by the China Medical Board of New York, Inc., the United States, Grant No.93-582.

Correspondence to: Prof. Hui Li, Director and Professor, Department of Epidemiology, Institute of Basic Medical Sciences, CAMS & PUMC, 5# Dong Dan San Tiao, Beijing 100005, China
Tel. 0086-10-65296971(O), 0086-10-65141591(H)

Received 2000-01-16 **Accepted** 2000-02-28

implemented in China and their effectiveness, which were used as the basis for evaluation, were selected from the related literature^[3,4] for the sake of fair comparison between the different endemic areas. The definition of these strategies is as follows: ① Low-dose immunization strategy is defined as without maternal predelivery HBeAg and HBsAg screening, and infancy vaccination with three or four doses (one dose of booster) of 10 µg plasma-derived hepatitis B vaccine, and yielding a protective effectiveness of 85%. ② Based on maternal predelivery HBeAg and HBsAg screening, high-dose immunization strategy is known as infancy vaccination with one of the following regimens: infant with maternal HBeAg- and HBsAg-negative only receives three doses of 10 µg plasma-derived hepatitis B vaccine; infant with maternal HBeAg and/or HBsAg-positive receives one dose of 30 µg and two doses of 10 µg plasma-derived hepatitis B vaccine; or three doses of 20 µg plasma-derived hepatitis B vaccine and one dose of hepatitis B immune globulin (HBIG); or three doses of 20 µg and one dose of 10 µg (for booster) plasma-derived hepatitis B vaccine. All provided a protective effectiveness of 90%.

Definition of heavy, medium and low endemic areas

The range of HBsAg-positive rate for heavy, medium and low endemic areas of HB is defined as over 11%, from 5% to 10%, and less than 4% respectively. Longan County, Jinan City and Beijing were selected as the representative areas for the heavy, medium and low endemic levels of HB in China, respectively. The HBsAg- positive rate for the whole population and pregnant women was 18.0% and 11.9% in Longan County, 7.59% and 5.40% in Jinan City, and 2.0% and 1.4% in Beijing, respectively. The data collected from these three places were used for CBA.

Study methods

CBA method was used to compare the data of economic benefit between the different places. Comprehensive weighted score analysis (CWSA) was made for determining the optimal immunization strategy. Definition and calculation formula relative to four scales for evaluation of the strategies are as follows: (a) proportion of individuals with HBsAg

carriage prevented among immunized population: HBsAg-positive rate before immunization-HBsAg-positive rate after immunization = HBsAg-positive rate before immunization \times protective effectiveness; (b) net benefit (NB) = total benefit-total cost; (c) benefit cost

ratio (BCR) =

here, the signal B, denotes benefit; C, cost; r , discount rate; t , time; n , lifetime saved. (d) Direct BCR (DBCR) was known as a BCR which only involved the expenses of medical treatment in hospital. The basic principle and procedure of CWSA: First, four kinds of standards, A,B,C,D, used for assessment of every strategy to endemic areas of HB were defined in terms of different weight score (from 0 to 4) of 4 scales. Standard A was designated as comprehensive effectiveness in four scales: 4 scores (very important) to scale I (HBsAg) which denoted the reduced proportion of HBsAg-positive rate between pre- and post-vaccination; 1 score (less important) to scale II (NB); 3 scores (important) to scale III (BCR), and 2 scores (fairly important) to scale IV (DBCR). Standard B: 4 scores to scale HBsAg; 3 scores to scale NB; 2 scores to scale BCR; and 1 score to scale DBCR. Standard C: 4 scores to scale HBsAg; 3 scores to scale NB; 3 scores to scale BCR; and 0 score (not important) to scale DBCR. Standard D: 0 score to scale HBsAg; 4 scores to scale NB; 4 scores to scale BCR; and 3 scores to scale DBCR. Then, the score rank for four scales was calculated according to their corresponding value in each strategy, the maximal score of any scale in all strategies was 10. The calculation of the score rank was that a measured or estimated value of the scale in each strategy was divided by the greatest measured or estimated value of this scale among all strategies being compared, then multiplied by 10. The total comprehensive scores for each strategy was calculated by the following formula: score rank for each strategy \times weighted score for each scale. Finally, based on the same standard, for example, B, the total comprehensive scores for all strategies were compared to screen a strategy with maximal scores. The strategy possessing greatest total comprehensive scores in all standards evaluated was considered as the optimal one.

Data analysis

All data was analyzed with the software of version SAS 6.0 and Excel 5.0.

RESULTS

Benefit from hepatitis B vaccination of different strategies in different endemic areas

Benefit of the low-dose strategy in three places CBA was conducted based on the actual epidemiologic data of Longan County, Shanghai and Jinan City,

and assuming that after the implementation of the infancy low-dose strategy same protective effectiveness of 85% and coverage of 100% could be yielded in these places. The results indicated that the outstanding benefit was obtained for all places in spite of their different economic development level and different endemicity. Longan had a lower value of benefit scales compared with Shanghai and Jinan except the DBCR scale. The greatest value of difference between BCR and DBCR excluding the cost of liver cancer was found in Longan (Table 1).

Table 1 Benefit of HB vaccination of the low-dose strategy for three places with different economic development level and different endemicity

	Place		
	Longan	Shanghai	Jinan
HBsAg-positive rate before vaccination (%)	18.0	10.2	7.6
No. of neonates in 1987	7666	12 000	18 519
Direct benefit*	286	345	562
Indirect benefit*	683	1571	1852
Total benefit*	969	1916	2414
Total cost*	18	22	42
Net benefit*	951	1893	2372
BCR	52.7	85.8	57.9
DBCR	15.5	15.4	13.5
BCR excluding cost of liver cancer	23.6	67.9	34.8
DBCR excluding cost of liver cancer	9.2	14.2	10.1
HBsAg-positive rate after vaccination (%)	3.1	2.2	1.5

*10 000 Yuan RMB.

Comparison of benefit from different strategies in three places Assuming that different immunization strategies had been implemented in each place, the results of CBA for three places showed that the low-dose strategy in Longan and Shanghai would provide the highest values in both scales, BCR and DBCR; the high-dose strategy (30 μ g + 10 μ g \times 2 regimens) in Jinan would yield a slightly higher BCR value compared with the low-dose strategy, 55.35 vs 54.52; and if excluding the influence of difference of economic level between the places (assuming that average personal income for three places was the same i.e. 10 000 in 1998), Longan would have a greater economic benefit, BCR, than Shanghai and Jinan.

Determination of the optimal immunization strategy in different endemic areas of HB

Analysis of sensitivity Based on the assuming parameters involving birth number (10 000), coverage (100%), screening proportion (90%), and sensitivity for screening (90%), the influence of changing endemicity level and strategies on benefit was determined. The results indicated that if the same immunization regimen and strategy was adopted, rank of NB value for every strategy would be seen in order of medium, heavy and low endemic

areas; if BCR of the changing immunization strategies in same endemic area was compared, the low-dose strategy for all endemic areas would yield the greatest BCR and DBCR compared with other strategy, leading to BCR value of 49.91, 54.53 and 37.68 for heavy medium and low endemic area respectively; and DBCR of 14.63, 12.69 and 5.61 for corresponding three endemic areas. No matter which strategy was taken, the greatest difference between DBCR and the BCR excluding liver cancer might be seen certainly in the heavy endemic area; the high-dose strategy would yield the greatest NB compared with other strategy in any endemic area.

Comprehensive weighted score analysis Total comprehensive score for each strategy of different endemic areas were calculated according to four scales of standard, A, B, C, D. The results indicated that when the goal of expectation (representative of standards A, B, C) was to decrease HBsAg-positive rate in general population, the low-dose strategy yielded the highest total comprehensive score. Even through ignoring the decrease of HBsAg-carriage, i.e. only concerning the economic benefit (representative of standard D), the low-dose strategy still yielded the highest total comprehensive score in different endemic areas. But whichever the four standards, the regimen of $10\text{ }\mu\text{g} \times 3 + \text{HBIG}$ classified into the low-dose strategy always had the least comprehensive score, compared with any regimen of both low and high-dose strategies. The details are shown in Table 2.

Table 2 Comprehensive weighted score analysis of the immunization strategies in different endemic areas

Endemic-area	Immunization strategy	Standard			
		A	B	C	D
Heavy	$10\text{ }\mu\text{g} \times 3$	97.3	96.2	96.2	107.9
	$10\text{ }\mu\text{g} \times 4$	84.7	88.5	88.5	90.2
	$10\text{ }\mu\text{g} \times 3 + \text{HBIG}$	83.4	89.9	89.9	86.5
	$30\text{ }\mu\text{g} + 10\text{ }\mu\text{g} \times 2^*$	93.1	95.9	95.9	100.4
	$20\text{ }\mu\text{g} \times 3 + 10\text{ }\mu\text{g}^*$	90.6	94.3	94.3	96.8
	$20\text{ }\mu\text{g} \times 3 + \text{HBIG}^*$	91.4	94.8	94.8	97.9
Medium	$10\text{ }\mu\text{g} \times 3$	97.3	96.2	96.2	107.9
	$10\text{ }\mu\text{g} \times 4$	84.7	88.5	88.5	90.2
	$10\text{ }\mu\text{g} \times 3 + \text{HBIG}$	80.5	88.1	88.1	82.4
	$30\text{ }\mu\text{g} + 10\text{ }\mu\text{g} \times 2^*$	92.6	95.6	95.6	99.6
	$20\text{ }\mu\text{g} \times 3 + 10\text{ }\mu\text{g}^*$	90.2	94.1	94.1	96.3
	$20\text{ }\mu\text{g} \times 3 + \text{HBIG}^*$	91.2	94.7	94.7	97.7
Low	$10\text{ }\mu\text{g} \times 3$	97.3	96.3	96.3	108.0
	$10\text{ }\mu\text{g} \times 4$	84.7	88.5	88.5	90.2
	$10\text{ }\mu\text{g} \times 3 + \text{HBIG}$	78.1	86.6	86.6	79.0
	$30\text{ }\mu\text{g} + 10\text{ }\mu\text{g} \times 2^*$	90.8	94.5	94.5	97.1
	$20\text{ }\mu\text{g} \times 3 + 10\text{ }\mu\text{g}^*$	88.3	92.9	92.9	93.6
	$20\text{ }\mu\text{g} \times 3 + \text{HBIG}^*$	89.6	93.7	93.7	95.4

*High dose strategy.

DISCUSSION

The results of CBA and sensitivity analysis on the actual data from Longan, Shanghai and Jinan indicated that the low-dose strategy yielded higher NB and BCR in Shanghai and Jinan with higher level of economic development; and DBCR in Longan was slightly higher than that in Shanghai and Jinan after excluding indirect benefit; and the distribution of HBsAg-positive rate in these three places was positively correlated with their DBCR, suggesting that the higher the endemicity level was, the bigger the DBCR obtained; the difference between BCR and BCR excluding expenses of liver cancer in Longan was the greatest compared with that in other two places, and the half of total expenses was used for the treatment of liver cancer in Longan, revealing that a significant economic benefit would be obtained in hyperendemic area of liver cancer assuming that the morbidity of liver cancer could be prevented through the HB vaccination. It is demonstrated from the results mentioned above that the low-dose regimen is an optimal strategy in economic benefit and hepatitis B control for areas with different endemic and economic levels/ However, the strategy, i.e., the maternal HBVMs screening before delivery and high dosage vaccination ($30\text{ }\mu\text{g} + 10\text{ }\mu\text{g} \times 2$), should be adopted to improve the protective effectiveness of HB vaccine. Also, the results of CWSA used for determining an optimal strategy demonstrated that for any endemicity level the low-dose strategy yielded the maximal comprehensive score compared with other strategies, providing same conclusion with CBA based on the actual data.

It is recommended that in different endemic areas of hepatitis B in China, the high-dose strategy is suitable for the economically developed areas in obtaining better protective effectiveness in decreasing HBsAg-positive rate. However, the low-dose strategy is optimally used for poor rural areas based on its outstanding economic benefit and better protection against HBV.

REFERENCES

- 1 Xu ZY, Xi LF, Fu TY, Zhou DK. Study on hepatitis B immune prevention strategy of Shanghai district. — V. Analysis of cost-benefit and making decision for hepatitis B immune prevention. *Shanghai Yufang Yixue Zazhi*, 1989;1:24-27
- 2 Liu ZQ, Zhao SL, Zhang YX, Ma MG, Wang H. Cost-benefit analysis of infant hepatitis B vaccine immunization prevention in Jinan city. *Zhonghua Liuxingbingxue Zazhi*, 1995;16:81-84
- 3 Li H, Li RC, Liao SS, Gong J, Zeng XJ, Li YP. Long-term effectiveness of infancy low dose hepatitis B vaccine immunization in Zhuang minority area in China. *World J Gastroentero*, 1999;5:122-124
- 4 Xia GL, Liu CB, Yan TQ, Ma JC, Yang JY, Liu YX. Prevalence of hepatitis B virus markers in children vaccinated by hepatitis B vaccine in five hepatitis B vaccine experimental areas of China. *Zhonghua Shiyao He Linchuang Bingduxue Zazhi*, 1995;9(Suppl):17-23

Edited by You DY
proofread by Sun SM

Analysis of point mutation in site 1896 of HBV precore and its detection in the tissues and serum of HCC patients

Yuan Wang¹, Hu Liu¹, Qing Zhou¹ and Xu Li²

Subject Headings hepatitis B virus; carcinoma, hepatocellular; precore; polymerase chain reaction; integration; mutation; liver neoplasms

Wang Y, Liu H, Zhou Q, Li X. Analysis of point mutation in site 1896 of HBV precore and its detection in the tissues and serum of HCC patients. *World J Gastroenterol*, 2000;6(3):395-397

INTRODUCTION

Hepatitis B is one of the common infectious diseases, which severely impairs the health of the people in our country and has close relationship to the initiation and progression of chronic hepatitis, cirrhosis, and liver cancer. The recent researches indicate that the mutation of HBV precore exists in the patients with these diseases as stated above^[1-5]. According to the recent publications, the mutation of HBV attracts great interests of investigators. The major mutation points in HBV precore are the point in sites 1896 (A1893) and 83 (A83), which are both of G→A point mutations^[6]. Based on the DNA sequence of precore region of HBV, the method of 3'-base specific polymerase chain reaction (3'-BS-PCR) is applied to analyze the 1896 site mutation of HBV^[7] in 126 clinical serum samples and 23 patients' tissues and sera whose tumors have been surgically excised and pathologically diagnosed.

MATERIALS AND METHODS

Reagents and Instruments

Primers were ordered from Life Technology Company, USA; Proteinase K, Taq Polymerase, MgCl₂, PCR reaction buffer ordered from Hua Mei Biotechnology Company; other reagents were of

¹Laboratory of Molecular Biology and Department of Biochemistry, Anhui Medical University, Hefei 230032, Anhui Province, China

²Department of Infectious Diseases, the First Affiliated Hospital of Anhui Medical University, Hefei 230032, Anhui Province, China
Dr. Yuan Wang, graduated from Anhui Medical University (1982) and Shanghai Medical University (1987) postdoctor in Vanderbilt University and Northwestern University, USA from 1993 to 1995, professor and director, majoring in molecular biology and biochemistry, having 42 papers published.

Project supported by the Natural Science Foundation of Anhui Province, No.9741006 and Natural Science Foundation of Anhui Educational Commission, No.JL-97-077.

Correspondence to: Dr. Yuan Wang, Laboratory of Molecular Biology, Box #109, Anhui Medical University, Hefei 230032, Anhui Province, China

Tel. 0086-551-2843963
Email. wangyuan@mail.hf.ah.cn

Received 2000-01-10 Accepted 2000-03-03

analytical purity and made in China. Hema Thermocycler was the product from Zhuhai Hema Medical Instruments Company.

Specimens

The 126 serum samples were collected from outpatients and inpatients of Department of Infectious Disease, the First Affiliated Hospital of Anhui Medical University from November 1996 to August 1997. Seventy-two patients were infected by HBV, and 14 by HAV. Forty were HBsAg negative diagnosed by the method of RPHA. The 23 samples of liver cancer tissues were the surgical specimens from HCC patients in Department of Surgery, the First Affiliated Hospital of Anhui Medical University who were corroborated by pathological diagnosis. The corresponding serum was obtained before operation. These patients are diagnosed according to the diagnostic criteria stipulated by the Sixth National Meeting of Hepatitis, 1990.

DNA extraction from serum

Into 125 µL of the serum to be examined, add 125 µL HBV DNA extraction buffer (200 mmol·L⁻¹ NaCl, 2 mmol·L⁻¹ EDTA, 1% SDS, 100 mmol·L⁻¹ Tris-HCl, pH 8.0) and 6.25 µL Proteinase K (2 g·L⁻¹). Incubate in 37°C water bath for 6 hours. Extract with phenol and chloroform, precipitate the HBV DNA with ethanol, dissolve in 20 µL sterile re-distilled water and store at -20°C.

DNA extraction from the liver cancer tissues

Into the 200 µg HCC tissue, add 500 µL of DNA extract buffer (100 mmol·L⁻¹ NaCl, 1 mmol·L⁻¹ EDTA, 0.5% SDS, 50 mmol·L⁻¹ Tris-HCl, pH 8.0). Homogenize on ice. Add 50 µL of Proteinase K (2 g·L⁻¹). Incubate in 37°C water bath for 6 hours. Extract with phenol and chloroform, precipitate the HBV DNA with ethanol, dissolve in 20 µL sterile re-distilled water and store at -20°C.

PCR

The primers are designed according to the recorded HBV-DNA sequence, the principle of 3'-BS-PCR, and the papers published by Goergen^[6] i.e. 3' primer (GW-1-1d) TCC ACA CTC CAA AAG ACA

(2287-2270), wild type 5' primer (GW-1-1a) GTG CCT TGG GTG GCT TTG (1879-1896) and mutant type 5' primer (GW-1-1b) GTG CCT TGG GTG GCT TTA (1879-1896). Into the 10 μ L DNA extracted from serum or tissue diluted into 5 ng \cdot μ L⁻¹, add PCR reaction buffer [10 mmol \cdot L⁻¹, Tris, 50 mmol \cdot L⁻¹ KCl, 2 mmol \cdot L⁻¹ MgCl₂, 0.001% Gelatin, 200 μ mol \cdot L⁻¹ dNTPs, 0.5 μ mol \cdot L⁻¹ primers (wild type: GW-1-1a+GW-1-1d; mutant type: GW-1-1a+GW-1-1b) and 0.5 μ L Taq DNA polymerase (3U \cdot μ L⁻¹), covered with mineral oil, run PCR: 93°C 1min, 64°C 1min, 72°C 1min, 30 cycles, 72°C 5min. Aspirate 8 μ L of PCR products, check the results with 1.5% agarose gel electrophoresis. The positive band is of 408bp.

RESULTS

3'-BS-PCR of HBV DNA

Using the specific oligonucleotides designed according to the DNA sequences of mutant and wild types the results showed that the amplified specific DNA of wild and mutant types of HBV in precode C were both of 408 bp. Figure 1 shows the PCR results of the DNA extracted from 126 patients' serum obtained at different stages, which demonstrates that constant results can be achieved when repeated. The PCR results of the 14 patients infected by HAV were all negative.

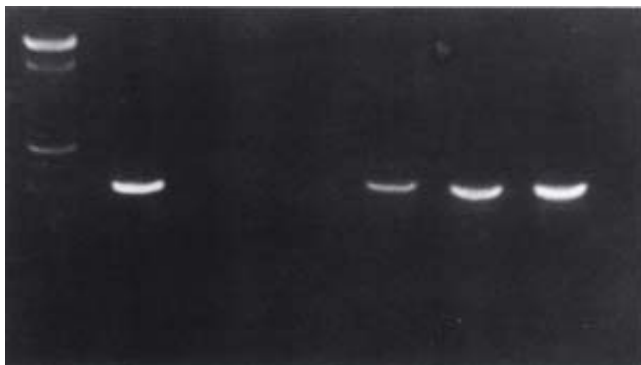


Figure 1 PCR results of HCC patients' point mutation in site 1896 of HBV precore.

1. 100bp DNA Marker; 2. positive control; 3. negative control; 4, 5. sample numbers

Analysis of the 126 patients' point mutation in site 1896 of HBV precore

Of the 72 patients with chronic hepatitis examined with the 3'-BS-PCR of HBV DNA, 58 were positive in wild type, 13 were positive in mutant type only, 21 were positive in both types. The positive rate of mutant type was 47.2% (34/72); the positive rate of mutant type only was 18.1%, the positive rate of both types was 29.1% (21/72). Neither of these types were detected in the 40 patients with negative HBsAg.

Detection of HBV precore gene in the 23 HCC patients (Table 1).

Table 1 The HBV precore and its mutant type detection in 23 HCC Patients n (%)

	Total	HBV precore positive	HBV precore negative	HBV precore positive		
				Mutant type	Wild type	Mixed type
Tissue	23(100%)	12(52.2)	6(26.1)	5(21.7)	12(52.2)	5(21.7)
Serum	23(100%)	7(30.4)	16(69.6)	6(26.1)	4(17.4)	3(13.0)

The positive rate of the 23 HCC patients' surgically excised tissues and pre-operational serum was 52.2% (12/23) and 30.4% (7/23) respectively. In order to exclude the possibility of contamination, negative controls and positive controls were performed each time.

DISCUSSION

The establishment of 3'-BS-PCR method for the analysis of point mutation in site 1896 of HBV precore

The mutation of HBV may have a close relationship to the continuous HBV infection and the deterioration of liver after the infection. The research on the mutation of HBV will greatly promote the clinical analysis of HBV infection and its subsequent diseases. The common methods to detect point mutation are DNA sequencing and SSCP, which are expensive, time-consuming and unsuitable for clinical practice. In order to fulfill the requirements of further researches on HBV mutation and its application to the clinic, we established the 3'-BS-PCR method for the analysis of point mutation in site 1896 of HBV precore.

According to the principle of primer design that only when the last base of primer's 3' end must strictly match its corresponding template could PCR be accomplished, the reports of Georger^[6] and the phenomenon that the nucleotide of site 1896 of HBV precore mutates from G to A, the corresponding 5' primers of wild and mutant types whose 3' terminal base are G and A respectively were designed to amplify the wild or mutant type DNA of the HBV precore region. Georger^[6] has successfully applied this kind of method to detect the point mutation of site 1896 in the HBV precore in the patients with positive anti-HBe results, which have been confirmed by DNA sequencing. The positive rates of this site's point mutation were slightly higher than the other reports^[9]. It may be because most patients investigated were inpatients from the Department of Infectious Diseases whose liver damages were more severe than those from outpatients. This explanation is supported by the recorded reports that the positive rates of mutant type are unanimous with the conditions of the liver

damages. The establishment of this method provides a new approach to study the HBV infection and analyze the liver damage.

The study on the integration of HBV precore gene in HCC

Many researches have shown that the infection of HBV has a close relationship with the carcinogenesis of liver cancer and is one of important factors inducing the liver cancer. With the research progresses in molecular oncology, two kinds of genes, oncogenes and anti-oncogenes, that have close relationship to carcinogenesis have been discovered. In the development of HCC, the activation of oncogene and the inactivation of anti-oncogene are frequent events, which cause the changes of the qualities or quantities of the important proteins that they are encoded and eventually lead to the carcinogenesis of normal cells. The integration of HBV DNA in the genome of the cells infected by the HBV is an important factor that brings the instability of chromosomes in liver cells^[8].

Therefore, it is meaningful to investigate the HBV-DNA fragments' integration and its effect on the activation of oncogene and inactivation of anti-oncogene. Our research shows that 12 of 23 primary HCC patients were found to have the HBV precore in the cancer tissues whose positive rate was 52.2%. Among these patients, the HBV precore DNA were detected in 7 patients' sera whose positive rate was 30.4%. The results indicate that the HBV precore gene widely exists in liver cancer tissues and the replication of HBV is accompanied by the development of HCC. HCC patients (21.8%,

5/23) had negative results in serum but positive results in cancer tissues, which indicates that these patients had HBV precore DNA fragments integrated in their liver cells and there was no virus replication. We plan to study whether there is an integration in the genome of liver cells using Southern Blot. Among these HBV precore positive patients, the patients with mutant type detected in the tissues were all wild type. Only half of the patients with mutant type detected in the serum were also wild type. A hypothesis could be made that the HBV precore may mutate during long host in the liver cell and may play an important role in the transformation of normal liver cells.

REFERENCES

- 1 Ulrich PP, Bhat RA, Kelly I, Brunetto MR, Bonino F, Vyas GN. A precore defective mutant of hepatitis B virus associated with eantigen-negative chronic liver disease. *J Med Virology*, 1990;32:109-118
- 2 Fattovich G, McIntyre G, Thursz M, Colman K, Ginliano G, Alberti A, Thomas HC, Carman WF. Hepatitis B virus precore/core variation and interferon therapy. *Hepatology*, 1995;22:1355-1362
- 3 Guptan RC, Thakur V, Sarin SK, Banerjee K, Khandekar P. Frequency and clinical profile of precore and surface hepatitis B mutants in Asian-Indian patients with chronic liver disease. *Am J Gastroenterol*, 1996;91:1312
- 4 Lubber B, Arnold N, Sturz M, Hohne M, Schirmacher P, Lauer U, Wienberg J, Hofschneider PH, Kekule AS. Hepatoma derived integrated HBV DNA causes multistage transformation *in vitro*. *Oncogene*, 1996;12:1597-1608
- 5 Robinson WS, Klote L, Aoki N. Hepadnaviruses in cirrhotic liver and hepatocellular carcinoma. *J Med Virol*, 1990;31:18-32
- 6 Georger B. Comparison of mutation specific PCR and direct sequencing of PCR-products for the detection of the HBV pre-C stop codon. *Hepatology*, 1992;16:232
- 7 Wang Y, Li X, Zhou Q. Analysis of precore site mutation of hepatitis B virus by polymerase chain reaction. *Anhui Yike Daxue Xuebao*, 1998;33:251-253
- 8 Robinson WS. The role of Hepatitis B virus in development of primary hepatocellular carcinoma. *J Gastro Hepatol*, 1992;7:622
- 9 Wang XF, Liu HD, Wang JR, Zhou F, Lei PJ. Studies of HBV precore region 1896 site mutation of patients with hepatitis B and hepatoma. *Zhonghua Chuanranbingxue Zazhi*, 1996;14:11-13

Edited by You DY
proofread by Sun SM

Orthotopic liver transplantation for fulminant hepatitis B

Xiao Shun He, Jie Fu Huang, Gui Hua Chen, Qian Fu, Xiao Feng Zhu, Min Qiang Lu, Guo Dong Wang and Xiang Dong Guan

Subject headings hepatitis B; liver transplantation; lamivudine

He XS, Huang JF, Chen GH, Fu Q, Zhu XF, Lu MQ, Wang GD, Guan XD. Orthotopic liver transplantation for fulminant hepatitis B. *World J Gastroentero*, 2000;6(3):398-399

INTRODUCTION

When fulminant hepatitis progresses to deep encephalopathy, with stage III or IV coma, it is commonly irreversible with a high mortality rate (80%-100%)^[1]. Liver transplantation may be the sole treatment of choice in such circumstances. However, the early results have been disappointing, largely due to the frequency of posttransplant HBV infection^[2,3]. This recurrent disease often develops in an aggressive manner characterized by high levels of HBV replication and rapidly progressive liver graft damage. In recent years, however, as new antiviral agents, such as lamivudine came into being, the patient's survival has much been improved. The purpose of this study is to assess the effect of OLTx in a series of 7 patients with fulminant hepatitis B, and to evaluate the efficiency of lamivudine on preventing patients from HBV reinfection.

MATERIALS AND METHODS

Between October 1993 and August 1999, 7 adult male patients with hepatitis B were referred for liver transplantation. Their age at the time of operation ranged from 32 years to 49 years (median age 42.9 years). All patients were positive for HBV surface antigen (HBsAg), and 2 had evidence of viral replication. The latter was demonstrated by positive hepatitis B e antigen or/and HBV-DNA. Patient profiles are shown in Table 1.

All patients received orthotopic liver

transplantation 1 to 10 days after admission. Initial immunosuppression with cyclosporine A (CsA), and methylprednisolone was used in all cases. In the latter 3 cases, tacrolimus (FK506) was given orally when the patients resumed oral intake. Doses were adjusted in the first month to maintain 12 h trough levels of 10 g/L to 15 g/L. Prophylaxis for cytomegalovirus infection was started immediately after surgery with acyclovir or ganciclovir for 2 weeks. Lamivudine was administered orally, 100 mg or 150 mg daily in 5 patients when it became commercially available, and the treatment was not interrupted in any patient.

RESULTS

All patients in this series recovered consciousness 24 h after OLTx. Of them, five recipients were still alive and well with normal liver function during a following up period of 3-7 months. One patient with grade III hepatic encephalopathy died due to HBV reinfection 36 days after liver transplant. Another patient with preoperative esophageal varicosis bleeding died of multi-organ failure 3 days after transplantation. Various medical and surgical complications occurred in two of the five survived patients. One developed recurrent onset of epilepsy necessitated continuous antiepileptic therapy. Another developed stenosis of inferior vena cava, which was successfully treated by balloon dilation and stent replacement.

No acute or chronic graft rejection occurred in any patient. In patient 1, viral replication disappeared within 1 month following OLTx and became positive thereafter. The other 6 patients had a negative HBsAg within 3 to 14 days after OLTx and all had a negative viral replication. No side effects were noted concerning lamivudine treatment.

DISCUSSION

Hepatitis B is a common disease in mainland China. It was estimated that HBsAg carriers accounted for 10% of the total population. However, the natural history of hepatitis B can be quite variable^[4]. Even once signs of portal hypertension develop, many patients can go years before complications develop that impair the quality of their lives. By contrast, others can have stable liver disease for quite some time and then deteriorate quickly, often related with bleeding or infection. Thus, it is difficult to make accurate decisions about the timing of liver transplantation. In general, once the patient's liver

Transplantation Surgery, First Affiliated Hospital of Sun Yat-Sen University of Medical Sciences, Guangzhou 510080, P.R.China

Dr. Xiao Shun He, MD, Ph.D., graduated from Sun Yat-Sen University of Medical Sciences, working as a visiting scholar in Australian National Liver Transplantation Unit between 1997-1998, now associate Professor and Deputy Director of Transplantation Surgery Department, majoring in liver transplantation, having 20 papers published.

Project supported by the Key Clinical Project of Ministry of Health. No. 97040230 and the Key Project of Scientific and Technological Committee of Guangdong Province No. 963003

Correspondence to: Dr. Xiao Shun He, Department of Transplantation Surgery, First Affiliated Hospital of Sun Yat-sen University of Medical Sciences, 58 Zhongshan Er Lu, Guangzhou 510080, China
Tel. 0086-20-87306082, Fax. 0086-20-87306082
Email. sean@gzsums.edu.cn

Received 2000-01-13 **Accepted** 2000-03-02

disease begins to impair air quality of life, the physician should consider an evaluation for transplantation. Based on this understanding, fulminant or sub-fulminant hepatitis is justifiable for liver transplantation. According to the experience of King's College Hospital in London, the selection criteria for transplantation in hepatitis B are based on the occurrence of three of the followings: a prothrombin time greater than 50 seconds; a jaundice to encephalopathy time of more than 7 days; non-A, non-B hepatitis or drug-induced hepatitis; age younger than 10 years or older than 40 years; bilirubin greater than 300 $\mu\text{mol/L}$; or the finding of a prothrombin time of greater than 100 seconds in isolation^[5]. In the present series, all 7 patients met the above mentioned criteria. The overall survival rate of our series was 71.4% after a 3-7 month follow-up period. The mortality rate of those patients with fulminant hepatitis B was 29.6%. Of the two patients who died, one died 5 weeks following OLTx of recurrent fulminant hepatitis B, indicating the high risk of HBV reinfection when the serum HBeAg was positive. The other patient died of multi-system organ failure on postoperative day 3. Nevertheless, the overall outcomes were to our satisfaction and support the continued application of liver transplantation as a therapeutic measure for fulminant hepatitis B.

It has been found that nearly 100% of patients showing evidence of active viral replication, i.e. serum HBV-DNA or/and HBeAg positive, and 70%-80% of those with HBV DNA or HBeAg negative prior to OLTx and received no immunoprophylaxis, developed recurrent HBV infection of the graft following OLTx^[6]. The recurrent disease may manifest as rapidly progressive disease. In our series, patient 1

developed fulminant hepatic failure 5 weeks following OLTx. Interferon (IFN) has been used both prophylactically and therapeutically after OLTx in patients with recurrent HBV, but it has proved to be mostly ineffective and may lead to further complications^[7]. In recent years, perioperative administration of hepatitis B immunoglobulin (HBIG) has been reported to reduce the incidence of recurrence. But, it requires prolonged parenteral treatment and does not suppress viral replication. Additionally, availability of HBIG could be limited and the costs related to prolonged use of HBIG are very high^[8]. These disadvantages of HBIG prevent it from wide clinical use. Because high level viral replication seems to be important in the pathogenesis of HBV recurrence, there has been great interest in the potential role of nucleoside analogue with anti-HBV activity. The most promising are lamivudine and fosciclovir. Both agents have been evaluated in both animal model of HBV and clinical trial and have been shown to rapidly suppress viral replication. Lamivudine prophylaxis after liver transplantation resulted in a complete and sustained suppression of viral replication in OLTx recipients^[9]. In our study, 5 patients received lamivudine treatment, no side effect has been identified, and the treatment was not interrupted in any patient. The doses of 100 mg daily suppressed HBV-DNA to undetectable levels in one patient. Serum HBsAg became negative and HBeAb became positive after transplantation in all the patients. No cases of HBV reinfection were noted in lamivudine-treated patients. The results indicated that lamivudine is a beneficial and well-tolerated therapy in OLTx with HBV infection. The long-term effects of lamivudine are being investigated.

Table 1 Details and results of 7 patients underwent OLTx for fulminant hepatitis B

Patients No.	Age/Sex	Medical history	Bilirubin ($\mu\text{mol/L}$)	Encephalopathy	ABO compatibility	Lamivudine regimen	Outcome	Cause of death
1	32/male		478.0	III	Identical	(-)	Died	HBV reinfection
2	44/male	Biliary surgery $\times 2$	756.1	I	Identical	(+)	Alive	
3	49/male	Nasopharyngeal carcinoma	141.3	I	Identical	(-)	Alive	
4	48/male	Epilepsy due to brain trauma, PE $\times 3$	787.1	II	Identical	(+)	Alive	
5	48/male	Hepato renal syndrome duodenal ulcer, PE $\times 4$	500.7	IV	Identical	(+)	Alive	
6	44/male	Esophageal varicosis bleeding, PE $\times 2$	937.5	III	Compatible	(+)	Died	Massive bleeding and multi-organ failure
7	35/male	Tuberculosis, PE $\times 5$	432.6	I	Incompatible	(+)	Alive	

PE: plasma exchange

REFERENCES

- Hodes JE, Grosfeld JL, Weber TR, Schreiner RL, Fitzgerald JF, David Mirkin L. Hepatic failure in infants on total parenteral nutrition (TPN): clinical and histopathologic observations. *J Pediatr Surg*, 1982;17:463-468
- Lake JR, Wright TL. Liver transplantation for patients with hepatitis B: what have we learned from our results. *Hepatology*, 1991;13:796-799
- O'Grady JG, Smith HM, Davies SE, Daniels HM, Donaldson PT, Tan KC, Portmann B, Alexandev GJ, Williams R. Hepatitis B virus reinfection after orthotopic liver transplantation: serological and clinical implications. *J Hepatol*, 1992;14:104-111
- Bonino F, Rosina F, Rizzetto M, Rizzi R, Chiaberge E, Tardano R, Callea F, Verme G. Chronic hepatitis in HBsAg carriers with serum HBV DNA and anti-HBe. *Gastroenterology*, 1986;90:1268-1273
- O'Grady JG, Alexander GJM, Hayllar KM, Williams R. Early indicators of prognosis in fulminant hepatic failure. *Gastroenterology*, 1989;97:439-445
- Ben Ari Z, Shmueli D, Mor E, Shaharabani E, Bar-Nathan N, Shapira Z, Tur-Kaspa R. Beneficial effect of lamivudine pre and post liver transplantation for hepatitis B infection. *Transplant Proc*, 1997;29:2687-2688
- Wright HI, Gavalier JS, Van Thiel DH. Preliminary experience with α -2b-interferon therapy of viral hepatitis in liver allograft recipients. *Transplantation*, 1992;53:121-124
- Nery JR, Weppler D, Rodriguez M, Ruiz P, Schiff ER, Tzakis AG. Efficacy of lamivudine in controlling hepatitis B virus recurrence after liver transplantation. *Transplantation*, 1998;65:1615-1621
- Gutfreund KS, Fischer KP, Tipples G, Ma M, Bain VG, Kneteman N, Tyrrell DLJ. Lamivudine results in a complete and sustained suppression of hepatitis B virus replication in patients requiring orthotopic liver transplantation for cirrhosis secondary to hepatitis B. *Hepatology*, 1995;22:328A

Edited by You DY
proofread by Sun SM

Dot immunogold filtration assay for rapid detection of anti-HAV IgM in Chinese

Feng Chan Han, Yu Hou, Xiao Jun Yan, Le Yi Xiao and Yan Hai Guo

Subject headings dot immunogold filtration assay; hepatitis A virus; immunoglobulin M/analysis

Han FC, Hou Y, Yan XJ, Xiao LY, Guo YH. Dot immunogold filtration assay for rapid detection of anti HAV IgM in Chinese. *World J Gastroentero*, 2000;6(3):400-401

INTRODUCTION

The hepatitis A virus specific immunoglobulin M(IgM) antibody is a specific serological marker for early diagnosis of hepatitis A. At present, the methods used at home or abroad for detecting anti-HAV IgM are RIA, ELISA and SPHAI. The dot immunogold combination assay that has been developed since 1989 is a new technique with the property of simple and rapid immunological detection, by using the red colloidal gold particles to label the antibodies as indicator, and the millipore filtering membrane coated with antigen as the carrier. Affected by filtration and condensation, the antigen antibody reaction is enabled to go on rapidly. When the reaction is positive, red dots appear on the membrane. It takes about 2 min to 4 min for the whole reaction to be carried out. With the above technique, we have established the dot immunogold filtration assay (DIGFA) for rapid detection of anti-HAV IgM with comparatively satisfactory results.

MATERIALS AND METHODS

Materials

The hepatitis A virus antigen (HAAG) was the cell-cultured antigen, some of which were purchased from the Reagent Factory of Chinese PLA 302 Hospital and the rest was prepared by our institute. The anti-human μ chain monoclonal antibody was purchased from the teaching and research group for immunology of our university. The sheep anti-human IgM antibody was purchased from the immunological room of Chinese PLA 302 Hospital. The chloroauric acid was the product of the Chendu Chemical Plant with the batch number of 93082. Part of the serum samples from hepatitis A patients was supplied by the Department of Epidemiology

Chinese PLA Institute of Gene Diagnosis, Fourth Military Medical University, 710033 Xi'an, Shaanxi Province, China
Dr. Feng Chan Han, graduated from Chinese PLA Fourth Military Medical University as a postgraduate in 1998, now a lecturer, having 12 papers published.

Correspondence to: Feng Chan Han, Chinese PLA Institute of Gene Diagnosis, Fourth Military Medical University, 17 Changle Xilu, -Xi'an 710033, Shaanxi Province, China
Tel. 0086-29-3374771
Email. hanfengchan@yeah.net

Received 2000-01-15 **Accepted** 2000-03-03

and the rest was collected from the Xi'an Municipal Children Hospital and the Railroad Central Hospital with diagnosis in accordance with the standards revised by the Shanghai Conference held in 1990. The sera of the patients suffering from epidemic hemorrhagic fever were supplied by Professor Sun of the Department of Epidemiology. The remaining serum samples were obtained from the Xijing Hospital. The ELISA kits for anti-HAV IgM detection were purchased from the Nanjing Military Medical Research Institute.

Methods

Principle The serum to be tested was put on the millipore membrane previously coated with HAAG. If there was anti-HAV IgM, the HAAG-anti-HAV IgM colloidal gold complex was formed on the membrane as red dots which were visible to the naked eyes.

Preparation of colloidal gold It was prepared according to the methods by Dar *et al*^[1]. Fifty mL of 0.2 g/L chloroauric acid was heated to the boiling point with 1.2 mL of the 10 g/L sodium citrate added later. The boiling lasted 5 min. The preparation was well done and finished when it became dark red in color.

Anti-human μ chain antibody colloidal gold labelling It was prepared according to reference^[2] with the main procedures as follows: Using 0.1 mol/L K_2CO_3 , 1 mL colloidal gold was regulated to have the pH of 8.0 or 9.0. With the help of magnetic stirring, the F(ab')₂ anti-human μ chain monoclonal antibody or sheep anti-human IgM was added. After 10 min, the bovine serum albumin (BSA) was added to get the concentration of 10 g/L. After that, the mixture was centrifuged at $2\,500 \times g$ for 5 min. The supernatant was further centrifuged at $12\,000 \times g$ for 20 min. The supernatant was discarded and the precipitate was dissolved by 5 g/L BSA-PBS, thus forming the colloidal gold labelling reagent.

Millipore filtering membrane treatment and antigen immobilization The nitrocellulose membrane with millipore diameter of 0.65 μm produced by the attached factory of the Beijing Chemical School was soaked by triple-distilled water and then dried spontaneously. The disc, 1 cm in diameter was made from the prepared membrane with a punch, was soaked in 0.05 mol/L carbonate buffer and then dried in air. One μL HAAG solution was dripped onto the center of the disc. After dried at room temperature, the disc was enclosed with 5 g/L BSA, then rinsed with the PBS-T twice for 10 min each time. After being dried, it was put into the self-made immune filtration plate.

Testing methods The immune filtration plate was numbered with the corresponding serum numbers, to the center of the membrane, dripped a drop of 0.01 mol/L PBS-T to activate the surface of the membrane. After the PBS-T was filtered into the membrane, 10 μ L of the serum was dripped slowly to the center of the membrane. Then, the membrane center was flushed by 2-3 drops of washing solution. After that, 30 μ L of the colloidal gold labelling reagent was added. After the latter was filtered into the membrane, the center was flushed with 2-3 drops of washing solution. Red dots in the center denote positive results, while colorless means negative.

Blocking test A: Ten μ L of anti-HAV IgM positive serum was added to 10 μ L of anti-human IgM working solution. B: Ten μ L of the positive serum was added to 20 μ L of the HAAg original solution and mixed evenly. The solution was kept in the water bath at 37°C for 1 h. The sera treated in both ways were put on the membrane. The DIGFA was made following the steps depicted above.

2-ME destruction tests Ten μ L of 0.2 mL/L β -mercaptoethanol (2-ME) was added to 10 μ L of anti-HAV IgM positive serum and mixed evenly. The solution was kept in water bath at 37°C for 1 h. The treated sera were used to do the tests of DIGFA as described above.

ELISA tests The tests were performed according to the operative instructions in a strict way.

RESULTS

Comparison between DIGFA and ELISA Two hundred and seventy nine serum samples were tested in a contrast way with the DIGFA and ELISA. The result was that 148 samples were positive and 125 samples negative with both methods. If the ELISA was used as the reference standard, the specificity of the DIGFA was 98.4% and the sensitivity 97.3%. The coincidental rate of both methods was 97.8%.

Blocking tests and 2-ME destruction tests Ten samples of anti-HAV IgM positive sera tested by the DIGFA and ELISA were chosen at random, all changed to negative after undergoing the blocking affect. Besides, the 10 serum samples which were treated by the 2-ME also changed to negative. This testifies that what was detected by the DIGFA was surely the anti-HAV IgM.

Results of detection on non-hepatitis A sera Forty serum samples from epidemic hemorrhagic fever patients, 10 serum samples with positive anti-HBc IgM and 41 serum samples from the blood donors were all negative when tested by the DIGFA.

Rheumatoid factor interference tests Twenty samples with positive rheumatoid factor (RF) were all shown negative results by DIGFA.

Repetitive tests Ten anti-HAV IgM positive samples and 10 negative samples which were chosen at random were tested repeatedly for five time. They all showed the identical results.

DISCUSSION

The dot immunogold test is a new immunological technique which has been developed in recent years^[1,3,4]. Since the millipore filtering membrane not only absorbs protein, but also affords rapid filtration and acts as capillaries, the antigen or antibody in serum is able to combine rapidly with the counterpart on the membrane. Moreover, as the colloidal gold labelling reagent is red in color, red dots appear after the combination takes place. Therefore, no color developing reagent is needed. This method that has aroused our interest greatly not only keeps with the sensitivity and specificity of the ELISA and RIA, but also with the advantage of affording prompt result.

In China, to detect Anti-HAV IgM, the ELISA and RIA are mainly used^[5,6], but the successful employment of the solid-phase immunoadsorption hemagglutination inhibition test^[7] has been reported. However, the drawbacks of ELISA and RIA lie on their requirement of prolonged operation time, complicated procedures and instruments, and some reagents having carcinogenic or radionuclide effects may be harmful to the handlers or polluted the environment if not properly disposed. Furthermore, the activity of HAAg is unstable and may be likely influenced by temperature, so it is hard to obtain a reagent kits with reliable efficiency. As for the solid-phase immunoadsorption hemagglutination inhibition test, the operation time is also long and no kit is available. The advantages in using DIGFA to test the Anti-HAV IgM are as follows: The operation period is shortened from a few hours to 5 min and the results are reliable and visible to the naked eye. The specificity and sensitivity are approximately equal to those of the ELISA and not influenced by RF. The HAAg from cultured cells is coated on the nitrocellulose millipore filtering membrane in a solid phase, with durable activity; the colloidal gold labelling reagent can be preserved beyond one year; the manipulations are simple and no sophisticated testing instrument required; the operator can be trained in a simple way, and may become acquainted with whole operation technique in a short time.

Therefore DIGFA is an ideal method utilized in the early diagnosis and the epidemiological study of hepatitis A.

REFERENCES

- 1 Dar VS, Ghosh S, Broor S. Rapid detection of rotavirus by using colloidal gold particles labeled with monoclonal antibody. *J Virol Methods*, 1994; 47:51-58
- 2 Xiao LY, Yan XJ, Chen YX, Li SQ, Guo YH, Su CZ, Hou Y, Liu J. Primary study of a dot immunogold filtration assay for rapid detection of HAV, HBV and HCV IgM. *Disi Junyi Daxue Xuebao*, 1995;16:176
- 3 Spielberg F, Kabeya CM, Ryder RW, Kifuani NK, Harris J, Bender TR, Heyward WL, Quinn TC. Field testing and comparative evaluation of rapid and visually read screening assays for antibody to human immunodeficiency virus. *Lancet*, 1989;1:580-584
- 4 Cao XK, Tao YX, Han S, Zhen ZG, Zhu EY. Application of dot immunogold filtration assay in the detection of serum alpha-fetoprotein. *Shanghai Mianyixue Zazhi*, 1991;11:154-156
- 5 Xu ZY. Application of the method of solid-phase enzyme labeling double sandwich for the detection of IgM antibody of hepatitis A. *Shanghai Yixue*, 1982;5:406-409
- 6 Zhang XT, Duo FQ, Zhu MB, Wu XM, Jiang YT. Detection of IgM antibody of hepatitis A by solid-phase radioimmunoassay. *Jiefangjun Yixue Zazhi*, 1982;7:213-216
- 7 Xiao LY, Wang SS, Xu DZ, Li YG, Zhou H, Chen YJ. Rapid detection of anti-HAV IgM by solid-phase immunosorption hemagglutination inhibition test. *Zhonghua Liuxingbingxue Zazhi*, 1992;13:229-231

Edited by You DY
proofread by Sun SM

Protective actions of salvianolic acid A on hepatocyte injured by peroxidation *in vitro*

Yi Yang Hu¹, Cheng Hai Liu¹, Run Ping Wang², Cheng Liu¹, Ping Liu¹, Da Yuang Zhu³

Subject headings Salvianolic acid A; hepatocyte; carbon tetrachloride; liver injury; lipid peroxidation; water soluble vitamin E; ALT; AST; superoxide dismutase; malondialdehyde; catalase; lactase dehydrogenase; glutathione peroxidase; glutathione

Hu YY, Liu CH, Wang RP, Liu C, Liu P, Zhu DY. Protective actions of salvianolic acid A on hepatocyte injured by peroxidation *in vitro*. *World J Gastroentero*, 2000;6(3):402-404

INTRODUCTION

Salvianolic radix, one of the most commonly used traditional Chinese herbs, was widely studied about its actions against liver injury and fibrosis, and was one of the focuses of recent research^[1,2]. Salvianolic acid-A (SA-A) was an aqueous soluble component of *Salvianolic radix*. In our previous work^[2], SA-A was found to have protective effects against liver injury and fibrosis induced by carbon tetrachloride (CCl₄) in rats. In order to investigate the effect of SA-A on peroxidation in hepatocytes, we induced the injured hepatocyte model by CCl₄ fumigation *in vitro*, treated the cell model with SA-A or aqueous soluble vitamin E (Vitamin E), the latter served as the control drug, and observed the influences of the drugs on the functions of the hepatocytes injured by peroxidation.

MATERIALS AND METHODS

Animals

Wistar rats, male, specific pathogens free (SPF), weighing 140 g-160 g, were provided by the Experimental Center of Animals, Shanghai University of Traditional Chinese Medicine.

Drug

SA-A, molecular formula C₂₆H₂₂O₁₀, molecular structure as Figure 1, weight 494, was extracted and

identified by Shanghai Institute of Materia Medica, Chinese Academy of Sciences. Vitamin E was purchased from Hoffman Co. USA.

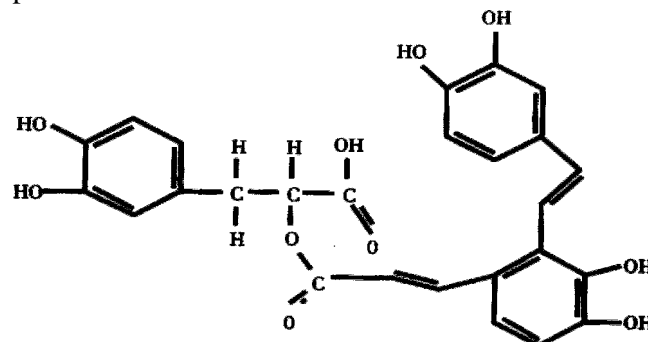


Figure 1 SA-A molecular structure.

Main reagents

Purified type III collagenase (specific activity, 960 U/mg), insulin and dexamethasone were purchased from Sigma Co. USA. Soybean trypsin was from Institute of Biochemistry, Chinese Academy of Science; ficoll was from Shanghai Second Chemical Reagent Factory; medium 199 (M199) from Gibco Co., USA; carbon tetrachloride (CCl₄), analytical grade, from Yixin Third Chemical Reagent Factory, Jiangsu Province; and newborn bovine serum (NBS) from Shanghai Sino-American Co.

Isolation and culture of hepatocytes

According to a modified method^[3], hepatocytes were isolated and primarily cultured from rats. In brief, after anesthesia with ether, the rat liver was perfused *in situ* with Ca²⁺ and Mg²⁺-free Hank's solution via the portal vein for 5 min, followed by perfusion with Hank's solution containing 0.5 g/L collagenase for 20 min. The liver was then excised and minced with forceps to remove Glisson's capsule and the liver cells dispersed. The liver cell suspension was filtrated with double layers of gauze and was adjusted to 2 × 10¹⁰/L. Then 5 mL cell suspension was added onto the top of 20 mL 492 g/L Ficoll, and centrifuged at 50 × g, 4°C, 5 min to purify the hepatocytes. The cell recovery was about 1 × 10¹⁰ cells per liver, the purity was more than 95% identified by the cell typical appearance via phase contrast microscope, and the viability was more than 90% assessed by trypan blue exclusion. Hepatocytes were suspended with M199

¹Institute of Liver Diseases, Shanghai University of Traditional Chinese Medicine, Shanghai 200032, China

²Now at Beijing Hospital of Traditional Chinese Medicine, Beijing 100011, China

³Shanghai Institute of Materia Medica, Chinese Academy of Sciences, Shanghai 200031, China

The project was supported by Shanghai Education Committee "Shuguang Program", No. 96 SG 26.

Correspondence to: Dr. Yi Yang Hu, Professor, Institute of Liver Diseases, Shanghai University of Traditional Chinese Medicine, Shanghai 200032, China

Tel. 0086-21-64174600 Ext.424, Fax. 0086-21-64036889

Email. hyy@shutcm.edu.cn

Received 2000-01-02 Accepted 2000-02-18

containing 5% (v/v) NBS to adjust their density to 5×10^8 cells/L, seeded on plastic dishes (Nunc, Denmark) and primarily cultured at 37°C in a humidified atmosphere of 50 mL/L CO₂ and 950 mL/L air.

Induction of hepatocyte peroxidative injured model

According to David method^[4], the peroxidatic injury of hepatocytes was induced by CCl₄ fumigation. Briefly, after 48 h of isolation and culture, the cells were placed in sealed box, to which 1 mL/L CCl₄ was added, and the cells were fumigated with CCl₄ at 37°C for 24 h.

Drug treatment

Normal hepatocytes in dishes were divided into the following groups: the normal, the control, vitamin E (2×10^{-3} mol/L^[5]) and SA-A treated groups at different concentrations (10^{-4} mol/L- 10^{-8} mol/L). All but the normal group, were incubated with vitamin E or SA-A at different concentrations and fumigated with CCl₄ spontaneously for 24 h, then the culture medium was collected respectively and stored at -70°C until assay.

Biochemical index assay

The ALT and AST in culture medium were assayed with Riman and Frankle method, malondialdehyde (MDA) with Bacon's method^[6]. Superoxide dismutase (SOD), catalase (CAT), lactase dehydrogenase (LDH), glutathione peroxidase (GSH-PX), glutathione (GSH) were measured following the protocols provided by the manufacturer (Jianchueng Biochemical Technological Institute, Nanjing).

Statistics

Chi-square test and *q* test.

RESULTS

The cell morphological changes

After 48 h of isolation and culture, primary hepatocytes gathered, attached and grew very well. At 24 h after fumigation with CCl₄, the hepatocytes partially shrank, their plasma membrane became rough and organelles swollen. When the cell models were incubated with SA-A or Vitamin E, the plasma membrane became smoother and the organelles less smother than those of controlled model cells.

Effects of SA-A or Vitamin E on ALT, AST and LDH activity in hepatocytes injured by peroxidation

The activities of ALT and AST both increased, while the former increase more obviously. LDH activity enhanced approximately 20 folds. SA-A inhibited these pathological increase in dosage

dependent manner, and among all concentrations tested the 10^{-4} mol/L SA-A had the best effect on the cell structure and enzymes. The effect of SA-A was better than that of Vitamin E, but 10^{-7} mol/L- 10^{-8} mol/L SA-A was not effective compared with the control (Table 1).

Effects of SA-A or Vitamin E on MDA contents and the activities of SOD and CAT in hepatocytes injured by peroxidation

MDA content in the control nearly doubled that of the normal, and the activities of SOD and CAT increased remarkably. SA-A decreased these pathological changes, and 10^{-4} mol/L SA-A had a significant inhibitory action. Vitamin E also decreased the MDA content markedly, but had no obvious influence on SOD activity (Table 2).

Effects of SA-A or Vitamin E on GSH content and GSH-PX activity in hepatocytes injured by peroxidation

After the hepatocytes were injured by peroxidation, the GSH-PX activity increased but GSH content decreased remarkably. 10^{-4} mol/L SA-A or Vitamin E inhibited the increase of GSH-PX activity and the decrease of GSH. For the extent of inhibition in GSH lowering, SA-A 10^{-4} mol/L is superior to Vitamin E (Table 2).

Table 1 Effects of SA-A on ALT, AST and LDH activities in hepatocytes injured for 24 h (*n* = 6, $\bar{x} \pm s$)

Group	ALT(U·L ⁻¹)	AST(U·L ⁻¹)	LDH(U·L ⁻¹)
Normal	18 ± 2.8 ^b	56 ± 3.8 ^b	77 ± 38 ^b
Control	103 ± 6.5	176 ± 9.1	1674 ± 128
10^{-4} mol/L SA-A	49 ± 2.9 ^{bd}	134 ± 5.0 ^{bd}	1050 ± 83 ^{bd}
10^{-5} mol/L SA-A	72 ± 3.9 ^{bd}	177 ± 8.3	1551 ± 88
10^{-6} mol/L SA-A	91 ± 11.1 ^a	177 ± 9.2	1602 ± 88
10^{-7} mol/L SA-A	96 ± 7.9	181 ± 6.7	1657 ± 81
10^{-8} mol/L SA-A	93 ± 11.4	181 ± 10.7	1684 ± 71
Vitamin E	86 ± 7.6 ^b	182 ± 10.7	1509 ± 30 ^a

^a*P* < 0.05; ^b*P* < 0.01, vs Control; ^d*P* < 0.01 vs Vitamin E.

Table 2 Effects of SA-A on the contents of MDA and GSH and the activities of SOD, CAT and GSH-PX in hepatocytes injured by peroxidation (*n* = 6, $\bar{x} \pm s$)

Group	MDA(μmol·L ⁻¹)	SOD(U·L ⁻¹)	CAT(U·L ⁻¹)	GSH(U·L ⁻¹)	GSH-PX(U·L ⁻¹)
Normal	5.11 ± 0.91 ^b	30.4 ± 2.86 ^b	12.8 ± 3.45 ^b	1.27 ± 0.13 ^b	16.7 ± 8.84 ^b
Control	9.17 ± 0.80	59.0 ± 2.23	86.6 ± 13.00	0.36 ± 0.07	90.9 ± 11.00
10^{-3} mol/L SA-A	6.79 ± 0.81 ^a	45.6 ± 3.26 ^{bd}	17.3 ± 3.59 ^{bd}	0.95 ± 0.02 ^{bd}	65.2 ± 1.24 ^a
10^{-4} mol/L SA-A	7.67 ± 1.11	55.2 ± 2.44	38.3 ± 11.82 ^b	0.40 ± 0.04	81.8 ± 17.54
10^{-5} mol/L SA-A	8.27 ± 1.50	57.6 ± 3.27	49.9 ± 6.78 ^b	0.38 ± 0.10	84.1 ± 19.11
Vitamin E	7.52 ± 0.69 ^a	55.8 ± 4.03	27.6 ± 3.22 ^b	0.49 ± 0.07 ^a	63.64 ± 10.57 ^a

^a*P* < 0.05, ^b*P* < 0.01, vs Control; ^d*P* < 0.01 vs Vitamin E.

DISCUSSION

In this study, 24 h after fumigation of hepatocytes with CCl₄, the ALT, AST and LDH all increased remarkably, the rate of elevation was in order of LDH, ALT and AST. It is suggested that the

hepatocytes were acutely injured, cell membrane integrity was broken and the enzymes in cell plasma leaked out. However, after the hepatocytes injured by peroxidation which were incubated with SA-A, the pathological increases of ALT, AST and LDH reduced markedly. It is indicated that SA-A had a potential effect against hepatocyte injury.

The free radicals and its triggered lipid peroxidation were involved in the main mechanisms by which carbon tetrachloride injured hepatocytes. MDA was one of main lipid peroxidatic products, its elevated levels could reflect the degrees of lipid peroxidatic injury in hepatocytes. GSH, a peroxide scavenger with a lower molecular weight, could eliminate superoxide anion and hydrogen peroxide. The content of GSH reflected the ability against peroxidation^[7]. In this study, GSH in hepatocytes of the model group was reduced remarkably, suggesting that the potency of antioxidation in injured cells was decreased. There were many other markers that could reflect lipid peroxidation, e.g. SOD, a scavenger of peroxide anion radicals, which could inhibit the initiation of lipid peroxidation by free radicals; GSH-PX, which could particularly catalyze the reductive action of GSH to H₂O₂ to protect the integrity of plasma membrane and functions; CAT etc. All the above-mentioned enzymes increased in the model cells. This may result from acute compensation after injury, and peroxidatic reaction stimulated by CCl₄ in

hepatocytes. SA-A markedly inhibits the increase of MDA level and the decrease of GSH, also reduced the activities of GSH-PX, CAT, SOD in different extents. Among these results, SA-A had better effect than vitamin E, which is a widely recognized antioxidation drug. It is indicated that SA-A had potential action against lipid peroxidation, this effect perhaps is the main mechanism of protection on liver injury. The results are also in accordance with the other reports^[8] and our previous work^[2].

REFERENCES

- 1 Deng HJ, Ma XH, Xu RL, Chen XM, Zhao YC, Yin L, Han DW. Study on mechanisms of protective action of Radix Salvia miltiorrhiza (RSM) against experimental hepatic injury in rats. *Zhongguo Zhongyao Zazhi*, 1992;17:233-236
- 2 Hu YY, Liu P, Liu C, Xu LM, Liu CH, Zhu DY, Huang MF. Actions of salvianolic acid A on CCl₄ poisoned liver injury and fibrosis in rats. *Zhongguo Yaoli Xuebao*, 1997;18:478-480
- 3 Alpini G, Phillips JO, Vroman B, Larusso NF. Recent advances in the isolation of liver cells. *Hepatology*, 1994;20:494-514
- 4 Johnston DE, Kroening C. Stimulation of prostaglandin synthesis in cultured liver cells by CCl₄. *Hepatology*, 1996;24:677-684
- 5 Zhu JL, Liu SL, Wu J, Tsyganskaya M, Kuncio GS, Zern MA. MG132, vitamin E and lithospermic acid A all inhibit TGHP induced damage to rat hepatocytes. *Hepatology*, 1996;24(4,part 2):335A
- 6 Bacon BR, Tavill AS, Brittenham GM, Park CH, Recknagel RO. Hepatic lipid peroxidation *in vivo* in rats with chronic iron overload. *J Clin Invest*, 1983;71:429-439
- 7 Gasso M, Rubio M, Varela G, Cabre M, Caballeria J, Alonso E, Deulofem R, Camps J, Gimenez A, Pajares M, Pares A, Mato JM, Rodes J. Effects of S-adenosylmethionine on lipid peroxidation and liver fibrogenesis in carbon tetrachloride induced cirrhosis. *J Hepatol*, 1996;25:200-205
- 8 Lin TJ, Liu GT. Protective effect of salvianolic acid A on heart and liver mitochondria injury induced by oxygen radicals in rats. *Zhongguo Yaolixue Yu Dulixue Zazhi*, 1991;5:276-281

Edited by You DY
proofread by Sun SM

Kupffer cell and apoptosis in experimental HCC

Hai Zhen Zhu, You Bing Ruan, Zhong Bi Wu and Chun Ming Zhang

Subject headings liver noplasm, experimental; diethylnitrosamine; apoptosis; protein P53; Kupffer's cell

Zhu HZ, Ruan YB, Wu ZB, Zhang CM. Kupffer cell and apoptosis in experimental HCC. *World J Gastroentero*, 2000;6(3):405-407

INTRODUCTION

Our previous study has proved that Kupffer cells may have an inhibitory effect on the process of hepatocarcinogenesis^[1], however, their inhibitory mechanism needs exploring deeply. We performed a comparative study on the expression of PCNA, Bax, P53 and apoptosis of liver cancer cells using immunohistochemical technology and terminal deoxynucleotidyl transferase (TdT)-mediated dUTP-digoxigenin nick end labeling (TUNEL) in the diethylnitrosamine-induced hepatocellular carcinoma (HCC) in rats with or without pretreatment with gadolinium chloride or zymosan which might effectively block or enhance the activity of Kupffer cells in order to know the role of Kupffer cells in apoptosis in the experimental HCC and explore further the inhibitory mechanism of Kupffer cells on the process of hepatocarcinogenesis.

MATERIALS AND METHODS

Establishment of animal models and pathological examination

One hundred and forty male Sprague-Dawley rats were divided into six groups. ① DENA group, 40 rats received diethylnitrosamine (DENA) at a dose of 70 mg/kg in distilled water once/wk till wk15. ② GC+DENA group, gadolinium chloride was injected iv at a dose of 10 mg/kg once 2 wk to suppress Kupffer cells in 40 rats till wk15 and these rats simultaneously received DENA just as DENA group. ③ ZM+DENA group, zymosan was injected iv at a dose of 20 mg/kg once 2 wk to activate Kupffer cells till wk15 and DENA was received just as DENA group. ④ GC group, gadolinium chloride was injected iv at a dose of 10 mg/kg in 0.85% NaCl once 2 wk till wk15. ⑤ ZM group, zymosan

was injected iv at a dose of 20 mg/kg in 0.85 % NaCl once 2 wk till wk15. ⑥ Control group, these rats were maintained on a standard laboratory diet and tap water. All rats were killed at the wk21 of hepatocarcinogenesis. The liver samples were taken, fixed in 40 mL/L paraformaldehyde and embedded in paraffin. Each specimen was cut into 5 µm serial slices, stained with hematoxylin-eosin and subjected to histopathological examination.

Immunohistochemical staining

The SP method was used, the 1st antibody was mouse-anti-human PCNA monoclonal antibody (Calbiochem Co., dilution 1 : 50), rabbit-anti-human Bax (Santa Cruz, dilution 1 : 50) and mouse-anti-human P53 monoclonal antibody (Novocastra Laboratories, dilution 1 : 50). The SP kit was purchased from Boehringer Mannheim, Germany. DAB staining was used. The dark brown staining of nuclei was taken as PCNA and P53-positive reaction. The dark brown granules in cytoplasm were taken as Bax-positive reaction. We used PBS to replace the 1st antibody as negative control.

Terminal deoxynucleotidyl transferase-mediated biotinylated-dutp nick end labeling method (TUNEL method)

In situ Cell Apoptosis Detection kit was purchased from Boehringer Mannheim, Germany. After deparaffinization and rehydration in ethanol, the sections were incubated with 0.2 mol/L HCl for 20 min at room temperature (RT). They were then deproteinized by incubation with 30mg/L proteinase (in 50mM Tris-HCl, pH 8.0; 5mM EDTA) for 30 min at RT. Terminal deoxynucleotidyl transferase (TdT) and biotinylated dUTP in TdT buffer (30mM Trizma base, pH 7.2; 140mM sodium cacodylate; 1mM cobalt chloride) were added to cover the sections, which were then incubated for 60 min in a humid atmosphere at 37°C. The sections then reacted with alkaline phosphatase (ALP) for 30 min at RT. Visualization was carried out with NBT/BCIP. Nuclei with clear blue staining were regarded as positive. TUNEL incubation solution without terminal deoxynucleotidyl transferase was used as negative control.

Proliferating index (PI) and apoptosis index (AI)
PI and AI were determined by Leitz ASM 68K image analyzing system purchased from Germany. Five visual fields (original magnification, 10 × 40)

Department of Ultrastructural Pathology, Tongji Medical University, Wuhan 430030, Hubei Province, China

Dr. Hai Zhen Zhu, graduated from Tongji Medical University in 1997, engaged in the researches of antitumor of Kupffer cell under the instruction of Professor You Bing Ruan, having four papers published.
Correspondence to: Hai Zhen Zhu, Department of Ultrastructural Pathology, Tongji Medical University, Wuhan 430030, Hubei Province, China

Received 2000-01-12 **Accepted** 2000-02-20

from every positive slide would be chosen and the TUNEL and PCNA-positive parenchymal cells as well as the total number of parenchymal cells in the same field would be counted. PI or AI was expressed as the percentage of the number of PCNA or TUNEL-positive parenchymal cells in the total parenchymal cells of the same field.

$$\text{Proliferating index (PI)} = \frac{\text{number of PCNA-positive cells}}{\text{number of total cells}} \times 100\%$$

$$\text{Apoptosis index (AI)} = \frac{\text{number of TUNEL-positive cells}}{\text{number of total cells}} \times 100\%$$

Statistical analysis

Fisher's exact test, Student's test and Spearman rank correlation were employed.

RESULTS

Macroscopic observation and histopathological examination (at wk 21 of hepatocarcinogenesis)

Neither the control group, nor the GC group and ZM group showed any changes macro and microscopically; on the contrary, the liver surface in DENA group and GC + DENA group were covered with a lot of white nodules. The diameter of the largest nodules was 0.5 cm in DENA group and 2.0 cm in GC+DENA group. These nodules were diagnosed as HCC histologically. Some white grey focal nodules scattered over the liver surface in ZM+DENA group, were also diagnosed as HCC with many apoptotic cells and apoptotic bodies.

Bax staining

Cytoplasm of cancer cells with clear brown staining was regarded as positive (Figure 1). The positive rates of Bax in ZM+DENA group, DENA group and GC+DENA group were 84.6% (11/13), 28.6% (2/7) and 27.3% (3/11) respectively. It was significantly higher in ZM+DENA group than that in DENA group (Fisher's exact test, $P < 0.05$).

P53 staining

A clear brown staining of the nuclei in cancer cells was regarded as positive (Figure 2). The positive rates of P53 in ZM+DENA group, DENA group and GC+DENA group were 76.9% (10/13), 14.3% (1/7) and 36.4% (4/11) respectively. It was markedly higher in ZM+DENA group than that in DENA group (Fisher's exact test, $P < 0.05$).

PCNA staining

Nuclei with clear brown staining were regarded as positive (Figure 3).

No expressions of Bax, P53 and PCNA in the control group, GC group and ZM group were found.

Apoptosis of cancer cells using TUNEL method

Apoptotic cells were observed in DENA group, GC+DENA group and ZM+DENA group by means of TUNEL method. The cells with clear nuclear labeling were defined as TUNEL-positive cells. Apoptotic cells were scattered in the cancer tissue (Figure 4).

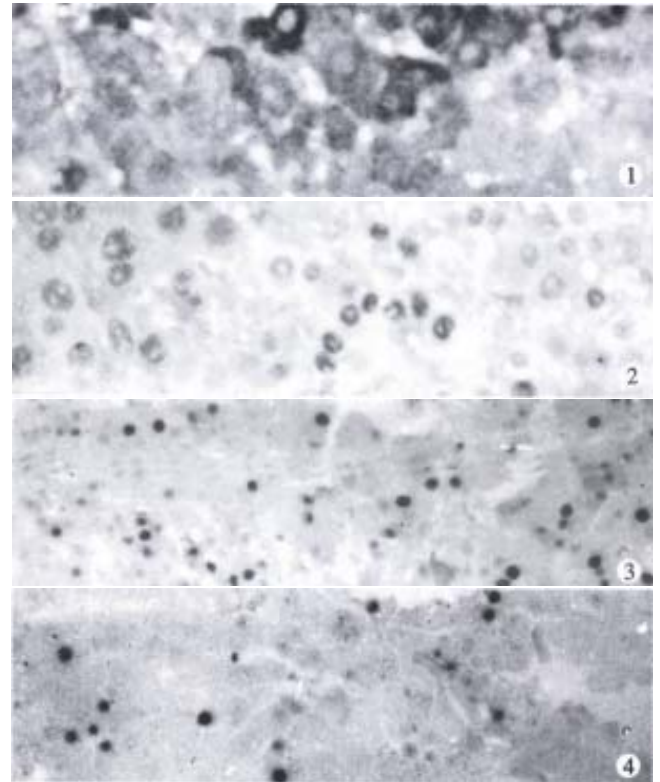


Figure 1 Expression of Bax in rat HCC in ZM+DENA group. SP $\times 400$

Figure 2 Expression of P53 in rat HCC in DENA group. SP $\times 400$

Figure 3 Expression of PCNA in rat HCC in DENA group. SP $\times 200$

Figure 4 Apoptotic cells in rat HCC in ZM+DENA group. TUNEL $\times 200$

Proliferating index (PI) and apoptosis index (AI) (Table 1)

Table 1 PI and AI in ZM+DENA group, DENA group and GC+DENA group

Groups	Number	PI(% , $\bar{x} \pm s$)	AI(% , $\bar{x} \pm s$)	PI/AI
ZM+DENA group	13	15.22 \pm 2.17 ^b	7.53 \pm 1.61 ^b	2.20
DENA group	7	24.97 \pm 2.53	4.36 \pm 1.18	5.73
GC+DENA group	11	38.69 \pm 3.17 ^b	2.52 \pm 0.81 ^b	15.40

^b $P < 0.01$, vs DENA group, Fisher's exact test.

Correlation between apoptosis index, Bax and P53 expression

There was a positive correlation between apoptosis index and Bax or P53 protein reactivity in ZM+DENA group, DENA group and GC+DENA group (Table 2).

Table 2 Correlation between apoptosis index and Bax or P53 expression

Groups	Bax-positive cases/total	AI vs Bax		P53-positive cases/total	AI vs P53	
		r_s	P		r_s	P
ZM+DENA group	11/13	0.63	<0.05	10/13	0.73	<0.05
DENA group	2/7	0.79	<0.05	1/7	0.61	
GC+DENA group	3/11	0.74	<0.01	4/11	0.82	<0.05

Spearman rank correlation.

DISCUSSION

Gadolinium chloride is believed to be a specific suppressor of Kupffer cells^[1,2]. Zymosan is an immunopotentiator and may be used to activate Kupffer cells^[3]. We performed a comparative study on apoptosis in DENA-induced hepatocellular carcinoma in rats with or without pretreatment with gadolinium chloride or zymosan which might effectively block or enhance the activity of Kupffer cells in order to clarify whether the Kupffer cells play a role in apoptosis of the experimental hepatocarcinogenesis or not.

Proliferating cell nuclear antigen (PCNA) is an auxiliary protein of DNA polymerase- δ . It accumulates little in the resting stage cell, but prominently in the nuclei of proliferating cells during G₁-late phase and S-phase and decreases in G₂-phase and M-phase. It is associated with cell proliferation and regarded as a biological marker for cell proliferation^[4]. Bax is a 21 000 protein with extensive amino acid homology with Bcl-2. This protein has been shown to form heterodimers with apoptosis inhibiting protein, Bcl₂, so it can induce cell apoptosis^[5]. When DNA is injured by toxicant, wild-type p53 drives cell to G₁ and arrests or inhibits cell proliferation until DNA is repaired. When nuclear DNA is badly damaged or cannot be repaired, wild-type p53 induces transcription of apoptotic genes and drives the cell to be in apoptosis^[6]. Gottlieb *et al*^[7] thought that overexpression of P53 was related to cell apoptosis. Zhao *et al*^[8] observed that there was a positive correlation between apoptosis index and P53 protein, and supported the role of P53 in regulating apoptosis in human HCC. The positive correlation between apoptosis index and P53 protein immunoreactivity observed in our study also supports these findings. A new method to detect apoptosis *in situ*, terminal deoxynucleotidyl transferase-mediated (TdT) dUTP-digoxigenin nick end labeling (TUNEL) was recently developed by Gavrieli *et al*^[9], and was applied to detect cell apoptosis of human HCC and other tumors^[10].

Our results showed that the positive rates of Bax and P53 protein were markedly higher in ZM +

DENA group than in DENA group with significant differences. Proliferating index and apoptosis index respectively increased or decreased in ZM+DENA group, DENA group and GC+DENA group successively. These results demonstrated that the blockage of Kupffer cells with gadolinium chloride might suppress cell apoptosis and the activation of Kupffer cells with zymosan might promote cell apoptosis in the experimental hepatocarcinogenesis.

One of the characteristic features of cancer is the continuous growth and the ratio of cell proliferation and cell apoptosis determine the fate of tumor growth^[11-13]. In normal tissues, apoptosis is an efficient way of eliminating transformed cells. However, inability of cells to undergo apoptosis may advance their development, both by allowing the accumulation of dividing cells and by impairing the elimination of genetic mutants that may harbor malignant potential^[11,12]. Our results proved that Kupffer cells could promote apoptosis in the experimental hepatocarcinogenesis and revealed further that they played an inhibitory role in hepatocarcinogenesis through inducing apoptosis of tumor cells.

REFERENCES

- 1 Zhu HZ, Ruan YB, Wu ZB, Ivankovic S. The influence of Kupffer cells on experimental hepatocarcinogenesis. *Zhonghua Binglixue Zazhi*, 1998;27:102-104
- 2 Kukan M, Vajdova K, Horecky J, Nagyova A, Mehendale HM, Trnovec T. Effects of blockade of Kupffer cells by gadolinium chloride on hepatobiliary function in cold ischemia reperfusion injury of rat liver. *Hepatology*, 1997;26:1250-1257
- 3 Decker K. Biologically active products of stimulated liver macrophages (Kupffer cells). *Eur J Biochem*, 1990;192:245-261
- 4 Celis JE, Celis A. Cell cycle dependent variations in the distribution of the nuclear protein cyclin proliferating cell nuclear antigen in cultured cells: Subdivision of S phase. *Proc Natl Acad Sci USA*, 1985;82:3262-3266
- 5 Hung WC, Chuang LY. Induction of apoptosis by sphingosine-1-phosphate in human hepatoma cells is associated with enhanced expression of bax gene product. *Biochem Biophys Res Commun*, 1996;229:11-15
- 6 Mitry RR, Sarraf CE, Wu CG, Pignatelli M, Habib NA. Wild type p53 induces apoptosis in Hep3B through up regulation of Bax expression. *Lab Invest*, 1997;77:369-378
- 7 Gottlieb TM, Oren M. p53 in growth control and neoplasia. *Biochim Biophys Acta*, 1996;1287:77-102
- 8 Zhao M, Zimmermann A. Apoptosis in human hepatocellular carcinoma and in liver cell dysplasia is correlated with p53 protein immunoreactivity. *J Clin Pathol*, 1997;50:394-400
- 9 Gavrieli Y, Sherman Y, Ben Sasson SA. Identification of programmed cell death *in situ* via specific labeling of nuclear DNA fragmentation. *J Cell Biol*, 1992;119:493-501
- 10 Hino N, Higashi T, Nouse K, Nakatsukasa H, Tsuji T. Apoptosis and proliferation of human hepatocellular carcinoma. *Liver*, 1996;16:123-129
- 11 Carson DA, Ribeiro JM. Apoptosis and disease. *Lancet*, 1993;341:1251-1254
- 12 Rotello RJ, Lieberman RC, Purchio AF, Gerschenson LE. Coordinated regulation of apoptosis and cell proliferation by transforming growth factor β 1 in cultured uterine epithelial cells. *Proc Natl Acad Sci USA*, 1991;88:3412-3415
- 13 Williams GT. Programmed cell death: apoptosis and oncogenesis. *Cell*, 1991;65:1097-1098

Clinical significance of serum intercellular adhesion molecule-1 detection in patients with hepatocellular carcinoma

Ming Hui Mei¹, Jing Xu¹, Qin Fen Shi², Jing Hong Yang¹, Qian Chen¹ and Li Ling Qin²

Subject headings carcinoma, hepatocellular/diagnosis; intercellular adhesion molecule-1; liver neoplasms/diagnosis; alpha-fetoprotein

Mei MH, Xu J, Shi QF, Yang JH, Chen Q, Qin LL. Clinical significance of serum intercellular adhesion molecule-1 detection in patients with hepatocellular carcinoma. *World J Gastroentero*, 2000;6(3):408-410

INTRODUCTION

Since the late 1980s, studies on the expression of intercellular adhesion molecule-1 (ICAM-1) in patients with malignancies have demonstrated that ICAM-1 may strongly express in two forms in such diseases: membranous one on the surface of tumor cells (membrane-bound ICAM-1) and soluble one in circulation (soluble ICAM-1, sICAM-1)^[1,2]. Furthermore, increased expression of sICAM-1 in various malignant diseases, such as gastric cancer, colonic and pancreatic cancer was reported by Tsujisaki *et al*^[3], who found that the incidence of positivity of sICAM-1 in the malignant diseases was significantly higher than that in benign diseases. Therefore, the diagnostic value of detecting sICAM-1 for some malignancies has been proposed^[3]. The recent studies on detecting serum sICAM-1 in patients with hepatocellular carcinoma (HCC) have revealed that serum levels of sICAM-1 were well correlated to progression and prognosis of the disease^[4-6], from which it has been considered that sICAM-1 may be useful for monitoring the response to treatment^[4]. However, whether sICAM-1 is a diagnostic marker is still controversial. Our recent study demonstrated that in HCC patients with normal or low levels of serum α -fetoprotein (AFP) measurement of sICAM-1 is of clinical value for detecting early HCC and its recurrence after hepatectomies^[7-9]. To further evaluate the clinical

significance of measuring sICAM-1 in HCC, the serum levels of sICAM-1 in 134 patients with HCC were examined and the results were analyzed.

MATERIALS AND METHODS

Patients

There were 134 patients with HCC, including 115 males and 19 females, aged from 12-80 years, median 49 years. The diagnosis of HCC for all patients was confirmed pathologically either by surgical resection of liver tumors or by liver biopsies. Tumor was less than 5 cm in diameter in 17 patients, less than 10 cm in 37 and more than 10 cm or with extrahepatic metastasis in 80 cases. Hepatitis B surface antigen (HBsAg) was positive in 112 cases and hepatitis C antibody positive in 10 patients. Surgical treatment was carried out in 68 patients, of whom 57 underwent tumor resection and 11 underwent laparotomy or selective catheterization of the hepatic artery. The rest of the patients were treated by transcatheter arterial embolization (TAE) or alcohol injection of tumors. As controls, serum levels of sICAM-1 were measured in 42 patients with chronic hepatitis B (CH), 40 with liver cirrhosis (LC) and 50 healthy blood donors.

Methods

Blood samples were collected early in the morning. The serum was immediately separated by centrifugation and frozen to -80°C. Concentrations of serum sICAM-1 were measured with an enzyme-linked immunosorbent assay kit (Biosource Europe, Fleurus, Belgium). The quantitative determinations of serum AFP in patients with HCC was done by radio-immunoassay (RIA), using an AFP kit (Jiuding Biological, Tianjin, China). The reference ranges of serum AFP concentration were classified as follows: above 200 µg/L, positive; 20 µg/L-200 µg/L, questionable positive; and below 20 µg/L, negative.

Statistical analysis

Data between groups were compared by Wilcoxon's Rank Sum test and Fisher test. $P < 0.05$ means significance statistically.

RESULTS

The median of sICAM-1 in 134 patients with HCC was 1801 µg/L, which was significantly higher than

¹Department of Hepatobiliary Surgery, ²Institute of Hepatobiliary Surgery, Guilin Medical College, Guilin 541001, Guangxi Province, China
Ming Hui Mei, M.D., graduated from Guangxi Medical College in 1968, from Tongji Medical University as a postgraduate in 1981 and from Hannover Medical University, Germany in 1989, receiving a doctor's degree of medicine, having more than 40 papers published.

Supported by the grants from the Guangxi Science and Technology Committee (No.9817093).

Correspondence to: Dr. Ming Hui Mei, Lequn Road 95, Department of Hepato-Biliary Surgery, Guilin Medical College, 541001 Guilin, PR China

Tel. 0086-773-2824373, Fax. 0086-773-2822194

Email. meimh@gliet.edu.cn

Received 2000-01-03 **Accepted** 2000-02-16

those in patients with CH (median = 462 $\mu\text{g/L}$), LC (median = 587 $\mu\text{g/L}$) and the healthy subjects (median = 305 $\mu\text{g/L}$) (Table 1). The compared analysis of serum levels of sICAM-1 and AFP in the HCC patients was shown in Table 2. Serum AFP concentration was positive in 85 cases, negative in 22 and questionable positive in 27. The serum levels of sICAM-1, in the corresponding patients were 2018, 1370 and 1453 $\mu\text{g/L}$ respectively. A correlated analysis of serum concentrations of AFP and sICAM-1 demonstrated that there was a close correlation between the two parameters in patients with AFP positive ($r = 0.249$, $P < 0.05$). However, the correlation did not exist in patients with AFP negative or questionable positive. Although the serum concentrations of AFP in these two groups of patients were normal or in a low level, that of sICAM-1 in these patients all exceeded 1000 $\mu\text{g/L}$, the median values of which showed no significant difference compared with the median of the whole group of HCC patients ($P > 0.05$). The ranges of serum levels of sICAM-1 in the patients with HCC are shown in Table 3. One hundred and seven patients (80%) had a sICAM-1 level higher than 1000 $\mu\text{g/L}$ and 126 (94%) higher than 700 $\mu\text{g/L}$. There was no close correlation between the serum value of sICAM-1 and the tumor size among 134 patients with HCC (Table 4). The medians of serum levels of sICAM-1 in patients with different sizes of tumor showed no significant difference ($P > 0.05$).

Table 1 Concentrations of serum sICAM-1 in patients with HCC and control groups

Group	Number of patients	sICAM-1 ($\mu\text{g/L}$) ^a
Normal control	50	305
CH	42	462
LC	40	587
HCC	134	1801 ^b

a median $P < 0.01$ vs compared with other groups; ^b $P < 0.01$ vs other groups each.

Table 2 Comparative analysis of serum levels of sICAM-1 and AFP in HCC patients

Group	Number of patients	sICAM-1 ($\mu\text{g/L}$) [*]	AFP ($\mu\text{g/L}$) [*]
AFP < 20 $\mu\text{g/L}$	22	1370	11
AFP 20-200 $\mu\text{g/L}$	27	1453	89
AFP > 200 $\mu\text{g/L}$	85	2018	31610

^{*}median.

Table 3 Ranges of serum sICAM-1 concentration in 134 patients with HCC

sICAM-1 ($\mu\text{g/L}$)	Number of patients	(%)
330-690	8	6
700-990	19	14
1000-1990	72	54
> 2000	35	26

Table 4 Serum concentrations of sICAM-1 and tumor size in 134 patients with HCC

Tumor size in diameter (cm)	sICAM-1 ($\mu\text{g/L}$) ^a	Number of patients
≤ 5	1518 ^b	17
< 10	1769	37
> 10	1897	80

a median; ^b $P > 0.05$ vs others groups each.

DISCUSSION

One obvious phenomenon from the present study was that a much higher level of sICAM-1 was observed in our HCC patients than those reported by the others [4,6,12]. According to the following researches, we may explain the discrepancies: It has been known that ICAM-1 expression can be upregulated by several cytokines [10,11], of which interferon-gamma (INF-gamma) was the main cytokine trigger for ICAM-1 expression in a human hepatoplastoma cell line. In addition, hepatitis B virus-DNA-transfected cells expressed membranous ICAM-1, the triggering mechanisms of which may be gene activation by virus genome or autocrine virus-induced hepatocellular cytokine production. Furthermore, the clinical research of relationship between serum levels of sICAM-1 and HCC showed that the high levels of sICAM-1 were closely related to the progression and prognosis of HCC [4,6,12]. In this study, the rate of hepatitis B infection was 84% (112/134) and 87% of the patients were in the middle or late stage of HCC (117/134). Thus it can be seen from our study that a high infectious rate of hepatitis B and a delayed diagnosis of HCC in this group of patients may be the main reasons for the high expression of serum levels of sICAM-1.

However, with regards to the study on sICAM-1 and HCC, one more important point, which is still controversial and to be resolved is whether detecting sICAM-1 in patients with HCC is of clinical significance for early diagnosing the disease and detecting its recurrence after surgical resection. As the study results by Hyodo *et al.* [4] showed that there was no difference in serum levels of sICAM-1 between their patients with HCC and liver cirrhosis. Based on this they declared that sICAM-1 is only a marker for progression and prognosis of the disease, but not a diagnostic marker for HCC. However, this conclusion was at odds with the observations from other reports [6,8,12], in which significantly higher serum levels of sICAM-1 in patients with HCC than those with LC, HC and healthy controls were demonstrated. The results of present study by the authors further confirmed the observations.

Moreover, the following results from the literatures seem to be more useful to resolve the controversial problem: enhanced expression of ICAM-1 on HCC cell surface exists in most patients with HCC (ranged from 80% to 96.2%) [5,13], which did not exist in peritumor and normal liver tissues. Regarding the association between membranous and soluble ICAM-1 expression, a highly consistent expression rate of the two forms of ICAM-1 was reported by Momosaki *et al.* [5]. They found that in tumor lines, the consistent expression rate of the two forms ICAM-1 was 87.5% (present or absent concomitantly). There were two forms of sICAM-1 in HCC patients: inflammation-associated sICAM-1 and HCC-specific circulating form of sICAM-1. The latter mainly came from HCC cells,

from which the membranous ICAM-1 were shed into the circulation continuously and became the important source of sICAM-1^[14]. In addition, recent studies by the authors^[9] found that regardless of positive or negative serum AFP, after a radical resection of liver tumor, the sICAM-1 level would be decreased to the normal within 1-2 months postoperatively. However, in patients underwent non-radical resection due to vascular invasions of the liver or extrahepatic metastasis, the serum levels of sICAM-1 will maintain at a high level. It has been suggested from all of the studies mentioned above that the high level of serum sICAM-1 in HCC may originate mainly from tumor itself. Thus we believe sICAM-1 in HCC patients may be a useful marker for detecting HCC and a monitor of recurrence after hepatectomy.

As the strong correlation between serum levels of sICAM-1 and AFP in patients with positive AFP was disclosed (Table 2), the clinical significance of sICAM-1 detection for diagnosing HCC will be focused on patients with normal or low levels of serum AFP. Serum AFP is still the best diagnostic marker for HCC. But AFP levels may be normal in 20%-40% of patients with HCC, depending on the severity of the disease^[15]. In China about 30% of HCC patients can not be diagnosed by this serum marker, which results in delayed diagnosis and, consequently, hampers efforts to improve effective surgical treatment of the disease. Therefore, more sensitive serum markers are required for detecting HCC.

From the study, one of the interesting results was that there were 22 (16.4%) and 27 (20.2%) patients with HCC, whose serum levels of AFP were negative (median = 11 µg/L) and questionable positive (median = 89 µg/L). However, that of sICAM-1 in those patients were 1370 and 1453 µg/L respectively (Table 2), which showed no significant difference compared with the median level of total group of HCC ($P>0.05$). Furthermore, analysis of ranges of sICAM-1 levels in patients with HCC demonstrated that 80% of the patients had a high serum level of sICAM-1 exceeding 1000 µg/L. According to the study by Shimizu *et al*^[6], sICAM-1 level above 1000 µg/L is a determinant for prognosis and progression of HCC, the proportion of patients with high levels of sICAM-1 (>1000 µg/L) in patients with HCC in our study was obviously higher than that of AFP (>200 µg/L). As mentioned in our previous studies the diagnosis of HCC should be strongly suspected when a patient with an uncertain intrahepatic lesion had a serum level of sICAM-1 higher than 1000 µg/L^[7]. The results of the present study further confirm our previous conclusion.

Another interesting finding from the study was

that a significant correlation between serum level of sICAM-1 and tumor size of HCC was not observed (Table 4). The median of sICAM-1 concentration in 17 patients with tumor diameter less than 5 cm was 1518 µg/L, among them 4 being negative, 8 questionable positive and 5 positive for AFP. In addition, a tumor recurrence was diagnosed in 4 of the 17 patients after 1-3 hepatectomies during the postoperative follow-up. The median of tumor size in the 4 cases was only 2.8 cm when recurrence was confirmed, however, the median of serum level of sICAM-1 in the same patients was 1378 µg/L. It was strongly suggested by our observation that measurement of sICAM-1 is of clinical significance in detecting early HCC and monitoring its recurrence postoperatively when tumor is small in diameter, particularly for patients with normal or low serum concentrations of AFP.

ACKNOWLEDGMENTS We are grateful to Professor S. Meuer, and Dr. B. Schraven, Institute of Immunology, Ruprecht-Karls-University, Heidelberg, Germany, for their suggestions, advice, and cooperation in this study.

REFERENCES

- Vogetseder W, Feichtinger H, Schulz TF, Schwaebler W, Tabaczewski P, Mitterer M, Boeck G, Marth C, Dapunt O, Mikuz G, Dierich MP. Expression of 7F7-antigen, a human adhesion molecule identical to intercellular adhesion molecule-1 (ICAM-1) in human carcinomas and their stromal fibroblasts. *Int J Cancer*, 1989;43:768-773
- Rothlein R, Mainolfi EA, Czajkowski M, Marlin SD. A form of circulating ICAM-1 in human serum. *J Immunol*, 1991;147:3788-3793
- Tsujiisaki M, Imai K, Hirata H, Hanzawa Y, Masuya J, Nakano T, Sugiyama T, Matsui M, Hinoda Y, Yachi A. Detection of circulating intercellular adhesion molecule-1 antigen in malignant diseases. *Clin Exp Immunol*, 1991;85:3-8
- Hyodo I, Jinno K, Tanimizu M, Hosokawa Y, Nishikawa Y, Akiyama M, Mandai K, Moriawaki S. Detection of circulating intercellular adhesion molecule-1 in hepatocellular carcinoma. *Int J Cancer*, 1993;55:775-779
- Momosaki S, Yano H, Ogasawara S, Higaki K, Hisaka T, Kojiro M. Expression of intercellular adhesion molecule-1 in human hepatocellular carcinoma. *Hepatology*, 1995;22:1708-1713
- Shimizu Y, Minemura M, Tsukishiro T, Kashu Y, Miyamoto M, Nishimori H, Higuchi K, Watanabe A. Serum concentration of intercellular adhesion molecule-1 in patients with hepatocellular carcinoma is a marker of the disease progression and prognosis. *Hepatology*, 1995;22:525-531
- Mei MH, Xu J, Shi QF, Chen Q, Qin LL. Measurement of serum intercellular adhesion molecule-1 in hepatocellular carcinoma and its clinical significance. *Zhonghua Yixue Zazhi*, 1999;79:200-201
- Mei MH, Xu J, Shi QF, Chen Q, Qin LL. Measurement of serum circulating intercellular adhesion molecule-1 and its clinical significance in hepatocellular carcinoma: preliminary report. *J Hepatobiliary Pancr Surg*, 1999;6:181-185
- Xu J, Mei MH, Shi QF, Chen Q, Qin LL. Clinical evaluation of measurement of serum intercellular adhesion molecule-1 in hepatocellular carcinoma. *Zhonghua Shiyian Waikao Zazhi*, 1998;15:514-515
- Dustin ML, Rothlein R, Bhan AK, Dinarello CA, Springer TA. Induction by IL 1 and interferon-γ: tissue distribution, biochemistry, and function of a natural adherence molecule (ICAM-1). *J Immunology*, 1986;137:245-254
- Zoehrens G, Armbrust T, Pirzer U, Bueschenfelde KHM, Ramadori G. Intercellular adhesion molecule 1 concentration in sera of patients with acute and chronic liver disease: relationship to disease activity and cirrhosis. *Hepatology*, 1993;18:798-802
- Adams DH, Mainolfi E, Burra P, Neuberger JM, Ayres R, Elias E, Rothlein R. Detecting of circulating intercellular adhesion molecule-1 in chronic liver diseases. *Hepatology*, 1992;16:810-814
- Torii A, Harada A, Nakao A, Nonami T, Ito M, Takagi H. Expression of intercellular adhesion molecule 1 in hepatocellular carcinoma. *J Surg Oncol*, 1993;53:239-242
- Hyodo I, Jinno K, Tanimizu M, Doi T, Nishikawa Y, Hosokawa Y, Moriawaki S. Intercellular adhesion molecule-1 release from human hepatocellular carcinoma. *Cancer Detect Prev*, 1996;20:308-315
- Giardina MG, Matarazzo M, Variale A, Morante R, Napoli A, Martino R. Serum Alpha-L-Fucosidase: a useful marker in the diagnosis of hepatocellular carcinoma. *Cancer*, 1992;70:1044-1048

Edited by You DY
proofread by Sun SM

Polymorphism of p16INK4a gene and rare mutation of p15INK4b gene exon2 in primary hepatocarcinoma

Yang Qin¹, Bo Li², Yong Shu Tan³, Zhi Lin Sun¹, Feng Qiong Zuo¹ and Ze Fang Sun¹

Subject headings p16INK4a gene; p15INK4b gene; polymorphism; mutation; hepatocarcinoma

Qin Y, Li B, Tan YS, Sun ZL, Zuo FQ, Sun ZF. Polymorphism of p16INK4a gene and rare mutation of p15INK4b gene exon2 in primary hepatocarcinoma. *World J Gastroentero*, 2000;6(3):411-414

INTRODUCTION

Hepatocellular carcinoma (HCC) is the most common cause of death from cancer in China. The mechanisms of hepatocarcinogenesis are not yet known clearly. p16INK4a gene, the multiple tumor suppressor gene 1 (MTS1), encodes P16 protein, which acts as an inhibitor by binding directly to CDK4 and CDK6 and preventing its association with a cyclin. It was supposed to exert negative control on cell proliferation. p15INK4b gene, multiple tumor suppressor gene 2 (MTS2), is a homologue of p16INK4a and has a similar role in control of cell proliferation. Both of them were mapped to chromosome 9p21 region^[1,2]. Although deletion or mutation of p16INK4a occurred in melanoma, biliary tract cancers, gastric carcinoma, hepatocarcinoma, and alterations of p15INK4b were shown in primary lung cancers, acute leukemia, biliary tract cancers and bladder tumors, there has been no report about whether p15INK4b gene altered in primary hepatocellular carcinoma^[3-9]. In the present study, exon 1, exon 2, exon 3 of p16INK4a and p15INK4b exon 2 in 35 HCC, 35 corresponding adjacent noncancerous liver

cirrhosis were analyzed for somatic mutation with PCR-SSCP and one case of aberrant SSCP DNA was cloned and sequenced.

MATERIALS AND METHODS

Specimens and extraction

Tissue specimens used in the study were paraffin embedded and stored in Department of Pathology, the First Affiliated Hospital, West China University of Medical Sciences from 1991-1993. The 35 samples of human primary hepatocarcinoma and 35 corresponding adjacent noncancerous liver cirrhosis were stained with HE and examined under microscope. More than 70% sections used in PCR were hepatocarcinoma sections. And more than 80% cirrhosis sections were the noncancerous liver cirrhosis sections. DNA was extracted from 1-3 sections (10 µm) of paraffin embedded tissue blocks with xylene, ethanol and phenol method, and dissolved in 50 µL of distilled water^[10]. Ten samples of normal human blood DNA were extracted with standard method. The concentration of DNA was determined with spectrophotometer.

PCR

The exons of p16INK4a gene and exon 2 of p15INK4b gene were amplified using the following primers (Table 1):

Table 1 Primers for p16INK4a and p15INK4b genes analysis

Gene	Primers	Fragment length (bp)	Ref
P16INK4a exon1	5'GGGAGCAGCATGGAGCCCC 3'(sense) 5'AGTCGCCCGCCATCCCCT 3'(antisense)	204	[6]
p16INK4a intron1	5'GGAAATTGGAAGCTGGAAGC 3'(sense)	168	[1]
and exon2	5'GCTGCCCATCATCATGACCT 3'(antisense)		
p16INK4a exon2	5'GGCAGGTCATGATGATGGGC 3'(sense)	362	[1]
and exon3	5'TCTGAGCTTTGGAAGCTCT 3'(antisense)		
P15INK4b exon2	5'GGCCGGCATCTCCATACCTG 3'(sense) 5'TGTGGGGCGGTGGGAACCTG 3'(antisense)	345	[9]

The PCR reaction was performed as follows: 200 ng DNA from paraffin embedded tissue or 100 ng DNA from normal human blood cells, 200 µmol/L each dATP, dGTP, dCTP and dTTP, 20 pmol primers, 1.5 u of Taq DNA polymerase (Sino-American Biotechnology Company) with a buffer provided by the manufacturer, in a total

¹Institute of Biochemistry and Molecular Biology, West China University of Medical Sciences, Chengdu 610041, Sichuan Province, China

²Department of General Surgery, The First Affiliated Hospital, West China University of Medical Sciences, Chengdu 610041, Sichuan Province, China

³Department of Pathology, The First Affiliated Hospital, West China University of Medical Sciences, Chengdu 610041, Sichuan Province, China

Dr. Yang Qin, graduated from Beijing Medical University as a postgraduate in 1987, associate professor of Institute of Biochemistry and Molecular Biology, West China University of Medical Sciences, as a research fellow supported by Wellcome Trust Fellowship, in MRC Virology Unit, Institute of Virology, Glasgow University in UK during 1993-1994 and as a research fellow in Virology Laboratory, School of Medicine, Catholic University of Louvain in Belgium between 1994 - 1995, majoring in molecular biology of cancer and molecular virology, having 21 papers published.

Project supported by the National Natural Science Foundation of China, No. 39670702

Correspondence to: Dr. Yang Qin, Institute of Biochemistry and Molecular Biology, West China University of Medical Sciences, Chengdu 610041, Sichuan Province, China

Received 2000-01-30 **Accepted** 2000-3-14

reaction volume of 25 μ L. The thermal cycle profile was 1min at 94°C, 1min at 66°C (p16 exon 1, 204 bp) or 57°C (p16 exon 2, 168 bp) or 55°C (p16 exon 2, exon 3, 362 bp) or 68°C (p15 exon 2), 2 min at 72°C, 40 cycles. The PCR reaction mixture for p16INK4a exon1 (204 bp) exon 2 and exon 3 (362 bp) contained 5% dimethyl sulfoxide.

SSCP

PCR products were directly subjected to silver-staining SSCP analysis according to the method of Peng *et al*^[11]. Ten μ L of PCR products were denatured in 30 μ L of 98% formamide, 10 mmol/L NaOH, 20 mmol/L EDTA, 0.05% (w/v) bromophenol blue and 0.05% (w/v) xylene cyanol, at 98°C for 5 min. The samples were immediately loaded on an 8% polyacrylamide gel and run at 1.25v/cm in 1 \times TBE in 4°C for approximately 14h. Ten μ L of PCR products of p16INK4a exon 2 and exon 3 (362 bp) was digested with *Sma* I. It generated two fragments (114 bp, 248 bp) which were then subjected to SSCP analysis. After electrophoresis, the gels were fixed, and stained with silver.

PCR cloning and sequencing

The gels were stained with silver. The staining was stopped by immersing the gel in 5% acetic acid, 16% methyl alcohol for 30 min. The gel was rinsed for 1 h in distilled water (changed each 5 min). The abnormal migration single strand DNA band of p15INK4b exon 2 was cut from gel and put into the same volume of distilled water. The gels were incubated in 37°C water bath for 4 h, centrifuged at 10 000r/min for 5 min, then the gel was discarded. The supernatant was extracted with phenol/chloroform, and chloroform. The DNA from approximately 90 mg gel was placed in the PCR mixture for amplification under the same conditions as the initial PCR.

Following reamplification by PCR, the PCR products were isolated on 1.8% agarose gel. The 345 bp DNA band was cut from the gel and purified with Glassmilk Isolation Kit (made in our Lab). The DNA was blunted and phosphorylated with *E.coli*- Klenow fragment and *T*₄ polynucleotide kinase, ligated to *Sma* I site of pUC118. The ligation reaction was transformed into *E.coli*- JM109. The recombinants were screened by minipreparation of plasmid and digesting with restriction endonuclease. The DNA from the clone was screened by PCR-SSCP to identify the clone containing the shift single strand and was sequenced on a ABI 377 DNA sequencer by CyberSyn BJ. Company.

RESULTS

Polymorphism of the p16INK4a gene intron 1 and exon 2

Mutation of p16INK4a gene was analyzed in 31 of

the 35 patients with HCC and 8 healthy blood donors. The PCR amplified 168 bp fragment of p16INK4a intron 1 and exon 2 containing 15 nucleotides within exon 2 and 153 nucleotides of its 5' flanking sequence within intron 1. Three patterns (A, B, B') of p16INK4a intron 1 and exon 2 (168 bp) at SSCP analysis were observed in hepatocellular carcinoma and corresponding adjacent noncancerous cirrhosis (Figure 1). The B pattern (48%, 15/31) outnumbered the B' pattern (26%, 8/31). A pattern was the least (13%, 3/31). Two patterns (B, B') at SSCP analysis were observed in healthy human blood cells. The B' pattern (62.5%, 5/8) outnumbered the B pattern (37.3%, 3/8). The PCR amplified 362 bp fragment covered exon 2, exon 3 and intron 2 sequences. The PCR products were cleaved into two fragments 114 bp and 248 bp by digesting with *Sma* I. Neither band shift nor polymorphism at SSCP analysis was observed. The PCR amplified 204 bp fragment containing exon 1 and 19 nucleotides of 5' flanking upstream sequence and 41 nucleotides of 3' flanking downstream sequence. No band shift was detected in all of the samples.

SSCP analysis of p15INK4b exon 2

A 345 bp fragment containing p15INK4 b gene exon 2 and 60 nucleotides of its 5' flanking sequence within intron 1 was amplified by PCR from all of the hepatocellular carcinomas, adjacent noncancerous cirrhosis and normal blood cells. No evidence of allele deletion was detected (Figure 2). On repeating SSCP analysis, one case of adjacent noncancerous cirrhosis showed an abnormal migration single strand (Figure 3). But no additional shift band was found in either the corresponding tumor tissue from the same patient or the other hepatocarcinoma and cirrhosis tissues. The identical migration single strand was detected in all of the 10 normal human blood cells. No evidence of polymorphism was found.

Cloning and sequencing of the abnormal single strand

The abnormal migration single strand DNA of C₅ (adjacent noncancerous cirrhosis) was purified and cloned in *Sma* I site of pUC118. The recombinant plasmid, pP15E₂, containing the p15INK4a exon 2 insert, was selected after minipreparation. The restriction endonuclease map analysis by *Hind*-III, *Eco*R I, *Bgl*II revealed that pP15E₂ plasmid contained a 345 bp insert (Figure 4) and the insert was placed in antisense orientation. PCR-SSCP analysis of the pP15E₂ showed an identical abnormal migration single strand with that of C₅ (Data not shown). Sequencing analysis of the insert of pP15E₂ indicated that its sequence was identical to that of p15INK4b exon 2 and its upstream 60 nucleotides reported by Kamb (Figure 5).

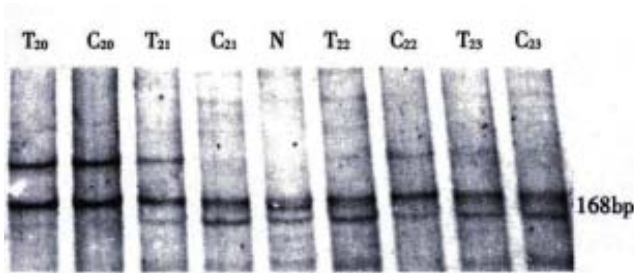


Figure 1 PCR-SSCP analysis of p16 gene intron 1 and exon 2. At the SSCP analysis T₂₀ and C₂₀ showed as A pattern; T₂₃ and C₂₃ showed as B pattern; T₂₁ and C₂₁ showed as B' and B pattern, respectively; T₂₂ and C₂₂ showed as B and B' pattern, respectively. T = Human hepatocarcinoma; C = Adjacent non-cancerous liver cirrhosis; N = Normal human leucocyte

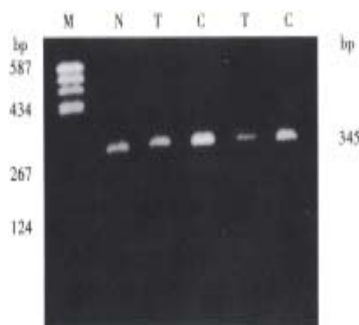


Figure 2 PCR product analysis of p15 gene exon 2 in human hepatocarcinoma on agarose gel. M = pBR322/Hea III; N = Normal human leucocyte; T = Human hepatocarcinoma; C = Adjacent non-cancerous liver cirrhosis

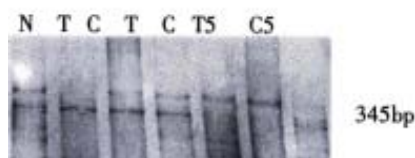


Figure 3 PCR-SSCP analysis of p15 gene exon 2. N = Normal human leucocyte; T = Human hepatocarcinoma; C = Adjacent non-cancerous liver cirrhosis

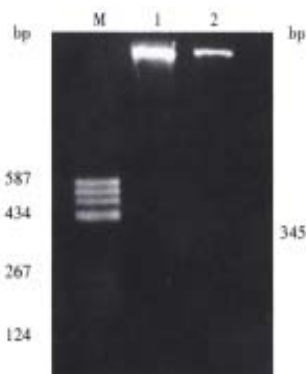


Figure 4 Restriction enzyme analysis of recombinant plasmid which contains aberrant single strand of p15 gene exon 2. M = pBR322/Hea III; 1 = Vector (pUC118) digested with *EcoR* I and *Hind* III; 2 = pP15E₂ digested with *EcoR* I and *Hind* III

Figure 5 The sequence of p15 gene exon 2 in pP15E₂ recombinant plasmid.

DISCUSSION

The p16INK4a gene has been confirmed to be a tumor-suppressor gene by the analysis of p16 gene knock-out mice and its abnormalities have been reported in various kinds of primary cancers and cell lines, such as malignant melanomas, gliomas, glioblastomas, and esophageal squamous-cell carcinomas^[1,12-14]. But there have been relatively few studies concerning the alteration of p16INK4a gene in hepatocellular carcinoma. Kita *et al* reported only three (5%) intragenic mutations of p16INK4a in primary HCC^[15]. Chaubert *et al* found four patients carried hemizygous germ-line point mutations of the p16INK4a gene, suggesting the existence of familial HCC involving this gene^[6]. Hui *et al* found higher proportion of HCCs may fail to express p16INK4a at the protein level^[16]. The general conclusion is that alterations of p16INK4a gene are infrequent in HCC. Our study showed polymorphism of p16INK4a intron 1 and exon 2 at SSCP pattern. The A pattern was only presented in HCC patients, not in the healthy blood donors. It is worthy to study whether people with the A pattern has HCC susceptibility. Five patients showed different SSCP patterns in tumor and noncancerous cirrhosis, most of which (4/5) occurred in large HCC (no statistical significance was revealed). It suggested that intragenic mutation may occur during the progression of HCC, and advanced HCC, but not in the early stages of HCC.

There is argument on whether the inactivation of p15INK4b contributes to the carcinogenesis. Okamoto *et al* observed that non-small-cell lung cancer showed homozygous deletions of p15INK4b (23%), somatic mutation (12%) in exon 2, G→A and C→A polymorphism (8%) within the noncoding sequence of 23 nucleotides and 27 nucleotides of 5' of exon 2, respectively. The latter was named 15Int1-27A gene pattern^[7]. But Russin *et al* detected only the 15Int1-27A polymorphism (13%), no mutation in non-small-cell lung cancers^[17]. Sill *et al* reported 15Int1-27A polymorphism (13%), no somatic mutation in 80 acute leukemia^[8]. Orlow *et al* observed deletions of p15INK4b in primary bladder tumors (8%). Yoshida reported no somatic mutation of p15INK4b gene in biliary tract cancers^[4]. The general

consensus is that frequency of mutation of p15INK4b in progression of cancer is very uncommon. In the present study no intragenic mutation of p15INK4b exon 2 was detected. Although one case of adjacent non-cancerous liver cirrhosis showed abnormal migration single strand, the cloning and sequencing of the aberrant SSCP DNA showed the sequence is identical to wild type p15INK4b exon 2 and 60 nucleotides upstream of exon 2^[1]. It suggested that intragenic mutation of p15INK5b exon 2 was an uncommon event in progression of HCC. This result is in agreement to the infrequent mutation of p16INK4a occurring in HCC, and also similar to the studies in AML, bladder cancers and biliary tract cancers^[4,8,9]. Whether the high frequency of p15INK4b somatic mutation in non-small cell lung cancers is related to the different types of tumor deserves further investigation.

REFERENCES

- 1 Kamb A, Gruis NA, Wever-feldhaus J, Liu QY, Harshman K, Tavitigian SV, Stockert E, Day III RS, Johnson BE, Skolnick MH. A cell cycle regulator potentially involved in genesis of many tumor types. *Sciences*, 1994;264:436-440
- 2 Hannon GJ, Beach D. p15INK4B is a potential effector of TGF- β induced cell cycle arrest. *Nature*, 1994;371:257-261
- 3 Nobori T, Miura K, Wu DJ, Lois A, Takabayashi K, Carson DA. Deletions of the cyclin dependent kinase-4 inhibitor gene in multiple human cancers. *Nature*, 1994;368:753-756
- 4 Yoshida S, Todoroki T, Ichikawa Y, Hanai S, Suzuki H, Hori M, Fukao K, Miwa M, Uchida K. Mutations of p16Ink4/CDKN2, p15Ink4B/MTS2 genes in biliary tract cancers. *Cancer Res*, 1995; 55:2756-2760
- 5 Wu MS, Shun CT, Sheu JC, Wang HP, Wang JT, Lee WJ, Chen CJ, Wang TH, Lin JT. Overexpression of mutant p53 and C-erbB-2 proteins and mutations of the p15 and p16 genes in human gastric carcinoma: with respect to histological subtypes and stages. *J Gastroenterol Hepatol*, 1998;13:305-310
- 6 Chaubert P, Gayer R, Zimmermann A, Fontollet C, Stamm B, Bosman F, Shaw P. Germ line mutations of the p16INK4 (MTS1) gene occur in a subset of patients with hepatocellular carcinoma. *Hepatology*, 1997;25:1376-1381
- 7 Okamoto A, Hussain SP, Hagiwara K, Spillare EA, Rusin MR, Demetrick DJ, Serrano M, Hannon GJ, Shiseki M, Zariwala M, Xiong Y, Beach DH. Mutations in the p16INK4/MTS1/CDKN2, p15INK4B/MTS2, and p18 genes in primary and metastatic lung cancer. *Cancer Res*, 1995;55:1448-1451
- 8 Sill H, Aguiar RCT, Schmidt H, Hochhaus A, Goldman JM, Cross NCP. Mutational analysis of the p15 and p16 genes in acute leukemias. *Br J Haematol*, 1996;92:681-6839 Orlow I, Lacombe L, Hannon GJ, Serrano M, Pellicer I, Dalbagni G, Reuter VE, Zhang ZF, Beach D, Cordon-Cardo C. Deletion of the p16 and p15 genes in human bladder tumors. *J Natl Cancer Inst*, 1995;87: 1524-1529
- 10 Wright DK, Manon MM. Sample preparation from paraffin-embedded tissues. In: Michael A Inns Eds. PCR Protocols A Guide to Methods and Applications. *San Diego; Academic Press Inc*, 1992: 153-158
- 11 Peng H, Du M, Ji J, Isaacson PG, Pan L. High-resolution SSCP analysis using polyacrylamide agarose composite gel and a background free silver staining method. *Bio Techniques*, 1995;19:410-414
- 12 Serrano M, Lee HW, Chin L, Cordon-Cardo C, Beach D, Depinho RA. Role of the INK4a locus in tumor suppression and cell mortality. *Cell*, 1996;85:27-37
- 13 Schmidt EE, Ichimura K, Reifemberger G, Collins VP. CDKN2 (p16/MTS1) gene deletion or CDK4 amplification occurs in the majority of glioblastomas. *Cancer Res*, 1994;54:6321-6324
- 14 Mori T, Miura K, Aoki T, Nishihira T, Mori S, Nakamura Y. Frequent somatic mutation of the MTS1/ CDKI (multiple tumor-suppressor/cyclin-dependent kinase 4 inhibitor) gene in esophageal squamous-cell carcinoma. *Cancer Res*, 1994;54:3396-3397
- 15 Kita R, Nishida N, Fukuda Y, Azechi H, Matsuoka Y, Komeda T, Sando T, Nakao K, Ishizaki K. Infrequent alterations of the p16INK4A gene in liver cancer. *Int J Cancer*, 1996;67:176-180
- 16 Hui AM, Sakamoto M, Kanai Y, Ino Y, Gotoh M, Yokota J, Hirohashi S. Inactivation of p16 INK4 in hepatocellular carcinoma. *Hepatology*, 1996;24:575-579
- 17 Rusin MR, Okamoto A, Chorazy M, Czyzewski K, Harasim J, Spillare EA, Hagiwara K, Hussain SP, Xiong Y, Demetrick DJ, Harris CC. Intragenic mutations of the p16INK4, p15 INK4B and p18 genes in primary non-small-cell lung cancers. *Int J Cancer*, 1996;65: 734-739

Edited by Zhu LH
proofread by Sun SM

Computed morphometric analysis and expression of alpha fetoprotein in hepatocellular carcinoma and its related lesion

Li Juan Shen¹, Zong Ji Zhang¹, Yang Ming Ou², Hua Xian Zhang¹, Run Huang¹, Yun He², Min Jie Wang² and Guo Shu Xu²

Subject headings liver neoplasms; carcinoma, hepatocellular; alpha fetoprotein; morphometry

Shen LJ, Zhang ZJ, Ou YM, Zhang HX, Huang R, He Y, Wang MJ, Xu GS. Computed morphometric analysis and expression of alpha fetoprotein in hepatocellular carcinoma and its related lesion. *World J Gastroentero*, 2000;6(3):415-416

INTRODUCTION

Hepatocellular carcinoma (HCC) is closely related with hepatitis and cirrhosis. In order to investigate the pathogenesis and early pathologic diagnosis of HCC, HCC and related lesions were analyzed qualitatively and quantitatively by automatic image analyser and immunohistochemical assay.

MATERIALS AND METHODS

Materials

Specimens obtained from surgical resection, autopsy and needle aspiration biopsy of livers during 1966-1997 were fixed in 10% formalin, embedded in paraffin, made into serial sections, and stained with routine HE. They were divided into seven groups: I. normal liver tissues used as controls (10 cases); II. chronic hepatitis (10 cases); III. chronic hepatitis with early cirrhosis (10 cases); IV. micronodular cirrhosis (13 cases); V. micronodular and macronodular mixed cirrhosis (14 cases); VI. paracancerous cirrhosis (27 cases); VII. HCC (39 cases).

All of the specimens were examined and diagnosed by two pathologists. The diagnosis of hepatitis and cirrhosis was referred to the standard of the Beijing Conference in 1995 and WHO's criteria.

Morphometry

Thirteen morphometric parameters were determined by the automatic image analyser (Type Q-900, Cambridge Company). And the sections were

enlarged 1000 times under light microscope on the screen of monitor. The cells and nuclei in the sections were traced by light pen. The automatic image analyser was used to determine the nucleus area (NA), the coefficient of variation of NA (NACV), the nucleus perimeter (NP), the nucleus diameter (ND), the roundness of nucleus (NR), the average volume of nucleus (NAV), the cell area (CA), the cell perimeter (CP), the cell diameter (CD), the cell roundness (CR) the average volume of cell (CAV), the ratio of area of the nucleocytoplasm (A-N/C), the ratio of volume of the nucleocytoplasm (V-N/C). After 50-100 cells in each section were examined at random, of the data were analysed by variance (q-test) and stepwise discriminational analysis. Then the equation of discriminational function was set up, the results were compared based on the histopathological classification.

Immunohistochemical staining

Mouse monoclonal antibody against human AFP and Immunostain S-P Kit were purchased from Fuzhou Maxim Biotechnical Company. Immunostaining of AFP was performed by the S-P method in each case. The procedures of S-P staining were taken according to the manufacturer's recommendations. The color was developed with diaminobenzidine and hematoxylin. Positive and negative controls were simultaneously used to ensure specificity and reliability of the staining.

RESULTS

Morphometry

The values of nucleus parameters (NA, NP, ND, NAV, A-N/C and V-N/C) increased gradually and those of cell parameters (CA, CP, CD and CAV) decreased gradually in the sequence of chronic hepatitis, cirrhosis without tumor, paracancerous cirrhosis and HCC. The difference was statistically significant between the group of HCC and the other groups without tumor ($P < 0.05$). The values of NACV, NR and CR in all groups varied irregularly. The values of most parameters (NA, NP, ND, CA, CP, CD, CAV, A-N/C and V-N/C) of the paracancerous cirrhosis were in between those of the cirrhosis without tumor and HCC. The difference was statistically significant ($P < 0.05$). The difference of the value of most parameters was not significant among chronic hepatitis with early cirrhosis, micronodular cirrhosis, mixed

¹Department of Pathology, Kunming Medical College, Kunming 650031, China

²Department of Image Analyses, Scientific Experiment Center Yunnan University, Kunming 650091

Dr. Li Juan Shen, graduated from Department of Medicine, Kunming Medical College in 1982, associate professor of pathology, majoring in hepatic pathology, having 15 papers published.

Supported by the Applied and Basic Scientific Research Fund of Yunnan Province, No.94C027Q.

Correspondence to: Dr. Li Juan Shen, Department of Pathology, Kunming Medical College, Kunming 650031, China
Tel. 0086-871-5338845

Received 2000-01-01 **Accepted** 2000-02-26

micronodular and macronodular cirrhosis ($P<0.05$). Results of stepwise discriminational analysis: because the difference of most parameters was not statistically significant among chronic hepatitis with early cirrhosis, micronodular cirrhosis, micronodular and macronodular mixed cirrhosis, the three groups were merged into one cirrhosis group of as a whole. Six of 13 parameters processed by stepwise discriminational analysis were chosen in chronic hepatitis (Y_1), cirrhosis without tumor (Y_2), paracancerous cirrhosis (Y_3) and HCC (Y_4). The equation of discriminational function was setup.

$$Y_1 = -526.540 - 32.768(NP) + 631.477(NR) + 6.046(CP) + 1.887(CA) + 19.264(A-N/C) - 0.016(CAV)$$

$$Y_2 = -453.402 - 29.633(NP) + 590.223(NR) + 5.466(CP) + 1.636(CA) + 17.903(A-N/C) - 0.011(CAV)$$

$$Y_3 = -441.556 - 28.851(NP) + 603.816(NR) + 3.875(CP) + 1.854(CA) + 17.991(A-N/C) - 0.014(CAV)$$

$$Y_4 = -623.687 - 36.878(NP) + 698.493(NR) + 5.217(CP) + 2.074(CA) + 23.555(A-N/C) - 0.011(CAV)$$

Fifty-three specimens had been tested, only one of the chronic hepatitis with early cirrhosis was falsely classified into chronic hepatitis and the general conformation rate was 98.2% to pathologic diagnosis.

Expression of AFP

Immunostaining of AFP was seen in paracancerous cirrhosis and HCC cytoplasms. The positive rates were 33.3% (9/27) and 43.6% (17/39) respectively. The expression of AFP was negative in hepatitis and cirrhosis without tumor. The positive rate of AFP in the paracancerous cirrhosis (33.3%) was significantly higher than in the cirrhosis without tumor (0%, 0/27) ($P<0.01$, $\chi^2 = 10.8$).

DISCUSSION

HCC which is related with hepatitis and cirrhosis, is one of the common malignant tumors in the world. Popper *et al* considered the occurrence of HCC was a multistep process: HBV infection → persistent inflammation → necrosis → regeneration and repair → hyperplasia → HCC. The course had been studied by morphometry and the results showed that the values of parameters of nucleus increased gradually and those of cells decreased gradually. These suggested that HCC was associated closely with hepatitis and cirrhosis, especially paracancerous cirrhosis.

Paracancerous cirrhosis differed essentially from cirrhosis without tumor. Ren *et al*^[1] considered the regenerative nodules in the paracancerous cirrhosis had regenerated more actively than those in the cirrhosis without tumor. Watanabe *et al*^[2] reported that the rate of dysplasia in the paracancerous cirrhosis (25.9%) was higher than that in the cirrhosis without tumor (12%). Dai

et al^[3] reported that some liver cells around the HCC triggered the closed gene to resynthesize AFP. Zhang^[4] reported that the re presented different degrees positive expression of AFP in the host hepatocytes around cancer and hepatocytes non-neoplastic animals in late stage experimental hepatocarcinoma in rats. All the results showed that the carcinogenesis in paracancerous cirrhosis was more liable to occur than in cirrhosis without tumor. We discovered that values of most parameters in the paracancerous cirrhosis were in between those of the cirrhosis without tumor and HCC by morphometry ($P<0.05$). The expression of AFP was positive in the paracancerous cirrhosis and negative in the cirrhosis without tumor ($P<0.01$). Evidently the paracancerous cirrhosis differed from the cirrhosis without tumor in the respect of function and morphology. It is more likely to be precancerous lesion than cirrhosis without tumor. The values of morphometric parameters in cirrhosis without tumor, regardless of early cirrhosis, micronodular cirrhosis or micronodular and macronodular mixed cirrhosis, were not different significantly. It suggested that the cirrhosis without tumor may be the result of regeneration and repair after HBV infection. Therefore, we inferred that the posthepatitis cirrhosis, the result of persistently affecting HBV, should be evolved into "precancerous cirrhosis" similar to paracancerous cirrhosis, and then some of liver cells were selectively developed into HCC in the circumstance suitable for carcinogenesis. The multisteps in the genesis of HCC may be HBV infection—chronic hepatitis—cirrhosis—"precancerous cirrhosis"—HCC. The paracancerous cirrhosis may be a sequential lesion of precancerous cirrhosis. This inference should be verified by further study. Now, since we can not differentiate the precancerous cirrhosis from the cirrhosis without tumor under light microscope, the precancerous cirrhosis was diagnosed merely by morphometry and immunohistochemical method, which suggested that the patient with precancerous cirrhosis would probably suffer from HCC in the near future or they had already suffered from HCC somewhere in the liver. It was significant to diagnose HCC as early as possible, especially by using needle aspiration biopsy of liver, thus to decrease the possibility of missing small HCC (SHCC, diameter ≤ 3 cm).

REFERENCES

- 1 Ren CS, Dai WJ, Zhao HL, Li GQ, Chen H, Wang W. Expression of p21 in hepatocellular carcinoma and liver cirrhosis and its relation with HBV infection. *Zhonghua Binglixue Zazhi*, 1991;20:88-90
- 2 Watanabe S, Okita K, Harada T, Kodama T, Numa Y, Takemoto T, Takahashi T. Morphologic studies of the liver cell dysplasia. *Cancer*, 1983;51:2197-2205
- 3 Dai YM, Yang LS, Mei F, Ni CR. Expression of AFP gene and cytoposition of its antigen protein in hepatocellular carcinoma and the liver cells surrounding tumor. *Zhonghua Yixue Zazhi*, 1989;69:625-629
- 4 Zhang JZ. Carcinohistogenesis and expression of alpha fetoprotein in experimental hepatocarcinoma. *Linchuang Yu Shiyang Binglixue Zazhi*, 1999;15:224-226

The new proof of neuro-endocrine-immune network—expression of islet amyloid polypeptide in plasma cells in gastric mucosa of peptic ulcer patients

Yan Huang¹, Shi Jun Lu², Jing Xia Dong³ and Feng Li³

Subject headings peptic ulcer; plasma cells; gastric mucosa; islet amyloid polypeptide (IAPP); neuro-endocrine-immune network

Huang Y, Lu SJ, Dong JX, Li F. The new proof of neuro-endocrine-immune network—expression of islet amyloid polypeptide in plasma cells in gastric mucosa of peptic ulcer patients. *World J Gastroentero*, 2000;6(3):417-418

INTRODUCTION

Peptic ulcer, as a common disease, seriously affected people's work and life. Its occurrence, development and change have close relationship with the change of people's moods. Animal experiment proved that significant changes occurred in the endocrine system of the gastric ulcer rats^[1]. Recent study also showed that the number of lymphocytes increased markedly in the gastric mucosa of peptic ulcer patients^[2]. All the above indicated that peptic ulcer is closely related neuro-endocrine-immune system. IAPP, a novel islet hormone, not only takes part in the regulation of blood glucose^[3], but also protects gastric mucosa^[4] and regulates gastrointestinal movements^[5]. On the basis of previous studies, we observed the expression change of IAPP and explored the relationship between the endocrine and the immune system in gastric mucosa of peptic ulcer patients, so as to provide morphologic data on the existence of neuro-endocrine-immune network and the changes in peptic ulcer.

MATERIALS AND METHODS

Twenty-one samples, including 6 cases from normal human stomach, 15 cases from gastrectomy of gastric ulcer patients, were collected. The paraffin

sections were prepared as usual. Immunohistochemical PAP method was used to show IAPP-IR cells. Briefly five-micron sections were placed on glass slides deparaffinized in xylene, rinsed in ethanol, and brought to PBS through a series of descending concentration of ethanol; endogenous peroxidase activity was blocked with methanol-H₂O₂ at room temperature for 30 min; rabbit anti-IAPP serum (peninsula, USA) was diluted 1/6000 with PBS, and the sections were incubated overnight at 4 °C. Goat anti-rabbit IgG (Huamei, Beijing) (1/50), peroxidase-anti-peroxidase (Capital Medical University) (1/100) and DAB kit (Zhongshan, Beijing) were used for staining. As the negative control, the primary antiserum was replaced by PBS and other steps were the same as stated above. All the sections were counterstained with Mayer hematoxylin.

RESULTS

The IAPP-IR cell was not observed in the gastric mucosa of normal subject (Figure 1A). In comparison, a great number of plasma cells IAPP-IR were found in the gastric mucosa of peptic ulcer patients (Figure 1B,C). Most of IAPP-IR plasma cells were weak and only a few were strong for IAPP staining (Figure 1D). Of the negative control sections, no immunoreactive product to IAPP was found in plasma cells (Figure 1E).

DISCUSSION

The gastric mucosa, in which there are a lot of neurons, endocrine cells and immunocytes that may interact with each other, is an important field for the study of neuro-endocrine-immune network. It will undoubtedly provide valuable data for the study on this network by exploring the change of immune-endocrine of gastric mucosa of peptic ulcer patients. Based on the observation of T and B lymphocytes which increase obviously in the gastric mucosa of peptic ulcer patients^[2] and the action of IAPP, a novel islet hormone, which inhibits gastric acid secretion^[6] and protects gastric mucosa^[4], we further studied the expression change of IAPP in the gastric mucosa. Unexpectedly, it was found that the plasma cells of gastric mucosa increased in number, moreover most of them expressed IAPP to some degree.

¹Department of Histology and Embryology, ²Department of Pathology, Weifang Medical College, Weifang 261042

³Department of Histology and Embryology, Beijing Medical University, Beijing 100083, China

Dr. Yan Huang, graduated from Beijing Medical University as a Ph.D in 1995, now professor and postgraduate tutor, majoring in neuroendocrine research, having 18 papers published.

Supported by the Foundation of Shandong Educational Committee
Correspondence to: Yan Huang, Department of Histology and Embryology, Weifang Medical College, Weifang 261042, Shandong Province, China

Tel. 0086-536-8271378

Email. yphytyt@wf-public.sd.cninfo.net

Received 2000-01-18 **Accepted** 2000-03-14

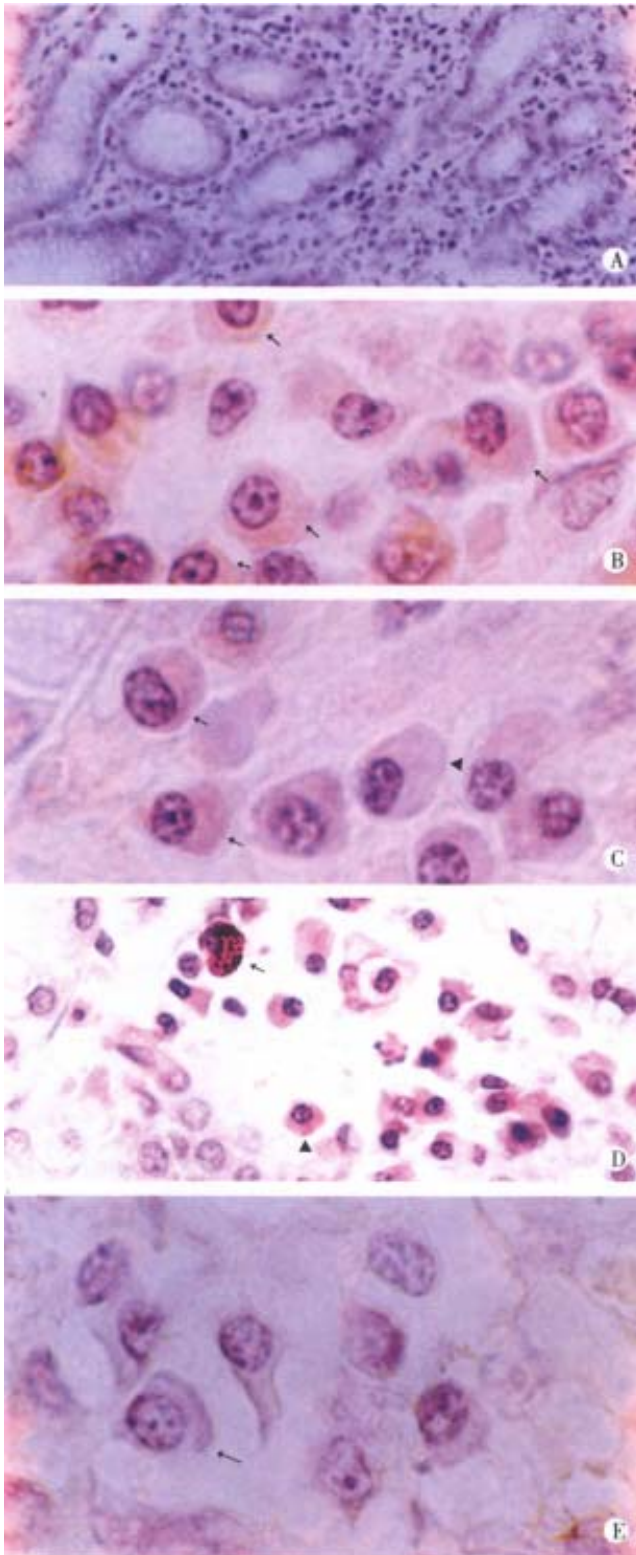


Figure 1 Immunohistochemical PAP method, Mayer Hematoxylin counterstained showing IAPP-IR cells.

A. The gastric mucosa of normal human, no IAPP-IR cell was found. $\times 200$

B-E. The gastric mucosa of peptic ulcer patients.
B. The more IAPP-IR plasma cells (\uparrow). $\times 1000$

C. The weak positive (\uparrow) and negative (\blacktriangle) plasma cells. $\times 1000$

D. The strong (\uparrow) and weak (\blacktriangle) positive IAPP-IR plasma cells. $\times 400$

E. The negative control section in which IAPP antiserum was replaced by PBS. (\uparrow) showing plasma cell. $\times 1000$

Firstly, the specificity of the above findings should be confirmed because there was no IAPP expression in the plasma cells on the negative control sections; and there were also IAPP-IR negative plasma cells around the positive ones. Secondly, the significance of IAPP expression in plasma cells should be studied. IAPP is mainly secreted by islet B cells^[7]. Recent study indicated that besides regulating blood glucose, IAPP could inhibit gastric acid secretion^[4], and protect gastric mucosa^[5]. IAPP-IR cells of islet were markedly increased during the healing process of rat gastric ulcer^[8]. The above-mentioned studies all suggested that IAPP is beneficial to ulcer healing. As it is known, the plasma cells of gastric mucosa come from B lymphocytes and they respond by synthesizing and secreting IgA. It is observed, for the first time, that plasma cells in gastric mucosa of peptic ulcer patients not only increased in the number, but also expressed IAPP. Combined with our previous observation that T and B lymphocytes of gastric mucosa increased in peptic ulcer patients, it is reasonable to infer that some plasma cells in gastric mucosa of peptic ulcer patients may transform to ones expressing IAPP so as to maintain the high level of IAPP in the gastric mucosa and help promote ulcer healing just as a growth factor^[9].

CONCLUSION

It is found, for the first time, that IAPP was expressed in plasma cells of gastric mucosa of peptic ulcer patients, which provides morphologic evidence for the existence of neuro-endocrine-immune network.

REFERENCES

- 1 Zheng ZT. Digestive Ulcer. Beijing: The People's Health Publishing House, 1998:306-325
- 2 Huang Y, Lu SJ, Dong JX, Li F. Changes of T and B lymphocytes in gastric mucosa of peptic ulcer patients. *Shijie Huaren Xiaohua Zazhi*, 1999;7:648
- 3 Ludvik B, Kautzky WA, Prager R, Thomaseth K, Pacini G. Amylin: history and overview. *Diabet Med*, 1997;14(Suppl 2):S9-13
- 4 Clementi G, Caruso A, Cutuli VM, Prato A, de-Bernardis E, Amico-Roxas M. Effect of amylin in various experimental models of gastric ulcer. *Eur J Pharmacol*, 1997;332:209-213
- 5 Gedulin BR, Young AA. Hypoglycemia overrides amylin-mediated regulation of gastric emptying in rats. *Diabetes*, 1998;47:93-97
- 6 Rossowski WJ, Jiang NY, Coy DH. Adrenomedullin, amylin, calcitonin gene-related peptide and their fragments are potent inhibitors of gastric acid secretion in rats. *Eur J Pharmacol*, 1997;336:51-63
- 7 Huang Y, Li ZC, Shi AR. Morphometric study on coexistence of islet amyloid polypeptide with insulin in rat pancreatic islet cells during postnatal development. *Acta Anatomica Sinica*, 1995;26:305-308
- 8 Li ZC, Shi AR. The morphometric study on IAPP-IR cells and Ins-IR cells of islet during the healing process of rat experimental gastric ulcer. *J Beijing Med Univ*, 1995;27:333-335
- 9 Wookey PJ, Tikellis C, Nobes M, Casley D, Cooper ME, Darby IA. Amylin as a growth factor during fetal and postnatal development of the rat kidney. *Kidney Int*, 1998;53:25-30

Edited by Zhu LH
proofread by Sun SM

Effect of gastrectomy on G-cell density and functional activity in dogs

Yu Qiang Chen¹, Wen Hu Guo², Zheng Ming Chen³, Lei Shi³ and Yan Xu Chen²

Subject headings gastrectomy; pylorus; G-cell; gastrin; peptic ulcer/surgery

Chen YQ, Guo WH, Chen ZM, Shi L, Chen YX. Effect of gastrectomy on G-cell density and functional activity in dogs. *World J Gastroentero*, 2000;6(3):419-420

INTRODUCTION

Billroth gastrectomy has some advantages of inhibiting acid secretion, low ulcer recurrence and low mortality. However, postoperative complications, such as dumping syndrome and reflux gastritis, often occurred as a result of pylorotomy^[1]. To minimize these complications, pylorus-preserving gastrectomy (PPG) had been performed for gastric ulcer with satisfied clinical results. Positive correlation was not found between ulcer recurrence and serum gastrin level^[2]. In this study, we performed distal partial gastrectomy with Billroth II anastomosis (DPG-BII), pylorus-preserving gastrectomy (PPG) and highly selective vagotomy (HSV) on dogs and investigated the relationship between different antrum disposal and gastric acid secretion, serum gastrin level and G-cell density and functional activity.

MATERIALS AND METHODS

Eighteen hybrid adult dogs, with body weight ranging from 10 kg to 20 kg, mean weight 13.9 kg, were randomly divided into 3 groups, and underwent PPG, DPG-BII or HSV respectively. In PPG group, antrum was strictly retained within 1.5 cm-2.0 cm and stomach was resected about 40%. DPG-BII, in which stomach was resected about 75%, and HSV were routinely done. After laparotomy biopsy was taken at antrum 2 cm beyond the pyloric sphincter, the first segmental duodenum and jejunum 4 cm beyond Treitz ligamenta, 3 mo after operation, biopsies were done again around the original biopsy sites. Gastric acid secretion was analyzed using neutralization method (subcutaneous injection of tetra-gastrin 4 µg/kg). Fasting and

postprandial serum gastrin levels were measured by radioimmunoassay. The G cell density and its functional activity were determined by immunohistochemical assay using an antigastrin antibody (Zymedco) at a dilution of 1:200 in PBS. G cell density was measured according to the method of Creutzfeldt^[3], in which G cell functional activity was divided into 4 grades, as follows: 1+, brown-red cytoplasm, without granule; 2+, minute brown granules, occupied within 1/3 cytoplasm area; 3+, brown granule or clusters occupied, 1/3-2/3 cytoplasm area; 4+, brown-black granules or clusters, above 2/3 cytoplasm area.

RESULTS

Effects of different operative procedures on gastric acid secretion

In DPG-BII, PPG and HSV groups, preoperative basal acid output (BAO) was 1.80 mmol/h, 2.25 mmol/h and 2.19 mmol/h; maximal acid output (MAO) was 5.19 mmol/h, 4.49 mmol/h and 5.30 mmol/h, respectively; 3 mo after operation, BAO decreased to 0.48 mmol/h, 0.98 mmol/h and 0.97 mmol/h; while MAO decreased to 1.04 mmol/h, 1.76 mmol/h and 1.29 mmol/h, respectively. Gastric acid secretion was significantly suppressed by 56%-80%, which showed that all of the three operations can effectively inhibit gastric acid secretion in dogs (Table 1).

Effects of different operative procedure on serum gastrin level

Pre and post-operative fasting and postprandial serum gastrin levels of DPG-BII, PPG and HSV groups are shown in Table 2. In DPG-BII, post-operative fasting and postprandial serum gastrin levels were significantly decreased ($P<0.05$), the inhibiting rate was 49.7% and 48.4% respectively; while in PPG, serum gastrin levels were slightly decreased with an inhibiting rate of 25.9% and 24.4%; in HSV, post-operative serum gastrin levels were increased by 65.2% and 54.1%, respectively.

Effects of different operative procedure on G cell density and functional activity

Postoperatively, G cell density increased in all sites checked. The increasing rate in duodenum was about 75.0% and 50.0% in antrum or residual antrum (Table 3). The increase in jejunum had no statistical significance.

Stained by immunohistochemical method, G cell was stained in brown color and there were brown-black granules in cytoplasm, which were the products of gastrin acted with its antibody and presented as the index of activity of G cell. If 1+

¹Department of General Surgery, Chinese PLA 174th Hospital, Xiamen 361003, Fujian Province, China

²Department of General Surgery, Chinese PLA Fuzhou General Hospital of Nanjing Command Area, Fuzhou 351003, Fujian Province, China

³State Lab for Tumor Cell Engineering of Xiamen University, Xiamen 361005, Fujian Province, China

Dr. Yu Qiang Chen, Ph.D, graduated from Xiamen University in 1998, now working as a doctor-in-chief in Chinese PLA 174th Hospital, having 10 papers published.

Correspondence to: Dr. Yu Qiang Chen, Department of General Surgery, Chinese PLA 174th Hospital, Xiamen 361003, Fujian Province, China

Tel. 0086-592-2040931, Fax. 0086-592-2040931

Email. chenylq@public.xm.fj.cn

Received 2000-01-05 **Accepted** 2000-02-21

and 2+ grade cell was taken as normal- or hypofunction, while 3+ and 4+ as hyperfunction, the number of grade 3+ and 4+ G cells as a whole constituted 44% and 60% of the total G cells examined in pre and post-operative specimens respectively, and particularly in duodenum the corresponding postoperative rate was 63%. It reveals that no matter what procedure of gastrectomy was performed, the post-operative G cell functional activity, especially in duodenum was enhanced with statistical significance (Table 4).

Table 1 Effects of different operative procedures on gastric acid secretion

Operation	Group	Preoperation (mmol/h)	Postoperation (mmol/h)	Inhibiting rate (%)
DPG-BII	BAO	1.80 ± 0.25	0.48 ± 0.20 ^b	73.7
	MAO	5.19 ± 0.56	1.04 ± 0.19 ^b	80.0
PPG	BAO	2.25 ± 0.27	0.98 ± 0.26 ^a	56.4
	MAO	4.49 ± 0.34	1.76 ± 0.19 ^b	60.7
HSV	BAO	2.19 ± 0.21	0.97 ± 0.26 ^a	55.9
	MAO	5.30 ± 0.14	1.29 ± 0.47 ^b	75.7

^aP<0.05; ^bP<0.01, vs preoperation.

Table 2 Effects of different operative procedure on serum gastrin level

Operation	Group	Pre-operation (ng/L)	Post-operation (ng/L)	Changing rate(%)
DPG-BII	fasting	179 ± 104	90 ± 117 ^a	↓ 49.7
	postprandial	181 ± 86	94 ± 39 ^a	↓ 48.8
PPG	fasting	190 ± 153	144 ± 63	↓ 25.9
	postprandial	239 ± 115	180 ± 47	↓ 24.4
HSV	fasting	100 ± 10	166 ± 75	↑ 65.2
	postprandial	103 ± 48	186 ± 63	↑ 54.1

^aP<0.05, vs preoperation.

Table 3 Effects of different operative procedure on G cell density

Operation	Site	Preoperation (cell/field)	Postoperation (cell/field)	Increasing rate(%)
DPG-BII	Duodenum	23.1 ± 5.0	41.3 ± 4.9 ^b	78.9
	Jejunum	1.1 ± 1.1	3.2 ± 3.0	190.4
PPG	Antrum	66.2 ± 2.1	103.3 ± 18.8 ^a	56.0
	Duodenum	15.6 ± 5.3	27.1 ± 3.6 ^a	74.3
HSV	Jejunum	1.0 ± 4.2	1.1 ± 1.9	11.0
	Antrum	69.8 ± 23.2	103.3 ± 19.3 ^b	47.6
	Duodenum	33.7 ± 15.1	60.1 ± 21.5	78.5
	Jejunum	5.5 ± 3.3	17.3 ± 9.2	218.3

^aP<0.05; ^bP<0.01, vs preoperation.

Table 4 Effects of different operations on G cell function

Operation	Site	Group	1+	2+	3+	4+
DPG-BII	Duodenum	Preoperation	21	142	106	29
		Postoperation	24	73	157	46 ^b
PPG	Antrum	Preoperation	32	136	71	61
		Postoperation	23	115	64	98 ^a
	Duodenum	Preoperation	50	124	81	45
		Postoperation	24	93	117	68 ^b
HSV	Antrum	Preoperation	55	105	84	56
		Postoperation	38	94	73	95 ^a
	Duodenum	Preoperation	67	107	74	52
		Postoperation	24	99	81	96 ^b

^aP<0.05; ^bP<0.01, vs preoperation.

DISCUSSION

According to the theory “no acid, no ulcer”, anti-acid secretion has been the dominant measure in treating peptic ulcer. For suppressing acid secretion, how to treat the antrum has been a much controversial question in general surgery^[4]. Total antrum excision would make the serum gastrin level and gastric acid output lowered, which was accompanied with relatively lower ulcer recurrence; on the other hand, damage of sphincter function resulted in dumping syndrome, reflux gastritis,

dyspepsia and even carcinogenesis of residual stomach^[1]. Under this condition PPG was presented, which not only removed the ulcer lesion and suppressed gastric acid secretion, but also preserved the sphincter function^[5]. Our results showed that all the three procedures can effectively inhibit gastric acid secretion in spite of the different postoperative serum gastrin levels. Clinically, similar results were observed that absolute serum gastrin value of patients were all kept within normal limits, regardless their gastrin level decreased or increased after DPG-BII, PPG or HSV^[2]. This implied that different disposal of antrum did not obviously affect the inhibition of gastric acid secretion.

Gastric acid secretion is a complex physiological process, which was regulated by several factors, such as vagus nerve, G cell, parietal cell and its receptor, some alimentary endocrine substances, gastric mucosal blood supply^[6]. Of them any change may inhibit the gastric and secretion and keep it at lower output level. In addition to regulating acid secretion, gastrin has important effects on nourishment of gastric mucosa and pancreas^[7]. Our results showed that there were many G cells in duodenum and jejunum besides antrum. After operation, the number of G cells in the nongastric tissue increased and their function enhanced, this was not only associated with the gastric acid depletion, but also was demanded by other physiological effects. Therefore it is evidently impossible and unnecessary to eliminate gastrin from serum by operation of peptic ulcer. To some extent, hypergastrinemia subsequent to treatment of peptic ulcer, such as HSV and antacid drugs, is the main determinant of ulcer healing^[8]. It is the key point that how to keep the whole function of sphincter. Fukushima *et al*^[5] has discovered that the length of preserved antrum was closely related to the residual stomach function. In our study, the length of preserved antrum was strictly limited within 1.5 cm to 2.0 cm, vomiting, decline of food intake and loss of body weight were not found postoperatively in the animals which suggested that the function of sphincter had been fairly maintained.

REFERENCES

- 1 Tersmette AC, Giardiello FM, Tytgat GN, Offerhaus GJ. Carcinogenesis after remote peptic ulcer surgery: the long-term prognosis of partial gastrectomy. *Scand J Gastroenterol*, 1995;212(Suppl 1): 96-99
- 2 Sasaki I, Fukushima K, Naito H, Matsuno S, Shiratori T, Maki T. Long-term results of pylorus-preserving gastrectomy for gastric ulcer. *Tohoku J Exp Med*, 1992;168:539-548
- 3 Creutzfeldt W, Arnold R, Creutzfeldt C, Track NS. Mucosal gastrin concentration, molecular forms of gastrin, number and ultrastructure of G-cells in patients with duodenal ulcer. *Gut*, 1976;17: 745-754
- 4 Brody FJ, Trad KS. Comparison of acid reduction in antiulcer operations. *Surg Endosc*, 1997;11:123-125
- 5 Fukushima K, Sasaki I, Naito H, Funayama Y, Kamiyama Y, Takahashi M, Matsuno S. Long-term follow-up study after pylorus preserving gastrectomy for gastric ulcer. *Nippon Geka Gakkai Zasshi*, 1991;92:401-410
- 6 Vakhrushev IaM, Ivanov LA. Changes in gastric secretory function in peptic ulcer patients after gastric resection. *Terapevt Arkh*, 1991;63:14-16
- 7 Halter F, Wilder Smith CH. Gastrin: friend or foe of peptic ulcer? *J Clin Gastroenterol*, 1991;13(Suppl 1):S75-82
- 8 Jones DB, Howden CW, Burget DW, Kerr GD, Hunt RH. Acid suppression in duodenal ulcer: a meta-analysis to define optimal dosing with antisecretory drugs. *Gut*, 1987;28:1120-1127

Edited by You DY
proofread by Sun SM

Enzymohistochemical study on burn effect on rat intestinal NOS

Qiu Gui Wang, Li Ya He, Ye Wen Chen and Song Lin Hu

Subject headings nitric oxide; burn; intestines; superoxide dismutase; MDA; GSH-PX

Wang QG, He LY, Chen YW, Hu SL. Enzymohistochemical study on burn effect on rat intestinal NOS. *World J Gastroentero*, 2000;6(3):421-423

INTRODUCTION

The blood irrigate flow obstruction, especially the gastrointestinal (GI) ischemia^[1], is the main factor of the damage to the digestive tract caused by serious burns. The effect of GI ischemia on the whole body is extensive and profound, which not only causes the increase of intestinal permeability and the movement of bacteria and toxin in the intestinal cavity, but releases a large quantity of inflammatory media. Neuroendocrine element after burns is closely related to intestinal damage^[2]. As is known at present, abundant nitric oxide synthase (NOS) is distributed in GI tract, whose product NO is a nonadrenergic and noncholinergic (NANC) restraining transmitter in enteric nervous system which participates extensively in various physiological functions in the intestinal tract^[3]. Few reports about the effects on intestinal NOS after serious burns are available. We used scalded rat model with degree III 40% of body surface area (TBSA), and enzymatic histological and biochemical methods to observe dynamically the active changes of empty myenteric plexus NOS and changes of jejunal tissue MDA SOD and GSH-PX and probe into the relationship between NOS and intestinal tissue and function damage as well as their mechanism so as to provide morphological experimental basis for clinical treatment.

MATERIALS AND METHODS

Materials

B-NADPH, TYPE, nitroblue tetrazolium (NBT) (Sigma); SOD reagent kit (Wuhan Xiehe Hospital Science and Technology Development Centre); thibarbiluric acid (Shanghai Reagent Factory); self-made phosphate buffer; and healthy SD rats weighing 250 g provided by the Animal Laboratory Centre of Tongji Medical University.

Methods

Eighty rats were randomly divided into five groups: sham-burn control (SBC) and 4 groups of 8, 24, 48

and 72 hours postburn, each group having 16 rats (40 were measured for biochemical indexes, and other 40 for morphological indexes). The rats, before being scalded, had their hair depilated on the neck and back with 80 g/L Na₂S under the anaesthesia with 100 g/L trichloroacetaldehy-demonohydrate after they became conscious, depilated parts were soaked into the 100°C boiling water for 16 sec and scalded to degree III 400g/L TBSA. They were then fed in different cages without treatment. And those in sham-burn control group were soaked into 37°C water.

Rats in different groups, after being scalded, were sacrificed at different time points, a 10 cm empty intestine was taken out and made into thick liquid. SOD activity was determined with modified pyrogallol auto-oxidation^[4]. GSH-PX activity by active DTNB^[5], and the content of MDA with modified thiobarbituric acid fluorescence analysis^[6].

The rats in each group were anaesthetized with 100 g/L trichloroacetaldehy demonohydrate (300 mg/kg), opened up to expose the heart, the blood was quickly rinsed away with 200 mL warm normal saline from left chamber through ascending aorta, and then 450 mL of 40 mL/L cold paraformaldehyde was instilled for one hour, a 10 cm empty intestine was taken out, the intestinal content was washed off and filled again with the same liquid to make the intestinal track full, both ends were ligated and fixed in the above-mentioned liquid (4°C) for 4 hours. The outer longitudinal tunica muscularis was peeled off carefully from the ring tunica muscularis and tela submucosa, and the specimens were made.

The specimens after being washed with 0.1 mol/L of PBS, was put into reduction type NADPH-d hatching liquid at 37°C for 50 min (consisting of 0.1 mol/L of PB (pH 8.0) which contained 30 g/L tritonx-100, 100 mol/L of nitroblue tetrazolium and 1 g/L of NADPH-d, and washed thoroughly with 0.1 mol/L of PBS. After reaction^[7], it was pasted onto a galative glass piece and conventionally dehydrated, made into transparency, sealed and observed under microscope. The staining result of NOS was achieved using IBAS automatic picture analyzer to determine semi-quantitatively the contents in myenteric plexus neuron NOS and internode bind NOS.

Statistical treatment

The data were expressed as $\bar{x} \pm s$, and *t* test was used to compare the results.

Department of Neurobiology Xianning Medical College, Xianning 437100, Hubei Province, China

Correspondence to: Qiu Gui Wang, Department of Neurobiology Xianning Medical College, Xianning 437100, Hubei Province, China

Received 2000-01-05 **Accepted** 2000-03-16

RESULTS

Changes of the contents of MDA, SOD, GSH-PX in the empty intestinal tissues of burned rats

The content of MDA in the empty intestinal tissues gradually rose with the time of burns; compared with the SBC, the contents in each group increased significantly ($P < 0.01$). But the activity of SOD and GSH-PX decreased markedly the difference being significant as compared with SBC ($P < 0.01$).

Active change of myenteric plexus NOS in the empty intestine of burned rats

Observation under light microscope In the control group, most ganglion cells in myenteric plexus and their scabrosity appeared strongly positive in NOS, while a small number had moderate staining, most being distributed around myenteric plexus and the cell being comparatively large and various in shape, i.e., ovate, triangle or irregular. There were NOS positive products in dark blue in the cytoplasm and the nucleus was negative. Most of intersegment bind fiber contained bulge, and some had division and intersect with varying size (Figure 1). In the group

of 8 hours post-burn, the cell NOS stain appeared obviously lighter but intersegment bind fiber had no obvious change (Figure 2). In the 24 hours post-burn group, ganglion cell NOS staining was intensified obviously with clear cell outline and larger size. Intersegment bind fiber and bulge became markedly dense (Figure 3). In the 48 to 72 hour post-burn groups, ganglion cell and intersegment bind fiber staining gradually became lighter, especially in those of 72 hour group (Figure 4), perikaryon and OD change of myenteric plexus NOS in the empty intestine of burned rats. In burned rats after 8 hours the OD of myenteric plexus and intersegment bind fiber NOS were significantly lower than that in the control group ($P < 0.01$) and in those after 24 hours, the OD of ganglion cells and intersegment bind fiber NOS was significantly higher than that in the control ($P < 0.01$); while in those after 48 to 72 hours, OD of ganglion cells and intersegment bind fiber NOS decreased gradually, being significantly different from the control group and those of 24 hours post-burn ($P < 0.01$).

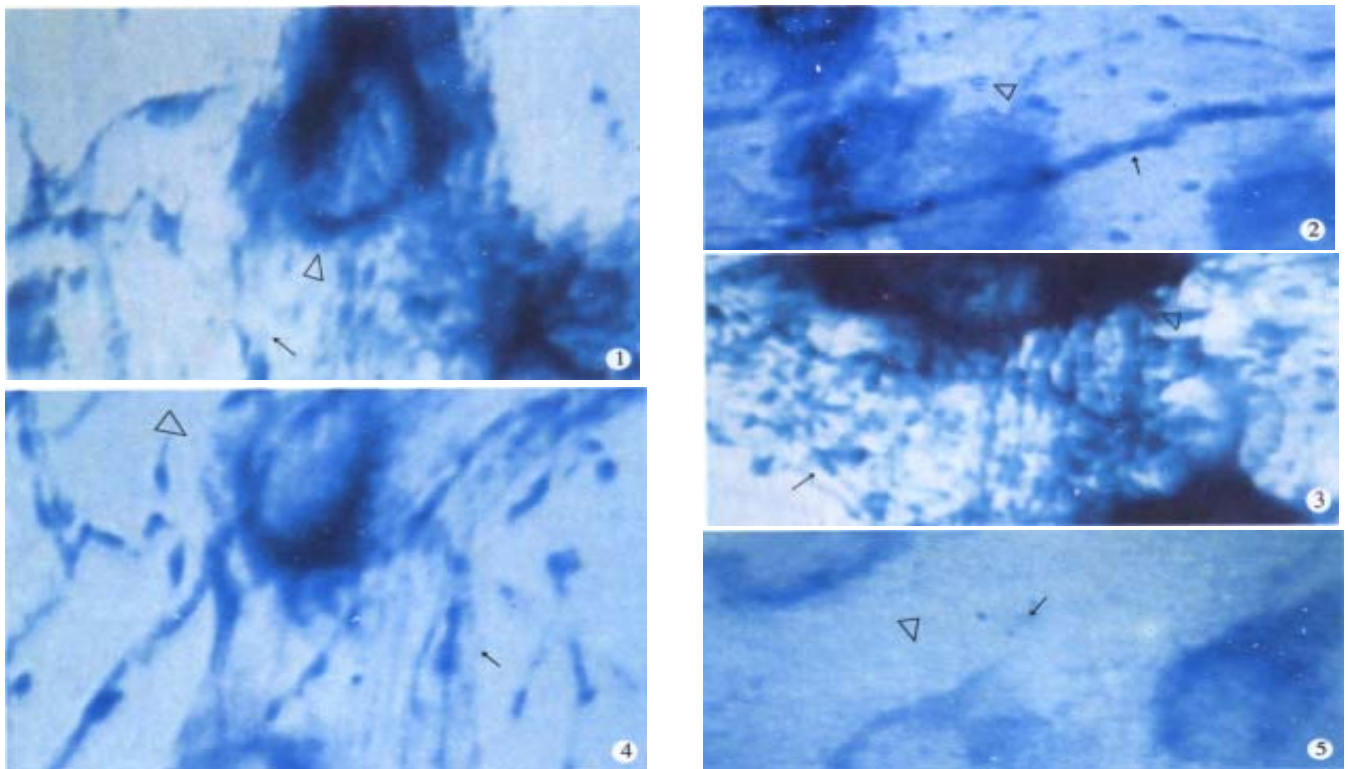


Figure 1 Myenteric plexus neuro bind ganglion cell (Δ) and positive reaction of NOS of intersegmental bundle (\uparrow) in the control group. $\times 400$

Figure 2 Myenteric plexus neuro bind ganglion cell (Δ) and positive reaction of NOS of intersegmental bundle (\uparrow) reduced obviously in the group of 8 hours post-burn. $\times 400$

Figure 3 Myenteric plexus neuro bind ganglion cell (Δ) and positive reaction of NOS of intersegmental bundle (\uparrow) increased obviously in the group of 24 hours post-burn. $\times 400$

Figure 4 Myenteric plexus neuro bind ganglion cell (Δ) and positive reaction of NOS of intersegmental bundle (\uparrow) reduced obviously in the group of 48 hours post-burn compared with the group of 24 hours post-burn. $\times 400$

Figure 5 Myenteric plexus neuro bind ganglion cell (Δ) and positive reaction of NOS of intersegmental bundle (\uparrow) reduced obviously in the group of 72 hours post-burn. $\times 400$

DISCUSSION

NO, a newly discovered active biosubstance in recent years, is a dual-functional messenger and venosity molecule with short half-life and instable nature. The *in vivo* NO, in the form of L-Arg as primer, exists through the catalyza tion of NOS, which indicates that the distribution of NOS is closely related to the physiological functions of NO. It is reasonable to infer bioeffects of NO through the research of NOS, Nathan *et al*^[8] divided NOS into two types, i.e. cNOS and iNOS. cNOS is mainly distributed in neurocyte and endothelium and catalyzes NO which acts chiefly as neurotransmitter and secondary messenger, while iNOS, mainly distributed in macrophage and endothelium cell, catalyzes NO, which has cytotoxic effect. However, the physiological effect of NO to the body depends chiefly on the quality and strength of stimulat ive elements, the dosage and reactive sites. Thus we can presume that after serious burns bad perfusion of intestinal blood, disorder of motor functions and damaged enteromycoderm may be related to the abnormal intestinal NOS activit y. It was suggested that MDA content in the jejunal tissues of the burned rats increased, the result was consistent with that of Peng *et al*^[9]. At the same time, SOD and GSH-PX antioxidase activities in jejunal tissues decreased after being burned, indicating that lipoperoxidation reactions participate in the pathophysiological course of the mucosal damage of burned rats. Some studies demonstrated that cNOS was distributed extensively in plexuses of GI wall, and its output NO was inhibitory neurotransmitter of NANC nerves in GI tract, which may cause angiectasis of intestinal tract and laxation of smooth muscles^[10]. Eight hours after serious burns myenteric plexus NOS activity decreased obviously in our experiment suggesting burn stress caused adrenergic nerve excitation, and inhibited NANC nerves, leading to the decrease of cNOS activity and the catalyzed NO, causing excessive contrac tion of smooth muscles. These may be the main causes in bad perfusion of intesti nal blood and disorder of motor functions. In this experiment, 24 hours post-burn, myenteric plexus NOS activity increased significantly, possibly because the enterogenous infection after serious burn, activated the endotoxin on macrophage cell of intestine to release a series of such body fluid agents as TNT IL-1, etc, leading to increased iNOS

activity. A large amount of high-concentr ation NO produced in this way had cytotoxic effects which further damaged the intestinal tissues. Excessive amounts of NO and O₂ free radicals produced more toxic ONOO⁻ free radicals which further react to produce HO[·], NO₂, NO₃⁻, etc. while HO[·] and NO₂ are catalyst of biomembrane lipid peroxidat ion and can cause a succession of peroxidation of high unsaturation and adipoaci d occurring on the membrane, thus producing a large amount of metabolin MDA wors ening the damage of intestinal tissues. Therefore 48-72 hours post-burn, we fou nd that intestinal myenteric plexus ganglion cell and perikaryon reduced obviously, and changes caused by the lowered NOS activity and other delayed neuronal damage. It can be inferred that NO in the intestine of seriously burned rats and ONOO⁻ reacted by O₂ are important mechanisms that NO damages intestin al structure and functions. It suggests that the damaged structure and functi ons in seriously burned rats are related to the increase of NOS activity. It is concluded that using the inhibitor of NOS to lower NOS activity level may be beneficial to lessening the degree of post-burn intestinal damage.

REFERENCES

- 1 Cui XL, Sheng ZY, Guo ZR, He LX, Zhao J, Ren XW. Mechanisms of early gastrointestinal ischemia after burn: hemodynamic and hemorrheologic features. *Zhonghua Zhengxing Shaoshang Waike Zazhi*, 1998;14:262-265
- 2 Hu DH, Chen B, Lin SX, Tang CW. Observation and analysis of postburn changes in substancep (sp) and sp peptidergic nerve fibers in the intestine of rat. *Chin J Plast Surg Burns*, 1996;12:93-97
- 3 Rand MJ. Nitrinergic transmission: nitric oxide as a mediator of non-adrenergic, on cholinergic neuro effector transmission. *Chom EXP Pharmacol Physio*, 1993;19:147
- 4 Deng BY, Yuan QS, Li WJ. Superoxide dismruse assayed by modified pyrogallolaut oxidation mothod. *Progress Biochem Biophysics*, 1991;18:163
- 5 Xia YM, Zhu LZ. The datermination of glutathione peroxidase in blood and tissue-DTNB direct method. *Weisheng Yanjiu*, 1987;16: 29-33
- 6 Zhang XM, Yan LJ, Chai JK, Zhou WQ, Wang LX. Improvement of the thiobarbituric acid fluorescence analysis of serum lipoperoxides. *Progress Biochem Biophysics*, 1996;23:175-179
- 7 Ding YQ, Lou XF, Wang YQ, Qin BZ. The distribution of nitric oxide synthase positive neurons and fibers and the origin of the positive fibers in the rat spinal cord. *Chin J Neuroanat*, 1993;9:81-87
- 8 Nathan C, Xie QW. Nitric oxide synthase Rdes tolls and controls. *Cell*, 1994;78:915
- 9 Peng YZ, Xiao GX, Wang DW, Zhang YP, Qin XJ. Role of lipid peroxidation in the mechanism of bacterial translocation from the gut after severe thermal injury in rats. *Disan Junyi Daxue Xuebao*, 1989;11:329-334
- 10 Nichols K, Kramtis A, Staines W. Histochemical localization of nitric oxide-synthesizing neurons and vascular sites in the guinea pig intestine. *Neuroscience*, 1992;51:791-799

Edited by Ma JY

Protective effect of electroacupuncture and moxibustion on gastric mucosal damage and its relation with nitric oxide in rats

Wen Fen Pei, Guan Sun Xu, Yong Sun, Shun Li Zhu and Dao Qin Zhang

Subjects headings acupuncture and moxibustion; nitric oxide; gastric mucosal damage; gastric mucosal blood flow; transmucosal potential difference; rats

Pei WF, Xu GS, Sun Y, Zhu SL, Zhang DQ. Protective effect of electroacupuncture and moxibustion on gastric mucosal damage and its relation with nitric oxide in rats. *World J Gastroentero*, 2000;6(3): 424-427

INTRODUCTION

Gastric mucosal injury is one of the common disorders, there are many reports subjected to its pathogenesis treatment and prevention^[1-4]. We investigated the protective effect of electroacupuncture and moxibustion of Zusanli point on gastric mucosal damage and its relation with nitric oxide (NO) on the animal model with acute gastric mucosal damage induced by ethanol. The detected indexes include the content of NO, gastric mucosal blood flow (GMBF), gastric mucosal lesion index (LI) and transmucosal potential difference (PD).

MATERIAL AND METHODS

Drugs L-arginine (L-arg)—the precursor of NO (purchased from Huamei Biological Engineering Corporation); Natrii Nitroprussidum (SNP)—the donor of NO (provided by Experimental Drug Plant of the Beijing Institute of Pharmaceutical Industry), diluted with distilled water prior to use, Nw-nitro- L-arginine (L-NNA), an inhibitor of NOS (produced by Sigma), and diluted with 0.2 mol·L⁻¹ PBS; 200 g·L⁻¹ pentobarbital sodium was prepared with distilled water immediately before use.

Animal grouping

Wistar rats weighing 180 g-250 g (provided by the Institute of Acupuncture and Moxibustion, Anhui College of Traditional Chinese Medicine) were

fasted for 12 h and allowed free access to water. The animals were divided into 16 groups randomly, including: control group (c), model (m), m+electroacupuncture (EA), m+moxibustion (M), L-arg+m, SNP+m, L-NNA+m, L-NNA+L-arg+m, L-arg+m+EA, L-arg+m+M, SNP+m+EA, SNP+m+M, L-NNA+m+EA, L-NNA+m+M, L-NNA+L-arg+m+EA, L-NNA+L-arg+m+M.

Preparation of acute gastric mucosal damage model^[5]

The rats fasted for 12 h were injected with pentobarbital intraperitoneally at a dose of (30-40) mg·Kg⁻¹. The middle line incision below xiphoid process after anesthesia was performed, then stomach was exposed and injected with 2 mL 700 mL/L ethanol, and the abdomen closed, 30 min later the preparation of model was fulfilled.

Experimental procedure

Different procedures were used for different groups. In groups injected drugs or equivalent amount of physiological saline, these were injected respectively into blood flow slowly through the great saphenous vein of the anesthetized rats 15 min before the preparation of the model. In groups which required electroacupuncture or moxibustion, were treated with electroacupuncture or moxibustion on bilateral Zusanli points after the model was successfully prepared. The electroacupuncture was performed with PCE₂ electroacupuncture therapy device on the condition of frequency 20Hz, voltage 5v-8v for 30 min (produced by the Institute of Acupuncture and Moxibustion of Anhui College of Traditional Chinese Medicine). During moxibustion, the lighted pure moxa-cigar was maintained 1 cm from the bilateral Zusanli points. The GMBF and PD values were measured for all rats. Then the blood was obtained through decapitation or from retro-ocular vessel for the NO assay. Subsequently the rat stomach was resected for the analysis of LI, and the mucosa from gastric antrum and the body for assaying NO contents.

Index detection

GMBF was assayed by analyzing hydrogen gas clearance curves^[6]; PD was assayed with direct Ag-

Department of Physiology, Anhui College of Traditional Chinese Medicine (TCM), Hefei 230038, Anhui Province, China

Dr. Wen Fen Pei, graduated from the Department of Medicine, Anhui Medical College in 1976. Associate professor, engaged in study of digestive physiology, having more than 10 papers published.

Supported by National Advanced Project of China (JL-93012)

Correspondence to: Dr. Wen Fen Pei, Department of Physiology, Anhui College of TCM, Hefei 230038, Anhui Province, China
Tel. 0086-551-2823237

Received 2000-01-25 **Accepted** 2000-03-02

AgCl. Electrode measurement technique^[7] with few alterations, i.e. the efficient electrode was put on the mucosa while the reference one on the serosa. The electric potential difference between two membranes was recorded. For the detection of LI, the stomach was resected and incised along the greater curvature, washed with physiological saline. Guth index assessment^[8] (slightly modified) was used to compute the damage, on a scale of grades 1-5 as follows: Grade 1, the petechia or ecchymosis, Grade 2, 3, 4 and 5, pathological focus of 1 mm; 1 mm-2 mm, 2 mm-4 mm, and over 4 mm, respectively. The NO content in blood and mucosa of gastric antrum and body were assayed based on the method from Green *et al*^[9]. The Kit for NO assay was provided by the Department of Biochemistry, Institute of Radiology, Academy of Medical Science of PLA. The analysis was based on the protocol, but the mucosa were homogenized before the assay.

Statistical analysis

All data were expressed as $\bar{x} \pm s$, and the Student's *t* test was used for the comparison between groups.

RESULTS

The effect of acupuncture and moxibustion of Zusanli point on GMBF, PD and LI in rats with the gastric mucosal damage (Table 1)

The mean of GMBF, PD in group m showed statistically significant difference compared with the control group ($P < 0.01$), demonstrating marked decrease of GMBF and PD after gastric mucosal damage, the integrity of gastric mucosa was depended on adequate blood flow. GMBF and PD in group m+M was obviously increased ($P < 0.01$) compared with group m, suggesting the electroacupuncture and moxibustion of Zusanli point may relieve and cure the gastric mucosal damage induced by ethanol.

Changes of NO content in blood and gastric mucosa and their relation with LI after electroacupuncture and moxibustion on the Zusanli point of rat models

From Table 1 we can find, NO contents in group m showed significant difference compared with normal control ($P < 0.01$); LI in group m+EA and group m+M was markedly lower than that in group m ($P < 0.01$). The results showed that the gastric mucosal damage aggravated as NO content decreased while NO content increased and the gastric mucosal damage relieved, which suggests that NO content is associated with the integrity of gastric mucosa.

Effect of L-NNA, L-arg and SNP on the response of electroacupuncture and moxibustion (Table 1)

The L-Arg (150 mg·Kg⁻¹), SNP (200 µg·Kg⁻¹) and L-NNA (3 mg·Kg⁻¹) were administered through the great saphenous vein respectively 15 min before administration of 700 mL/L ethanol in different groups. After that the electroacupuncture and moxibustion of Zusanli point were performed for 30 min. Subsequently, the GMBF, PD and LI as well as NO content in blood and gastric mucosa were assayed and detected respectively in each group. It was found that there was little difference in the indexes when group L-arg +m and group SNP+m were compared with group m+EA or group m+M ($P < 0.05$), indicating the function of electroacupuncture and moxibustion on gastric mucosal damage was similar to that of L-arg or SNP. Comparing group L-Arg+m+EA (or M) and group SNP+m+EA (or M) with group m+EA (or M), and group SNP+m+EA (or M) with group m+EA (or M), NO content, GMBF and PD values were markedly increased, and LI value was obviously decreased ($P < 0.01$ or $P < 0.05$), which suggested that electroacupuncture and moxibustion of Zusanli point had the effect of strengthening NO pathway and protecting gastric mucosa.

In comparison of group L-NNA+m with group m, NO content, GMBF and PD value decreased, and LI value increased ($P < 0.01$ or $P < 0.05$), showing that L-NNA aggravated ethanol induced gastric mucosal damage. When we compared group L-NNA+m+EA (or M) with group m+EA (or M), NO content, GMBF and PD value also decreased, but LI value increased ($P < 0.01$ or $P < 0.05$), which suggests L-NNA decreased the protective action of electroacupuncture and moxibustion on gastric damage. While we compared group L-NNA +L-arg +m+EA (or M) with group L-NNA+m+EA (or M), NO contents, GMBF and PD value increased and LI value decreased ($P < 0.01$ or $P < 0.05$), demonstrating L-arg may reverse the inhibitory function of L-NNA. In conclusion, the above mentioned results further suggest that the protective action on gastric mucosa by the electroacupuncture and moxibustion of Zusanli point is NO mediated.

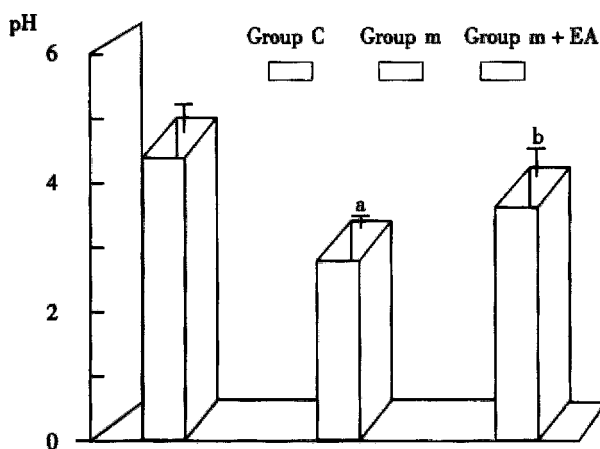
Effect of electroacupuncture of Zusanli point on pH value of gastric fluid (Figure 1)

pH in group c was 4.33 ± 0.40 and that in Group m 2.92 ± 0.37 , decreasing significantly in the latter group ($P < 0.01$). The pH value in Group m+EA, 3.84 ± 0.69 was much higher than that in Group m indicating 700 mL/L ethanol promotes the stomach to secrete acids while electroacupuncture inhibits the secretion.

Table 1 Effect of electroacupuncture and moxibustion of Zusanli point on LI, GMBF, PD and NO after gastric mucosal damage in rats ($\bar{x} \pm s$)

Group	n	LI	GMBF (mL·min ⁻¹ ·100g ⁻¹)	PD (mV)	NO	
					Blood (μmol·L ⁻¹)	Antrum (ng·mg ⁻¹)
C	5	0	138.20 ± 4.37	20.82 ± 0.99	21.12 ± 1.89	53.30 ± 2.65
m	5	45.6 ± 3.2 ^a	60.60 ± 6.09 ^a	11.85 ± 0.82 ^a	12.84 ± 1.54 ^a	35.17 ± 1.57 ^a
m + EA	5	31.4 ± 3.3 ^c	92.55 ± 6.35 ^c	15.84 ± 0.48 ^c	18.65 ± 0.69 ^c	48.51 ± 2.12 ^c
m + M	5	33.8 ± 2.4 ^c	95.91 ± 5.59 ^c	15.96 ± 0.34 ^c	18.53 ± 1.04 ^c	48.49 ± 2.39 ^c
L-arg + m	5	32.4 ± 3.2	106.22 ± 5.30	17.73 ± 0.22	18.93 ± 1.30	47.57 ± 2.86
SNP + m	5	30.0 ± 3.1	104.03 ± 7.57	17.89 ± 0.39	19.07 ± 1.29	47.18 ± 2.17
L-NNL + m	5	55.8 ± 2.8 ^b	56.85 ± 5.96 ^d	6.97 ± 0.32 ^c	8.37 ± 0.27 ^b	27.29 ± 1.71 ^b
L-NNA + L-arg + m	5	46.8 ± 2.6	78.90 ± 5.10	10.93 ± 0.39	12.10 ± 1.23	33.76 ± 2.44
L-arg + m + EA	5	21.0 ± 0.9 ^e	121.50 ± 3.55 ^d	18.14 ± 0.44	24.70 ± 0.75 ^d	50.63 ± 2.34
L-arg + m + M	5	27.1 ± 2.7 ^d	97.46 ± 4.90	16.08 ± 0.45	21.06 ± 1.17	44.26 ± 2.01
SNP + m + EA	5	20.9 ± 0.8 ^e	118.50 ± 4.21 ^d	17.79 ± 0.59	24.80 ± 0.50 ^d	45.17 ± 2.01
SNP + m + M	5	26.8 ± 2.2 ^d	101.11 ± 5.23	14.73 ± 0.61	23.14 ± 1.52 ^d	43.33 ± 1.97
L-NNA + m + EA	6	41.8 ± 2.1 ^e	73.57 ± 5.43 ^d	11.87 ± 0.41 ^d	12.37 ± 1.78 ^e	39.25 ± 1.66 ^d
L-NNA + m + M	6	40.5 ± 3.0 ^d	66.42 ± 5.42 ^e	10.25 ± 0.72 ^e	11.43 ± 1.03 ^e	32.17 ± 2.35 ^e
L-NNA + L-arg + m + EA	5	31.0 ± 1.2 ^g	95.00 ± 3.78 ^f	16.15 ± 0.74 ^g	19.24 ± 0.54 ^g	51.51 ± 2.14 ^f
L-NNA + L-arg + m + M	5	31.5 ± 2.1 ^g	70.76 ± 4.78	11.81 ± 0.53	12.88 ± 0.68	36.37 ± 2.29

^a*P*<0.01 vs Group C; ^b*P*<0.05, ^c*P*<0.01 vs Group m; ^d*P*<0.05, ^e*P*<0.01 vs Group m+EA (or M); ^f*P*<0.05, ^g*P*<0.01 vs Group L-NNA+m+EA (or M).

**Figure 1** Effect of electroacupuncture on pH value with gastric mucosal damage in rats.

^a*P*<0.01 vs Group C; ^b*P*<0.01 vs Group m.

DISCUSSION

Acupuncture and moxibustion may treat and prevent gastrointestinal disorders, the mechanism of which is being further investigated. The acupuncture and moxibustion on Zusanli points show the two-way regulation of gastrointestinal function. In recent years, it is frequently reported that they may relieve symptom and promote the ulcer healing to certain extent^[1-4]. There is relative point specificity, the first choice is the Zusanli point in stomach channel of foot yangming. Our study investigated the therapeutic and protective effect of the acupuncture and moxibustion on acute gastric mucosal damage induced by 700 mL/L ethanol. It is found that

GMBF and PD value as well as NO content, pH value in rat gastric mucosa of model group with acupuncture and moxibustion increased more markedly than those without any therapy (*P*<0.01), while the gastric mucosal damage alleviated (*P*<0.01) which denotes the therapeutic and protective effect of acupuncture and moxibustion on the damage and suggests that the protective action is related with the level of NO content.

NO is a small molecular gas produced from the precursor L-Arg under the NOS catalysis. The process is called as L-Arg-NO pathway, NOS activity plays a key role in NO synthesis. NOS is existed in many kinds of tissues including vascular endothelial cell, thrombocyte, brain cell, renal epithelial cell, macrophage, neutrophil, hepatocyte, etc. Some factors can induce the expression of NOS and increase the NO synthesis. As a special bioinformational molecule, the neurotransmitter or the humoral factor, NO involves in the functional regulation and pathophysiology of many diseases. Our study investigates the protective effect of acupuncture and moxibustion on acute gastric mucosal damage and in the meantime measures NO content in blood and gastric mucosa and finds that NO content is negatively correlated with the severity of gastric mucosal damage, which proves that the protective action of acupuncture and moxibustion of Zusanli point is NO mediated; and in other words NO involves in the regulative effect of acupuncture and

moxibustion on gastrointestinal function.

The good balance between NO and ET keeps the endothelium intact. If the unbalance is developed, the gastric mucosal damage will be formed and the gastric dysfunction presented. Our study showed^[1] that when NO content decreased ET content increased and gastric mucosal damage aggravated, and on the contrary, the damage alleviated. Our results have verified it. When L-arg or SNP was administered 15 min before establishing the model with 700 mL/L ethanol; NO content was higher than that in the model group and concurrently GMBF and PD value increased, and LI value decreased; if NOS inhibitor -L-NNA was given, NO content, GMBF and PD value were lower than those in the model group while LI value increased, which indicates that NO plays an important role in maintaining the intact gastric mucosa. GMBF decrease may prominently respond to the gastric mucosal damage after ethanol induction. It is thought that NO is an EDRF, which is capable of relaxing the vascular smooth muscle obviously. Our research further confirmed that the vascular relaxing action of NO can protect gastric mucosa from damage.

NO initiates the protective effect of acupuncture and moxibustion on gastric mucosa, which has been proved in our work. During experiment, in the model rats, the NO content in their blood and gastric mucosa increased after acupuncture and moxibustion were performed, and GMBF and PD values were also increased while LI value decreased. If L-NNA was preliminarily given, the above effect of acupuncture and moxibustion of Zusanli point disappeared, but concurrently given L-arg, the action of L-NNA could be reversed. In addition, if L-arg or SNP was preliminarily administered and then the model established, NO content in the group with the acupuncture and moxibustion of Zusanli point increased more than that in the corresponding groups without acupuncture and moxibustion, moreover, GMBF and PD values increased and LI decreased correspondingly, showing the synergetic action between them. The above phenomena further confirm that the acupuncture and moxibustion of Zusanli points alleviate gastric mucosal damage, which is NO mediated, and this illustrates that the acupuncture and moxibustion of Zusanli point can activate endogenous NOS.

As far as the possible mechanism why Zusanli point can initiate NO system is concerned, we consider that the main nerves regulating gastric function are vagus nerves, the dorsal vagus nucleus (DMV) being the major motor nucleus. The efficient stimulus transmitted to DMV by the somatic sensory nerves through the spinal cord. DMV also receives afferent information from gastrointestinal tract and integrates other information from central nervous system (CNS), and transfers to the stomach by efferent vagus nerves, resulting in the increase of NO synthesis and release.

The possible mechanism about how NO can protect gastric mucosa from damage is as follows: NO acts as one of endothelial diastolic factors which can cause the dilatation of vascular smooth muscles, resulting in GMBF increase, improvement of blood supply of gastric mucosa, maintaining the integrity of gastric mucosal epithelium, protecting the gastric mucosa from the stimulation of gastric contents and from damage, preventing from H⁺ invasion and keeping normal ionic concentration gradient across gastric mucosa as well as maintaining appropriate PD value, while acupuncture and moxibustion may activate NOS to increase the synthesis and release of NO. Further research remains to be done as how does the acupuncture and moxibustion activate NOS.

REFERENCES

- 1 Xu GS, Wang ZJ, Zhu SL, Chen QZ, Jiao J, Zhang DQ. Nitric Oxide participates in protective effects of acupuncture on gastric mucosal damages in rats. *Anhui Zhongyi Xueyuan Xuebao*, 1996;15:36-38
- 2 Ma TF, Yang Z. Therapeutic effect and mechanism of acupuncture on digestive tract disease. In: Ed Zhou Lu. *Gastrointestinal physiology*. Peking: Science press, 1991:755-772
- 3 Qiao XF, Yin KJ. Therapeutic effect and mechanism of moxibustion on experimental gastric ulcer in rats. *Zhenci Yanjiu*, 1992;17:270-273
- 4 Xu GS, Zhang QQ, Liu WZ, Leng JP. Effect and mechanism of Moxibustion on gastric electric activity in rabbits. *Zhenci Yanjiu*, 1992;17:274-276
- 5 Masuda E, Kawano S, Nagano K, Tsuji S, Takei Y, Tsujii M, Oshita M, Michida T, Kobayashi I, Nakama A, Fusamoto H, Kamada T. Endogenous nitric oxide modulates ethanol induced gastric mucosal injury in rats. *Gastroenterology*, 1995;108:58-64
- 6 Livingston EH, Reedy T, Leung FW, Guth PH. Computerized curve fitting in the analysis of hydrogen gas clearance curves. *Am J Physiol*, 1989;257:G668-675
- 7 Xu GS, Sun Y, Wang ZJ, Zhang DQ, Gu XJ. Effects of electroacupuncture on gastric mucosal blood flow and transmucosal potential difference in stress rats. *Huaren Xiaohua Zazhi*, 1998;6:4-6
- 8 Guth PH, Aures D, Paulsen G. Topical aspirin plus HCl gastric lesions in rat. *Gastroenterology*, 1979;76:88-93
- 9 Green LC, Tannenbaum SR, Goldman P. Nitrate synthesis in the germfree and conventional rat. *Science*, 1981;212:56-58

Edited by You DY
proofread by Sun SM

Research of *Helicobacter pylori* infection in precancerous gastric lesions

Xiao Qiang Zhuang¹ and San Ren Lin²

Subject headings *Helicobacter pylori*; precancerous gastric lesions

Zhuang XQ, Lin SR. Research of *Helicobacter pylori* infection in precancerous gastric lesions. *World J Gastroentero*, 2000;6(3):428-429

INTRODUCTION

Helicobacter pylori (*Hp*) infection has been considered to play significant roles in pathogenesis of peptic ulcer. Additionally *Hp* is associated with the development of gastric epithelial hyperplasia and lymphoid malignancies. The International Agency for Research on Cancer has classified *Hp* as a class I carcinogen and a definite cause of gastric cancer in humans. *Hp* infection first causes chronic active gastritis and may slowly lead to infection of whole stomach. In the late stages of infection, mucosal atrophy and intestinal metaplasia (IM), and even dysplasia (DYS) occur^[1]. Chronic atrophic gastritis (CAG), IM and DYS are considered markers for development of gastric cancer in high-risk individuals. In our study we analyzed *Hp* infection prevalence in 486 patients with precancerous gastric lesions.

MATERIALS AND METHODS

The mucosal biopsy specimens were collected from 486 patients subjected to routine gastroscopy, including 163 cases of CSG, 207 cases of CAG, 71 cases of IM and 45 cases of DYS. Biopsies were taken from five sites in the stomach: one from the antrum, four from the lesser and greater curvature of gastric body and gastric antrum. Each biopsy was classified according to the presence or absence of CSG, CAG, IM and DYS, and scanned by Warthin-Starry method.

Data analysis was made with *Chi-square* test. Statistical significance was defined as $P < 0.05$.

RESULTS

Table 1 Relation between precancerous gastric lesions and age and sex

Variables	n	CSG		CAG		IM		DYS	
		n	%	n	%	n	%	n	%
Sex									
Male	314	96	30.6	142	45.2	43	13.7	33	10.5
Female	172	67	38.9	65	37.8	28	16.3	12	7
Age (yrs)									
≤40	184	64	34.9	98	53.5	13	7.0 ^a	9	4.6 ^b
41-55	171	52	30.3	70	41.2	30	17.3	19	10.8
≥56	131	40	30.5	46	35.4	28	21.1 ^a	17	13.0 ^b

^a $P < 0.05$, ^b $P < 0.05$.

Gastric pathology data was available for 486 cases. As shown in Table 1, there was no significant difference between the two sexes ($P > 0.05$), but the prevalence rates increased with age, being significantly higher in ≥56 age group than ≤40 group for IM and DYS ($P < 0.05$).

Table 2 *Hp* infection rate in precancerous gastric lesions

Variables	n	Hp(+)		Hp(-)	
		n	%	n	%
CSG	163	39	23.9	124	76.1
CAG	207	88	42.5 ^a	119	57.5
IM	71	54	76.1 ^b	17	23.9
DYS	45	40	88.9 ^c	5	11.1

^a $P < 0.05$, CAG vs CSG; ^b $P < 0.01$, IM vs CSG; ^c $P < 0.01$, DYS vs CSG.

The prevalence of *Hp* increased steadily with increasing severity of gastric histopathology (Table 2). The detection rates of *Hp* in IM (76.1%) and DYS (88.9%) were significantly higher than that in CSG (23.9%, $P < 0.01$), and in CAG than in CSG ($P < 0.05$).

Table 3 *Hp* infection distribution in precancerous gastric lesions by biopsy sites

Variables	n	ALC		AGC		A		BLC		BGC	
		n	%	n	%	n	%	n	%	n	%
CSG	39	37	94.9	36	92.3	32	82.1	18	46.2	10	25.6
CAG	88	84	95.4	80	90.9	78	88.6	53	59.9	41	46.2
IM	54	49	90.7	46	85.2	40	74.1	34	62.7 ^a	32	58.8 ^a
DYS	40	36	90.0	33	82.5	30	75.0	28	70.0 ^b	26	63.9 ^b

ALC:antral lesser curvature; AGC:antral greater curvature; A: angulus; BLC:body, lesser curvature; BGC:body, greater curvature
^a $P < 0.05$, IM vs CSG; ^b $P < 0.05$, DYS vs CSG.

¹Department of Gastroenterology, General Hospital, of Guangzhou Command Area, Guangzhou 510010, Guangdong Province, China

²Department of Gastroenterology, The Third Hospital of Beijing Medical University, Beijing 100083, China

Dr. Xiao Qiang Zhuang, associate professor Master of Gastroenterology, having 31 papers published.

Correspondence to: Xiao Qiang Zhuang, Department of Gastroenterology, General Hospital of Chinese PLA Guangzhou Command Area, Guangzhou 510010, China

Tel. 0086-20-86664097

Received 2000-02-05 Accepted 2000-03-18

As shown in Table 3, the prevalence of *Hp* positivity tended to increase from BLC to BGC, *Hp* positive rates in IM and DYS were significantly higher than that in CSG in both BLC and BGC ($P < 0.05$).

DISCUSSION

The first compelling evidence linking *Hp* infection to gastric carcinoma was generated by seroepidemiologic studies^[2,3], bacterial seropositivity was significantly more common in those with gastric adenocarcinoma, with an odds ratio ranging from 2.8 to 6.0, suggesting a strong association between *Hp* and gastric malignancy.

Hp infection was related to both the intestinal and diffuse types of cancer as well as the precancerous lesion of IM or DYS^[4], and greater than 70% of gastric carcinomas are linked to IM, although DYS may also be seen without neoplastic disease.

Our study demonstrated that the prevalence rates of precancerous lesions varied with age, for IM and DYS, it had an upward trend with aging, while for CSG, it had a downward trend with aging, but were not different between the two sexes. The prevalence

rose steadily with increasing severity of gastric histopathology, the detection rates of *Hp* in CAG (42.5%), IM (76.1%) and DYS (88.9%) were significantly higher than that in CSG (23.9%), suggesting that *Hp* may play a role in late as well as early stages of carcinogenesis.

Our study also showed that *Hp* positive rates in IM and DYS were significantly higher than that in CSG in the lesser and greater curvature of gastric body, suggesting the more serious the gastric histopathology, the higher the *Hp* infection rate, furthermore, the higher level of *Hp* infection site. The study suggests we should take multiple site biopsy for histopathology and *Hp* examination.

REFERENCES

- 1 Kuipers EJ. *Helicobacter pylori* and the risk and management of associated diseases: gastritis, ulcer disease, atrophic gastritis and gastric cancer. *Aliment Pharmacol Ther*, 1997;11(Suppl 1):71-88
- 2 Nomura A, Stemmermann GN, Chyou PH, Kato I, Perez-Perez GI, Blaser MJ. *Helicobacter pylori* infection and gastric carcinoma among Japanese Americans in Hawaii. *New Engl J Med*, 1991;325:1132-1136
- 3 Parsonnet J, Friedman GD, Vandersteen DP, Chang Y, Vogelstein JH, Orentreich N, Sibley RK. *Helicobacter pylori* infection and the risk of gastric carcinoma. *New Engl J Med*, 1991;325:1127-1131
- 4 Craanen ME, Dekker W, Blok P, Ferwerda J, Tytgat GN. Intestinal metaplasia and *Helicobacter pylori*: an endoscopic biopsic study of the gastric antrum. *Cut*, 1992;33:16-20

Edited by Zhu LH
proofread by Sun SM

Antisense telomerase RNA induced human gastric cancer cell apoptosis

Fang Xin Zhang¹, Xue Yong Zhang², Dai Ming Fan², Zi Yun Deng¹, Yan Yan², Han Ping Wu¹ and Jun Jie Fan¹

Subject headings stomach neoplasms; RNA, antisense; telomere; gene therapy

Zhang FX, Zhang XY, Fan DM, Deng ZY, Yan Y, Wu HP, Fan JJ. Antisense telomerase RNA induced human gastric cancer cell apoptosis. *World J Gastroentero*, 2000;6(3):430-432

INTRODUCTION

Human tissue homeostasis is precisely regulated by cellular division, differentiation and death. Normal human somatic cells progressively lose telomere restriction fragment (TRF) length with each successive cell division, eventually leading to cellular quiescence, chromosomal end-degradation and apoptosis^[1]. On the contrary, stabilization of telomere lengths by expressing telomerase, an RNA-dependent DNA polymerase, may be involved in cellular immortality and carcinogenesis^[2-4]. Changes of telomerase activity and telomere lengths have been found in almost all human cancers^[4-10], but the evidence of their relationship with immortalization of cancers cell remain to be directly demonstrated. Since shortened telomere was first discovered in Hela cells with antisense RNA techniques in 1995^[11], anticancer agents based on inhibition of telomerase RNA have been reported^[12,13]. However, the relationship between telomerase inhibition and cell apoptosis has not been fully understood. In this study, we investigated the effect of blocking telomerase activity on apoptosis of human gastric cancer cells *in vitro* using an antisense vector for human telomerase RNA component (hTR) into human gastric cancer cells.

MATERIALS AND METHODS

Reagents

EcoRI, *BaI* I, *SaI* I, SP6 or T7 polymerases (Promega), hygromycin (Boehringer Mannheim) and lipofectamine (Gibco BRL) were commercially obtained. Antisense hTR expression construct vector (pBBS212) and hTR recombinant plasmid (pGRN83) were kindly donated by Dr Villeponteau (Geron Corporation, USA).

Cell line

The human gastric cancer cell line SGC7901 (Fourth Military Medical University, China) was cultured in RPMI1640 (Gibco BRL) containing 100 mL/L fetal bovine serum.

Transfection of antisense hTR expression vector

The TRC₃ piece (hTR) was flanked by 2 *EcoRI* sites and was inserted into *EcoRI* site of pBBS212 to make the plasmids pBBS-hTR, which can express the antisense of hTR under the MPSV promoter^[11,14]. Cells at density of 2×10^5 /well (2 mL) in 6 well plates were transfected with purified plasmids (pBBS-hTR) and a selectable marker, hygromycin, by lipofectin procedure as described^[15]. As a control, cells were transfected either with an hTR-free plasmid (pBBS212) containing hygromycin marker or with hygromycin alone. Four clonal cells from each group were used for a series of experiments.

hTR expression by blot hybridization

Total RNA was prepared from each group cells by RNA isolation kit (Promega). PGR N83 was lined with *BaI* I or *SaI* I and transcribed *in vitro* using T7 RNA polymerase and SP6 RNA polymerase respectively. The transcription was carried out according to the manufacturer's instructions in the presence of 370GBq [α -³²P]UTP (Beijing Huri Co, China). Then a sense hTR or antisense hTR probe synthesized was used for RNA blot hybridization^[15].

Telomerase assay

Cell extracts were prepared by detergent CHAPS (Pierce), and telomerase activity was measured by telomeric repeat amplification protocol (TRAP) methods as described by Kim *et al*^[5,16]. The TRAP reaction products were separated by 100 g/L polyacrylamide gel electrophoresis and autoradiographed. The basal level of telomerase activity was measured by serial dilution of the protein extracts.

Determination of TRF length

Genomic DNA extracted from the gene transfected cells and the control cells were digested with *HinfI* and *RsaI*. DNA samples (8 μ g each) were loaded onto a 8 g/L agarose gel and electrophoresed for bromophenol blue to the bottom of gel at 90V. The gel was dried, denatured, neutralized and hybridized to a 5'-[³²P](TTAGGG)₄ probe (T₄ polynucleotide kinase, Promega) and *autoradi-*

¹Department of Gastroenterology, Lanzhou PLA General Hospital, Lanzhou 730050, Gansu Province, China

²Institute of Digestive Diseases, the Fourth Military Medical University, Xi'an 710033, Shaanxi Province, China

Supported by the Natural Science Foundation of Gansu Province, China, No.ZS981-A23-086-Y

Correspondence to: Dr. Fang Xin Zhang, Department of Gastroenterology, Chinese Lanzhou General Hospital, Lanzhou 730050, Gansu Province, China

Email: zhangfx@lz.gs.cninfo.net

Received 2000-01-21 **Accepted** 2000-03-18

ographed 48 h at -20°C ^[2,17].

Cell cycle analysis

Cells in log phase growth were collected, washed twice with phosphate buffered saline (PBS) and fixed in 70 mL/L ethanol at 4°C overnight. Cells were washed with PBS, digested with 20 mg/L RNase A at room temperature for 1 h, and then resuspended in 50 mg/L propidium iodide solution. Cell cycle was analyzed on the FAC/Scan (ELITEESP, Coulter Co) using a computer program interfaced with the integrator.

Ultrastructural observation

Ultrastructure in the gene transfected cells was observed under a transmissive electron microscope (JEM-2000EX, Japan).

RESULTS

Antisense telomerase RNA inhibited the sense telomerase RNA expression in the gene transfected cells. Antisense hTR expression was high and sense hTR expression was weak in RNA blot hybridization analysis (Figure 1). Sense hTR suppression rate analyzed by thin layer scanning reached 60% (Figure 1). Antisense RNA to hTR mediating telomerase activity was down-regulated in the gene transfected cells but not in the control plasmids transfected cells (Figure 2). Mean TRF length of

the gene transfected cells (11.0 ± 5.6) was also shorter than that of the control plasmids transfected cells (Figure 3). Compared with the control plasmids transfected cells, G1 phase decreased by 25% in the gene transfected cells and its apoptotic peak reached in 46.2% of cell cycle in a computer apoptotic program analysis (Figure 4). Either denaturation and necrosis or chromatin compaction and apoptotic body appeared in the gene transfected cells while the non-gene transfected cells showed no changes of this kind (Figure 5).

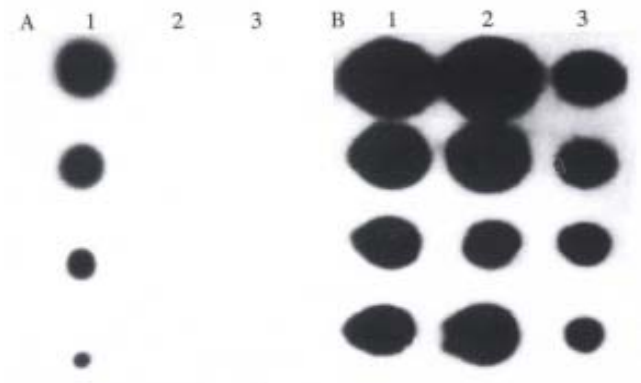


Figure 1 Blotting hybridization of hTR. (A) Antisense hTR expression. (B) Sense hTR expression. (1) SGC7901 cells. (2) SGC7901 cells transduced with control vector (pBBS). (3) SGC7901 cells transduced with vector expressing antisense hTR (pBBS-hTR).



Figure 2 Telomerase activity of SGC7901 cells analyzed by TRAP. (A) SGC7901 cells transduced with control vector (pBBS). (B) SGC7901 cells transduced with vector expressing antisense hTR (pBBS-hTR).

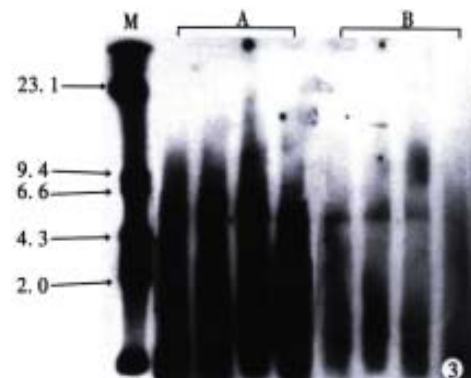


Figure 3 Telomeric lengths of SGC7901 cells analyzed by hybridization of nucleic acids directly in agarose gels. (M) λ -DNA/Hind III Molecular Markers. (A) SGC7901 cells transduced with control vector (pBBS). (B) SGC7901 cells transduced with antisense hTR expressing vector (pBBS-hTR).

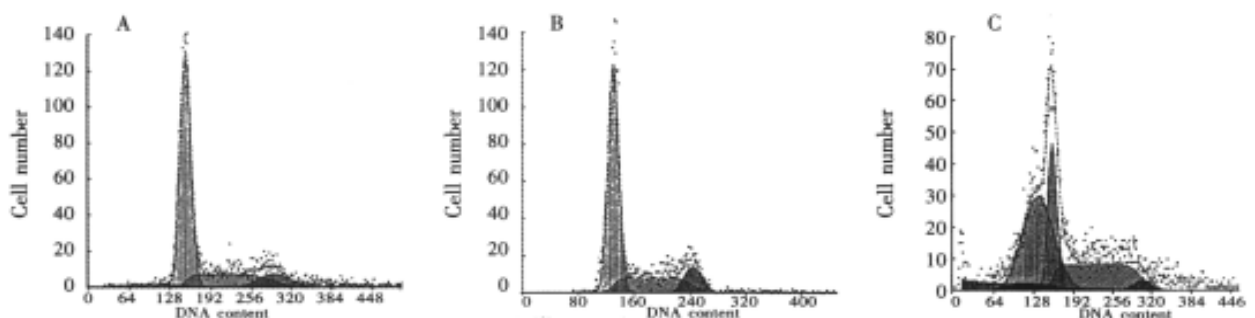


Figure 4 Cell cycle analyzed by flow cytometry. (A) SGC7901 cells. (B) SGC7901 cells transduced with control vector (pBBS). (C) SGC7901 cells transduced with vector expressing antisense hTR (pBBS-hTR).

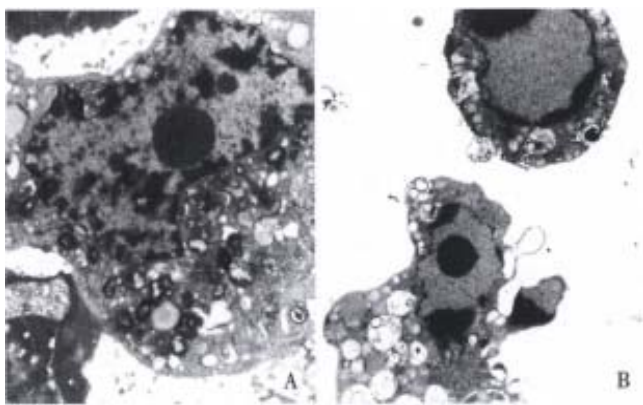


Figure 5 Ultrastructure observed under transmissive electron microscope. (A) SGC7901 cells transduced with control vector (pBBS). (B) SGC7901 cells transduced with antisense hTR expressing vector (pBBS-hTR).

DISCUSSION

Cell apoptosis is closely associated with tumorigenesis, tumor growth and tumor metastasis. Changes of telomere lengths may play an important role in maintaining cell division, proliferation, apoptosis and immortalization^[2,4]. Normal human somatic cells progressively lose their telomeric sequence with replicative senescence till cell "crisis" or apoptosis occurred^[4,18,19]. In contrast, almost all tumor cells and tissues express telomerase and maintain telomere length through an indefinite number of cell divisions^[4-10,19-24]. Antisense hTR, hammerhead ribozyme TeloRZ and antisense oligonucleotide against hTR could suppress tumor cell growth by inhibiting telomerase activity or shortening TRF length^[11-13]. Therefore, it has been proposed that antisense RNA based on telomerase inhibition may potentially reverse uncontrolled proliferation of tumor cells and induce apoptosis of cancer cells^[25,26]. The present study is undertaken to investigate the possible relationship between the antisense hTR expression and apoptosis of human gastric cancer cells.

Our study has demonstrated that the antisense hTR expression level of SGC7901 cells was high. Based on the histogram of flow cytometry, G1 phase was arrested and there was a typical apoptotic peak in the antisense hTR expression vector transfected cells. Meanwhile, compaction of nuclear chromatin and apoptotic body were observed under a transmissive electron microscope. These results suggest that antisense hTR may mediate apoptosis of human gastric cells. Also, we have found that the antisense hTR expression of SGC7901 cell could down-regulate telomerase activity and shorten telomere length. This supports the changes of telomere length and telomerase activity in antisense hTR transfected tumor cells^[11,12], indicating that telomerase can mediate telomeric sequence replication in gastric cancer cells

and that shortening of telomere length by the antisense hTR may be associated with apoptosis of human gastric cancer. Thus, the induction of cell apoptosis in SGC7901 cells expressing antisense hTR demonstrates the potential of telomerase inhibition as a therapeutic target for human cancer.

REFERENCES

- 1 Pathak S, Dave BJ, Gagos S. Chromosome alterations in cancer development and apoptosis. *In Vivo*, 1994;8:843-850
- 2 Counter CM, Avilion AA, LeFeuvre CE, Stewart NG, Greider CW, Harley CB, Bacchetti S. Telomere shortening associated with chromosome instability is arrested in immortal cells which express telomerase activity. *EMBO J*, 1992;5:1921-1929
- 3 Wright WE, Brasikyte D, Piatyszek MA, Shay JW. Experimental elongation of telomeres extends the lifespan of immortal X normal cell hybrids. *EMBO J*, 1996;15:1734-1741
- 4 Rhyu MS. Telomeres, telomerase, and immortality. *J Natl Cancer Inst*, 1995;87:884-894
- 5 Kim NW, Piatyszek MA, Prowse KR, Harley CB, West MD, Ho PLC, Coviello GM, Wright WE, Weinrich SL, Shay JW. Specific association of human telomerase activity with immortal cells and cancer. *Science*, 1994;266:2011-2015
- 6 Counter CM, Hirte HW, Bacchetti S, Harley CB. Telomerase activity in human ovarian carcinoma. *Proc Natl Acad Sci USA*, 1994;91:2900-2904
- 7 Zhang FX, Zhang XY, Fan DM, Deng ZY, Yan Y. Expression of telomere and telomerase in human primary gastric carcinoma. *Zhonghua Binglixue Zazhi*, 1998;27:429-432
- 8 Zhang FX, Zhang XY, Fan DM, Den ZY. Analysis of telomere length in human gastric cancer and precancerous. *Zhonghua Xiaohua Neijing Zazhi*, 1998;15:351-352
- 9 Zhang FX, Zhang XY, Fan DM, Yan Y, Xu ZK. Telomerase activity in gastric cancer and precancerous. *Disi Junyi Daxue Xuebao*, 1998;19:457-459
- 10 Park KH, Rha SY, Kim CH, Kim TS, Yoo NC, Kim JH, Roh JK, Noh SH, Min JS, Lee KS, Kim BS, Chung HC. Telomerase activity and telomere lengths in various cell lines: changes of telomerase activity can be another method for chemosensitivity evaluation. *Int J Oncol*, 1998;13:489-495
- 11 Feng JL, Funk WD, Wang SS, Weinrich SL, Avilion AA, Chiu CP, Adams RR, Chang E, Allsopp RC, Yu JH, Le S, West MD, Harley CB, Andrews WH, Greider CW, Villeponteau B. The RNA component of human telomerase. *Science*, 1995;269:1236-1240
- 12 Kanazawa Y, Ohkawa K, Ueda K, Mita E, Takehara T, Sasaki Y, Kasahara A, Hayashi N. Hammerhead ribozyme mediated inhibition of telomerase activity in extracts of human hepatocellular carcinoma cells. *Biochem Biophys Res Communication*, 1996;225:570-576
- 13 Kondo S, Kondo Y, Li GY, Silverman RH, Cowell JK. Targeted therapy of human malignant glioma in a mouse model by 2-5 A antisense directed against telomerase RNA. *Oncogene*, 1998;16:3323-3330
- 14 Lin JH, Wang MP, Andrews WH, Wydro R, Moser J. Expression efficiency of the human thrombomodulin encoding gene in various vector and host systems. *Gene*, 1994;147:287-292
- 15 Davis LG, Kuehl WM, Battey JF. Basic methods in molecular biology. *Norwalk Connecticut: Appleton Lange*, 1997:189-633
- 16 Piatyszek MA, Kim NW, Weinrich SL, Hiyama K, Hiyama E, Wright WE, Shay JW. Detection of telomerase activity in human cells and tumors by a telomeric repeat amplification protocol (TRAP). *Methods Cell*, 1995;17:1-15
- 17 Tsao SGS, Brunk CF, Pearlman RE. Hybridization of nucleic acids directly in agarose gels. *Analytical Biochem*, 1983;131:365-372
- 18 Levy MZ, Allsopp RC, Futcher AB, Greider CW, Harley CB. Telomere end-replication problem and cell aging. *J Mol Biol*, 1992;225:951-960
- 19 Holt SE, Wright WE, Shay JW. Multiple pathways for the regulation of telomerase activity. *Eur J Cancer*, 1997;5:761-766
- 20 Brown T, Aldous W, Lance R, Blaser J, Baker T, Williard W. The association between telomerase, p53, and clinical staging in colorectal cancer. *Am J Surg*, 1998;175:364-366
- 21 Kyo S, Takakura M, Tanaka M, Kanaya T, Inoue M. Telomerase activity in cervical cancer is quantitatively distinct from that in its precursor lesions. *Int J Cancer*, 1998;79:66-70
- 22 Suda T, Isokawa O, Aoyagi Y, Nomoto M, Tsukada K, Shimizu T, Suzuki Y, Naito A, Igarashi H, Yanagi M, Takahashi T, Asakura H. Quantitation of telomerase activity in hepatocellular carcinoma: a possible aid for a prediction of recurrent diseases in the remnant liver. *Hepatology*, 1998;27:402-406
- 23 Seol JG, Kim ES, Park WH, Jung CW, Kim BK, Lee YY. Telomerase activity in acute myelogenous leukaemia: clinical and biological implications. *Br J Haematol*, 1998;100:156-165
- 24 Asai A, Kiyozuka Y, Yoshida R, Fujii T, Hioki K, Tsubura A. Telomere length, telomerase activity and telomerase RNA expression in human esophageal cancer cells: correlation with cell proliferation, differentiation and chemosensitivity to anticancer drugs. *Anticancer Res*, 1998;18:1465-1472
- 25 Morin GB. Is telomerase a universal cancer target. *J Natl Cancer Inst*, 1995;12:859-860
- 26 Yokoyama Y, Takahashi Y, Shinohara A, Lian ZL, Wan XY, Niwa K, Tamaya T. Attenuation of telomerase activity by a hammerhead ribozyme targeting the template region of telomerase RNA in endometrial carcinoma cells. *Cancer Res*, 1998;58:5406-5410

Edited by Ma JY

Expression of lung resistance protein in patients with gastric carcinoma and its clinical significance

Zhong Min Liu¹, Nan Hai Shou² and Xi Hong Jiang²

Subject headings lung resistance protein/expression; pathology ; gastric cancer; drug resistance

Liu ZM, Shou NH, Jiang XH. Expression of lung resistance protein in patients with gastric carcinoma and its clinical significance. *World J Gastroentero*, 2000;6(3):433-434

INTRODUCTION

The efficacy of chemotherapy in the treatment of cancer patients is often hampered by the presence or appearance of multidrug resistance (MDR) of tumor cells. One of the most important mechanisms of MDR is overexpression of P-glycoprotein (Pgp) which is encoded by *mdr1* gene^[1]. Recently, another MDR-related protein, lung resistance protein (LRP), has been identified^[2]. Our primary study indicated that LRP overexpressed in gastrointestinal carcinoma^[3]. In this paper, the expression of LRP in human gastric carcinoma and its significance were studied.

MATERIALS AND METHODS

Patients

All the 36 patients (21 men, 15 women; aged 32-78 years, mean age 54.6 years) were in-patients of our hospital admitted between September 1997-August 1998 and surgically resected specimens were diagnosed as adenocarcinoma by pathologists. No patients received chemotherapy before operation.

Methods

The expression of LRP in tumor tissues was detected by SABC (streptavidin-biotin complex) immunohistochemical staining as described before^[4], and in 14 of 36 specimens, the LRP was also analysed by flow cytometry (FCM), the matched mucosas served as normal controls, and peripheral blood lymphocytes as negative controls. The specific LRP monoclonal antibody LRP-56 was kindly supplied by Dr. R.J. Scheper

(Department of Pathology, Free University Hospital, Amsterdam, the Netherlands), and the SABC immunohisto-chemical kit was purchased from Boster Biotechnology Company (Wuhan).

RESULTS

Expression of LRP in gastric carcinoma tissues

The LRP positive rate was 72.2% (26/36). LRP immunoreactivity was cytoplasmic, and in some specimens, the interstitial cells were also LRP immunostained. The intensity of the reactions was frequently strong and, in general, most of the cancer cells were LRP-positive in LRP-positive tissues.

Expression of LRP and pathologic parameters

The relationship between LRP expression and pathologic parameters is shown in Table 1. The LRP expression in highly and moderately differentiated carcinoma (9/9) was higher than that in mucoid carcinoma (6/11). There was no association between LRP expression and tumor size, lymphodal involvement, serosal invasion, or TNM stages.

Expression of LRP detected by FCM

LRP expression was at low to moderate levels in gastric cancer tissues (0%-20% in 10 patients, 21%-40% in 2 patients, and 41%-60% in 2 patients), and the mean LRP positivity rate was $29.9\% \pm 9.8\%$, significantly higher than that in normal ($16.9\% \pm 7.5\%$, $t = 3.94$, $P < 0.01$) and negative controls ($1.72\% \pm 0.23\%$, $t = 5.63$, $P < 0.01$).

Table 1 The pathologic parameters and expression of LRP

Pathologic parameters	LRP(+) n	LRP(-) n
Tumor size		
<3 cm	7	2
3 cm-5 cm	11	3
>5 cm	8	5
Differentiation		
well	1	0
moderate	8	0
poor	11	5
mucoid	6	5 ^a
Nodal metastasis		
(-)	15	2
(+)	11	8
Serosal invasion		
(-)	7	3
(+)	19	7
TNM stage		
I	6	1
II	8	3
III	9	3
IV	3	3
N	26	10

^a $P < 0.05$, vs well and moderately differentiated carcinoma. n: number of cases

¹Department of General Surgery, First Teaching Hospital of Taishan Medical College, Tai'an 271000, Shandong Province, China

²Department of General Surgery, Affiliated Hospital of Shandong Medical University, Jinan 250012, Shandong Province, China
Dr. Zhong Min Liu, graduated from Shandong Medical University in 1990, and received Ph. D. degree of General Surgery from Shandong Medical University in 1999, engaged in research of general surgical oncology, having 20 papers published.

Correspondence to: Zhong Min Liu, Department of General Surgery, First Teaching Hospital of Taishan Medical College, 29 Longtan Road, Tai'an 271000, Shandong Province, China

Tel. 0086-538-8224161 Ext.8387, Fax. 0086-538-8223227

Received 2000-01-25 **Accepted** 2000-03-28

DISCUSSION

LRP is the human major vault transporter protein and is suggested to confer anticancer drug resistance. The mechanism that LRP confers MDR is unknown, but concerning the reduced nuclear accumulation of daunorubicin in the LRP-overexpressing MDR cell line 2R120 and the evidence supporting a role of vaults as transporter unit of the nuclear pore complexes, it is tempting to hypothesize that LRP can mediate drug resistance by regulating both the cytoplasmic redistribution and the nucleocytoplasmic transport of drugs^[5]. LRP was overexpressed in ovarian cancer, leukemia, and several cancer cell lines of MDR phenotype, and LRP is of high predictive value for response to chemotherapy and prognosis^[6,7]. Ikeda *et al*^[8] quantitated the level of LRP mRNA expression in 10 gastric cancer cell lines by RT-PCR, and examined the relationship between its level in these cells and their sensitivities to anticancer drugs. LRP mRNA was expressed in all cell lines, and LRP correlated with the resistance to cisplatin. But up to now, there has been no study about LRP expression in specimens of gastric cancer and the relationship between LRP expression and pathologic parameters. Our study revealed that LRP was frequently overexpressed in untreated gastric cancer, suggesting that gastric carcinoma holds high intrinsic resistance. Analysis of LRP can help evaluate the chemosensitivity of patients to anticancer drugs, and choose more effective drugs.

Meanwhile, our results disclosed that LRP positivity rates in well and moderately differentiated carcinomas were 100%, in poorly differentiated cancer was 11/16, and in mucoid carcinoma was 6/11, showing the descending tendency, and LRP positivity rate in patients with well and moderately differentiated adenocarcinoma was higher than that in mucoid carcinoma, which was consistent with the clinical observation that well-differentiated cancer cells have less satisfactory chemosensitivity than poorly differentiated. LRP expression was independent on tumor size, lymph nodal

involvement, serosal invasion, and TNM stage, indicating that these parameters represent the progression of the tumor only, and have no correlation to chemotherapy drug sensitivity. Our previous studies showed that *mdr1* mRNA and MRP were overexpressed in gastric carcinoma^[9,3], and the present study demonstrated that LRP overexpressed in gastric cancer, suggesting that MDR can be mediated by all of them simultaneously, and combined administration of different MDR reversing agents, which can overcome MDR by increasing the intracellular drug accumulation of cancer cells, could achieve a better effect.

REFERENCES

- 1 Fujii H, Tanigawa N, Muraoka R, Shimomatsuya T, Tanaka T. Clinical significance of multidrug resistance and P-glycoprotein expression in patients with gastric carcinoma. *J Surg Oncol*, 1995;58:63-69
- 2 Scheper RJ, Broxterman HJ, Scheffer GL, Kaaijk P, Dalton WS, van Heijningen THM, van Kalken CK, Slovak ML, de Vries EGE, van der Valk P, Meijer CJLM, Pinedo HM. Overexpression of a M_r 11 000 vesicular protein in non-P-glycoprotein mediated multidrug resistance. *Cancer Res*, 1993;53:1475-1479
- 3 Liu ZM, Shou NH. Expression of multidrug resistance related protein and lung resistance protein in gastrointestinal carcinoma and their clinical significance. *Shijie Huaren Xiaohua Zazhi*, 1999;7:95
- 4 Schroeijers AB, Scheffer GL, Flens MJ, Meijer GA, Izquierdo MA, van der Valk P, Scheper RJ. Immunohistochemical detection of the human major vault protein LRP with two monoclonal antibodies in formalin-fixed, paraffin-embedded tissues. *Am J Pathol*, 1998;152:373-378
- 5 Izquierdo MA, Scheffer GL, Flens MJ, Schroeijers AB, van der Valk P, Scheper RJ. Major vault protein LRP-related multidrug resistance. *Eur J Cancer*, 1996;32A:979-984
- 6 Izquierdo MA, van der Zee AGJ, Vermorken JB, van der Valk P, Belien JAM, Giaccone G, Scheffer GL, Flens MJ, Pinedo HM, Kenemans P, Meijer CJLM, de Vries EGE, Scheper RJ. Drug resistance associated marker Lrp for prediction of response to chemotherapy and prognosis in advanced ovarian carcinoma. *J Natl Cancer Inst*, 1995;87:1230-1237
- 7 Izquierdo MA, Shoemaker RH, Flens MJ, Scheffer GL, Wu L, Prather TR, Scheper RJ. Overlapping phenotypes of multidrug resistance among panels of human cancer cell lines. *Int J Cancer*, 1996;65:230-237
- 8 Ikeda K, Oka M, Narasaki F, Fukuda M, Nakamura T, Nagashima S, Terashi K, Sato SI, Kawabata S, Mizuta Y, Soda H, Kohno S. Lung resistance related protein gene expression and drug sensitivity in human gastric and lung cancer cells. *Anticancer Res*, 1998;18:3077-3080
- 9 Liu ZM, Shou NH. Significance of *mdr1* gene-expression in gastric carcinoma tissue. *Shijie Huaren Xiaohua Zazhi*, 1999;7:145-146

Edited by Zhu LH
proofread by Sun SM

A study on arsenic trioxide inducing *in vitro* apoptosis of gastric cancer cell lines

Qin Long Gu¹, Ning Li Li², Zheng Gang Zhu¹, Hao Ran Yin¹ and Yan Zhen Lin¹

Subject headings Arsenic Trioxide (As₂O₃); gastric cancer cell; apoptosis

Gu QL, Li NL, Zhu ZG, Yin HR, Lin YZ. A study on arsenic trioxide inducing *in vitro* apoptosis of gastric cancer cell lines. *World J Gastroenterol*, 2000;6(3):435-437

INTRODUCTION

Cell apoptosis, which involves the biologic regulation of the numbers and vital activity of cells, is an important metabolic process in both normal cells and tumor cells. Delayed process of cell apoptosis will probably lead to a disturbance of metabolism, and occurrence and development of neoplasms. Song *et al* have proved the relationship between apoptosis delay and tumor development through inhibition of cell apoptosis induced by tumor promotor^[1]. Thus, induction of cell apoptosis could be a new strategic measure against tumor. In this paper, we studied whether arsenic oxide will induce apoptosis of gastric cancer cell lines (GCCL) to explore the use of such chemical agent against gastric cancer in clinic.

MATERIALS AND METHODS

Target cells

Human gastric cancer cell lines, MKN45 and SGC7901 (provided by Chinese Academy of Sciences) were used as target cells. Human leukemia cell line K562 and human peripheral blood lymphocytes (PBL) were used as controls. All of cells were cultured in RPMI 1640 medium (GIBICO-BRL), supplemented with 10% heat-inactivated fetal calf serum, 100U/mL penicillin and 100mg/mL streptomycin, in a humidified atmosphere of 95% air/5% CO₂ at 37°C. The numbers of four kinds of cells were maintained at 1 × 10⁶/mL by daily adjusting cell concentration.

¹Department of Surgery, Ruijin Hospital, Shanghai Institute of Digestive Surgery, Shanghai Second Medical University, Shanghai 200025, China

²Shanghai Immunology Institute, Shanghai 200025, China

Dr. Qin Long Gu, graduated from Bengbu Medical College in 1977, acquired MD & PhD degree in surgery from Shanghai Second Medical University in 1994, majoring in research in the field of tumor biological therapy and having 40 papers published.

Correspondence to: Prof. Qin Long Gu, Director, Division of Scientific Research, Deputy Director of Shanghai Institute of Digestive Surgery, 227 Chongqing Nan Road, Shanghai 200025, China. Tel. 0086-10-63841391, Fax. 0086-10-63841391. Email. kyc@koala.ahamu.edu.cn

Received 2000-01-03 **Accepted** 2000-03-12

Product of arsenic trioxide (As₂O₃)

Ai-Lin No.1 containing As₂O₃ was prepared by pharmacy of our hospital. Stock solution was made at the concentration of 1mmol/L with phosphate-buffered saline (PBS) and diluted with RPMI 1640 to working concentration before use.

Cytocide test

MTT[3-(4,5-dimethylthiazoyl-2-yl)2,5-diphenyltetrazoliumbromide]colorimetric analysis was used to measure the cytocide rate of As₂O₃. Well grown cells were collected and were put into 96 well culture plate at 1 × 10⁴/well. As₂O₃ was added to culture plate at the concentration of 5 μmol/well, while cells stuck on wall, 6 duplicate wells were set up in each sample in both experimental and control groups. Cells were cultured for 24 h, 48 h and 72 h separately, MTT(5 mg/mL) was added at 10 μL/well. Acidulated isopropanol was finally added at 100 μL/well-after 2 h culture; values of OD570 were obtained on autocolorimeter. Cytocide rate was calculated by the following formula:

$$\text{Cytocide rate(\%)} = \frac{\text{Control OD} - \text{Experimental OD}}{\text{Control OD}} \times 100\%$$

Apoptosis detection

Cell treatment MKN45 and SGC7901 cells of 10⁶ were treated with As₂O₃ of the concentration of 5 μmol and 10 μmol, or with 5-Fu (0.5 g/L), or without any treatment as control. Cells were harvested after 24 h, 48 h and 72 h culture for apoptosis detection.

TDTlabel Consulting Gregory modified method^[2]: PBS containing 1% formalin was added to cells at 4°C. Thirty min later, it was washed twice with PBS, then reacted with 0.5 μg terminal deoxynucleotidyl transferase (TDT) and 0.5 μmol biotinylated dUTP at 37°C for 30 min. Afterwards it was washed again with PBS, finally labelled by affinitin-fluorescein isothiocyanate (FITC) at room temperature for 30 min. DNA strand will be broken off during apoptosis, which can be labelled by dUTP and the positive observable fluorescences were seen under fluorescent microscope.

Flow cytometry(FCM) assays and fluorescent photographing The stimulating wave length of FCM (Becton Dickson FAC Scan) is 488 nm, FITC detection spectrum is between 80 and 630 nm. A total of 2000 cells were counted. Results were recorded and analyzed automatically.

Preparation of specimen for electronic microscopy
MKN45 cells treated with As_2O_3 of concentration of $10 \mu\text{mol}$ for 72 h were washed with PBS and fetal calf serum; 25% glutaraldehyde was added to fix the cell specimens for 12 h. Then it was washed twice with 0.1 mol/L phosphoric buffer solution; the specimens were fixed with 1% osmic acid, and were dehydrated step by step with alcohol and acetone; then covered up with Epon 812 epoxy resin. Sections were made by ultramicrotome and dyed with uranium acetate and citric acid, and finally observed under transmission electronic microscope.

RESULTS

Cytocidal rate of As_2O_3 on GCCL

Our results showed that As_2O_3 had higher cytotoxicity on GCCL than on K562 ($P < 0.05$). The effect of cytocidal was observed at 24 h after reaction, and it increased with time (Table 1).

Table 1 Cytocidal effects of As_2O_3 ($5 \mu\text{mol}$) on various cell categories (% $\bar{x} \pm s$)

Group	MKN45	7901	K562	PBL
24 h	69.45 ± 11.12	68.27 ± 8.27	51.36 ± 10.25^a	30.31 ± 5.12^b
48 h	71.40 ± 10.15	69.04 ± 11.31	57.11 ± 7.45^a	35.67 ± 4.37^b
72 h	80.53 ± 10.18	82.74 ± 9.14	65.33 ± 8.24^a	39.74 ± 8.27^b

Comparison of cytocidal rate between GCCL and controls by As_2O_3 , $^aP < 0.05$ ($t > 2.2262$), $^bP < 0.01$ ($t > 3.250$).

Table 2 Apoptosis rate(%) of MKN45 by different treatment methods ($\bar{x} \pm s$)

Group	Controls	5-Fu	As_2O_3 1	As_2O_3 2
24 h	4.71 ± 0.36	18.04 ± 1.50	32.33 ± 3.75^a	60.02 ± 7.41^b
48 h	14.90 ± 0.94	24.39 ± 3.45	90.59 ± 10.35^b	97.05 ± 8.24^b
72 h	28.98 ± 3.12	41.47 ± 2.24	98.10 ± 13.24^b	98.75 ± 11.53^b

Comparison of apoptosis rate between As_2O_3 and 5-Fu group, $^aP < 0.05$ ($t > 2.2262$), $^bP < 0.01$ ($t > 3.250$).

GCCL apoptosis rate induced by As_2O_3

As shown in Table 2, apoptosis rates of 2 kinds of GCCL induced by 5-Fu were also obviously higher than natural cell apoptosis rate, of controls, which suggested that antitumor drug can kill tumor cells by inducing cell apoptosis. Nevertheless, a more significant cytocidal effect of As_2O_3 on GCCL was demonstrated in our study compared with that of 5-Fu. We found that apoptosis rate of GCCL induced by As_2O_3 is correlated with the concentration and reaction time of As_2O_3 (Table 3).

Table 3 Apoptosis rate (%) of SGC7901 by different treatment methods ($\bar{x} \pm s$)

Group	Controls	5-Fu	As_2O_3 1	As_2O_3 2
48 h	7.44 ± 0.60	34.28 ± 4.15	51.33 ± 5.16^a	78.31 ± 9.14^b
72 h	30.90 ± 2.54	56.32 ± 4.56	78.15 ± 6.78^a	89.28 ± 10.26^b

Comparison of apoptosis rate between As_2O_3 and 5-Fu group, $^aP < 0.05$ ($t > 2.2262$), $^bP < 0.01$ ($t > 3.250$).

The morphology of GCCL apoptosis under fluorescent microscope:

Under fluorescent microscope, the apoptosis cell can be seen after being terminally labelled (positive), but nonapoptotic cells were not labelled by fluorescein isothiocyanate (negative). The positive staining showed bright green fluorescence. Fluorescent spots appeared in early stage, and these fluorescent bodies gathered like a bunch of grapes in late stage. The cellular volume can be seen shrunken under the microscope.

The morphology of GCCL apoptosis under electronic microscope:

Under the transmission electronic microscope, typical morphologic changes of apoptotic GCCL (mainly cell nucleus) took place after treatment of As_2O_3 . These changes included cell nucleus fixation and shrinkage of GCCL, chromatin condensation, and fragmentation of apoptotic bodies. These changes coexisted.

DISCUSSION

Some researchers have proposed that the uncontrolled growth of neoplasms would be due to the loss of the nature of autoapoptosis rather than over proliferation. Previous studies have proved that there existed autoapoptosis blockage in tumor cells. Lauwers *et al* [3] examined bcl-2 gene in 46 cases of gastric adenocarcinoma by immunochemical method, revealing 75% positivity. Of bcl-2 gene in tumor tissues, which indicated that apoptosis was blocked in gastric cancer. Bcl-2 has been considered as one of survival genes which plays an important role in the specific-inhibition of tumor cell apoptosis [4]. Based on these findings, a new proposal of inducing apoptosis to inhibit tumor growth was introduced [5]. Many factors such as high temperature, cytokine, radiations and all kinds of anti-tumor chemotherapy drugs have a certain effect on inducing tumor cells apoptosis. But some of these are not satisfactory. Our aim is to find a specific-agent which can induce apoptosis of tumor cells. Vollmers *et al* [6] reported the suppressive effects of monoclonal antibody (SC-1) on both *in vitro* proliferation of gastric cancer cell line and growth of a tumor inoculated on nude mice. The inhibition of proliferation of tumor cells was produced through the induction of autoapoptosis, which has been proved by the observation of ultrastructure.

Arsenic is a major composition of traditional Chinese medicine, white arsenic. White arsenic has been considered as a carcinogen. It can inactivate some important enzymes in cells, change the metabolic process and induce chromosome aberration [7]. Zhang *et al* [8] reported a satisfactory result by using As_2O_3 for the treatment of early acute promyelocytic leukemia (APL). Complete remission was 73.3% in patients after the first therapeutic course, and 52.83% in recurrent

patients. The longest remission period of APL patient was over 10 years. No obvious toxic reactions were found when As₂O₃ was given by iv drip, which is appropriate. Similar result has also been obtained by researchers at Shanghai Institute of Hematology of Shanghai Ruijin Hospital^[9,10]. Recently, Zhang *et al*^[11] demonstrated that Arsenic Oxide can inhibit growth of lymphosarcoma cells and induce apoptosis to these cells.

Based on the above studies, we applied As₂O₃ for the treatment of GI solid tumor. The results from *in vitro* study are impressive. Proliferation of MKN45 and SGC7901 was inhibited by As₂O₃ through apoptosis induction. Results also showed that As₂O₃ has a stronger effect of apoptosis induction than 5-Fu. Induction of apoptosis was enhanced with increase of concentration and time of As₂O₃. The question is what the optimal dosage is for clinical use so as to produce maximal effect with no toxicity. Further comprehensive researches are needed to clarify the significance of As₂O₃ for the treatment of GI solid tumors.

REFERENCES

- 1 Song Q, Baxter GD, Kovacs EM, Findik D, Lavin MF. Inhibition of apoptosis in human tumour cells by okadaic acid. *J Cell Physiol*, 1992;153:550-556
- 2 Li NL, Shen BH, Zheng ZX, Zhou GY. Detection of DNA strand breaks in drug induced apoptosis of HL-60 and U937 cells by in situ terminal deoxynucleotidyl transferase. *Zhongliu*, 1996;16:391-393
- 3 Lauwers GY, Scott GV, Karpeh MS. Immuno-histochemical evaluation of bcl-2 protein expression in gastric adenocarcinomas. *Cancer*, 1995;75:2209-2213
- 4 Hockenbery D, Nunez G, Milliman C, Schreiber RD, Korsmeyer SJ. Bcl-2 is an inner mitochondrial membrane protein that blocks programmed cell death. *Nature*, 1990;348:334-336
- 5 Sachs L, Lotem J. Control of programmed cell death in normal and leukemic cells: new implications for therapy. *Blood*, 1993;82:15-21
- 6 Vollmers HP, Dammrich J, Ribbert H, Wozniak E, Muller Hermelink HK. Apoptosis of stomach carcinoma-Hermelink by a human monoclonal antibody. *Cancer*, 1995;76:550-558
- 7 Dong JT, Luo XM. Effects of arsenic on DNA damage and repair in human fetal lung fibroblasts. *Mutat Res*, 1994;315:11-15
- 8 Zhang P, Wang SY, Hu LH, Shi FD, Qiu FQ, Hong LJ, Han XY, Yang HF, Song YZ, Liu YP, Zhou J, Jin ZJ. Treatment of acute promyelocytic leukemia with intravenous arsenic trioxide. *Zhonghua Xueyexue Zazhi*, 1996;17:58-60
- 9 Chen GQ, Zhu J, Shi XG, Ni JH, Zhong HJ, Si GY, Jin XL, Tang W, Li XS, Xong SM, Shen ZX, Sun GL, Ma J, Zhang P, Zhang TD, Gazin C, Naoe T, Chen SJ, Wang ZY, Chen Z. In vitro studies on cellular and molecular mechanisms of arsenic trioxide in the treatment of acute promyelocytic leukemia: As₂O₃ induces NB4 cell apoptosis with down regulation of bcl-2 expression and modulation of PML-RAR α /PML proteins. *Blood*, 1996;88:1052-1061
- 10 Sun YP, Chen GQ, Cai X, Huang Y, Sheng SY, Jia PM, Sheng YL, Yu Y, Chen SJ, Wang ZY, Chen Z. Phenylarsine oxide induces apoptosis in acute promyelocytic leukemia cell line NB4. *Aizheng*, 1999;18:1-4
- 11 Zhang W, Ohnishi K, Shigeno K, Fujisawa S, Naito K, Nakamura S, Takeshita K, Takeshita A, Ohno R. The induction of apoptosis and cell cycle arrest by arsenic trioxide in lymphoid neoplasms. *Leukemia*, 1998;12:1383-1391

Edited by Zhu LH
proofread by Sun SM

Relationship between collagen IV expression and biological behavior of gastric cancer

Zhen Ning Wang and Hui Mian Xu

Subject headings stomach neoplasms; collagen IV; biological behavior; immunohistochemistry

Wang ZN, Xu HM. Relationship between collagen IV expression and biological behavior of gastric cancer. *World J Gastroenterol*, 2000;6(3): 438-439

INTRODUCTION

Conceivably the presence of basement membrane (BM) in a neoplasm might be a result of interaction of tumor cells with the extracellular matrix. Collagen IV is one of the major intrinsic components of BM. Recent study^[1] has shown that collagen IV has cell adhesion function and is involved in the process of tumor invasion and metastasis, including colorectal cancer^[2] and breast cancer. But there are few systematic studies on gastric cancer and the results are equivocal. In this study we evaluated the expression of collagen IV immunohistochemically in 148 advanced gastric cancer cases in an attempt to clarify the relationship between the patterns of expression and the biological behavior of gastric cancer.

MATERIALS AND METHODS

Patients

Surgical specimens (148) of gastric carcinomas resected at the Oncology Department of China Medical University from 1988 to 1992 were studied. Routinely formalin-fixed and paraffin-embedded tissue blocks were sectioned at 5 μ m thickness. HE-stained slides were also collected and available.

Immunohistochemistry

The avidin-biotin-peroxidase complex (ABC) method by Hsu *et al*^[3] was applied. Briefly, paraffin sections were deparaffinized, dehydrated and pretreated with pepsin (0.1% in 0.1M-HCl for one hour at 37°C) to restore the immunoreactivity to type IV collagen. After blocking of endogenous peroxidase with 0.3% H₂O₂ in methanol and

washing in phosphate-buffered saline (PBS) for 3 \times 5 min, the sections were incubated with anti-collagen IV monoclonal antibody (Dako Putts Co., diluted 1:75) overnight at 4°C in a moist chamber. After washing in PBS the sections were incubated with secondary antibody for 30 min and ABC for 60 min at 37°C, then sections were stained with 0.05% DAB freshly prepared to visualize the immunoreactivity. Tumors were classified as "positive" with regard to the immunoreactivity for collagen IV when there was unequivocal immunostaining of the matrix components at least in one representative area of the tumor.

Statistical analysis

Statistical analysis was performed by χ^2 test.

RESULTS

Collagen IV stained the basement membrane of normal gastric glands and vessels and also the basement membrane of the smooth muscle cells in the muscular layers of the gastric wall.

Relationship between collagen IV expression and histological type, growth pattern of gastric cancer

Seventy patients (47%) has continuous or, more frequently, disrupted linear structures around cancerous gland ducts or solid nests of tumor cells. The positive rates in undifferentiated or signet ring cell cancers were much lower than those in other cancers ($P < 0.01$). Fifty-five percent of carcinomas with the nest-fashioned growth pattern showed collagen IV positive staining (Table 1), which was slightly lower than the percentage of collagen-IV positive carcinomas with mass-fashioned growth pattern, but significantly higher than that of diffuse-gastric carcinomas ($P < 0.01$).

Relationship between the distribution of collagen IV and liver metastasis of gastric cancer

The distribution patterns of collagen IV in cancer tissue in gastric wall are quite different. Collagen IV was seen less often in the deep layer than in the mucosa. Collagen IV positive BM was found in 70 (47%) of 148 patients in the mucosa and only 36 (24%) in the deep layer of stomach. Based on the difference of collagen IV distribution, we divided the cases into three groups as follow: Group A, tumors positive for collagen IV in both mucosa and deep layer; Group B, tumors positive for collagen IV in mucosa but negative in deep layer; Group C,

Oncology Department, China Medical University, Shenyang 110001, Liaoning Province, China

Dr. Zhen Ning Wang, graduated from China Medical University as a postgraduate in 1996, lecturer of oncology, major in oncology, having 4 papers published.

Supported by National Clinical Major Program of Ministry of Public Health, No.97100250

Correspondence to: Dr. Zhen Ning Wang, Oncology Department, China Medical University, Shenyang 110001, Liaoning Province, China
Tel. 0086-24-23256666 Ext.6227

Email: josie@pub.sy.ln.cn

Received 2000-01-05 **Accepted** 2000-02-26

tumors negative for collagen IV. From Table 2, we can find that liver metastasis rate in Group A is much higher than that in Group B or C ($P < 0.01$).

Table 1 Relationship between collagen IV expression and histological type, growth pattern of gastric cancer

Type	Number	Collagen IV n(%)	
		(+)	(-)
Growth pattern			
Mass-like	56	43(77)	13(23)
Nest-like	38	21(55)	17(45)
Diffuse	54	7(13)	47(87)
Histological type			
Well differentiated	37	30(81)	7(19)
Moderately differentiated	22	13(59)	9(41)
Poorly differentiated	23	10(43)	13(57)
Undifferentiated	27	3(11)	24(89)
Signet-net cell	25	2(8)	23(92)
Mucoid	14	12(86)	2(14)

Table 2 Relationship between the distribution of collagen IV and liver metastasis of gastric cancer

Liver-metastasis	Group A n = 36(%)	Group B n = 34(%)	Group C n = 78(%)
(+)	10(28)	2(6)	1(1)
(-)	26(72)	32(94)	77(99)

The blood vessels BM in gastric wall are also positively stained

In differentiated carcinoma, a large number of blood vessels were observed in the vicinity of cancer glands and collagen IV was localized around the blood vessels and cancer glands. But in poorly differentiated carcinoma, only a small number of blood vessels were distributed sporadically in stroma. In addition, vasoinvasion of tumor cells were highlighted by collagen IV immunostaining of the blood vessels BM.

DISCUSSION

Normal basement membrane is one of the biological barriers to tumor invasion and metastasis. In carcinomas, a dynamic interaction occurs at the interface between tumor cells and the surrounding extracellular matrix components. Tumor cells not only destroyed the basement membrane by producing collagenase, including the specific type IV collagenase, but also synthesize the components of basement membrane^[4]. And also as a host reaction to the invading tumor, extracellular matrix components may be deposited around the tumor cells. The appearance of these components may symbolize the characteristic of the tumor and reflect its biological behavior. Collagen IV is one of the major components of the basement membrane, Burtin *et al*^[5] showed that expression of collagen IV was related to the differentiation of the colorectal cancer.

Histological growth pattern could be considered as the objective indicator of the biological behavior of gastric cancer. In this study, we found that the presence of collagen IV containing basement membrane was closely related to the growth

pattern. In mass or nest-fashioned growth pattern of gastric carcinomas, continuous or disrupted linear structures stained positively for collagen IV can be seen around cancerous glands or solid nests of tumor cells. But only a few scattered spots or patches were positively stained in diffuse gastric carcinomas, most of which were undifferentiated or signet ring cell carcinomas. Our study demonstrated that the attenuation or absence of collagen IV expression was frequently seen in poorly differentiated and diffusely infiltrating gastric cancers. That is, the loss and irregular distribution of collagen IV expression could be considered as a biological marker of cancer cells which had strong invading ability. This finding may be concerned with these tumor cells which could produce collagenase with higher activity or had poorer potential of collagen IV synthesis.

The prognosis of patients with advanced gastric cancer is poor because the likelihood of recurrence is high. The most common patterns of recurrence are peritoneal implantation and liver metastasis. According to our study, the distribution patterns of collagen IV are related to liver metastasis in gastric cancer. Positive expressions of collagen IV in mucosa and deep layer of gastric cancer are accompanied by much higher incidence of liver metastasis. Vascular spreading of gastric cancer, which is different from direct invasion, is a multi-step process in which cells must migrate from the primary tumor and invade blood vessels. David L *et al*^[6] found that the expression of collagen IV was related to invading potential of tumor cells to blood vessels. All these findings support the hypothesis that collagen IV may play an important role in the metastatic process after migration from the primary tumor. The principal mechanism is an interesting subject for further studies. In conclusion, collagen IV-positive basement membrane in the deep layer of gastric wall in cancer tissue might be a risk factor for liver metastasis. In addition, collagen IV immunostaining facilitates recognition of vasoinvasion by highlighting the basement membrane of vessels.

REFERENCES

- 1 Martinez-Hernandez A, Amenta PS. The basement membrane in pathology. *Lab Invest*, 1983;48:656-677
- 2 Havenith MG, Arends JW, Simon R, Volovics A, Wiggers T, Bosman FT. Type IV collagen immunoreactivity in colorectal cancer. Prognostic value of basement membrane deposition. *Cancer*, 1988;62:2207-2211
- 3 Hsu SM, Raine L, Fanger H. A comparative study of the peroxidase-antiperoxidase method and an avidin biotin complex method for studying polypeptide hormones with radioimmunoassay antibodies. *Am J Clin Pathol*, 1981;75:734-738
- 4 Liotta LA, Terranova VP, Lanzer WL, Russo R, Seigel GP, Garbisa S. Basement membrane attachment and degradation by metastatic tumor cells. In: Kuehn K, New trends in basement membrane research. *New York: Raven*, 1982:277-286
- 5 Burtin P, Chavanel G, Foidart JM, Martin E. Antigens of the basement membrane and the peritumoral stroma in human colonic adenocarcinomas: an immunofluorescence study. *Int J Cancer*, 1982;30:13-20
- 6 David L, Nesland JM, Holm R, Sobrinho-Simoes M. Expression of laminin, collagen IV, fibronectin, and type IV collagenase in gastric carcinoma. An immunohistochemical study of 87 patients. *Cancer*, 1994;73:518-527

Edited by You DY
proofread by Sun SM

The effect of mast cell on the induction of *Helicobacter pylori* infection in Mongolian gerbils

Jing Chi¹, Miao Lu¹, Bao Yu Fu¹, S Nakajima² and T Hattori²

Subject headings diseases models, animal; Mongolian gerbils; *Helicobacter pylori*; mast cell; *Helicobacter* infections

Chi J, Lu M, Fu BY, Nakajima S, Hattori T. The effect of mast cell on the induction of *Helicobacter pylori* infection in Mongolian gerbils. *World J Gastroentero*, 2000;6(3):440-441

INTRODUCTION

Since 1982, *Helicobacter pylori* (Hp) has been successfully isolated and cultured^[1], and the fact many diseases such as gastritis, peptic ulcer, gastric carcinoma and gastric lymphoma were related to Hp, and Hp as an etiological organism, has attracted much attention. In 1991 Yokata *et al*^[2] first induced the Hp infection in Mongolian gerbils. From then on researches on Hp infection and its eradication exploded worldwide. Nakajima *et al*^[3] reported that mast cells were increased in gastric mucosa and submucosa of patients with Hp infection and found degranulated mast cells in these tissues. Now it is known that high affinity IgE and Fc segment receptors exist on the mast cell surface. When IgE bound to these receptors, mast cells degranulated and then many kinds of bioactive mediators were secreted so that the inflammatory process could be effected. Therefore it is extremely important to understand the relationship between degranulation of mast cells in the mucosa infected with Hp and the inflammatory response, and to conjecture of the effect of mast cells on the pathogenesis of Hp infection. This study observed the inflammation of gastric mucosa and the morphology, density, distribution and degranulation of mast cells in the infected gerbils using the histochemical or immunohistochemical methods and electron microscopy to elucidate the effect of mast cells on the pathogenesis of Hp infection.

¹Department of Gastroenterology, First Affiliated Hospital of China Medical University, Shenyang 110001, China

²First Department of Pathology, Shiga, University Of Medical Sciences, Japan

Dr. Jing Chi, graduated and received medical bachelor degree from China Medical University, awarded master, and doctor degree in 1992 and 1999 respectively, fifteen papers have been published since graduation.

Correspondence to: Jing Chi, Department of Gastroenterology, First Affiliated Hospital of China Medical University, Shenyang 110001, Liaoning Province, China

Tel. 0086-24-23256666 Ext.6199

Received 2000-01-16 **Accepted** 2000-02-28

MATERIALS AND METHODS

Animals

Thirteen male Mongolian gerbils infected with Hp for 1 mo to 3 mos were allocated to the experimental group, while 5 male Mongolian gerbils with out Hp infection to the control group.

The induction of animal models

Six-week-old specific pathogen-free/sea male Mongolian gerbils and Hp ATCC 43504 were used. The gerbils were subjected to ATCC 43504 and ethanol treatment according to the method described by Hirayama *et al*^[4]. Normal subjects were treated with the same amount of Brucella Broth. The gerbils infected with Hp were injected with BrdU subcutaneously one hour before sacrifice. A portion of the stomach was fixed in MFAA^[5] and embedded in paraffin, and cut in sequential 3 µm-4 µm section for light microscopy; the remainder was fixed in 25 g/L Glutaldehyde, serially dehydrated in ethanol, postfixed in 10 g/L osmium acid, embedded in Epon, and cut in 60 nm ultrathin sections for electron microscopy.

Staining of mast cells

Alcian blue (AB1.0)/ PAS staining The immunohistochemical staining of anti-mast cell monoclonal antibody, MSRM4 (produced by Moredum Scientific Limited Co. Britain, diluted 200 folds) by LsAB method was applied.

Double-staining AB staining was followed by anti-BrdU Ab and anti-CD3 lymphatic Ab complex staining to observe the cellular marking rate of mast cells in S-phase and their relationship with T lymphocytes.

Staining for electron microscopy with uranyl acetate and lead citrate

Bactericidal treatment Positive group was defined at 6 mos after Hp infection and then was cured with triad treatment (Lansoprazole, Ampicillin, Clarithromycin) for 2 wks continuously. At wk 4, wk 8 and wk 12 after withdrawal of medication, the gerbils were sacrificed to observe the changes in distribution, amount and degranulation of mast cells before and after bactericidal treatment.

Counting of mast cells At the magnification employed (× 400), the positive mast cells in the mucosa and the epithelial layer in gastric antrum and body in 5 consecutive areas were counted and

their mean values represented the density of positive cells in this particular area. All the data according to different areas were divided into different groups for further statistic treatment and analysis compared with the normal subjects.

RESULTS

Light microscopy

Mast cells appeared blue stained with AB/ PAS and brown when immunohistochemical staining was used. Positive mast cells, filled with granules in cytoplasm, dispersed in epithelium, lamina propria and submucosa and also commonly in muscular layer, having a close relationship with the vessels and nerves in submucosa and muscular layer. All of the above picture rarely appeared in the gastric tissues of normal gerbils. At 2 wk after *Hp* infection, the mast cells began to increase in amount with a tendency of inflammatory-dependence, significantly different from the normal group ($P < 0.001$). On the double staining section, there existed varied amounts of blue heterophilic granules in the cytoplasm and the nucleus was brown. The mast cells with these morphologic characteristics corresponded to the cells in S-phase. The increase of cells in S-phase signified the active hyperplasia in the progression of inflammation. The double staining of CD3 and mast cells indicated that a great deal of mast cells were around the lymphatic follicles in which CD3 existed. The amount of mast cells decreased 1 mo after bactericidal treatment and recovered to the normal level 3 mos after treatment.

Electron microscopy

Under the normal circumstances, the specific high-electron density granules in cells were stable and existed independently, while in inflammatory state the mast cells were activated to degranulate and form vacuoles and tended to be vacuolated after the fusion of vacuoles.

DISCUSSION

It is well known that mast cells exist widely in trachea, digestive tract, skin and many other organs and play an important role in the pathogenesis of allergic reaction characterized by bronchial asthma and urticaria. Recent studies on mast cells found direct or indirect evidences to reveal the close relationship between the mast cells and the injury of gastric mucosa^[6]. The mast cells located in human gastroenteral tract and induced by pathogen or some antigens, may secrete bioactive substances such as

histamine and prostaglandin, which increase the secretion of gastric acid, and then trigger a series of events: the injury of tissues and the inflammation of mucosa. The rapid development in recent years on the cell culture and molecular biology provides the possibility of explaining that various cytokines can cause the activation and proliferation of mast cells and mast cells can produce and secrete these cytokines. TNF α , GM-CSF, IL-6 and IL-8 can act as the precursor in the local inflammatory reaction which leads to the infiltration of inflammatory cells, and at the same time modulates the development and proliferation of themselves-the autoregulative process. The results of this study showed that the mast cells in gastric mucosa with infection of *Hp* increased significantly, the infiltration of lymphatic cells depended on the appearance of mast cells and the conspicuous increase of degranulation of mast cells in inflammatory areas was related to the degree of gastritis. All of the above supported the fact that mast cells play a role in the occurrence and development of the pathogenicity of *Hp*. It has been reported that some of the mast cells have the function of extending and movement so that the mast cells can penetrate the basal membrane and move toward the interepithelial space. During the moving process, degranulation appears gradually, which results in the phenomena of vacuolation. Therefore, some researchers believe that mast cells of mucosa-type are the active state of mast cells of conjugated-type. At present, the mechanism of the degranulation of mast cells remains unclear. The relationship between mast cells and *Hp* infection and the effect of the mediator secreted by mast cells on the pathophysiology of *Hp* infected gastric diseases need further investigation.

REFERENCES

- 1 Warren JR. Unidentified curved bacilli on gastric epithelium in active chronic gastritis. *Lancet*, 1983;1273-1275
- 2 Yokota K, Kurebayashi Y, Takayama Y, Hayashi S, Isogai H, Isogai E, Imai K, Yabana T, Yachi A, Oguma K. Colonization of *Helicobacter pylori* in the gastric mucosa of Mongolian gerbils. *Microbiol Immunol*, 1991;35:475-480
- 3 Nakajima S, Krishnan B, Ota H, Segura AM, Hattori T, Graham DY, Genta RM. Mast cell involvement in gastritis with or without *Helicobacter pylori* infection. *Gastroenterology*, 1997;113:746-754
- 4 Hirayama F, Takagi S, Yokoyama Y, Iwao E, Ikeda Y. Establishment of gastric *Helicobacter pylori* infection in Mongolian gerbils. *J Gastroenterol*, 1996;31(Suppl 1X):24-28
- 5 Nakajima S, Arizono N, Hattori T, Bamba T. Increase in mucosal and connective tissue type mast cells in the stomach with acetic acid induced ulcer in rat. *APMIS*, 1996;104:19-29
- 6 Scudamore CL, McMillan L, Thornton EM, Wright SH, Newlands GFJ, Miller HRP. Mast cell heterogeneity in the gastrointestinal tract. *Am J Pathol*, 1997;150:1661-1672

Effect of *Helicobacter pylori* infection on gastric epithelial cell proliferation

Hong Gao, Ji Yao Wang, Xi Zhong Shen and Jian Jun Liu

Subject headings *Helicobacter pylori*; cell proliferation; vacAs1a strain; gastric epithelial cell

Gao H, Wang JY, Shen XZ, Liu JJ. Effect of *Helicobacter pylori* infection on gastric epithelial cell proliferation. *World J Gastroentero*, 2000;6(3):442-444

INTRODUCTION

Helicobacter pylori (*H. pylori*) infection is one of the main pathogens of chronic gastritis and duodenal ulcer (DU), and it may be considered as a risk factor in the incidence of gastric cancer^[1]. *H. pylori* infection may lead to the anomaly of gastric epithelial cell proliferation which is closely related to the development of gastric cancer. Vacuolating cytotoxin (VacA) is an important virulence and vacA subtype determines the toxic activity^[2]. According to its signal sequence, it can be grouped into type s1a, s1b, s1c and s2^[3,4]. Strains harboring vacAs1a are more closely related with digestive diseases^[5] and may be the strains with high toxicity. The effect of *H. pylori* infection on gastric epithelial cell proliferation depends on the vacA subtype^[6]. The report of the effect of strains with vacAs1a on gastric epithelial cell proliferation has not been found in China. We particularly study the effect of this strain in order to reveal whether the patients suffering from *H. pylori* infection have accelerated proliferation of gastric epithelium compared with non-infected patients, and whether the strains harboring vacAs1a have more severe effect on it.

MATERIALS AND METHODS

Patients

Patients suffering from dyspepsia underwent diagnostic endoscopy and biopsy. Those taking H₂ antagonists, proton pump inhibitors, non-steroidal anti-inflammatory drugs, antibiotics or bismuth salts were excluded from the study. Patients with gastric ulcer or cancer were also excluded. Eighty-four patients with chronic gastritis (CSG) and 16 patients with duodenal ulcer (DU) with mean age of 46.45 years (22 years - 76 years) entered the

study. Biopsy specimens were taken from the site approximately 2 cm-5 cm from the pylori.

Histology and diagnosis of *H. pylori* infection

Two antral and one corpus biopsy specimens were routinely processed, and stained with haematoxylin and eosin. Examine *H. pylori* by fast urease test, modified Giemsa stain and culture. At least two positive results of test regarded as *H. pylori* infection.

Immunohistochemistry

An antral biopsy specimen was put immediately into RPMI containing bromodeoxyuridine (BrdU, 5 g/L). It was immersed in a waterbath for 60 min at 37°C and then fixed in Carnoy solution. Sections were stained with anti-BrdU antibody by ABC technique. The nuclei of proliferative cell were stained. Five hundred epithelial cells were counted and the number of positively stained epithelial cell nuclei expressed in percentage as labelling index (LI%). All sections were examined by the same person who was unaware of the subject's *H. pylori* status.

Polymerase chain reaction

H. pylori DNA was extracted routinely, vacAs1a amplified by PCR, 50 µL reaction solution contains the following: 1 × reaction buffer, dNTP mixture (0.2mM each), vacAs1a primers (0.2µM each), 1.25 unit Taq DNA polymerase and 4 µL template. PCR program comprises predenaturation at 94°C for 5 min, followed by 37 cycles of 1 min at 94°C, 90s at 52°C, 45s at 72°C, and a final incubation at 72°C for 7 min. PCR products were inspected by electrophoresis on 2% agarose gels stained by ethidium bromide. It is regarded as vacAs1a positive if a clear band can be seen at 190bp. Primers: 5'-GTCAGCATCACACCGCAAC-3', 5'-CTGCTTG-AATG CGCCAAAC-3'^[3].

Statistics

LI% is transformed to arcsin LI% 1/2, *t* test, Chisquare and multi variate linear-regression analysis were used to deal with the data.

RESULTS

The prevalence of *H. pylori* infection in CSG patients was 50%, and that of DU reached 93.75% (*P*<0.01), but the disparity of vacAs1a proportion between *H. pylori* positive CSG and DU was not significant (43.59% vs 58.33%, *P*>0.05).

There is significant difference on LI% between

Department of Internal Medicine, Zhongshan Hospital, Shanghai Medical University, Shanghai 200032, China

Hong Gao, graduated from Shanghai Medical University in 1999, master, instructor in digestive medicine.

Correspondence to: Dr. Ji Yao Wang, Department of Internal Medicine, Zhongshan Hospital, Shanghai Medical University, 180 Fenglin Road, Shanghai 200032, China
Tel. 0086-21-64041990
Email: <jywang@shmu.edu.cn

Received 2000-01-07 Accepted 2000-02-29

CSG and DU ($P < 0.05$), but considering the different prevalence of *H. pylori* infection, we got negative result ($P > 0.05$) from comparing the LI% between positive cases of CSG and DU. The results (Table 1) of analyzing the effect of *H. pylori* infection and its different strains on proliferation, showed that patients with *H. pylori* had higher LI% ($6.14\% \pm 1.21\%$) than *H. pylori* negative ones ($2.43\% \pm 0.61\%$, $P < 0.001$). Patients harboring vacA s1a strains had significantly higher gastric epithelial cell proliferation LI% ($n = 24$, $8.00\% \pm 1.46\%$) than those with non-vacA s1a strains ($n = 27$, $4.51\% \pm 0.86\%$, $P < 0.02$) or noninfected patients ($P < 0.001$).

The sections were graded into mild, moderate and severe according to the extent of inflammation and intestinal metaplasia. Statistics shows a close relationship between inflammation and *H. pylori* status ($P < 0.005$), however it is negative on metaplasia ($P > 0.05$). No significant relationship was found between inflammation and vacA s1a genotype ($P > 0.05$).

The results show that inflammation and neutrophil infiltration were closely related to epithelial cell proliferation ($P < 0.001$), but not to metaplasia ($P > 0.05$). Multivariate linear-regression analysis shows that among the factors, such as age, sex, DU, inflammation, neutrophil infiltration, intestinal metaplasia, vacA s1a strains, non-vacA s1a strains and so on, vacA s1a strain and inflammation are the independent factors influencing the epithelial cell proliferation.

Table 1 BrdU LI% of the patients ($\bar{x} \pm s$)

	LI%	case number
H.pylori-positive	6.14 ± 1.21^a	57 [§]
vacA s1a positive	8.00 ± 1.46^{ae}	24
vacA s1a negative	4.51 ± 0.86^c	27
H.pylori-negative	2.43 ± 0.61	43

^a $P < 0.001$ vs *H. pylori* negative patients; ^c $P < 0.01$ vs *H. pylori* negative patients; ^e $P < 0.02$ vs non-vacA s1a *H. pylori* patients; [§]vacA s1a were not examined in 6 cases because of loss of specimens.

Table 2 Multivariate linear-regression analysis

LI%	coefficient	SD	t	P> t	95%confidence interval
vacA s1a	4.47	1.37	3.27	0.002	1.76 7.19
inflammatory coefficient	3.89	1.21	3.22	0.002	1.49 6.30
	4.50	1.89	2.38	0.019	0.75 8.26

DISCUSSION

The genesis of gastric cancer is the result of long-term effect of multiple factors of environment and host. Epidemiological investigation and histological evidences showed that *H. pylori* infection was related to gastric cancer independently. *H. pylori* infection induced gastric epithelial cell proliferation, increase of mitosis and mutation^[7]. Because of the unstability of the genome of the proliferative cell, hyperproliferation increases the

possibility of DNA damage and aneuploidy. Dysplasia may evolve into carcinoma if damaged DNA cannot be repaired on time or fail in promoting the apoptosis system. Accelerated cellular proliferation rate is the property of malignant tissue and has been confirmed in gastric carcinoma^[8].

The genesis of most gastric adenocarcinomas is believed to follow a series of defined histologic steps from normal gastric mucosa to chronic gastritis, atrophic gastritis, intestinal metaplasia, and neoplasia^[9]. It has been postulated that *H. pylori* plays a causative role at the early phases in this chain of malignant progression^[10]. Therefore, we studied CSG and DU patients (part of them had intestinal metaplasia).

The prevalence of *H. pylori* in DU patients (93.75%) was much higher than that in CSG (50%) which supports the conclusion that *H. pylori* is a closely associated pathogen of DU.

It is reported that gastric epithelial cell proliferation in *H. pylori* associated gastritis patients increased prominently compared with normal control subjects and patients with *H. pylori* negative chronic gastritis, and it reduced after *H. pylori* was eradicated^[11-16]. Our results are in agreement with these reports.

No significant difference was found on BrdU LI% between *H. pylori* positive DU and CSG patients which reveals that the existence of DU does not alter the status of proliferation, some factors other than hyperproliferation such as increased apoptosis may play an important role, in the genesis of DU by keeping the dynamic equilibrium of the epithelium^[17-20]. But some CSG patients cannot keep efficiently this equilibrium, in other words, the proliferation increases without corresponding apoptosis, DNA is prone to be attacked by other carcinogens, resulting in canceration.

About 50% population infected by *H. pylori*, gastric cancer or DU only occurred in a small portion of them. This may be associated with many factors, one of the determinants is the virulence of the strain infected.

Compared with the non-vacA s1a strains infected patients, epithelial cell proliferation of the vacA s1a strains infected patients was much higher. So vacA s1a *H. pylori* strains may be able to promote the epithelial cell proliferation. Multivariate linear-regression shows that vacA s1a strain is an independent influencing factor, which further supports the conclusion that vacA s1a strain is of high virulence. In view of the importance of hyperproliferation during the genesis of gastric cancer, vacA s1a strain may play a critical role in it.

There is much difference on the constitution of the vacA subtype of *H. pylori* according to the reports from different areas. The proportion of vacA s1a strains varied greatly^[3,21]. There have been few reports on the genotype of vacA in China. She *et al* reported the relationship between 60 *H. pylori* strains and the alimentary diseases. The relevance

ratios of vacAs1 in gastric cancer, peptic ulcer and chronic gastritis were 87.5%, 78.9% and 9.1% respectively^[22]. There was obvious geographical discrepancy in the distribution of *H. pylori* vacA subtype.

We found that intestinal metaplasia had nothing to do with *H. pylori* infection, this result corresponds with the report of Cahill *et al.* We also found that intestinal metaplasia was not correlated with proliferation, which differs with some other reports in its clinical importance, the relationship with gastric cancer and effect on cell proliferation. Therefore, we cannot draw conclusion that intestinal metaplasia is not associated with proliferation. Further studies will be conducted.

The mechanism that *H. pylori* and its different strains accelerate proliferation is not clear. Ricci *et al* found VacA can inhibit cell proliferation *in vitro*, while cytotoxin-associated gene (CagA) does not affect proliferation^[23]. *H. pylori* can induce proliferation *in vivo*, so *H. pylori* may act by this suggesting that *H. pylori* based on its ability of inciting inflammatory reaction, influencing the gastrin secretion, but not the direct action of virulences to exact the effect on cell proliferation.

Inflammation and neutrophil filtration are both associated with *H. pylori* infection. That means *H. pylori* infection can arouse acute and chronic inflammation. Accelerated proliferation is related to the extent of inflammation, and the latter is highly related to *H. pylori* infection. This points out that *H. pylori* infection may promote proliferation by inflammation, which was once reported by Lynch *et al*^[11,12]. It is also shown that inflammation acts on proliferation as an independent factor. *H. pylori* infection affects proliferation at least partly by inflammatory action. On the contrary patients harboring vacAs1a strains have similar inflammatory response to those with non-vacAs1a strains, but their ability of inducing proliferation differed. Thereby *H. pylori* may promote proliferation by inflammation, and vacAs1a strains may act by the mechanism other than inflammation, such as the increase of ammonia^[24], gastrin^[25], and the decrease of ascorbic acid concentration^[26,27].

We found that *H. pylori* infection was closely related to gastric epithelial cell proliferation, and the vacAs1a strains had higher activity. The vacAs1a strain and extent of inflammation affect proliferation independently. But the effect of *H. pylori* and its different strains on apoptosis is not clear and needs further studies. Besides, *H. pylori* can be typed into m1 and m2 strains according to vacA middle sequence, and positive or negative cagA. They may have different effects on proliferation and apoptosis, these may play important roles in the pathogenicity of *H. pylori*.

REFERENCES

- 1 Parsonnet J, Friedman GD, Vandersteen DP, Chang Y, Vogelstein JH, Orentreich N, Sibley RK. Helicobacter pylori infection and the risk of gastric carcinoma. *N Engl J Med*, 1991;325:1127-1131
- 2 Atherton JC. The clinical relevance of strain types of Helicobacter pylori. *Gut*, 1997;40:701-703
- 3 Atherton JC, Cao P, Peek RM, Tummuru MKR, Blaser MJ, Corer TL. Mosaicism in vacuolating cytotoxin alleles of Helicobacter pylori. Association of specific vacA types with cytotoxin production and peptic ulceration. *J Biol Chem*, 1995;270:17771-17777
- 4 van Doorn LJ, Figueiredo C, Sanna R, Pena S, Midolo P, Enders KWNG, Atherton JC, Blaser MJ, Quint WGV. Expanding allelic diversity of Helicobacter pylori vacA. *J Clin Microbiol*, 1998;36:2597-2603
- 5 Atherton JC, Peek RM, Tham KT, Cover TL, Blaser MJ. Clinical and pathological importance of heterogeneity in vacA, the Vacuolating cytotoxin gene of Helicobacter pylori. *Gastroenterology*, 1997;112:92-99
- 6 Peek RM, Moss SF, Tham KT, Pérez-Pérez GI, Wang S, Miller GG, Atherton JC, Holt PR, Blaser MJ. Helicobacter pylori CagA⁺ strains and dissociation of gastric epithelial cell proliferation from apoptosis. *J Natl Cancer Inst*, 1997;89:863-868
- 7 Ames BN, Gold LS. Too many rodent carcinogens: mitogenesis increases mutagenesis. *Science*, 1990;249:970-971
- 8 Ohyama S, Yonemura Y, Miyazaki I. Proliferative activity and malignancy in human gastric cancers. Significance of the proliferation rate and its clinical applications. *Cancer*, 1992;69:314-321
- 9 Correa P. Human gastric carcinogenesis: a multistep and multifactorial process—first American cancer society award lecture on cancer epidemiology and prevention. *Cancer Res*, 1992;52:6735-6740
- 10 Cahill RJ, Kilgallen C, Beattie S, Hamilton H, O'Morain C. Gastric epithelial cell kinetics in the progression from normal mucosa to gastric carcinoma. *Gut*, 1996;38:177-181
- 11 Lynch DAF, Mapstone NP, Clarke AMT, Sobata GM, Jackson P, Morrison L, Dixon MF, Quirke P, Axon ATR. Cell proliferation in Helicobacter pylori associated gastritis and the effect of eradication therapy. *Gut*, 1995;36:346-350
- 12 Hibi K, Mitomi H, Koizumi W, Tanabe S, Saigenji K, Okayasu I. Enhanced cellular proliferation and p53 accumulation in gastric mucosa chronically infected with Helicobacter pylori. *Am J Clin Pathol*, 1997;108:26-34
- 13 Abdel-wahab M, Attallah AM, Elshal MF, Abdel-Raouf M, Zalata KR, El-Ghawalby N, Ezzat F. Cellular proliferation and ploidy of the gastric mucosa: the role of Helicobacter pylori. *Hepato-Gastroenterology*, 1997;44:880-885
- 14 Murakami K, Fujioka T, Kodama R, Kuhota T, Tokieda M, Nasu M. Helicobacter pylori infection accelerates human gastric mucosal cell proliferation. *J Gastroenterol*, 1997;32:184-188
- 15 Eraser AG, Sim R, Sankey EA, Dhillon AP, Pounder RE. Effect of eradication of Helicobacter pylori on gastric epithelial cell proliferation. *Aliment Pharmacol Ther*, 1994;8:167-173
- 16 Berstad AE, Hatlebakk JG, Maartmann-Moe H, Berstad A, Brandtzaeg P. Helicobacter pylori gastritis and epithelial cell proliferation in patients with reflux oesophagitis after treatment with lansoprazole. *Gut*, 1997;41:740-747
- 17 Moss SF, Calam J, Agarwal B, Wang S, Holt PR. Induction of gastric epithelial apoptosis by Helicobacter pylori. *Gut*, 1996;38:498-501
- 18 Wagner S, Beil W, Westermann J, Logan RPH, Bock CT, Trautwein C, Bleck JS, Manns MP. Regulation of gastric epithelial cell growth by Helicobacter pylori: evidence for a major role of apoptosis. *Gastroenterology*, 1997;113:1836-1847
- 19 Jones NL, Shannon PT, Cutz E, Yeger H, Sherman PM. Increase in proliferation and apoptosis of gastric epithelial cells early in the natural history of Helicobacter pylori infection. *Am J Pathol*, 1997;151:1695-1703
- 20 Chen G, Sordillo EM, Ramey WG, Reidy J, Holt PR, Krajewski S. Apoptosis in gastric epithelial cells is induced by Helicobacter pylori and accompanied by increased expression of BAK. *Biochem Biophys Res Commun*, 1997;239:626-632
- 21 van Doorn LJ, Figueiredo C, Megraud F, Pena S, Midolo P, De Magalhães Queiroz DM, Carneiro F, Vanderborght B, Pegado MDGF, Sanna R, DeBoer W, Schneeberger PM, Correa P, Enders KWNG, Atherton J, Blaser MJ, Quint WGV. Geographic distribution of vacA Allelic types of Helicobacter pylori. *Gastroenterology*, 1999;116:823-830
- 22 She FF, Shi BS, Chen YX. The examination and importance of Campylobacter pylori VacA S1 gene. *Fujian Yike Daxue Xuebao*, 1997;31:22-24
- 23 Ricci V, Ciacci C, Zarrilli R, Sommi P, Tummuru MKR, Blanco CDV, Bruni CB, Cover TL, Blaser MJ, Romano M. Effect of Helicobacter pylori on gastric epithelial cell migration and proliferation in vitro: role of VacA and CagA. *Infect Immun*, 1996;64:2829-2833
- 24 Tsujii M, Kawano S, Tsuji S, Ito T, Nagann K, Sasaki Y, Hayashi N, Fusamoto H, Kamada T. Cell kinetics of mucosal atrophy in rat stomach induced by long-term administration of ammonia. *Gastroenterology*, 1993;104:796-801
- 25 Sobhani I, Vallot T, Mignon M. Helicobacter pylori, a rediscovered bacterium. Implication in gastroduodenal diseases. *Presse Med*, 1995;24:73-75, 76, 78-79
- 26 Sobala GM, Crabtree JE, Dixon MF, Schorah CJ, Taylor JD, Rathbone BJ, Heatley RV, Axon ATR. Acute Helicobacter pylori infection: clinical features, local and systemic immune response, gastric mucosal histology and gastric juice ascorbic acid concentrations. *Gut*, 1991;32:1415-1418
- 27 Ruiz B, Rood JC, Fonham ETH, Malcom GT, Hunter FM, Sobhan M, Johnson WD, Correa P. Vitamin C concentration in gastric juice before and after anti-Helicobacter pylori treatment. *Am J Gastroenterol*, 1994;89:533-539

Edited by You DY and Ma JY
proofread by Sun SM

Effects of radical cholecystectomy on nutritional and immune status in patients with gallbladder carcinoma

Xing Yuan Jiao, Jing Sen Shi, Jian Sheng Wang, Yi Jun Yang and Ping He

Subject headings gallbladder neoplasms/immunology; cholecystectomy; nutritional status; immune status

Jiao XY, Shi JS, Wang JS, Yang YJ, He P. Effects of radical cholecystectomy on nutritional and immune status in patients with gallbladder carcinoma. *World J Gastroenterol*, 2000;6(3):445-447

INTRODUCTION

Carcinoma of the gallbladder is the most common neoplasm in biliary tract, and its incidence has been rising in recent years. The rate of correct diagnosis in early gallbladder carcinoma has been raised after the wide use of CT, ultrasound scans and frozen section examination. Now radical cholecystectomy is advocated as the best management for patients with early gallbladder carcinoma. In the present study, the diagnosis of 27 patients with gallbladder carcinoma was confirmed correct, and the patients underwent radical cholecystectomy, and their nutritional and immune assessments were performed pre- and post-operatively.

PATIENTS AND METHODS

Patients

From September 1993 to December 1997, 27 patients with gallbladder carcinoma who had undergone radical cholecystectomy were selected, and they were admitted to the First and Second Affiliated Hospitals of Xi'an Medical University. The patients included eight males, aged 46-65 years, with a mean of 57 years; nineteen females, aged 50-67 years, with the mean of 59 years. Four patients were diagnosed as having polyposis preoperatively, and diagnosed as carcinoma during the operation by the frozen section technique. In five patients with preoperative diagnosis of carcinoma, metastasis had not been found during the operation. No severe systemic disease was found, e.g. recent myocardial infarction, cerebral vascular accidents, uncontrollable diabetes mellitus or hypertension. Antibiotics were administered

postoperatively to prevent infection, intravenous infusion was routinely administered immediately after surgery and maintained at least for one week. The tumors were graded as stage I, II and III (Nevin stage) by histological examination. All of the resected specimens were sent for histological examination. No chemotherapy or radiotherapy was administered preoperatively.

Methods

The nutritional and immune status of the patients were assessed preoperatively (1 wk before surgery), and on d 3, d 7, d 14 and d 21 postoperatively.

Nutritional assessment Biochemical parameters evaluating the patient's nutritional status consisted of serum levels of albumin, cholesterol, iron, magnesium, zinc, and transferrin determined by an automated calorimetric technique (SMAC), and total iron binding capacity (TIBC) determined by radioimmunoassay.

Immune studies The immune status includes T lymphocyte subpopulation-CD₄, CD₈; immunoglobulins (IgG, IgA and IgM); complements (C₃ and C₄); and serum interleukin-2 and soluble interleukin-2 receptor were evaluated. T lymphocyte subpopulation assessment: blood samples were taken with venopuncture and anticoagulated by heparin. Mononuclear cells were isolated after the sample had been washed twice with Hank's balanced salt solution, and the concentration of the cells was regulated at $2 \times 10^2/\text{mL}$ with RPMI-1840 (Cow serum). Cell suspensions (0.2 mL) were placed in 24-well plates, and added cow serum 0.1 mL, PHA 0.05 mL, LPS 0.05 mL and 10% RPMI-1640 0.6 mL respectively. The plates were incubated at 37°C with 5% CO₂ for 72 h. Cultured supernatants were harvested and kept at -30°C. The cell suspension was assigned equally into three parts, which was washed once, added with CD₄ and CD₈ monoclonal antibody (monoclonal antibody was provided by Luo Yang Hua Mei Co.), stand for 2 h at 4°C; then each was washed twice again; a sheep-anti-mouse IgG fluorescent antibody 50 µL was added into each tube, stand for 2 h at 4°C, and washed twice again. After harvesting, cell suspension was studied under the fluorescence microscopy and the scintillation cells were quantitated as percentage of 100 or 200 lymphocytes.

Hepato-biliary Research Lab, First Affiliated Hospital of Xi'an Medical University, Xi'an 710061, Shaanxi Province, China

Xing Yuan Jiao, graduated from Xi'an Medical University with bachelor degree in 1991 and master degree in 1997 in the same university, now studying for doctor degree in general surgery, having 4 papers published.

Correspondence to: Xing Yuan Jiao, Hepato-biliary Research Lab, First Affiliated Hospital of Xi'an Medical University, Xi'an 710061, Shaanxi Province, China

Tel. 0086-29-5261696

Received 2000-01-18 Accepted 2000-03-14

Assay of IgA, IgG, IgM and complements Serum IgG, IgA, IgM, C₃ and C₄ were quantitated by nephelometric immunoassay.

Assay of serum IL-2, sIL-2R Serum IL-2 and sIL-2 levels were measured by a "Sandwich" enzyme-linked immunosorbent assay with two antibodies, the diagnostic reagents were supplied by Norman Bethune Medical University.

Statistical analysis

For each variable, multiple analysis of variance for repeated measurements was used to compare the values measured before operation with those measured at four subsequent time points. The results were presented as mean and standard error ($\bar{x} \pm s$) based on the mixed model of repeated measurement analysis. Statistical analysis was performed with SAS software. *P* values <0.05 were considered statistically significant.

RESULTS

The results of the nutritional and immunological assessment at various time points are demonstrated in Table 1.

Preoperation

As shown in Table 1, in patients with gallbladder carcinoma, the preoperative nutritional and immune status was all within the assigned normal ranges.

Third postoperative day

All the nutritional parameters decreased greatly after surgery, especially the serum iron, transferrin, cholesterol, TIBC, magnesium, and zinc ($P<0.01$, respectively).

The serum levels of immunoglobulins (IgA, IgG, IgM) and C₃, C₄ complements decreased significantly ($P<0.01$), serum IL-2 levels, CD₄ and CD₈ levels also reduced greatly ($P<0.01$), and CD₈ and sIL-2R levels increased significantly ($P<0.01$).

First postoperative week

Compared with the third postoperative day, all the nutritional parameters increased slightly, particularly the serum albumin, magnesium. Serum cholesterol, TIBC, transferrin, iron and zinc were still lower than their preoperative levels ($P<0.01$). CD₄, CD₈, CD₄/CD₈, IL-2, sIL-2 values differed significantly from those of the preoperative stage ($P<0.01$). The serum levels of immunoglobulins (IgG, IgA, IgM) and complements (C₃ and C₄) were significantly higher than those of the third postoperative day, but they were still lower than those of the preoperative day.

Second postoperative week

Compared with the third postoperative day and the first postoperative week, albumin, magnesium and zinc recovered to the preoperative levels ($P>0.05$), however, the levels of TIBC, transferrin and iron were still significantly lower than those of the preoperative ones ($P<0.01$). Compared with the third postoperative day and the first postoperative week, the serum levels of immunoglobulins (IgG, IgA, IgM) and complements (C₃ and C₄) gradually recovered, and IL-2, CD₄, CD₈, sIL-2R levels and CD₄/CD₈ ratio were not statistically different from the preoperative levels.

Third postoperative week

The nutritional evaluation showed continuous improvement in the third postoperative week, most of the nutritional parameters returned to the preoperative levels, except for the serum levels of iron, transferrin and TIBC. The immune parameters IL-2, sIL-2R, CD₄, CD₈, CD₄/CD₈ ratio, C₃, C₄ immunoglobulin levels (IgG, IgA, IgM) also returned to the preoperative levels, with no statistical difference ($P>0.05$).

Table 1 Nutritional and immunity status in patients with gallbladder carcinoma ($\bar{x} \pm s$)

Parameters	Preoperative	Postoperative			
		3rd day	1st week	2nd week	3rd week
Nutrition					
Albumin(g/mL)	3.6 \pm 0.07	3.01 \pm 0.14 ^b	3.49 \pm 0.13 ^a	3.50 \pm 0.12	3.58 \pm 0.15
Cholesterol(mg/dL)	215 \pm 7.81	78.16 \pm 7.22 ^b	85.23 \pm 7.41 ^b	131.45 \pm 6.85 ^b	148.62 \pm 8.41 ^b
TIBC(μ g/dL)	251.15 \pm 12.95	129.18 \pm 8.15 ^b	162.67 \pm 9.83 ^b	194.15 \pm 10.15 ^b	199.34 \pm 9.68 ^b
Transferrin(mg/dL)	221.07 \pm 12.11	99.77 \pm 8.98 ^b	131.29 \pm 9.01 ^b	175.25 \pm 9.31 ^b	186.21 \pm 10.18 ^b
Iron(mg/dL)	65.12 \pm 6.15	23.39 \pm 4.93 ^b	23.41 \pm 5.01 ^b	32.47 \pm 5.42 ^b	39.87 \pm 5.87 ^b
Magnesium(mg/dL)	2.13 \pm 0.06	1.57 \pm 0.05 ^b	1.99 \pm 0.05 ^b	2.04 \pm 0.06	2.06 \pm 0.06
Zinc(mg/dL)	106.1 \pm 3.56	59.85 \pm 5.13 ^b	88.66 \pm 4.43 ^b	105.8 \pm 3.71	109.9 \pm 3.81
Immunity					
C ₃ (mg/dL)	148.1 \pm 5.15	70.21 \pm 5.6 ^b	96.23 \pm 4.68 ^b	118.56 \pm 5.11 ^a	123.73 \pm 6.22
C ₄ (mg/dL)	25.15 \pm 1.15	14.38 \pm 1.41 ^b	18.79 \pm 1.45 ^a	24.82 \pm 1.21	24.98 \pm 1.16
T lymphocyte subpopulation					
CD ₄ (%)	44.15 \pm 2.01	33.22 \pm 1.88 ^b	39.96 \pm 2.02 ^b	42.37 \pm 2.00 ^a	43.99 \pm 1.97
CD ₈ (%)	34.12 \pm 1.69	29.47 \pm 3.77 ^b	26.21 \pm 3.13 ^b	39.69 \pm 3.00 ^b	35.81 \pm 1.20
CD ₄ /CD ₈ (ratio)	1.3 \pm 0.18	1.1 \pm 0.08 ^b	1.5 \pm 0.19 ^b	1.07 \pm 0.14 ^b	1.20 \pm 0.16 ^b
IL-2(IU/mL)	9.95 \pm 2.95	4.81 \pm 1.81 ^b	5.99 \pm 2.30 ^b	8.41 \pm 2.93 ^a	9.89 \pm 3.01
sIL-2R(U/mL)	754.2 \pm 141.5	478.3 \pm 87.57 ^b	597.4 \pm 96.81 ^b	692.1 \pm 112.6	748.9 \pm 138.8

For each variable, multiple repeated measurements analysis of variance and *t* test were used to compare the values before operation with those measured after operation, ^a $P<0.05$, ^b $P<0.01$, vs before operation.

DISCUSSION

Carcinoma of the gallbladder is one of the most common neoplasms in biliary tract, and 40%-100% cases are complicated with gallstones^[1,2], but correct diagnosis of gallbladder carcinoma in its early stage accounted for only 19.1%, and 53.3% cases are always diagnosed as cholecystitis and gallstone^[3-5]. More and more clinical experiences indicate that radical cholecystectomy for early carcinoma is the most effective treatment^[6-8]. In the present study, though all patients with gallbladder carcinoma were well prepared to receive the radical cholecystectomy, their nutritional and immune status still deteriorated remarkably immediately after the extensive surgical resection. The reasons might be that: ① Large volume of body fluid lost during and after the surgery; ② the radical cholecystectomy is a complex operation needing long time and wide scope of resection. Sumiyoshi^[9] and Wang *et al.*^[10] studied the effect of surgery as an injury factor on nutritional and immune status in patients with carcinoma, it is coincident with our findings in this report. Our investigation showed that all of the nutritional parameters but the serum levels of iron, TIBC and transferrin recovered within 3 wk after operation. Hickey *et al.*^[11] advocated that supplemental vitamins and minerals, e.g. iron should be given postoperatively when deficiencies are suspected. Our conclusion is that adequate iron should be supplemented after the radical cholecystectomy for gallbladder carcinoma in the third postoperative week, and the serum levels of minerals should be monitored routinely after surgery.

The immune study showed remarkable decrease of serum IgA, IgM, IgG and C₃, C₄ complement, IL-2, CD₄, CD₄/CD₈ ratio, and the remarkable increase of serum sIL-2R and CD₈ ($P < 0.01$) on d3 after operation. IL-2 is a T-cell derived soluble lymphokine whose main bioactivity is to stimulate the activated T cell (Th, Ts, Tc) to reproduce continually, proliferate and is the key mediator in cell and humoral immunity and immune regulation. The balance between IL-2 and its receptor regulates the immune status. T cell serves as the center in controlling cellular immune status which can affect directly the occurrence, development and progression of tumor^[12]. T cell's regulating function is mainly performed by CD₄ and CD₈ T cells. CD₄⁺ T cells can help B cell produce antibody and CD₈⁺ T cells can suppress B cell to produce antibody. The stable balance between them keeps normal immune response of the organism. Surgery, as an injurious factor, broke the balance between CD₄ and CD₈, however T cell's immune regulating function is demanded finally by the organism. In gallbladder carcinoma in an early stage, the serum IL-2, CD₄, CD₈, CD₄/CD₈ ratio, sIL-2R recovered remarkably in the first postoperative week. In early

postoperative stage, the serum levels of immunoglobulins and complement reduced remarkably. This evidence suggests the results are possibly influenced by surgical stress and the diluting effect of the postoperative massive fluid therapy. The immune parameters returned to the preoperative levels within 2 wk-3 wk after surgery, suggesting that T cell plays a more important role in the immune regulating system.

The present study suggests that radical cholecystectomy for early gallbladder carcinoma might have a mild and transient adverse effect on the cell-mediated immune response during the early postoperative period. Because of tumor's own direct products, tumor cell's metabolites and immuno-complex in body circulation, which depress the anti-tumor action of the immune cells^[13,14], patients' immune status deteriorated remarkably in the middle and late stage. For gallbladder carcinoma, radical cholecystectomy in its early stage with complete resection of the tumor and removal of lymphnodes should be performed, thus the immune inhibitors in the tumor mass can be excluded. These factors played important roles in the recovery of immune function.

REFERENCES

- Shi JS, Zhou LS, Wang ZR, Luo J, Wang L, Hao XY, Ma QJ, Li FZ, Wang T, Ren B, Lu Y, Liu SG. Retrospective analysis of 830 extra-hepatic biliary carcinoma. *Zhonghua Waike Zazhi*, 1997; 35:645-647
- Ekbohm A, Hsieh CC, Yuen J, Tricopoulos D, McLaughlin JK, Lan SJ, Adami HO. Gallstones and bile duct cancer. *Lancet*, 1993;342: 1262-1265
- Chijiwa K, Sumiyoshi K, Nakayama F. Impact of recent advances in hepatobiliary imaging techniques on the preoperative diagnosis of carcinoma of the gallbladder. *World J Surg*, 1991;15:322-327
- Henson DE, Albores Saavedra J, Corle D. Carcinoma of the gallbladder: histologic types, stage of disease, grade, and survival rates. *Cancer*, 1992;70:1493-1496
- Sumiyoshi K, Nagai E, Chijiwa K, Nakayama F. Pathology of carcinoma of the gallbladder. *World J Surg*, 1991;15:315-321
- Busse PM, Cady B, Bothe A Jr., Jenkins R, McDermott WV, Steele G Jr., Stone MD. Intraoperative radiation therapy for carcinoma of the gallbladder. *World J Surg*, 1991;15:352-356
- Gagner M, Rossi RL. Radical operations for carcinoma of the gallbladder: present status in North America. *World J Surg*, 1991; 15:344-347
- Gall FP, Kockerling F, Scheele J, Schneider C, Hohenberger W. Radical operations for carcinoma of the gallbladder: present status in Germany. *World J Surg*, 1991;15:328-336
- Mulvihill SJ, Pellegrini CA. Postoperative care. In: Current surgical diagnosis. 10th ed. VS: Lange Medical Publication, 1994:15-23
- Wang LS, Lin HY, Chang CJ, Fahn HJ, Huang MH, Jeff Lin CF. Effects of en bloc esophagectomy on nutritional and immune status in patients with esophageal carcinoma. *J Surg Oncol*, 1998; 67:90-98
- Hickey MS, Arbeit JM, Way LW. Surgical metabolism and nutrition. In: Current surgical diagnosis and treatment. 10th ed. VS: Lange Medical Publication, 1994:143-194
- Lotze MT, Finn OJ. Recent advance in cellular immunology: implications for immunity to cancer. *Immunol Today*, 1991;11:190-194
- Jiao XY, Shi JS, Gao JS, Zhou LS. Determination of levels of cellular immunity and humoral immunity in patients with gallbladder carcinoma. *Zhongguo Puwai Jichu Yu Lingchuang Zazhi*, 1999;6:227-229
- Jiao XY, Shi JS, Gao JS, Zhou LS, Han WS, Liu G, Lu Y. Study on the serum IL-2, sIL-2R and CEA levels in patients with gallbladder carcinoma. *Zhonghua Gandan Waike Zazhi*, 1999;5:342

Intraoperative endoscopic sphincterotomy for common bile duct stones during laparoscopic cholecystectomy

De Fei Hong¹, Ming Gao², Urs Bryner³, Xiu Jun Cai¹ and Yi Ping Mou¹

Subject headings laparoscopic cholecystectomy; common bile duct stones; endoscopic sphincterotomy

Hong DF, Gao M, Bryner U, Cai XJ, Mou YP. Intraoperative endoscopic sphincterotomy for common bile duct stones during laparoscopic cholecystectomy. *World J Gastroentero*, 2000;6(3):448-450

INTRODUCTION

The advent of laparoscopic cholecystectomy (LC) in the late 1980s gained widespread acceptance within a short period of time and has become the preferred treatment for symptomatic gallstones^[1-7], but the management of coexisting gallbladder and common bile duct (CBD) stones has remained controversial because the various strategies proposed have their limitations^[8-12]. In fact, choledocholithiasis is found in 10%-15% of patients with cholecystolithiasis, and most authors agree that at least 90% of CBD stones are secondary to those of the gallbladder, and that CBD stones must be extracted in a timely manner in order to avoid consequent complications which would otherwise occur in at least 90% of patients^[1-4]. This paper will introduce and evaluate a new approach of management of coexisting gallbladder and CBD stones-intraoperative endoscopic sphincterotomy (IOES).

MATERIALS AND METHODS

From December 1997 to August 1999, twenty-seven patients with cholelithiasis and CBD stones were treated by LC and IOES. Choledocholithiasis was detected in 9 patients by preoperative ultrasonography and 18 routine intraoperative cholangiography (IOC). They were 5 males and 22 females. The youngest patient was 23 years old, the oldest being 74 years, averaging 50.3 years. The preoperative diagnoses are summarized in Table 1. All patients were treated according to a standard

protocol (Figure 1).

Table 1 Preoperative diagnosis of 27 cases

Preoperative diagnosis	No. of patients
Acute cholecystitis with multiple gallstones	3
Chronic cholecystitis with multiple gallstones	15
Acute cholecystitis with multiple gallstones and CBDs	3
Chronic cholecystitis with multiple gallstones and CBDs	6

Figure 1 Protocol of treatment of 27 cases. LF: liver function; US: ultrasonography; LC: laparoscopic cholecystectomy; IOC: intraoperative fluorocholangiography; CBD: common bile duct; IOES: intraoperative endoscopic sphincterotomy.

LC was undertaken by the four trocar technique and IOC was performed according to the technique described by Alfred Cuschieri and Hong^[1,2]. As soon as the CBD stones were confirmed, the endoscopist was expected on call. The patient lay in supine position, after deflating abdominal CO₂, the endoscope (Olympus JF100 or a side-view JF100, JF140) was advanced into the duodenum. Once the position of ampulla of Vater was determined, EST was undertaken routinely. The size of sphincterotomy was about 0.8 cm-1.5 cm. The CBD stones were extracted in different ways according to their size, shape and number. The small stones (less than 8 mm) were expelled into the duodenum with the help of surgeons by injecting normal saline through the cholangiogram catheter, medium sized stones (8 mm-15 mm) were extracted with the basket (Olympus FG-23Q-1) or by a balloon (Wilson-cook EBL-12-200, EBL-8.5-200) monitored under fluoroscopy, large stones (more than 15 mm in diameter) were eliminated by basket or balloon after mechanical lithotripsy. After IOES and removal of CBD stones, the repeated IOC was performed to make sure that there were no retained CBD stones. The endoscope was withdrawn while aspirating the residual air. The LC was then completed.

¹Department of General Surgery, Sir Run Run Shaw Hospital, Zhejiang University, Hangzhou 310016, Zhejiang Province, China

²Department of Gastroenterology, Sir Run Run Shaw Hospital, Zhejiang University, Hangzhou 310016, Zhejiang Province, China

³Loma Linda University Medical Center, United States

Dr. De Fei Hong, graduated from Zhejiang University as a postgraduate in 1999, fellow of general surgery, major in hepato-biliary disease, having 14 papers published in international journal.

Correspondence to: Dr. De Fei Hong, Department of General Surgery, Sir Run Run Shaw Hospital, Zhejiang University, Hangzhou 310016, Zhejiang Province, China

Tel. 0086-571-6090073 Ext.2288

Received 2000-01-15 **Accepted** 2000-02-26

RESULTS

The IOES was technically successful in 26 of 27 patients (96.30%) and the CBD stones were removed in all of these cases (100%). In 5 cases, the stones were expelled into the intestinal tract spontaneously, in 17 cases, extracted by basket or balloon and in 4 cases, removed after mechanical lithotripsy. The number of CBD stones ranged from 1 to 15, and the size of the stones varied from 3 mm to 16 mm. In one case, IOES failed because the sphincterome could not cannulate the ampulla of Vater due to stones impacted tightly the distal portion of CBD. Two cases were complicated with mild acute pancreatitis (7.69%) which resolved within 3 d and 7 d being fasted and intravenously supplemented fluid. No other complications occurred. There were no operative mortalities. The average operation time of LC combined with IOES was about 160 min (from 80 min to 210 min). All but 3 cases recovered uneventfully leaving bed and resuming food 8 h-24 h after LC and IOES. One patient developed pneumothorax after LC procedure. In the other two cases recovery was delayed due to the complication of mild acute pancreatitis (mentioned above). The mean duration of hospital stay was 1 d to 26 d ($3 \text{ d} \pm 1 \text{ d}$). The patient who had the pneumothorax was discharged on the 26 th postoperative day.

DISCUSSION

It is well known that LC has become the primary method of treatment of symptomatic gallstones. Of the 500 000 cholecystectomies performed annually in the United States, 85% of them are estimated now to be performed laparoscopically^[13]. In China LC is also rapidly accepted. Likewise, the introduction of ERCP and EST in the 1970s rapidly revolutionized the management of CBD stones. Numerous series of cases have shown successful endoscopic clearance of the CBD stones in approximately 90% of patients, complications of EST occur in 5%-15%, most of these are minor, and the mortality is less than 1%. New instrumentation is being developed and improved continuously enabling the endoscopist-surgeon to deal more and more successfully and creatively with a variety of intra-abdominal conditions^[4-6]. But the management of coexisting gallbladder and CBD stones is now more controversial than before, because many approaches to resolve this problem have their limitations besides the expense and time (Table 2)^[8-12].

From May 1994 to November 1997, 1794 cases of LC and IOC were performed in our hospital. In about 7%-8% of patients with cholecystolithiasis^[2,3], CBD stones were also found, we removed them by various methods such as converting to open choledochostomy, laparoscopic choledochostomy, laparoscopic choledochoscopy via

cystic duct and postoperative EST. The results revealed that there was no best procedure for the patients, some shortcomings existed as shown in Table 2. Therefore, we employed a new approach of IOES from December 1997 to August 1999 to remove CBD stones identified at the time of LC.

Table 2 Alternatives of management of coexisting gallbladder and CBD stones

Methods	Shortcomings
Convert to open choledochostomy	loss of all advantages of minimally invasive surgery
Laparoscopic transcystic duct choledochoscopy	limited by cystic duct anatomy and risk associated with cystic duct dilation
Laparoscopic choledochostomy	Installation of T-tube and high technical demand
Preoperative ERCP and EST	hard to precisely predict preoperative CBD stones; if failed, subsequent operation should be considered
Postoperative ERCP and EST	If failed, another operation should be performed

The major advantages of combining LC and EST into one procedure are encouraging. The obvious benefit is that the patients have both problems solved at one session. But our 27 cases treated by LC combined with IOES only represent some of the common bile duct explorations done at our hospital during this period due to the following reasons (among 1485 LC cases during this period). First, some surgeons in our department thought that IOES presents significant logistic difficulties in coordinating the necessary personnel and equipment. Second, it was thought that the supine position may increase the technical difficulty of EST^[8-12]. But in our experience it is easier to remove the CBD stones by a combination of LC with IOES than by pre- or postoperative EST. The endoscopist gets benefit from general anesthesia. The surgeons can help the endoscopist to locate the proper position of the ampulla of Vater and irrigate the CBD by injecting normal saline through the cholangiography catheter. Small or fragmented stones can be washed out with normal saline irrigation. Medium or large sized stones in CBD can be removed with the help of a basket or balloon and by lithotripsy. By deflating the peritoneal cavity of CO₂, the endoscopist was able to insufflate the duodenum adequately for performing IOES, after aspirating the gastrointestinal air, LC was more easily accomplished. From our study, IOES was successful in 26 (96.30%) of 27 patients and CBD stones were cleared in all of them (100%), only two cases were complicated with mild acute pancreatitis (7.69%) resolved within 3 d-7 d with intravenous fluid and fasting. No death occurred postoperatively. The case of pneumothorax after LC recovered by conservative management. The total operative time compares favorably with that of

standard LC with CBD exploration in our hospital.

We recommend IOES as a valid alternative approach to the removal of CBD stones during LC. It has been safe and effective, and less traumatic to the patient than other intraoperative procedures or pre- or postoperative EST.

REFERENCES

- Cuschieri A, Berci G, Paz-Partlow M, Nathanson LK, Sackier J. Laparoscopic Biliary Surgery. Second Edition. 1992. Black Scientific Publications
- Hong DF, Li JD, Cai XJ, Wang YD, Wang XF, Wei Q, Yuan XM, Chen WJ, Li LB, Suong XY, Bryner U. The special role of routine intraoperative cholangiography in laparoscopic cholecystectomy. *Zhonghua Gandan Waike Zazhi*, 1998;4:101-103
- Cai XJ, Wang XF, Hong DF, Li LB, Li JD, Bryan F. The application of intraoperative cholangiography in laparoscopic cholecystectomy. *Zhonghua Waike Zazhi*, 1999;37:427-428
- Liu CL, Lai ECS, Lo CM, Chu KM, Fan ST, Wong J. Combined laparoscopic and endoscopic approach in patients with cholelithiasis and choledocholithiasis. *Surgery*, 1996;119:534-537
- Kullman E, Borch K, Lindstrom E, Svanvik J, Anderberg B. Management of bile duct stones in the era of laparoscopic cholecystectomy: Appraisal of routine operative cholangiography and endoscopic treatment. *Eur J Surg*, 1996;162:873-880
- Gong JP, Zhou YB, Wang SG, Gu HG, He ZP. Effect of endoscopic retrograde cholangiopancreatography, endoscopic sphincterotomy in assisting laparoscopic cholecystectomy for cholelithiasis. *Zhonghua Xiaohua Nei Jing Zazhi*, 1997;14:229-231
- Phillips EH, Carroll BJ, Pearlstein R, Daykovsky L, Fallas MJ. Laparoscopic choledochoscopy and extraction of common bile duct stones. *World J Surg*, 1993;17:22-28
- Deslandres E, Gagner M, Pomp A, Rheault M, Leduc R, Clermont R, Gratton J, Bernard EJ. Intraoperative endoscopic sphincterotomy for common bile duct stones during laparoscopic cholecystectomy. *Gastrointes Endos*, 1993;39:54-57
- Grieve DA, Merrett ND, Matthews AR, Wilson R. Left lateral laparoscopic cholecystectomy and its relevance to choledocholithiasis. *Aust N Z J Surg*, 1993;63:715-718
- Fitzgibbons RJ, Deeik RK, Martinez Serna T. Eight years experience with the use of a transcystic common bile duct duodenal double-lumen catheter for the treatment of choledocholithiasis. *Surgery*, 1998;124:699-706
- Cavina E, Franceschi M, Sidoti F, Goletti O, Buccianti P, Chiarugi M. Laparo-endoscopic "rendezvous": a new technique in the choledocholithiasis treatment. *Hepato Gastroenterology*, 1998;45:1430-1435
- Nakajima H, Okubo H, Masuko Y, Osawa S, Ogasawara K, Kambayashi M, Hata Y, Oku T, Takahashi T. Intraoperative endoscopic sphincterotomy during laparoscopic cholecystectomy. *Endoscopy*, 1996;28:264
- Gholson CF, Dungan C, Neff G, Ferguson R, Favrot D, Nandy I, Banish P, Sittig K. Suspected biliary complications after laparoscopic and open cholecystectomy leading to endoscopic cholangiography. A retrospective comparison. *Dig Dis Sci*, 1998;43:534-539

Edited by You DY and Ma JY
proofread by Sun SM

Pathogenetic effects of platelet activating factor on enterogenic endotoxemia after burn

Pei Wu Yu¹, Guang Xia Xiao², Wei Ling Fu², Jian Cheng Yuan², Li Xin Zhou² and Xiao Jian Qin²

Subject headings Platelet activating factor; burn; endotoxemia ; intestinal permeability

Yu PW, Xiao GX, Fu WL, Yuan JC, Zhou LX, Qin XJ. Pathogenetic effects of platelet activating factor on enterogenic endotoxemia after burn. *World J Gastroentero*, 2000;6(3):451-453

INTRODUCTION

Previous clinical and experimental studies have indicated that an early endotoxemia occurred after a major burn. It is unlikely that burn wound sepsis is the source of circulating endotoxin in less than 12 hour after burn. Increasing evidence demonstrates that the bacteria and endotoxin in the gastrointestinal tract can pass through the gut barrier into blood circulation to form enterogenic endotoxemia following burn^[1-3]. However, its pathogenesis remains poorly understood. Platelet activating factor (PAF), an endogenous phospholipid mediator, has recently been proposed as a critical mediator in shock, sepsis and multiple organ failure^[4,5]. In this study, the relationship between changes of PAF and enterogenic endotoxemia was observed on rat models with 30% TBSA III° burn. The purpose was to investigate the pathogenetic effects of PAF on the occurrence of enterogenic endotoxemia after burn.

MATERIALS AND METHODS

Animals

Wistar rats, male or female, weighing 220 g ± 30 g were used, they were provided by Laboratory of Animal Experiment, Institute of Burn Research, Third Military Medical University.

Experimental design

Animals were randomly divided into three groups. Group 1 (*n* = 10): normal rats served as control. Group 2 (*n* = 40): burned rats that had undergone

30% TBSA III° burn. Group 3 (*n* = 40): treated rats that received PAF antagonist WEB 2170 (5 mg/kg) by intraperitoneal injection after burn. WEB 2170 was provided by Boeringer Ingelheim *Pharmac*-euticals Inc, Germany.

Animals were killed on 6, 12, 24 and 48 hours postburn. Blood and terminal ileum were obtained from all animals for assay of PAF and endotoxin.

Burn model

Rats were anesthetized intraperitoneally with ketamine hydrochloride 80 mL/kg body weight, and their backs were shaved. They were placed in a mould that left approximately 30% area of their body surface exposed. These exposed surface s were immersed in 92°C water for 18s. This type of burn injury is a full-thick ness burn. Animals were resuscitated with 40 mL/kg of lactated Ringer's solution.

Measurement of PAF contents in blood and intestinal tissue

Blood (1mL) was collected into polypropylene tube containing 5 mL of methanol. The methanolic extract was separated by centrifugation. The supernata nts were collected and chloroform and water were added to effect phase separation. The lower chloroform-rich phase contained all PAF activity. Chloroform was evaporated under a stream of nitrogen. The samples were stored under -20°C. Segments of ileum tissue (200 mg) were added to 2 mL of 0.25% bovine serum albumin, and after homogenization, the mixture was added to 2 mL of cold acetone, and then centrifuged. Two mL of chloroform as added to the superna tants. After a further centrifugation, the thin layer chloroform containing PAF was collected and evaporated by nitrogen. PAF activity was bioassayed by the aggregation of rabbit washed platelets.

Measurement of intestinal mucosal permeability

After overnight fast, rats were anesthetized, a midline abdominal incision was made. Fifteen cm segments of ileum were isolated, cannulated proximally and distally, and perfused continuously with saline at rate of 1 mL/min-2 mL/min. ^{99m}Tc DTPA (5.55-7.4MBq/kg) was injected via the carotid ve in and allowed to equilibrate for 30 min. After that, a 10 min perfusion fluid and 1mL blood were collected for measurement of activity of ^{99m}Tc

¹Department of General Surgery, Southwest Hospital, Third Military Medical University, Chongqing 400038, China

²Institute of Burn Research, Southwest Hospital, Third Military Medical University, Chongqing 400038, China

Dr. Pei Wu Yu, graduated from the Third Military Medical University in 1984, now associate professor of surgery, majoring in gastrointestinal surgery, having 28 papers published.

Project supported by the National Natural Science Foundation of China, No.39290700.

Correspondence to: Dr. Pei Wu Yu, Department of General Surgery, Southwest Hospital, Third Military Medical University, Chongqing 400038, China

Tel. 0086-23-68754097

Received 2000-01-11 **Accepted** 2000-02-16

DTPA. The animals were killed and the perfused ileal segment was excised and weighed. DTPA clearance was calculated using the following formula: DTPA clearance = (cpm perfusate \times Q)/(cpm plasma \times W), and was expressed as mL/min \cdot 100g. Where Q is the rate of perfusion; W, the weight of perfused ileum.

Measurement of plasma endotoxin

Plasma endotoxin was assayed with chromogenic limulus amoebocyte lysate technique.

Statistical analysis

All data were expressed as $\bar{x} \pm s$, and statistical analyses were made using Student's *t* test.

RESULTS

The changes of PAF content

PAF contents of blood and intestinal tissue in burn group were significantly higher than those in control group ($P < 0.01$). The peak level occurred at 12 h postburn. In PAF-antagonist treatment group, the PAF contents of blood and intestinal tissue were significantly decreased compared with burn group, but were higher than those in control group

(Table 1).

The changes of intestinal mucosal permeability

The intestinal mucosal permeability increased significantly at 6h postburn and kept increasing during 48 h postburn compared with control group. The intestinal mucosal permeability in treatment group was lower than those in burn group (Table 2).

The changes of plasma endotoxin

The levels of plasma endotoxin in burn group were significantly higher than those in control group. The levels of plasma endotoxin in treatment group were significantly lower than those in burn group (Table 3).

Correlation analysis

The correlations between intestinal PAF and intestinal mucosal permeability, blood PAF and plasma endotoxin, intestinal mucosal permeability and plasma endotoxin in burn group were analyzed. The results showed positive correlation among the above three pairs with $P < 0.01$, $r = 0.94$, 0.93 and 0.95 respectively.

Table 1 Levels of PAF in blood and intestinal tissue ($\bar{x} \pm s$)

Group	n		After burn (h)			
			6	12	24	48
Control	10					
Blood($\mu\text{g/L}$)		0.56 ± 0.07				
Intestine(ng/g)		0.41 ± 0.06				
Burn	40					
Blood($\mu\text{g/L}$)			1.72 ± 0.21^b	2.76 ± 0.25^b	1.54 ± 0.24^b	1.19 ± 0.13^b
Intestine(ng/g)			1.80 ± 0.21^b	2.34 ± 0.18^b	1.68 ± 0.15^b	1.42 ± 0.16^b
Treatment	40					
Blood($\mu\text{g/L}$)			0.84 ± 0.16^{da}	1.46 ± 0.27^{db}	0.93 ± 0.18^{ca}	0.71 ± 0.15^c
Intestine(ng/g)			0.67 ± 0.07^{da}	1.24 ± 0.13^{dbaa}	0.83 ± 0.12^{da}	0.64 ± 0.08^{da}

^a $P < 0.05$, ^b $P < 0.01$ vs control; ^c $P < 0.05$, ^d $P < 0.01$ vs burn group.

Table 2 Changes of intestinal mucosal permeability ($\text{mL} \cdot \text{min}^{-1} \cdot 100\text{g}^{-1}$, $\bar{x} \pm s$)

Group	n		After burn (h)			
			6	12	24	48
Control	10	0.07 ± 0.02				
Burn	40		0.33 ± 0.14^b	0.58 ± 0.18^b	0.21 ± 0.07^b	0.13 ± 0.04^b
Treatment	40		0.19 ± 0.05^{db}	0.27 ± 0.06^{db}	0.10 ± 0.04^{da}	0.08 ± 0.03^c

^a $P < 0.05$, ^b $P < 0.01$ vs control; ^c $P < 0.05$, ^d $P < 0.01$ vs burn group.

Table 3 Levels of plasma endotoxin (ng/L , $\bar{x} \pm s$)

Group	n		After burn (h)			
			6	12	24	48
Control	10	34 ± 8				
Burn	40		93 ± 28^b	129 ± 32^b	90 ± 22^b	59 ± 16^b
Treatment	40		57 ± 15^{ca}	66 ± 13^{db}	50 ± 10^{da}	43 ± 8^c

^a $P < 0.05$, ^b $P < 0.01$ vs control, ^c $P < 0.05$, ^d $P < 0.01$ vs burn group.

DISCUSSION

The pathogenesis of enterogenic endotoxemia remains poorly understood. It is considered that the main cause is injury of intestinal mucosal barrier. Under physiological condition, the intestinal mucosa functions as a major local defense barrier preventing intestinal bacteria and endotoxin from invading distant organs and tissues. However, under the circumstances of trauma, shock and sepsis, the impairment of intestinal barrier may result from ischemic damage of the intestinal mucosa, the bacteria and endotoxin in gastrointestinal tract can pass through the intestinal barrier to mesenteric lymph nodes and systemic organs, resulting in enterogenic sepsis (endotoxemia)^[6,7]. There is increasing evidence that enterogenic sepsis may play an important role in the development of systemic infection as well as multiple organ failure^[8,9]. The present study results show that increased intestinal permeability after burn is an important cause of enterogenic endotoxemia.

PAF is a phospholipid mediator released from stimulated leukocytes, platelets, endothelial and mast cells^[10,11]. It has been regarded as an important endogenous mediator of shock, sepsis and multiple organ failure. Our study demonstrated that PAF contents in blood and intestinal tissue after burn were all significantly increased and were positively correlated with the increase of intestinal permeability and plasma endotoxin. Treatment with PAF antagonist can significantly decrease intestinal permeability and plasma endotoxin. These suggest that PAF is involved in the process of increasing the intestinal permeability after burn and is also an important factor leading to enterogenic endotoxemia.

Previous studies showed that endotoxin can stimulate directly or indirectly macrophages and endothelial cells to release PAF, which also

mediates some endotoxin-induced pathologic processes of multiple organ injury^[12,13]. It is suggested that a PAF-endotoxin positive feedback relationship existed in the body. Therefore, administration of PAF antagonists has an important effect on preventing and treating enterogenic endotoxemia.

REFERENCES

- 1 Jones WG, Barber AE, Minei JP, Fahey III TJ, Shires III GT, Shires GT. Differential pathophysiology of bacterial translocation after thermal injury and sepsis. *Ann Surg*, 1991;214:24-30
- 2 LeVoyer T, Cioffi WG, Pratt L, Shippee R, McManus WF, Mason AD, Pruitt BA. Alterations in intestinal permeability after thermal injury. *Arch Surg*, 1992;127:26-30
- 3 Gianotti L, Braga M, Vaiani R, Almondo F, DiCarlo V. Experimental gut-derived endotoxaemia and bacteraemia are reduced by systemic administration of monoclonal anti LPS antibodies. *Burns*, 1996;22:120-124
- 4 Anderson BO, Bensard DD, Harken AH, Colorado D. The role of platelet activating factor and its antagonists in shock, sepsis and multiple organ failure. *Surg Gynecol Obstet*, 1991;172:415-424
- 5 Beyer AJ, Smalley DM, Shyr YM, Wood JG, Cheung LY. PAF and CD18 mediate neutrophil infiltration in upper gastrointestinal tract during intra-abdominal sepsis. *Am J Physiol*, 1998;275:G467-G472
- 6 Wilmore DW, Smith RJ, O'Dwyer ST, Jacobs DO, Ziegler TR, Wang XD. The gut: a central organ after surgical stress. *Surgery*, 1988;104:917-922
- 7 Fink MP. Gastrointestinal mucosal injury in experimental models of shock, trauma, and sepsis. *Crit Care Med*, 1991;19:627-640
- 8 Fukushima R, Gianotti L, Alexander JW, Pyles T. The degree of bacterial translocation is a determinant factor for mortality after burn injury and is improved by prostaglandin analogs. *Ann Surg*, 1992;216:438-445
- 9 Moore FA, Moore EE. Evolving concepts in the pathogenesis of postinjury multiple organ failure. *Surg Clin North Am*, 1995;75:257-277
- 10 Snyder F. Platelet activating factor and related acetylated lipids as potent biologically active cellular mediators. *Am J Physiol*, 1990;259:C697-C708
- 11 Kubes P, Arfors KE, Granger DN. Platelet-activating factor induced mucosal dysfunction: role of oxidants and granulocytes. *Am J Physiol*, 1991;260:G965-G971
- 12 Torley LW, Pickett WC, Carroll ML, Kohler CA, Schaub RE, Wissner A. Studies of the effect of platelet activating factor antagonist, CL184,005, in animal models of Gramnegative bacterial sepsis. *Antimicrob Agents Chemother*, 1992;36:1971-1977
- 13 Fletcher JR, Disimone AG, Earnest MA. Platelet activating factor receptor antagonist improves survival and attenuates eicosanoid release in severe endotoxemia. *Ann Surg*, 1990;211:312-316

Edited by You DY and Zhu LH
proofread by Sun SM

Ultrastructural localization of glutathione S-transferase-pi in human colorectal cancer cells

Wen Jun Guo¹, Guang De Zhou¹, Hong Juan Wu¹, Yu Qing Liu¹, Rui Guang Wu² and Wei Dong Zhang¹

Subject headings colorectal neoplasms; GST-pi; immunoelectron microscope; colloid gold

Guo WJ, Zhou GD, Wu HJ, Liu YQ, Wu RG, Zhang WD. Glutathione S-transferase-pi in colorectal cancer cells. *World J Gastroentero*, 2000;6(3):454-455

INTRODUCTION

Placental form glutathione S-transferase (GST-pi) is a group of isoenzymes with protein combining ability. Since the reports showing that GST-pi was significantly increased in proliferative hepatic nodule induced by chemical carcinogen and in well differentiated carcinoma^[1], more studies have shown^[2-4] that GST-pi expressed highly in neoplasm, and could be regarded as a tumor marker. GST-pi has the antimutagenesis and antitumor ability, and is related closely with the resistance of tumor to anticancer drugs. As the description about the immunoelectron microscopical localization of GST-pi in human colorectal cancer cells was not available, we have observed the ultrastructural localization of GST-pi in colorectal cancer cells, and explored the distribution of GST-pi in these cells and its relationship with colorectal carcinogenesis.

MATERIALS AND METHODS

Fresh colorectal cancer tissues ($n = 6$) were obtained from surgical specimens, and the colorectal mucosal tissues ($n = 3$) more than 10 cm away from the cancer served as controls.

Reagents Monoclonal mouse anti-GST-pi antibody (Dako Company); 10 nm colloid gold labeled goat anti-mouse IgG (Institute of Basic Medicine, Academy of Military Medical Science).

Tissue processing All fresh blocks of tissue were fixed with 2.5 mL/L glutaraldehyde and 40 mL/L

paraformaldehyde, routinely dehydrated and embedded in Epon 812. Ultrathin sections were placed on nickel grids, treated with 30 mL/L H₂O₂ (15 min), washed thoroughly with 0.05M, pH 7.4 TBS, blocked with 1% bovine serum (30 min), dropped mouse anti-GST-pi monoclonal antibody (1:20), and placed in refrigerator (4°C) overnight. Washed with 0.05M, pH 7.4 TBS, then with 0.02M, pH 8.2 TBS, dropped 10 nm colloid gold labeled goat anti-mouse IgG (1:10), stand in room temperature for 1 h, washed with TBS, and restained with uranyl acetate followed by lead citrate. The first antibody was replaced by TBS as control. These specimens were observed under electron microscope.

RESULTS

The most significant ultrastructural change of colorectal cancer cell occurred in the nucleus. It was large and irregular in shape, with peripheral aggregation of heterochromatin and plenty of ribosomes and large nucleoli. There were colloid gold labeled GST-pi positive particles in all of the six cancer specimens. The positive particles were round in shape, high and clear electron density, distributed as clusters or spots in cancer cells. The majority of positive particles were in mitochondria, lysosomes and some plasma, and some also presented in nuclei (Figure 1) or in the periphery of nuclei (Figure 2). The positive particles accumulated in lumps. Visible positive particles were never found in normal control cells.



Figure 1 GST-pi positive particles present in nuclei. EM × 40 000

¹Department of Pathology, Weifang Medical College, Weifang 261042, Shandong Province, China

²Weifang People's Hospital, Weifang 261041, Shandong Province, China

Dr. Wen Jun Guo, graduated from Weifang Medical College in 1979, now associate professor of pathology, majoring gastrointestinal tumor immunopathology and having more than 30 papers published.

Correspondence to: Dr. Wen Jun Guo, Department of Pathology, Weifang Medical College, Weifang 261042, Shandong Province, China. Tel. 0086-536-8213047

Received 2000-01-18 **Accepted** 2000-02-28

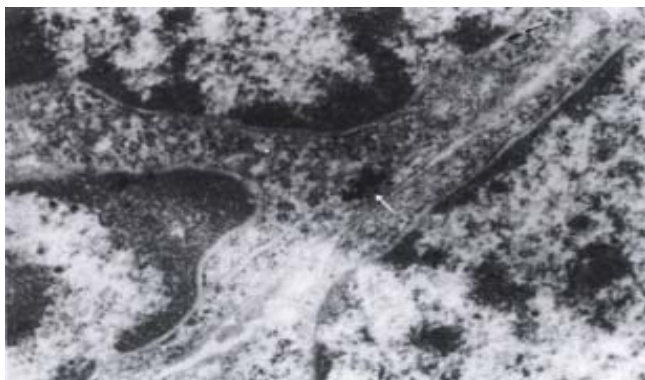


Figure 2 GST-pi positive particles present in the periphery of nuclei. EM $\times 25\ 000$

DISCUSSION

Biological characters of GST-pi

Placental form of glutathione included rat and human forms named GST-p and GST- π respectively. Because they presented generally in placenta according to the new category, they were nominated as GST-placental isoenzyme (GST-pi) as a whole. GST-pi could detoxify chemical mutagenesis, cancer promoter, lipid and DNA hyperoxidase, and protect normal cells from the influence of cancerigenic materials, so that GST-pi played an important role in the anti-mutation and anti-cancer process. As an important enzyme of detoxification, GST-pi was controlled by the gene. The high expression of GST-pi gene occurred while the carcinogen acted on the cells to induce their mutation^[5]. The high expression of GST-pi in many neoplasms was related to the resistance of anticancer drugs. Katagiri *et al* reported that the expression of GST-pi negatively correlated to the sensitivity of anticancer drug in testicular tumor^[6]. Dong J suggested that the expression of GST-pi closely related to resistance of anticancer drug in ovarigenic neoplasm^[7]. GST-pi could be regarded as a marker in evaluating the effect of tumorectomy, or in predicting the drug resistance of tumor cells. High expression of GST-pi in precancer and cancer of liver, and the protein synthesis ability could be blocked by cyclohexamide, which showed that GST-pi was controlled in transcription level. This may be the molecular base of the cancer cells in

getting cytotoxic drug resistance. We found that GST-pi expressed only in cancer cells, but not in normal cells, suggesting that this might be related to the action of carcinogen. GST-pi specific expression in colorectal cancer cells may be used as a marker for diagnosis of colorectal carcinoma.

Ultrastructural localization of GST-pi

We found that GST-pi was located in cytoplasm, mitochondria, lysosomes and nucleus adjacent to nuclear membrane of colorectal cancer cells. These agreed with immunohistochemical studies^[8]. But normal mucosa occasionally showed slight positivity in immunohistochemical studies. This is different from our findings. It might be related to the weak expression in normal mucosa. There were few studies about the GST-pi ultrastructural localization. In our study, GST-pi positive particles were found not only in cytoplasm, but also in nucleus. Chen M reported the same result in bladder carcinoma^[9]. Why was GST-pi positive particles present in nucleus? We think this can be an atavism, and if so it could not be used as a marker indicating colorectal cancer. Whether it is a right concept or not needs further studies.

REFERENCES

- 1 Sato K, Kitahara A, Satch K, Ishikawa T, Tatematsu M, Ito N. The placental form of glutathione S-transferase as a new marker protein for preneoplasia in rat chemical hepatocarcinogenesis. *Gann*, 1984;75:199-202
- 2 Tsuchida S, Sekine Y, Shineha R, Nishihira T, Sato K. Elevation of the placental glutathione S-transferase form (GST- π) in tumor tissues and the levels in sera of patients with cancer. *Cancer Res*, 1989;49:5225-5229
- 3 Cairns J, Wright C, Cattani AR, Hall AG, Cantwell BJ, Harris AL, Horne CHW. Immunohistochemical demonstration of glutathione S transferases in primary human breast carcinomas. *J Pathol*, 1992;166:19-25
- 4 Hamada SI, Kamada M, Furumoto H, Hirao T, Aono T. Expression of glutathione S-transferase- π in human ovarian cancer as an indicator of resistance to chemotherapy. *Gynecol Oncol*, 1994;52:313-319
- 5 Liu YB, Chen YJ, Yin Y, Yang XJ, Yang YJ, Wu DZ. The glutathione-S-transferase activity and the gene expression of GST- π in 56 tumor patients. *Aizheng*, 1995;14:1
- 6 Katagiri A, Tomita Y, Nishiyama T, Kimura M, Sato S. Immunohistochemical detection of P-glycoprotein and GST-pi in testis cancer. *Br J Cancer*, 1993;68:125-129
- 7 Huang J, Gu MJ, Chen CL. Expression of glutathione-S-transferase- π in operative specimens an marker of chemoresistance in patients with ovarian cancer. *Zhonghua Fuchanke Zazhi*, 1997;32:458
- 8 Guo WJ, Wu HJ, Liu YQ, Zhang WD, Guo AH, Huang WB. The value of GST-pi in the early diagnosis of colon-rectal carcinoma. *Weifang Yixueyuan Xuebao*, 1999;21:3
- 9 Chen M, Sui YG, You GC, Xu ZS, Feng SZ. Localization of glutathione S-transferase π in human bladder neoplasms. *Zhonghua Miniao Waike Zazhi*, 1998;19:391

Edited by You DY and Ma JY
proofread by Sun SM

Case Reports

Life threatening vitamin B₁₂ deficiency: will timely screening make a difference?

T.S. Dharmarajan¹, S. Lakshmi Narayanan² and Rajiv D. Poduval³

Subject headings vitamin B₁₂ deficiency/therapy; anemia, sickle cell; gastric mucosa; biopsy; anemia, pernicious; toxicity

Dharmarajan TS, Narayanan SL, Poduval RD. Life threatening vitamin B₁₂ deficiency: will timely screening make a difference?. *World J Gastroentero*, 2000;6(3):456-457

INTRODUCTION

While Vit.B12 deficiency is common, with a prevalence of about 15% in the elderly^[1-3], and recommendations for treatment available, detection of deficiency at the pre-clinical stage by appropriate screening does not always take place. Our report is an example of life threatening Vit.B12 deficiency diagnosed at age 56, with the onset of Vit.B12 depletion likely to have begun in the previous decade. Further, the patient had sickle cell trait along with Vit.B12 deficiency, a combination only sporadically reported.

CASE REPORT

A 56 year old caucasian male with no significant past medical illness presented to our University hospital with a history of lethargy, weakness, anorexia, pallor and icteric sclera for a few months. He denied use of medications inclusive of acid lowering agents (H₂ blockers or proton pump inhibitors) and vitamins of any kind. Dietary habits were omnivorous. Physical examination confirmed marked pallor and jaundice. Vital signs were stable; rest of the examination including nervous system was unremarkable.

Hemoglobin: 24g • L⁻¹, Hematocrit: 6.9%, MCV: 75fl, Platelet: 64 × 10⁹ • L⁻¹, Corrected reticulocyte count: 0.004, Blood smear: anisocytosis, poikilocytosis and macroovalocytosis with hypersegmented neutrophils, Folate: 12.1 µg • L⁻¹, Iron: 1.57 µg • L⁻¹, TIBC: 59, Ferritin: 764 µg L⁻¹, LDH: 15500U/L, and Haptoglobin: 31 mg • L⁻¹. Hemoglobin electrophoresis: HbA 0.67, HbS 0.30. Direct

Coomb's test: negative. Vitamin B12: 57ng L⁻¹ (Normal 200-900ng L⁻¹), Intrinsic factor antibodies: positive. Bone marrow aspirate and biopsy: erythroid hyperplasia with megaloblastic features. Upper endoscopy and gastric biopsy revealed chronic gastritis with mucosal atrophy. Colonoscopy was normal except for hemorrhoids.

Therapy included a total of 6 units of packed red blood cells. Vitamin B12 therapy was initiated as daily intramuscular injections, 1 000 µg daily for 3 days. Clinical improvement was dramatic and the patient was discharged shortly.

DISCUSSION

Our patient presented with pancytopenia and a life-threatening drop in Hb to 24 g • L⁻¹. Though the hematologic manifestations were severe, interestingly, there was no evidence of peripheral neuropathy, myelopathy, dementia or any neuropsychiatric manifestations. In view of omnivorous dietary habits, a dietary deficiency from inadequate consumption of Vit. B12 was unlikely. Neither was the patient on any antacids or other acid lowering agents. Proton pump inhibitors and H₂ blockers, widely used as prescription and over the counter agents for upper gastrointestinal symptoms have been associated with Vit. B12 deficiency. Acid peptic activity is important in the initial step where Vit. B12 is separated from food protein; lack of acid may cause food-cobalamin malabsorption, a common cause of Vit.B12 deficiency^[4,5].

An average omnivorous American diet provides 5 µg-15µg of Vit.B12 per day. Animal products such as meat, poultry, fish, eggs and dairy products are rich sources of Vit.B12. Plant sources contain Vit.B12 only if they are contaminated with microorganisms^[6,7]. As a result, vegans are at a higher risk of becoming Vit. B12 deficient over a period of time. When consumed, Vit.B12 attaches to an 'R' binder (haptocorrin) present in saliva, after it is separated from food protein by acid in the stomach. The pancreas secretes proteases, which at an alkaline pH beyond the stomach digests the 'R' binder facilitating the attachment of intrinsic factor (IF) to B12. IF-B12 complex is absorbed via receptors in the distal ileum. An efficient enterohepatic circulation of Vit.B12, wherein most of the Vit.B12 secreted in the bile is reabsorbed, is the reason why it takes anywhere upto 20 years to become Vit.B12 deficient if one stops consuming

¹Chief, Division of Geriatrics, Director, Geriatric Medicine Fellowship Program Our Lady of Mercy University Medical Center, 600 E 233rd Street, Bronx, NY 10466

²Resident, Internal Medicine Our Lady of Mercy Medical Center

³Chief Medical Resident, Internal Medicine Our Lady of Mercy Medical Center

Correspondence to: T. S. Dharmarajan, MD, FACP, AGSF 31 Pheasant Run Scarsdale, NY 10583

Tel. (718)-920-9041, Fax. (914)-723-4297

Received 2000-03-20 **Accepted** 2000-04-26

Vit.B12^[6,8].

PA was the most likely cause of Vit.B12 deficiency in our patient. The age of onset with advanced disease by mid fifties and absence of any other basis like gastric or small intestinal surgery, chronic pancreatitis, *Crohn's* disease and other causes of malabsorption makes PA the probable diagnosis. The presence of IF antibodies, which is more specific for PA than parietal cell antibodies and seen in about 40% of patients with PA, lends credence to our assumption^[9]. The additional finding of Vit.B12 deficiency with sickle cell trait in this patient is not common. Patients with severe sickle cell disease may have unrecognized Vit. B12 deficiency^[10]. Furthermore, routine folate supplementation in sickle cell anemia prior to determining Vit.B12 status has been considered risky, as it can mask the findings of Vit.B12 deficiency^[11].

The spectrum of Vit.B12 deficiency has been elaborately described in 4 stages^[8,12]. Stages 1 and 2 represent Vit.B12 depletion and stages 3 & 4 represent Vit.B12 deficiency with lab abnormalities and clinical manifestations. Our patient presented with full-blown stage 4 disease, suggesting that he would have been in the pre-clinical stage for many years prior to presentation. Screening for Vit.B12 deficiency would avert the morbidity associated with deficiency states. While in the past there have been no precise guidelines for screening, more recently several approaches have been described. Screening is aimed at reaching a diagnosis at the onset of depletion, i.e. at the pre-clinical stage. The literature suggests several options-from doing nothing until one is symptomatic, to screening all individuals, or an individualized approach^[4,13,14].

Our approach to screening and treatment of Vit. B12 deficiency has been described previously^[13]. Here initial screening is recommended for a select group of individuals at first contact. Included are patients with unexplained anemia, gastritis, acid lowering states from use of certain drugs, autoimmune diseases, HIV disease, *Crohn's* disease, multiple sclerosis, thyroid disease, malabsorption syndromes and vegans. In all other patients the initial screening is recommended at age 50, and thereafter every 5 years until age 65. Annual screening is suggested after age 65. Although normal Vit.B12 levels range from 200 to 900ng • L⁻¹, values between 200 and 400ng • L⁻¹ may need further evaluation including serum (or urine) homocysteine and methyl malonic acid to assess for presence of true deficiency^[13,14].

Treatment for Vit.B12 deficiency is generally initiated with intramuscular injections of Vit.B12, the usual dose being 1 000 µg daily for 3-5 days. Doses vary from 100 to 1 000 µg • d⁻¹ larger doses are accompanied by greater losses in the urine^[6]. Maintenance therapy may be by any of 3 routes intramuscular (IM), oral or intranasal. IM

injections are given every 1 to 3 months. Oral administration necessitates larger doses; 500 to 1 000 µg • d⁻¹ are needed to ensure absorption in PA where 1% maybe absorbed even in the absence of IF^[15]. However compliance with oral administration will always remain in question. Intranasal administration of Vit.B12 has been approved in 1998; this form of Vit.B12 is administered weekly (500 µg • wk⁻¹) and attains levels comparable to maintenance with IM route^[13,15].

CONCLUSION

The case illustrates the importance and need for timely screening for Vit.B12 deficiency. Delay in diagnosis and treatment resulted in a near fatal presentation of a common disease. The primary care physician should be aware that there is a window of opportunity for diagnosis and treatment; several complications of Vit.B12 deficiency are irreversible if early treatment is not provided. The treatment modalities are several and inexpensive, with no side effects. Selection of screening tests and choice of maintenance therapy may be individualized based on patient and physician preferences. Timely screening and treatment of Vit. B12 deficiency will make a difference.

REFERENCES

- 1 Stabler S, Lindenbaum J, Allen R. Vitamin B12 deficiency in the elderly: current dilemmas. *Am J Clin Nutr*, 1997;66:741-749
- 2 Dharmarajan TS, Norkus EP. Vitamin B12 deficiency in the elderly-population based research. In: Herbert V. Vitamin B12 deficiency. London: Royal Society of Medicine Press Ltd, 1999: 27-33
- 3 Lindenbaum J, Rosenberg IH, Wilson PW, Stabler SP, Allen RH. Prevalence of cobalamin deficiency in the Framingham elderly population. *Am J Clin Nutr*, 1994;60:2-11
- 4 Carmel R. Cobalamin, the stomach and aging. *Am J Clin Nutr*, 1997;66:750-759
- 5 Katz PO. Gastroesophageal reflux disease. *J Am Geriatr Soc*, 1998; 46:1558-1565
- 6 Herbert V, Das KC. Folic acid and vitamin B12. In: Shils ME, Olson JA, Shike M. Modern nutrition in health and disease. 8th ed. Philadelphia. Lea and Febiger, 1994:402-425
- 7 Herbert V. Vitamin B12: Plant sources, requirements and assay. *Am J Clin Nutr*, 1988;48:852-858
- 8 Herbert V. Vitamin B12-an overview. In: Herbert V. Vitamin B12 deficiency. London: Royal Society of Medicine Press Ltd, 1999:1-8
- 9 Friedman LS, Peterson WL. Peptic ulcer and related disorders. In: Fauci A, Braunwald E, Isselbacher K, Wilson J, Martin J, Kasper D. Harrison's principles of internal medicine. 14th ed. New York: Mcgraw Hill Pub, 1998;284:1596-1616
- 10 AlMomen AK. Diminished vitamin B12 levels in patients with severe sickle cell disease. *J Intern Med*, 1995;237:551-555
- 11 Sinow RM, Johnson CS, Karnaze DS, Siegel ME, Carmel R. Unsuspected pernicious anemia in a patient with sickle cell disease receiving routine folate supplementation. *Arch Intern Med*, 1987; 147:1828-1829
- 12 Herbert V. Staging vitamin B12 (cobalamin) status in vegetarians. *Am J Clin Nutr*, 1994;59(Suppl):1213S-1222S
- 13 Dharmarajan TS, Norkus EP. An algorithmic approach to the screening of vitamin B12 status and the treatment of identified deficiency. In: Herbert V. Vitamin B12 deficiency. London: Royal Society of Medicine Press Ltd, 1999:49-52
- 14 Stabler SP. Screening the older population for cobalamin deficiency. *J Am Geriatr Soc*, 1995;43:1290-1297
- 15 Elia M. Oral or parenteral therapy for B12 deficiency. *Lancet*, 1998; 352:1721-1722

Edited by Pan BR

Liver inflammatory pseudotumor or parasitic granuloma ?

Xiao Long Ji, Ming Shi Shen and Tong Yin

Subject headings inflammatory pseudotumor; parasitic granuloma; ascariasis larva; liver disease

Ji XL, Shen MS, Yin T. Liver inflammatory pseudotumor or parasitic granuloma. *World J Gastroenterol*, 2000;6(3):458-460

INTRODUCTION

Liver pseudotumor is a very rare benign lesion. Since the first case reported by Pack and Baker in 1953^[1], only 40 cases had been reported up to 1996. The diagnostic challenge of hepatic inflammatory pseudotumor is emphasized by the fact that most of the reported cases were diagnosed by surgical procedures.

Pathogenesis and etiology of hepatic inflammatory pseudotumor are uncertain. We report a case of hepatic pseudotumor that was suspected to be a well-differentiated hepatocellular carcinoma based on abdominal ultrasound, CT and MRI, but the final diagnosis is parasitic granuloma of ascariasis larva after hepatic lobectomy.

CASE REPORT

A soldierly multiple focal hepatic lesion was discovered in a 52-year-old man under the examination of ultrasonography when he was undergoing the regular physical examination in 1998-12. The ultrasonography showed that the nodule appeared as well defined, hypoechoic and hypovascular irregular solid mass without posterior acoustic enhancement on ultrasound (Figure 1). Subsequently, CT scan and MRI also demonstrated the existence of the lesion in the frontal segment of the right hepatic lobe (Figures 2, 3). In January 1999, a fine needle aspiration biopsy was performed on the lesion and the cytological examination showed the possibility of the well differentiated hepatocellular carcinoma. Therefore, the patient underwent the hepatectomy on January 12, 1999.

Pathological findings

Gross findings: The specimen of partial hepatic lobectomy measured 10 cm × 8 cm × 6 cm in size. The cut surface of the lesion contained several pale nodules, which were well-defined and slightly hardened. The center of the nodule was soft and pale-brownish in color, but the contour appearance of the surrounded liver was normal.

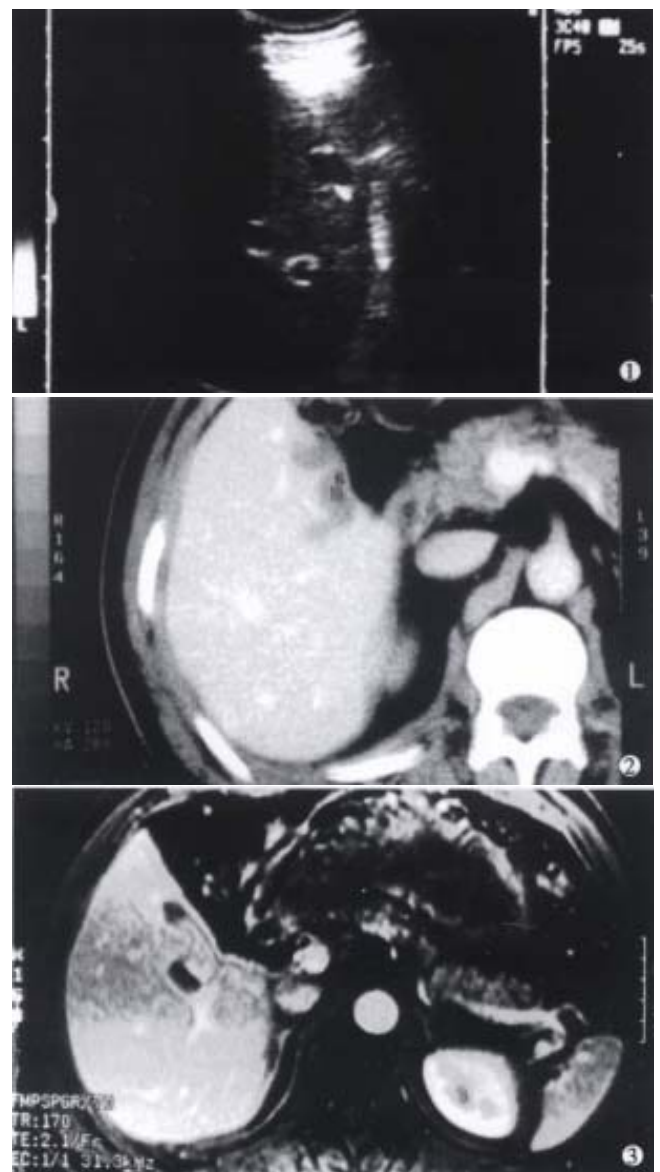


Figure 1 A nodule appeared as well-defined, hypoechoic and hypovascular irregular solid mass by ultrasonography.

Figure 2 Two nodules of low density without early enhancement detected on CT scans.

Figure 3 Two nodules of low signal intensity on T1WI and iso-signal intensity on T2WI by MRI.

Department of Pathology, General Hospital of Chinese PLA, Beijing 100853, China

Xiao Long Ji, graduated from The Third Military Medical University, specialized in the pathology of gastroenterology, having 250 papers published.

Correspondence to: Dr. Xiao Long Ji, Department of Pathology, General Hospital of Chinese PLA, Beijing 100853, China
Tel. 0086-10-68228362

Email: xlj@plagh.com.cn

Received 2000-01-16 Accepted 2000-03-05

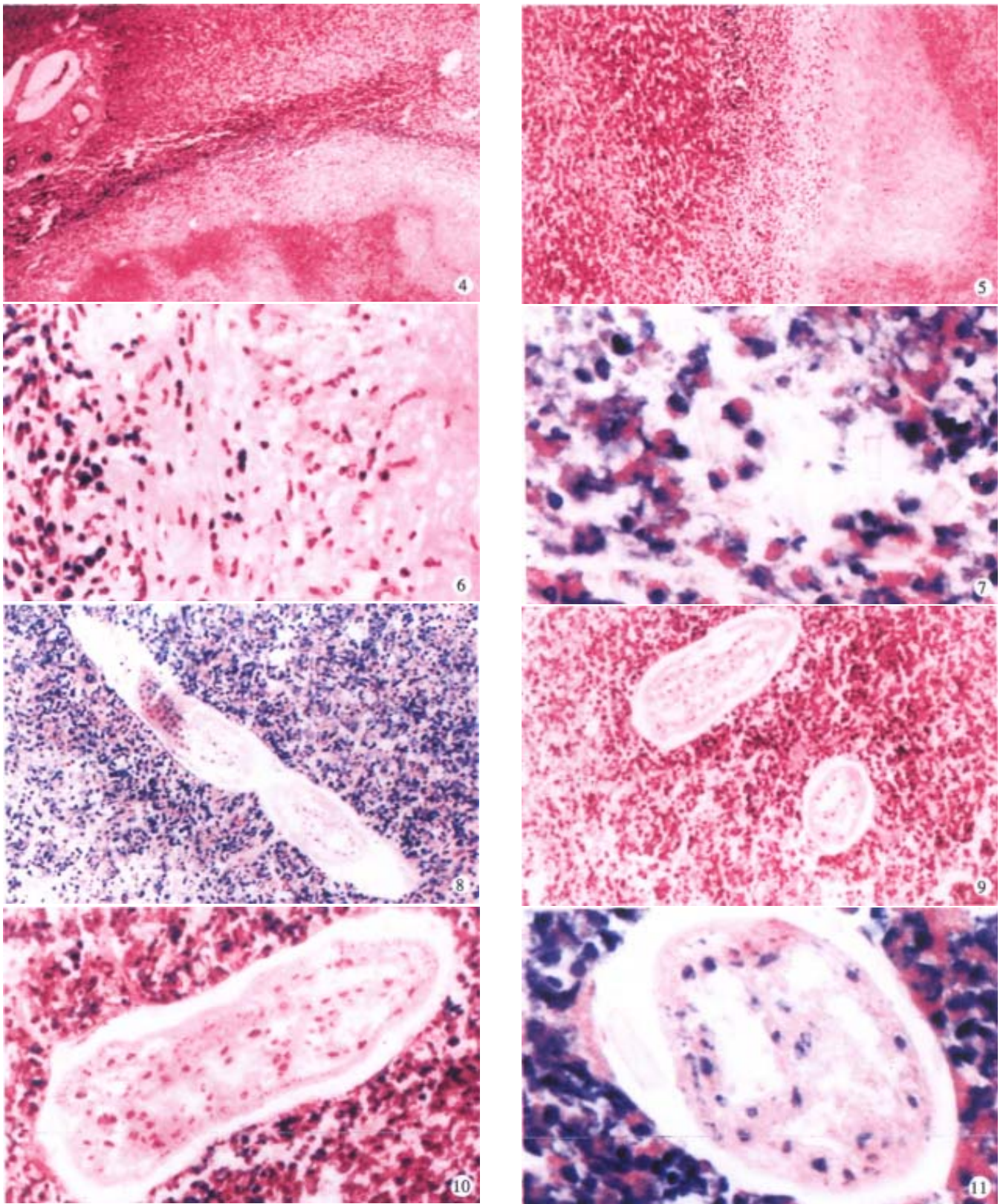


Figure 4 Solitary necrotic nodules of the liver. HE \times 50

Figure 5 Central necrotic core enclosed by a hyalinised fibr otic capsule. HE \times 100

Figure 6 Hyalinised fibrotic capsule infiltrated with eosino phils and lymphocytes. HE \times 200

Figure 7 Charcot-Leyden's crystals and eosinophils in the necrotic center. HE \times 400

Figure 8 One degenerated larva in the center of necrotic nodule. HE \times 100

Figure 9 Two pieces of the degenerated larva in the necrotic center of the nodule. HE \times 200

Figure 10 Necrotic cells around the larva. HE \times 200

Figure 11 Degenerated larva with Charcot-Leyden's crystals . HE \times 400

Microscopic findings

Histopathologic examination. The lesion contained a large area of necrosis with irregular border (Figure 4), around which there are fibrosis and infiltration of lymphocytes, plasma cells and eosinophils (Figures 5,6). In the center of the necrotic lesion, there are many Charcot-Leyden's crystals (Figure 7). The parasite infection was suspected and 26 pieces of tissues from the specimen were sectioned and embedded to find out the pathogen. Finally several parasites with certain morphologic architecture could be found in the sphacelus of the same section (Figures 8,9) only in one of the slides. Although the cells of the parasites were degenerated or necrosed, the viscus and somatic texture could still be recognized (Figures 10,11).

DISCUSSION

Inflammatory pseudotumors are rare benign lesions which may occur in anywhere of the body. They are usually associated with fever, pain and mass formation, and are frequently misdiagnosed as malignant neoplasm. Clinical manifestations and laboratory findings are similar in hepatic pseudotumor and hepatocellular carcinoma. The differential diagnosis between these two is difficult merely based on the images from ultrasonic and radiological examinations. The diagnostic challenge of hepatic inflammatory pseudotumor is emphasized by the fact that most of the reported cases were diagnosed after surgical procedures.

Liver pseudotumors are especially rare and the etiology and pathogenesis are uncertain. Infection was considered as a possible etiology^[2]. Only two cases with organisms were reported: *Escherichia coli* was detected in one case^[3], and Gram-positive cocci in the other^[4]. Other suggested mechanisms include an immune reaction, liver hemorrhage and necrosis,

occlusive phlebitis of hepatic veins, and local reaction to biliary tract^[5]. This is the first case in the literature which demonstrated that the ascariasis larva was found in the necrotic focus of the liver and it was primarily diagnosed as inflammatory pseudotumor. It was suggested that more sections should be taken when hepatic inflammatory pseudotumor was suspected.

The life cycle of ascariasis is complex but well understood. Adult male and female worms live in the small intestine, usually the jejunum, where each gravid female worm produces 200 000 to 250 000 eggs daily. Fertilized eggs pass in the feces and develop into infective eggs in 3 to 4 weeks. The eggs hatch in the small intestine, and the emerging larvae penetrate the intestinal wall, enter the portal vein or intestinal lymphatic vessels, migrate through the liver to the heart, and are pumped through the pulmonary arteries to the lungs. In the lungs, the larvae break out of capillaries into the air spaces. These larvae migrate up from the bronchi to the trachea and down to the esophagus. In the intestine, the larvae develop into sexually mature adults^[6]. From this life cycle, we postulate that the larvae are arrested in the liver during their migration through the liver and become a necrotic nodule.

REFERENCES

- 1 Pack GT, Baker HW. Total right hepatic lobectomy. Report of a case. *Ann Surg*, 1953;138:253-258
- 2 Horiuchi R, Uchida T, Kojima T, Shikata T. Inflammatory pseudotumor of the liver. *Cancer*, 1990;65:1583-1590
- 3 Standiford SB, Sobel H, Dasmahapatra KS. Inflammatory pseudotumor of the liver. *J Surg Oncol*, 1989;40:283-287
- 4 Lupovitch A, Chen R, Mishra S. Inflammatory pseudotumor of the liver. Report of the fine needle aspiration cytologic findings in a case initially misdiagnosed as malignant. *Acta Cytol*, 1989;33:259-262
- 5 Gollapudi P, Chejfec G, Zarling EJ. Spontaneous regression of hepatic pseudotumor. *Am J Gastroenterol*, 1992;87:214-217
- 6 Binford CH, Connor DH. Pathology of tropical and extraordinary diseases: an atlas. Washington D. C: *Armed Forces Instit of Pathol*, 1976:463-464

Edited by You DY and Ma JY
proofread by Sun SM

Renal amyloidosis as a late complication of Crohn's disease: a case report and review of the literature from Japan

Osamu Saitoh¹, Keishi Kojima¹, Tsutomu Teranishi¹, Ken Nakagawa¹, Masanobu Kayazawa¹, Masashi Nanri¹, Yutaro Egashira², Ichiro Hirata¹ and Ken-ichi Katsu¹

Subject headings Crohn's disease/complication; renal amyloidosis; amyloid deposits

Saitoh O, Kojima K, Teranishi T, Nakagawa K, Kayazawa M, Nanri M, Egashira Y, Hirata I, Katsu KI. Renal amyloidosis as a late complication of Crohn's disease: a case report and review of the literature from Japan. *World J Gastroentero*, 2000;6(3):461-464

INTRODUCTION

Secondary amyloidosis is a rare but serious complication of Crohn's disease (CD). The incidence of the association of secondary amyloidosis in patients with CD has been reported to be 0.5%-8% in Western countries [1-6]. However, in Japan, the number of patients with CD complicated by amyloidosis is limited. The characteristics of their clinical manifestations and the incidence of association are uncertain. Therefore, we report herein a patient with Crohn's disease who developed amyloidosis 13 years after the onset of CD. The diagnosis of renal amyloidosis was confirmed by renal biopsy. We also reviewed the literature concerning amyloidosis associated with CD in Japan.

CASE REPORT

The patient was a 29-year-old Japanese female. In May 1985, at the age of 14, she developed diarrhea. In March 1986, she developed fever and arthralgia. A diagnosis of CD was made by endoscopic and radiographic examinations. Thereafter, she received corticosteroids and sulfasalazine. However, hospitalization was required several times. In May 1993, severe stenosis of the ascending colon was found as shown in Figure 1. Therefore, subtotal colectomy, ileocecal resection, and ileosigmoid anastomosis were performed. As shown

in Figure 2, surgical specimen of the terminal ileum, cecum, and ascending colon (May 26, 1993) showed thickening of the bowel wall, cobblestone appearance, and longitudinal ulceration. Histological findings showed transmural inflammation and noncaseating epithelioid cell granuloma. In February, 1997, the patient was admitted because of fever, anemia, and hypoproteinemia. As shown in Figure 3, gastrografin enema examination performed on May 8, 1997 showed a stricture around the ileosigmoid anastomosis. The anastomosis and part of the remaining ileum were resected because of the stenosis. Cholecystectomy was also performed because of gallstones (the biggest stone measured 11 mm × 5 mm, five stones in total, pigmented). Immediately after surgery, right ureteral stricture due to retroperitoneal involvement was found and indwelling double J-catheter was placed. In August 1998, she was admitted because of anemia and hypoproteinemia. Her family history was unremarkable. Her height was 158 cm and body weight was 39.5 kg. Physical examination revealed marked pretibial edema. Laboratory findings included the followings: WBC $7.9 \times 10^9/L$, RBC $2.25 \times 10^{12}/L$, Hb-69 g/L, Ht 0.216, platelet $360 \times 10^9/L$, total protein 53 g/L, albumin 11 g/L, CRP 8.9 mg/dL (normal: less than 0.25 mg/dL), serum amyloid A protein (SAA) 235 $\mu g/dL$ (normal: less than 8 $\mu g/dL$), BUN 7.5 mmol/L, creatinine 145 $\mu mol/L$, creatinine clearance 0.38 mL/s, and urinary protein 9.3 g/day. Renal biopsy was performed in November 1998. As shown in Figure 4, amyloid deposition was found in the mesangial areas and blood vessels. The deposits were Congo red positive. The positive staining disappeared after pretreatment with potassium permanganate. The deposits immunoreacted with the antibody directed against amyloid A (AA)-amyloid. Colonoscopy revealed small discrete ulcerations around J-pouch. The amyloid deposition was not observed in the digestive tract. The electrocardiogram was normal. Ultrasonography did not show any abnormal findings in the heart. Thyroid was not swollen. Thyroid function tests were normal. Administration of prednisolone (40 mg/day) and 5-aminosalicylate (5-ASA) (2.25g/day) normalized serum levels of

¹Second Department of Internal Medicine, ²First Department of Pathology, Osaka Medical College, Takatsuki, Japan

Osamu Saitoh MD, Ph.D, graduated from Osaka Medical College in 1979, now an assistant professor of internal medicine specialized in gastrointestinal diseases, having 150 papers published.

This work was supported in part by Grant-in-Aid 10670518 (to Osamu Saitoh) for Scientific Research from the Ministry of Education, Science, Sports, and Culture, Japan

Correspondence to: Osamu Saitoh, Second Department of Internal Medicine, Osaka Medical College, 2-7 Daigakumachi, Takatsuki, Osaka 569-8686, Japan

Tel. 81-726-83-1221, Fax. 81-726-84-6532

Email. saito@poh.osaka-med.ac.jp

Received 2000-01-17 **Accepted** 2000-02-26

acute phase protein such as CRP and SAA. However, massive proteinuria and hypoalbuminemia persisted. Then, when the dosage of prednisolone was reduced to 10 mg/day, serum CRP and amyloid A protein became positive. Thereafter, azathiopurine (50 mg/d ay) was administered in addition to 5-ASA (2.25 g/day) and prednisolone (10 mg/day).

The onset of CD in this patient was May 1985. Diagnosis was made in March 1986. Proteinuria developed in July 1997. Massive proteinuria developed in April 1998. Creatinine clearance was decreased in July 1997. Amyloid deposits were supposed to have already been present in mid 1997.

DISCUSSION

There is wide geographic variation in the incidence of secondary amyloidosis, occurring in 6%-8% of patients with CD in Northern Europe^[2,4,5], 2% in England^[3], but only 0.5%-0.9% in the United States^[1,6]. However, in Japan, the incidence of secondary amyloidosis in patients with CD remains uncertain. Only 18 Japanese patients with CD complicated by secondary amyloidosis have been reported in the literature from Japan (Table 1)^[7-22].

Secondary amyloidosis is caused by extracellular deposition of the N-terminal AA fragment of the circulating acute phase plasma protein SAA. Secondary amyloidosis can complicate any inflammatory condition in which there is a sustained acute-phase response including CD, rheumatoid arthritis, and chronic sepsis. It has been reported that the activity of the underlying inflammation is an important factor in the development and progression of secondary amyloidosis. In the 18 Japanese patients with CD complicated by

amyloidosis, there were no patients who maintained prolonged remission. Therefore, in CD as well, the disease activity is considered an important factor in the development of secondary amyloidosis. In the present patient, surgery had already been performed two times as the disease activity could not be controlled by medical treatment. Nevertheless, serum CRP remained positive. Moreover, in the present patient, the involvement of the retroperitoneum caused right ureteral stricture.

Inflammation is thought to precede the development of secondary amyloidosis. However, the time-course and progression of secondary amyloidosis are not understood well. In animal experiments, amyloid deposits were found 18h or a few weeks after inflammatory stimuli^[23-25]. Various factors have been reported to influence the susceptibility, onset, and progression of murine amyloidosis^[26,27]. It remains controversial whether amyloidosis is a late complication of CD. In the present patient, nephrotic syndrome developed and the diagnosis of secondary amyloidosis was made 13 years after the onset of CD. When proteinuria was initially detected, it had already been 12 years since the onset of CD. In the literature, the time lapse between the onset of CD and the diagnosis of amyloidosis has been reported to range from 3 to 15 years or from 1 to 21 years^[28,29]. In 11 of the 18 Japanese patients, more than 5 years had passed after the onset of CD. The longest period was 18 years. Conversely, in 2 patients, the diagnosis of amyloidosis preceded that of CD. When CD was diagnosed in these 2 patients, the lesion of CD had already become typical. These findings suggest that secondary amyloidosis usually occurs as a late complication of CD. However, as the onset of CD is usually gradual, CD and secondary amyloidosis may be diagnosed almost simultaneously.

Table 1 Japanese Crohn's disease patients complicated by secondary amyloidosis

Case	Age	Sex	Sites of CD	Duration of CD prior to amyloidosis diagnosis	Clinical course of CD before amyloidosis diagnosis	Major clinical manifestation of amyloidosis	type of amyloid	Proteinuria	Author (year)
1	23	M	I,C	6 year	Not well controlled	Intestinal	AA	Present	Oshima T <i>et al.</i> (1988)
2	28	M	I,C	9 year	Not well controlled	Renal	AA	Present	Tsutsui R <i>et al.</i> (1988)
3	37	M	I,C,R	11 year	Not well controlled	Renal	AA	Present	Araki T <i>et al.</i> (1989)
4	20	F	C	4 year	Not well controlled	Renal	AA	Present	Kikuchi H <i>et al.</i> (1989)
5	25	M	I	0 [#]		Renal	AA	Present	Momiyama Y <i>et al.</i> (1989)
6	28	M	J,C	0		Renal	AA	Present	Takashima H <i>et al.</i> (1990)
7	24	M	I	0		Intestinal	AA	None	Itoh T <i>et al.</i> (1991)
8	44	M	I	8 year	Not well controlled	Intestinal	AA	None	Sakai Y <i>et al.</i> (1992)
9	26	M	I,C	13 year	Not well controlled	Renal	AA	Present	Ohwan T <i>et al.</i> (1994)
10	34	M	I,C	15 year	Unknown	Intestinal	AA	None	Yamamoto J <i>et al.</i> (1994)
11	28	M	I	12 year	Not well controlled	Renal	AA	Present	Itoh F <i>et al.</i> (1996)
12	28	M	I	7 year	Not well controlled	Renal	AA	Present	Itoh F <i>et al.</i> (1996)
13	26	M	C	4.5 year	Not well controlled	Renal	AA	Present	Yoshinaga Y <i>et al.</i> (1996)
14	43	M	C,R	15 year	Not well controlled	Renal	AA	Present	Yoshinaga Y <i>et al.</i> (1996)
15	21	M	I,C	3.5 year	Not well controlled	Renal	AA	Present	Horie Y <i>et al.</i> (1997)
16	43	M	C,R	18 year	Not well controlled	Renal	AA	Present	Muro K <i>et al.</i> (1998)
17	35	F	C	0 [#]		Renal	AA	Present	Taki F <i>et al.</i> (1998)
18	26	M	C	11 year	Unknown	Thyroid	AA	Present	Habu S <i>et al.</i> (1999)
19	29	F	I,C,R	13 year	Not well controlled	Renal	AA	Present	Present case (1999)

[#]:The diagnosis of amyloidosis preceded that of Crohn's disease. CD: Crohn's disease, J: jejunum, I: ileum, C: colon, R: rectum, AA: amyloid A

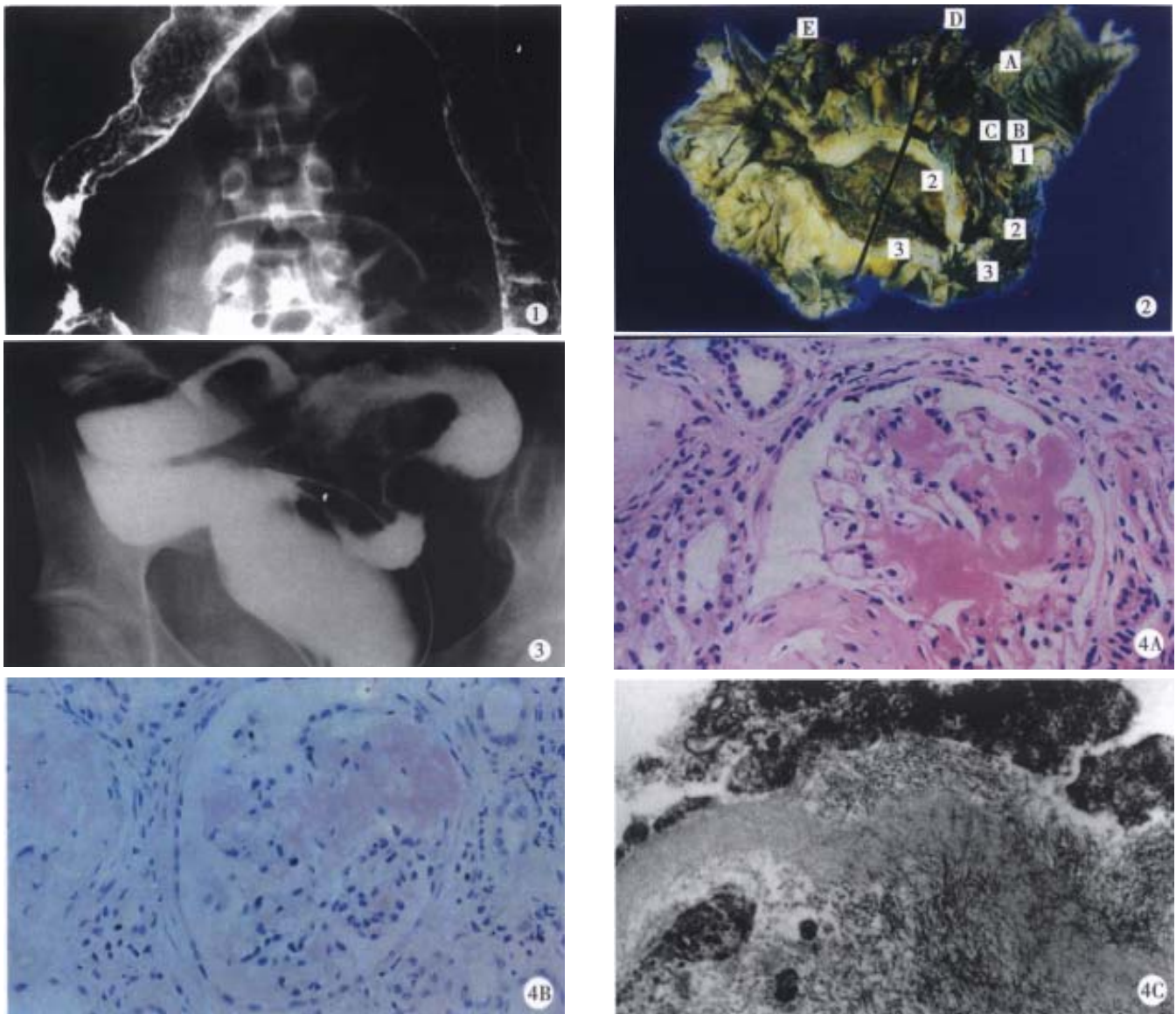


Figure 1 Barium enema examination performed on March 18, 1993. Stricture associated with cobblestone appearance was seen in the ascending colon. Small inflammatory polyps were observed in the transverse colon and descending colon.

Figure 2 Surgical specimen of the terminal ileum, cecum, and ascending colon (May 26, 1993). Thickening of the bowel wall, cobblestone appearance, and longitudinal ulceration were found. Histologically, transmural inflammation and noncaseating epithelioid cell granuloma were found.

Figure 3 Gastrografen enema examination performed on May 8, 1997. A stricture was seen around the ileosigmoid anastomosis.

Figure 4 Findings of the renal biopsy.

A. Histological findings (hematoxylin and eosin). Amorphous, eosin-stained deposits were seen in the mesangial areas.

B. Histological findings (Congo red stain). The deposits were Congo red positive. Congo red stain showed reddish pink deposits that demonstrated apple-green birefringence when examined under polarized light.

C. Electron microscopic findings. Fine fibrils (8 to 10-nm in diameter) arranged randomly or in bundles were found in the mesangium.

The kidney is involved in the majority of patients with secondary amyloidosis. The resulting renal insufficiency caused a deterioration in the prognosis of the patient. Azathiopurine^[30], colchicine^[31,32], dimethylsulfoxide^[33], and elemental diet^[19] have been proposed as the treatment for secondary amyloidosis. However, the effectiveness of this regimen has not been established. Therefore, prevention or early diagnosis and treatment are important. In 15 of the

18 Japanese patients, the kidney was involved by amyloidosis. And in 13 of the 15 patients, renal involvement was the main clinical manifestation of amyloidosis. In only one of the 15 patients^[19], the amount of urinary protein decreased to less than 0.3 g/day since the initiation of elemental diet therapy. In the remaining 14 patients, however, neither proteinuria nor impaired renal function improved after various therapeutic attempts.

Therefore, regular urine test for proteinuria

would be useful for early diagnosis of amyloidosis regardless of the interval since onset of CD. To prevent the development and progression of secondary amyloidosis, it is probably important to maintain CD in the remission.

ACKNOWLEDGEMENT The authors thank the doctors of Osaka Medical College Hospital for their invaluable contributions to the study of this case.

REFERENCES

- Greenstein AJ, Janowitz HD, Sachar DB. The extra-intestinal complication of Crohn's disease and ulcerative colitis: a study of 700 patients. *Medicine Baltimore*, 1976;55:401-412
- Fausa O, Nygaard K, Elgjo K. Amyloidosis and Crohn's disease. *Scand J Gastroenterol*, 1977;12:657-662
- Cooke WT, Mallas E, Prior P. Crohn's disease: course, treatment and long term prognosis. *Q J Med*, 1980;49:363-384
- Lind E, Fausa O, Gjone E, Mogensen SB. Crohn's disease. Treatment and outcome. *Scand J Gastroenterol*, 1985;20:1014-1018
- Weternan IT, Biemond I, Pena AS. Mortality and causes of death in Crohn's disease. Review of 50 years' experience in Leiden University Hospital. *Gut*, 1990;31:1387-1390
- Greenstein AJ, Sachar DB, Panday AKN, Dikman SH, Meyers S, Heimann T, Gumaste V, Werther JL, Janowitz HD. Amyloidosis and inflammatory bowel disease. A 50-year experience with 25 patients. *Medicine Baltimore*, 1992;71:261-270
- Oshima T, Fujimoto K, Kounoue E, Shibuya T, Ishibashi H, Niho Y, Iida M, Guo K, Nakamura K. A case of Crohn's disease associated with secondary amyloidosis. *J Jpn Soc Internal Med*, 1988;77:1233-1237
- Tsutsui R, Okada M, Yao T, Murayama H, Iwashita A, Yokota T. Crohn's disease associated with amyloidosis, report of a case. *Stomach Intestine*, 1988;23:195-201
- Araki T, Ohmori H, Kosaka K, Ohashi Y. A case of amyloidosis secondary to Crohn's disease. *Jpn J Gastroenterol*, 1989;86:2227-2231
- Kikuchi H, Saito H, Nakajima H, Uno R, Suzuki K, Sano M, Munakata A, Yoshida Y. A case report of Crohn's disease complicated with renal amyloidosis. *Jpn J Gastroenterol*, 1989;86:2579-2582
- Momiyama Y, Nagata H, Nakao T. Crohn's disease associated with amyloidosis. A case discovered by persistent proteinuria. *J Jpn Soc Internal Med*, 1989;78:398-403
- Takashima H, Kisu T, Yamaoka K, Uchida Y, Mori H, Koike Y, Nojiri I, Miyabara S. A case of Crohn's disease associated with nephrotic syndrome due to secondary amyloidosis. *Gastroenterol Endosc*, 1990;32:2393-2398
- Itoh T, Kawanami C, Kishi K, Kitajima N, Kinoshita Y, Takenaka M, Kodama K, Kishihara M, Inatome T, Inoh T, Tachibana H, Matsumoto Y, Takahashi H, Nakamura T. Crohn's disease associated with secondary amyloidosis: a case report. *Jpn J Gastroenterol*, 1991;88:730-734
- Sakai Y, Araki Y, Kawakubo K, Kohroggi N, Lida M, Fujishima M. A case of Crohn's disease associated with amyloidosis. *Jpn J Clin Exp Med*, 1992;69:1147-1154
- Ohwan T, Takano M, Takagi K, Fujiyoshi T, Fujimoto N, Nozaki R, Etoh K, Kikuchi R, Kii F, Tanaka S, Gakiya I, Tsuchihashi N. A case of Crohn's disease in siblings associated with amyloidosis. *J Jpn Soc Coloproctol*, 1994;47:448-454
- Yamamoto J, Nagae T, Uchida Y, Takenaka K, Sakurai T, Matsui T, Yao T, Yamada Y, Iwashita A. Secondary amyloidosis found by routine duodenoscopy during the course of Crohn's disease, report of a case. *Stomach Intestine*, 1994;29:1437-1443
- Itoh F, Honda S, Nishimura S, Hinoda H, Imai K. Crohn's disease associated with amyloidosis. Report of two cases. *JJPEN*, 1996;18:73-74
- Yoshinaga Y, Nagase S, Kishida M, Odawara M, Tagashira M, Yamawaki Y, Fujino K, matsumoto M, Urakubo N, Morisaki F, Ohta T. Renal amyloidosis secondary to Crohn's disease. Report of two cases. *Med J Onomichi Municipa Hosp*, 1996;12:47-54
- Horie Y, Chiba M, Miura K, Iizuka M, Masamune O, Komatsuda A, Ebina T. Crohn's disease associated with renal amyloidosis successfully treated with an elemental diet. *J Gastroenterol*, 1997;32:663-667
- Muro K, Kobayashi M, Shimizu Y, Kikuchi S, Yamaguchi N, Inadome Y, Watanabe T, Koyama A. A case of systemic AA amyloidosis complicating Crohn's disease. *Jpn J Nephrol*, 1998;40:284-289
- Taki F, Tomiyoshi Y, Matsunaga K, Mizuguchi M, Iwakiri R, Ikeda Y, Kou Y, Miyazono M, Sakemi T. A case of Crohn's disease detected by amyloid nephropathy. *Kidney Dialysis*, 1998;45:135-137
- Habu S, Watanobe H, Kimura K, Suda T. A case of amyloid goiter secondary to Crohn's Disease. *Endocrine J*, 1999;46:179-182
- Kisilevsky R, Boudreau L. Kinetics of amyloid deposition. I. The effects of amyloidenhancing factor and splenectomy. *Lab Invest*, 1983;48:53-59
- Sipe JD, Carreras I, Gonnerman WA, Cathcart ES, de Beer MC, de Beer FC. Characterization of the inbred CE/J mouse strain as amyloid resistant. *Am J Pathol*, 1993;143:1480-1485
- Graether SP, Young ID, Kisilevsky R. Early detection of inflammation-associated amyloid in murine spleen using thioflavin T fluorescence of tissue homogenates: implications for amyloidogenesis. *Amyloid*, 1996;3:20-27
- Botto M, Hawkins PN, Bickerstaff MC, Herbert J, Bygrave AE, McBride A, Hutchinson WL, Tennent GA, Walport MJ, Pepys MB. Amyloid deposition is delayed in mice with targeted deletion of the serum amyloid P component gene. *Nat Med*, 1997;3:855-859
- Kindy MS, Rader DJ. Reduction in amyloid A amyloid formation in apolipoprotein-E deficient mice. *Am J Pathol*, 1998;152:1387-1395
- Lowdell CP, Shousha S, Parkins RA. The incidence of amyloidosis complicating inflammatory bowel disease. A prospective survey of 177 patients. *Dis Colon Rectum*, 1986;29:351-354
- Rashid H, Blake D, Gokal R, Gooptu D, Kerr DN. The association of renal amyloidosis with regional enteritis (Crohn's disease). Report of two cases and review of the literature. *Clin Nephrol*, 1980;14:154-157
- Verbanck J, Lameire N, Praet M, Ringoir S, Elewaut A, Barbier F. Renal amyloidosis as complication of Crohn's disease. *Acta Clin Belg*, 1979;34:6-13
- Ravid M, Shapira J, Kedar I, Feigl D. Regression of amyloidosis secondary to granulomatous ileitis following surgical resection and colchicine administration. *Acta Hepatogastroenterol*, 1979;26:513-515
- Meyers S. Systemic amyloidosis complicating inflammatory bowel disease. *Gastroenterology*, 1997;113:731
- Ravid M, Shapira J, Lang R, Kedar I. Prolonged dimethylsulphoxide treatment in 13 patients with systemic amyloidosis. *Ann Rheum Dis*, 1982;41:587-592

Edited by You DY